

**Synthesis, reactivity and application to asymmetric catalysis
of small and medium sized chiral poly-substituted heterocycles**

By

Michelle LeeAnn Bezanson

*A thesis submitted to McGill University in partial fulfillment of the
requirements for the degree of Doctor of Philosophy*

Department of Chemistry,

McGill University

Montréal, QC, Canada

August 2016

© Michelle Bezanson 2016

I would like to dedicate this thesis to my family: my wonderful and supportive parents, Brent Bezanson and Linda McKenzie-Bezanson, as well as my sisters, Brianne and Danielle.

Copyright Statement

Some of the material included in the following thesis is adapted from published papers and is under copyright:

Chapters 2 and 3 reproduce material published in Bezanson, M.; Pottel, J.; Bilbeisi, R.; Toumieux, S.; Cueto, M.; Moitessier, N. Stereo- and Regioselective Synthesis of Polysubstituted Chiral 1,4-Oxazepanes. *J. Org. Chem.* **2013**, *78*, 872. ©American Chemical Society (2012). The ACS grants blanket permission for authors to use their work in their dissertation.

Chapters 1 and 4 are drafts of manuscripts to be submitted for publication.

Abstract

The majority of marketed drugs and fine chemicals contain some sort of cyclic structure, emphasizing the need for these types of structures in industry. Seven-membered rings however are uncommon, possibly due to the limited methods to synthesize them in an expedient fashion with good stereoselectivity. Despite the existence of several oxazepane containing bioactive molecules and natural products, little effort has been put into synthesizing these structures. In this thesis, we explore the synthesis of 1,4-oxazepanes via a key halocycloetherification reaction. We investigate the substrate scope of the reaction as well as details of the mechanism. The regioselectivity and relative stereochemistry can be easily controlled by manipulating the substitution of the starting material; the absolute stereochemistry was investigated using computational techniques and was determined to arise from reaction of the lowest energy ground state conformation as formation of the bromiranium ion had no transition state. From this point, the reactivity of the oxazepanes was investigated. Under fluoride-mediated conditions, *N*-Ns protected oxazepanes featuring a C3 ester underwent a unique ring closure accompanied by loss of SO₂ and migration of *para*-nitrophenyl to yield a series of 4-oxa-1-azabicyclo[4.1.0]heptanes. The mechanism of this reaction is currently under investigation using computational techniques and will be reported in due course. Derivatives of both 1,4-oxazepanes and 4-oxa-1-azabicyclo[4.1.0]heptanes were then probed as organocatalysts in a variety of reactions: secondary amine derivatives of 1,4-oxazepanes and 1,4-morpholines were investigated as organocatalysts in Diels-Alder cycloaddition and aldol reactions, giving products in low yields for the morpholine derivative and unfortunately not catalyzing the reaction at all in the case of the oxazepanes; 4-oxa-1-azabicyclo[4.1.0]heptanes featuring tertiary amines were investigated as ligands for OsO₄ for asymmetric dihydroxylation of olefins yet unfortunately did not induce any asymmetry and only racemic mixtures were obtained; and finally, amino alcohol derivatives of 4-oxa-1-azabicyclo[4.1.0]heptanes and also some carbohydrate-based amino alcohol scaffolds were discussed as organocatalysts for the addition of diethylzinc to benzaldehyde, leading to 1-phenyl-1-propanol in up to 78 % yield and up to 33 %ee.

Résumé

La grande majorité des médicaments et des produits de chimie fine contiennent un ou plusieurs cycles dans leur structure, les rendant dès lors indispensables dans l'industrie chimique. Cependant, les cycles à sept éléments sont relativement rares, possiblement en raison du manque de méthode de synthèse efficiente et stéréosélective. Malgré l'existence de plusieurs molécules bioactives et produits naturels contenant un oxazépane, peu d'efforts ont été faits pour la synthèse de ces composés. Dans cette thèse, nous explorons la synthèse de 1,4-oxazépanes via la réaction d'halocycloétherification. Nous étudions également l'étendue ainsi que les détails mécanistiques de la réaction. La régiosélectivité et stéréochimie relative peuvent facilement être contrôlées en modifiant la substitution du produit de départ. La stéréochimie absolue, étudiée par le biais de techniques computationnelles, se trouva être déterminée par la réaction de la conformation possédant l'état fondamental de plus basse énergie étant donné que la formation de l'ion bromiranium ne possède pas d'état de transition. La réactivité des oxazépanes ainsi obtenus a été étudiée. Sous des conditions de réactions contenant du fluor, les oxazépanes protégés (*N*-Ns) et possédant un ester à la position C3 subissent une fermeture de cycle accompagnée par la perte de SO₂ et la migration du groupement *para*-nitrophenyle afin de produire une série de 4-oxa-1-azabicyclo[4.1.0]heptanes. Le mécanisme de cette réaction est en cours d'étude par méthodes computationnelle et sera rapporté en temps voulu. Des dérivés de 1,4-oxazépanes et de 4-oxa-1-azabicyclo[4.1.0]heptanes ont ensuite été utilisés comme organocatalyseurs dans différentes réactions : les dérivés de 1,4-oxazépanes contenant une amine secondaire ont été utilisés comme organocatalyseurs dans les réactions de Diels-Alder ainsi qu'aldol, menant à des produits avec de faibles rendements pour le dérivé morpholine et malheureusement aucune réaction n'a été observée dans le cas des dérivés oxazépanes; la possibilité d'utiliser les 4-oxa-1-azabicyclo[4.1.0]heptanes contenant une amine tertiaire comme ligand de OsO₄ dans la dihydroxylation asymétrique d'oléfines a également été considérée, malheureusement sans succès avec la production de mélanges racémiques uniquement; et finalement, les dérivés amino alcool de 4-oxa-1-azabicyclo[4.1.0]heptanes et de carbohydrates ont été considérés pour l'addition de diéthylzinc sur du benzaldéhyde, formant du 1-phényl-1-propanol avec des rendements allant jusqu'à 78 % et jusqu'à 33 % ee.

Acknowledgements

First, I would like to acknowledge my supervisor, Professor Nicolas Moitessier, for all his support and advice over the course of my degree. His style of supervision has made graduate school exactly what I wanted it to be: I have learned so much from Nic, he gave me the freedom to pursue whatever chemistry I thought was interesting and he has always put the best interest of all his students first. Thank you so much Nic, it has been a pleasure.

I would also like to thank all the wonderful support staff in the McGill Chemistry department, particularly Fred Morin and Robin Stein in the NMR facility, Nadim Saadé and Alexander Wahba in the mass spectrometry facility as well as Chantal Marotte who is indispensable, every graduate student and faculty member in the department would be lost without her excellent management. Although not a member of McGill staff, I would additionally like to thank my friend Igor Huskic for his technical assistance with obtaining most of the crystal structures presented in this thesis.

I could not have gotten through this degree without the amazing people that I have had the pleasure of working with in the Moitessier lab over the years. In the lab, fellow graduate students Dr. Stephane De Cesco, Rodrigo Barroso, Sylvain Rocheleau, Paolo Schiavini, Jessica Plescia, Naëla Janmamode, post-doctoral fellows Dr. Sébastien Deslandes and Dr. Gaëlle Mariaule and undergraduates Dave Levan, Eric Ma, Tazkia Hassan, Michael Cueto, Stephanie Abraham and Jonathan O'Mondays. On the computational side of the group, Dr. Joshua Pottel, who I would like to particularly acknowledge for his wonderful work that we collaborated on and who I had the pleasure of publishing with, as well as other fellow graduate students Zhaomin (Leo) Liu, Anna Tomberg, Jerry Kurian, Mihai Burai Patrascu, post-doctoral fellows Dr. Valerie Campagna-Slater, Dr. Nathanael Weill and Dr. Stephen Jones Barigye, research associate Dr. Eric Therien, and undergraduate and good friend, Andy Arrowsmith. Additionally, I have been fortunate enough to share office space with the Auclair group and I would like to acknowledge them for being wonderful colleagues, I would like to note particularly Vanja Polic, Jack Cheong, Fabien Hammerer, Siqi Zhu and Eric Habib for wonderful office conversation, both scientific and purely entertaining.

There are several other people that I would like to acknowledge for being wonderful role models for what a graduate student should be: hard working, helpful and brilliant. Those people

that stood out to me include Rodrigo Mendoza-Sanchez, Daniel Rivalti, Katerina Krumova and Joris De Schutter.

Perhaps the most important part of graduate school has been meeting some of the most remarkable people I have ever had the chance to meet in my life and now have the honour to call my friends: Lana Greene, who helped immensely with the transition of moving from Nova Scotia to Montreal because she was going through the same thing; Mary Bateman, who I have known since our undergraduate degrees at Dalhousie and who is genuinely one of the nicest people I have ever met and without doubt the best roommate I have ever had; Julia Schneider, who is too wonderful for words to possibly describe, I absolutely adore everything about you; Jevgenijs Tjutrins, who started this adventure at the same time as me and has been one of my best friends throughout and the perfect person to understand all of the frustrations that have happened along the way; Laure Kayser, your constant optimism is inspiring, you are great and you push everyone around you to be great and I really admire that about you; Monika Rak, you seem superhuman sometimes with everything you do and your ridiculousness and awkwardness are some of my favourite things about you ; Thomas Knauber, one of the most unique people I have met and an original member of the drinking team, To Canada!; and finally Graeme Cambridge, thank you for loving me and supporting me and putting up with me, I did not know how much I needed you until I found you.

Lastly, I am incredibly grateful for my friends and family back in Nova Scotia. I know most of you never understand me when I talk about what it is I do but I appreciate you at least trying to listen. Particularly, huge thanks to my sisters, Brianne and Danielle, and my parents Brent and Linda. I love you all so much and I could not have done this without your love and support.

Thank you everyone!

Table of contents

CHAPTER 1 SYNTHESIS OF SMALL & MEDIUM SIZED HETEROCYCLES BY HALIRANIUM-MEDIATED CYCLIZATION

1.1	Halofunctionalization	1
1.2	Baldwin's rules	4
1.3	Intramolecular halocycloetherification.....	6
1.3.1	3- <i>exo</i> halocycloetherification	7
1.3.2	3- <i>endo</i> halocycloetherification	10
1.3.3	4- <i>exo</i> halocycloetherification	11
1.3.4	4- <i>endo</i> halocycloetherification	17
1.3.5	5- <i>exo</i> halocycloetherification	20
1.3.5.1	Diastereoselective Halocycloetherification.....	20
1.3.5.2	Catalytic Enantioselective Halocycloetherification	29
1.3.6	5- <i>endo</i> halocycloetherification	36
1.3.7	6- <i>exo</i> halocycloetherification	45
1.3.8	6- <i>endo</i> halocycloetherification	55
1.4	Conclusion and Perspective.....	61
1.5	References	62

CHAPTER 2 SYNTHESIS OF CHIRAL POLYSUBSTITUTED OXAZEPANES AND MORPHOLINES

2.1	Preface	67
2.2	Introduction	68
2.3	Results and Discussion.....	74
2.3.1	Design of synthetic strategy	74
2.3.2	Preparation of unsaturated alcohols.....	75
2.3.3	Key Cyclization	77
2.4	Conclusions	88
2.5	Experimental	89
2.5.1	General considerations and procedures	89
2.5.2	Experimental data	90
2.6	References	109

CHAPTER 3 CHARACTERIZATION & MECHANISTIC STUDY OF THE FORMATION OF REGIO- & STEREOSELECTIVE OXAZEPANES AND MORPHOLINES

3.1	Preface	111
3.2	Introduction	112
3.3	Results and Discussion.....	118
3.3.1	Mechanism.....	118
3.3.2	Regiochemistry.....	119
3.3.3	Stereochemistry	126
3.3.3.1	Relative Stereochemistry.....	130
3.3.3.2	Diastereomers.....	131
3.4	Conclusions	133
3.5	Experimental	134
3.5.1	General considerations and procedure.....	134
3.5.2	Computational methods.....	135
3.5.3	Experimental data	136
3.6	References	148

CHAPTER 4 FLUORIDE-MEDIATED DESULFONYLATIVE INTRAMOLECULAR CYCLIZATION TO FUSED AND BRIDGED BICYCLIC COMPOUNDS

4.1	Preface	149
4.2	Introduction	150
4.3	Results and Discussion.....	151
4.3.1	Characterization.....	151
4.3.2	Probing the reaction conditions	152
4.3.3	Substrate scope	155
4.3.4	Proposed mechanism	162
4.4	Conclusion.....	170
4.5	Experimental Section	170
4.5.1	General considerations	170
4.5.2	Experimental Data	171
4.6	References	177

CHAPTER 5 EFFORTS IN THE SYNTHESIS OF CYCLIC CHIRAL AMINES FOR APPLICATIONS IN ASYMMETRIC ORGANOCATALYSIS

5.1	Preface	178
5.2	Introduction	179
5.3	Results and Discussion.....	181
5.3.1	Development of chiral polysubstituted oxazepane and morpholine secondary amines as organocatalysts for Diels-Alder and aldol reactions	181
5.3.2	Efforts into removal of sulfonamide protecting groups.....	183
5.3.3	Diels-Alder catalysis.....	190
5.3.4	Aldol catalysis.....	191
5.3.5	Chiral tertiary amines as ligands for catalytic asymmetric dihydroxylation.....	193
5.3.6	Chiral bicyclic aziridinols as organocatalysts for diethylzinc addition to benzaldehyde 196	
5.3.7	Synthesis of amine alcohols.....	199
5.3.8	Diethylzinc addition catalysis.....	199
5.3.9	Carbohydrate-based amino alcohols as organocatalysts for diethylzinc addition to benzaldehyde	200
5.3.10	Asymmetric Catalyst Evaluation (ACE)	200
5.3.11	Efforts into the synthesis of carbohydrate-based amino alcohols.....	203
5.4	Conclusion.....	208
5.5	Experimental	209
5.5	References	215

CHAPTER 6 CONCLUSIONS AND PERSPECTIVES

6.1	Conclusions	218
6.2	Perspectives.....	220
6.3	References	222

Table of figures

Figure 1.1.	Nomenclature of halogen cations.	2
Figure 1.2.	Baldwin's rules for ring closure.	5

Figure 1.3. Ambiguity of naming system accompanying the cyclization of a cyclic precursor (1.16) to give bridged bicycles (1.18a and 1.18b).....	6
Figure 1.4. a) Bürgi-Dunitz angle of attack of nucleophiles onto olefins required for <i>trig</i> cyclizations and b) intramolecular cyclization unable to attack at the correct angle.....	11
Figure 1.5. Stereochemical model of 4- <i>exo-trig</i> iodocycloetherification to make oxetanes in a) a diastereoselective manner and b,c) an enantioselective manner; X _C = Evans auxiliary.....	14
Figure 1.6. Explanation of observed stereochemistry selectivity presented in Table 1.9.....	26
Figure 1.7. Structure of tetronasin (1.146) with the tetrahydrofuran portion of interest highlighted in blue.....	40
Figure 1.8. Incorrect stereochemical outcome of the 5- <i>endo</i> cyclizations of <i>cis</i> -(<i>E</i>)-1.147, <i>cis</i> -(<i>Z</i>)-1.147, <i>trans</i> -(<i>E</i>)-1.147 and <i>trans</i> -(<i>Z</i>)-1.147 mediated by I ⁺ and PhSe ⁺ , as misassigned by Barton and Lipshutz.....	40
Figure 1.9. Transition state of 1.159 showing the stabilization provided by the ester group that makes the reaction less susceptible to intermolecular attack of water to form halohydrins.....	41
Figure 1.10. Proposed transition state for 5- <i>endo</i> iodocycloetherification of transformations shown in Table 1.15.	43
Figure 1.11. Structure of natural product usneoidone E (1.185).	49
Figure 1.12. Proposed structure of waol A (1.214), structures of TAN-2483A (1.216) and TAN-2483B (1.217), revised structure of waol A (1.218) and structures of massarilactone B (1.219) and fusidilactone B (1.220).....	59
Figure 2.1. Reported synthetic oxazepanes.....	68
Figure 2.2. General synthetic strategy.	75
Figure 3.1. a) Symmetric bromiranium ion from symmetric olefin (3.1) and asymmetric bromiraniums from unsymmetric olefin (3.2) and symmetric olefin (3.3), bond lengths come from PM3-optimized geometries; b) Rapid equilibration of asymmetric β-halocarboocations through the symmetric bromiranium ion.....	112
Figure 3.2 a) Example of selectivity observed depending on the alkene substituents; b) Formation of a bromonium ion; c) Stereochemistry scrambling from olefin-to-olefin transfer, LB = Lewis Base.....	119
Figure 3.3. Expected signals in HMBC for 2.42j and 2.43j.....	124

Figure 3.4. HMBC for 2.42j; the red line shows an inconclusive signal between C2 and what may or may not be H7; the blue line shows a clear signal between H2 and C7, necessitating the regiochemistry shown.	124
Figure 3.5. HMBC for 2.43j; the blue line shows a clear signal between H2 and C6, necessitating the regiochemistry shown.	125
Figure 3.6. Solid-state molecular structure confirming the regiochemistry and stereochemistry of 2.42e.	130
Figure 3.7. Potential energy surface of the reaction between NBS-H ⁺ and <i>trans</i> -butene.	132
Figure 3.8. Stereochemical outcome from simple conformational analysis (2.41c).	133
Figure 3.9. Summary of observed selectivity based on the structure of the starting material. ...	134
Figure 4.1. Complexity from simple building blocks.	150
Figure 4.2. Fluoride-mediated intramolecular rearrangement of 2.42f. Ellipsoids shown at 50 % probability level; crystal structure is of (±)-4.1 (the enantiomer shown will be referred to as 4.1a, the enantiomer not shown will be referred to as 4.1b).	152
Figure 4.3. Mechanism for the formation of 4.2b.	156
Figure 4.4. Migration of <i>para</i> -nitrophenyl in nosyl-protected proline ester reported previously. ¹⁹	157
Figure 4.5. Assigned structure of 4.1c based on analogy of its NMR spectrum with that of 4.2fa. Ellipsoids shown at 50 % probability level.	158
Figure 4.6. Tentative mechanisms for the formation of 4.2fd.	159
Figure 4.7. Formation of carbocation intermediate 4.7 from 2.42f.	163
Figure 4.8. Compound 2.42f: conformation leading towards 4.1a (top), conformation with C6 proton anti-periplanar to the ether oxygen leading to elimination of bromine (bottom).	164
Figure 4.9. Ring opening of 2.42f leading to the production of its diastereomer 4.9.	165
Figure 4.10. Loss of HF to produce the intermediate enolates 4.10a and 4.10b from 2.42f and 4.9, respectively.	166
Figure 4.11. Formation of product 4.1a from enolate 4.10a (same for 4.1b from 4.10b).	167
Figure 4.12. Investigation of alternative pathways leading to 4.1b.	168
Figure 4.13. Overall energy profile (kcal/mol) for reaction mechanism leading from 2.42f to 4.1a (blue) and to 4.1b (green).	169
Figure 5.1. Gibbs free energy profile of an asymmetrically catalyzed addition reaction.	179

Figure 5.2. LUMO-activation mechanism of α,β -unsaturated carbonyls via Lewis acids or amines.	180
Figure 5.3. Asymmetric reactions catalyzed by chiral amines.	181
Figure 5.4. Suggested TS for the proline-catalyzed aldol reaction (5.7) and oxazepane-based potential organocatalysts featuring a secondary amine (5.8), an amino acid (5.9) and diphenyl(trimethylsilyl)oxy amine (5.10).	183
Figure 5.5. 4-oxa-1-azabicyclo[4.1.0]heptane scaffolds of interest as tertiary amine organocatalysts in the asymmetric dihydroxylation reaction.....	194
Figure 5.6. Heterodimer (5.55) and homodimer (5.56).	199
Figure 5.7. Pseudo-enantiomeric structures of carbohydrates.	201
Figure 5.8. a) Predicted selective mannose-based amino alcohol 5.60 and predicted less selective glucose-based amino alcohol 5.61; b) ACE output of highly structured transition state of diethylzinc addition to benzaldehyde using 5.60 as an organocatalyst.	203
Figure 6.1. Synthetic versatility of 1,4-oxazepanes.....	221
Figure 6.2. Potential sulfonamide protecting group.....	222

Table of schemes

Scheme 1.1. Generally accepted mechanism of halofunctionalization.....	1
Scheme 1.2. Proposed mechanism of alkene-to-alkene transfer of bromiranium ion leading to stereochemistry scrambling	2
Scheme 1.3. Intramolecular halocycloetherification	4
Scheme 1.4. Hypothetical depiction of a 4- <i>endo-trig</i> cyclization.	5
Scheme 1.5. 3- <i>exo-trig</i> chlorocycloetherification of 2-cycloalkenols via a boat-like transition state.	7
Scheme 1.6. Stereochemical differences in bromoepoxides formed through a) dibromination-S _N 2 sequence reaction and b) direct epoxidation from bromiranium ion. (<i>E</i>)-olefin: R ₁ = CH ₃ , R ₂ = H; (<i>Z</i>)-olefin: R ₁ = H, R ₂ = CH ₃	8
Scheme 1.7. Oxetane synthesis by 4- <i>exo</i> halocycloetherification.	11
Scheme 1.8. 4- <i>exo-trig</i> bromocycloetherification of oxanorbornene derivative 1.39 to synthesize oxetane 1.40.	13
Scheme 1.9. Oxetane formation through silicon-directed 4- <i>exo</i> bromocycloetherification.	13

Scheme 1.10. Synthesis of [2.2.0] fused ketal by iodocycloetherification.	15
Scheme 1.11. Competing a) 4- <i>exo</i> cyclization and b) iodonium opening mechanisms to give 1.58.	16
Scheme 1.12. 4- <i>exo-trig</i> cyclization of 1.59 with I ₂ /HTIB to give oxetane 1.60.	17
Scheme 1.13. Stereochemical course of 5- <i>exo</i> halocycloetherification.....	20
Scheme 1.14. Enantiomeric synthesis of polysubstituted tetrahydrofurans.	22
Scheme 1.15. Synthesis of pentalenofurane compounds by haloetherification.....	23
Scheme 1.16. Formation of bromomethyltetrahydrofuran through 5- <i>exo</i> bromocycloetherification of <i>n</i> -pentenylglycosides.	24
Scheme 1.17. Discrimination of cyclic and acyclic prochiral dienes.	26
Scheme 1.18. a) Catalytic cycle of desymmetrizing <i>meso</i> -diols using norbornene derived aldehydes; b) olefin selectivity of haloetherification reaction.	27
Scheme 1.19. Desymmetrization of symmetric alkenediols via Ti-catalyzed iodocycloetherification.	30
Scheme 1.20. Iodocycloetherification of γ -hydroxy- <i>cis</i> -alkenes using salen-metal complexes and NCS.....	31
Scheme 1.21. Asymmetric iodocycloetherification of γ -hydroxyalkenes in the presence of (<i>R</i>)- BINOL-Ti(IV) complex.....	31
Scheme 1.22. Chiral phosphoric acid catalysts to make asymmetric haliranium ions as reported by a) Hennecke and b) Shi.	33
Scheme 1.23. Stereochemical consequences of a) (<i>Z</i>)-configuration and b) (<i>E</i>)-configuration olefin geometry on the halocycloetherification of symmetric alkenediols.	35
Scheme 1.24. Desymmetrization of olefinic 1,3-diols using a) C ₂ -symmetric sulfide catalysts and b) quinidine derived catalyst.	36
Scheme 1.25. Deconjugative aldol-iodocycloetherification sequence reaction to make polysubstituted tetrahydrofurans.....	38
Scheme 1.26. Competition between 6- <i>exo</i> lactoization and 5- <i>endo</i> etherification, R ₁ = H, SiR ₃ . 41	
Scheme 1.27. 5- <i>endo</i> iodocycloetherification of 1.163a and 1.163b.....	44
Scheme 1.28. a) Formation of <i>trans</i> -2,5-disubstituted tetrahydrofuran via 5- <i>exo</i> iodocycloetherification, b) formation of <i>cis</i> -2,6-disubstituted tetrahydropyran via 6- <i>exo</i> iodocycloetherification and c) the stereochemical explanation of those cyclizations.	47

Scheme 1.29. Formation of spiroketals through a 5- <i>exo</i> -6- <i>exo</i> double iodocycloetherification sequence.....	48
Scheme 1.30. Transition states and selectivity of iodocycloetherification of <i>trans</i> -1.186 and <i>cis</i> -1.186.....	50
Scheme 1.31. Synthesis of attenol A (1.194) using 6- <i>exo</i> iodocycloetherification as a protecting group for a 5-alken-1-ol fragment.....	52
Scheme 1.32. Substrate-controlled enantioselective 6- <i>exo</i> iodocycloetherification reaction to make the A-ring in the total synthesis of (+)-Lasonolide (1.198).	53
Scheme 1.33. Nicolaou's total synthesis of (+)-azaspriacid-1 (1.201) utilizing a 6- <i>exo</i> iodocycloetherification at a late stage in the synthesis.	54
Scheme 1.34. 6- <i>endo</i> bromocycloetherification of polyenes using TBCO.	55
Scheme 1.35. Diastereoselective 6- <i>endo</i> synthesis of tetrahydropyrans and subsequent stereospecific ring contraction to <i>trans</i> -2,5-disubstituted tetrahydrofurans.	56
Scheme 1.36. Kinetic and thermodynamic control of iodocycloetherification. Conditions: a) I ₂ , THF, H ₂ O, 25 °C, 96 h; b) NIS, CH ₂ Cl ₂ , NaHCO ₃ , 0 °C, 3 h.	58
Scheme 1.37. Stereoselective 6- <i>endo</i> iodocycloetherification in the synthesis and efforts towards the confirmation of the revised structure of waol A (1.218).....	60
Scheme 1.38. Synthesis of a tricyclic ring structure via 6- <i>endo</i> iodocycloetherification.....	61
Scheme 2.1. a) Synthesis of oxazepanes by ring expansion as reported by Kaneko, <i>et al.</i> , b) platinum-catalyzed synthesis of fused bicyclic oxazepane containing acetals as reported by Diéguez-Vásquez, <i>et al.</i> and c) synthesis of 1,4-oxazepanes from Garner aldehydes as reported by Panda, <i>et al.</i>	69
Scheme 2.2. Synthesis of 1,4-oxazepanes 2.14 from carbonates 2.12 and dinucleophiles 2.13. .	70
Scheme 2.3. Synthesis of chiral substituted oxazepanes from 1) Gharpure and Prasad, b) Bode and coworkers and c) Brady and Carreria.	72
Scheme 2.4. Synthesis of 2.30 via a coupling, cyclization, reduction sequence of reactions.	73
Scheme 2.5. Lewis acid mediated synthesis of 1,4-oxazepanes from a) alkenols and b) oxiranols.	73
Scheme 3.1. Synthesis of 1,4-oxazepane 3.8 from a chiral enamine precursor.....	113
Scheme 3.2. Regioselectivity of aminoalkylation using monosubstituted epoxide.....	114
Scheme 3.3. One-pot stereoselective synthesis of 3.18.	114

Scheme 3.4. Enantioselective synthesis of a) Reboxetine (3.19) and b) carnitine acetyltransferase inhibitor (3.22) using NBS-induced electrophilic multicomponent synthesis.....	115
Scheme 3.5. Selenocycloetherification of perhydrobenzoxazines 3.23 induced by benzeneselenyl chloride to make 1,4-oxazepanes 3.24a,b. $R_1 = R_5 = H$, $R_2 = CH_3$ or H , $R_3 = CH_3$ or Ph , $R_4 = H$ or Ph	116
Scheme 3.6. Hypervalent-iodine-mediated 6- <i>exo</i> cyclization to synthesize 2,3,6-trisubstituted morpholines.....	117
Scheme 3.7. Regioselectivity of 2.42a.....	121
Scheme 3.8. Regioselectivity of 2.43b.....	122
Scheme 3.9. Competition of regioselectivity between 2.42j and 2.43j.....	123
Scheme 5.1. Catalytic cycle for Diels-Alder cycloadditions catalyzed by secondary amines operating via an iminium catalysis generic mode of activation.....	182
Scheme 5.2. Efforts to remove sulfonamide protecting groups via a deprotection-protection strategy.....	185
Scheme 5.3. a) Boc-deprotection and b) Bn deprotection attempt.	186
Scheme 5.4. Fluoride-mediated rearrangement of 5.15 to morpholine 5.17.	187
Scheme 5.5. Attempt to synthesize 5.10 by introducing diphenyl addition to the synthesis at an early stage.	188
Scheme 5.6. Attempt to synthesize 5.10 by introducing diphenyl addition to the synthesis at a middle stage.	189
Scheme 5.7. Attempt to remove sulfonamide protecting group and isolate 5.9-HCl.	190
Scheme 5.8. Catalytic cycle of asymmetric dihydroxylation with $K_3Fe(CN)_6$ as the co-oxidant.	194
Scheme 5.9. Amino alcohol organocatalyzed diethylzinc addition to benzaldehyde.....	196
Scheme 5.10. DAIB-catalyzed diethylzinc addition to aryl aldehydes.	197
Scheme 5.11. Catalytic cycle diethylzinc addition to benzaldehyde as catalyzed by DAIB (applies generally to amino alcohols).....	198
Scheme 5.12. Ester reduction.....	199
Scheme 5.13. Organocatalyzed diethylzinc addition to benzaldehyde using carbohydrate-based amino alcohol 5.59.....	201
Scheme 5.14. Retrosynthetic analysis of 5.60.	204

Scheme 5.15. Retrosynthetic analysis of 5.61.	205
Scheme 5.16. Benzylidene protection of 5.69.	205
Scheme 5.17. Triflation of C2 hydroxyl to give 5.67 followed by S _N 2 displacement of triflate by NaN ₃ to give 5.66.	206
Scheme 5.18. Reduction of azide 5.66 to amine 5.65 using a) PPh ₃ and b) LiAlH ₄	206
Scheme 5.19. a) Over-alkylation of 5.72 using MeI and b) Esweiler-Clarke reaction to yield 5.71.	207
Scheme 5.20. Fischer glycosylation to yield 5.74 followed by subsequent benzylidene protection to afford 5.73.	207
Scheme 5.21. Deacetylation of 5.73 followed by over-alkylation of 5.72 using MeI or alternative Eschweiler-Clarke conditions to successfully yield 5.71.	208

Table of tables

Table 1.1. Enantiospecificity of acetolysis	3
Table 1.2. Baldwin's Rules	4
Table 1.3. Iodocycloetherification of allyl alcohols with I(coll) ₂ ClO ₄	9
Table 1.4. Substrate variation in the enantioselective 3- <i>exo</i> iodocycloetherification of allyl alcohols.	10
Table 1.5. 4- <i>exo-trig</i> iodocycloetherification of homoallylic alcohols with I(coll) ₂ ClO ₄ to synthesize oxetanes as reported by Schauble <i>et al.</i>	12
Table 1.6. Reaction of cinnamyl alcohols with Br(coll) ₂ PF ₆ to make oxetanes.	18
Table 1.7. Synthesis of oxetanes by 4- <i>endo-trig</i> bromocycloetherification. ^a	19
Table 1.8. Iodocycloetherifications of 4-penen-1,3-diols.	21
Table 1.9. Acetal expansion via halofunctionalization to make chiral 1,4-diols.	25
Table 1.10. Iodocycloetherification of ene ketals.	28
Table 1.11. Lewis base catalyzed bromo- and iodocycloetherification of alkenols.	29
Table 1.12. Bromocycloetherification using Lewis base/chiral Brønsted acid cooperative catalysis	32
Table 1.13. Diastereoselective 5- <i>endo</i> iodocycloetherification to make <i>trans</i> -2,5-disubstituted tetrahydrofurans. ^a	37
Table 1.14. Enantioselective 5- <i>endo</i> iodocycloetherification using Evans auxiliary. ^a	39

Table 1.15. Iodocycloetherification of 3-alkene-1,2-diols and derivatives.	42
Table 1.16. Scope of catalytic asymmetric 5- <i>endo</i> chlorocycloetherification of homoallylic alcohols.	45
Table 1.17. Acetal expansion via halofunctionalization to make chiral 1,4-diols.	48
Table 1.18. Substrate effect on Pd(II)-catalyzed iodocycloetherification.	51
Table 1.19. Effects of chiral auxiliaries on the stereoselectivity of 6- <i>endo</i> bromocycloetherification of enamides.	57
Table 2.1. One-pot synthesis of 1,4-oxazepanes via ring-opening of aziridines and azetidines. .	70
Table 2.2. <i>N</i> -Ts protection and alkylation.	75
Table 2.3. Oxazepanes by haloetherification of <i>N</i> -Ts protected derivatives.	78
Table 2.4. Condition optimization.	80
Table 2.5. <i>N</i> -Ns protection and alkylation.	81
Table 2.6. Oxazepanes by haloetherification of <i>N</i> -Ns protected derivatives.	84
Table 3.1. Rationale for diastereoselectivity.	117
Table 3.2. Baldwin's rules	120
Table 3.3. NOESY signals used to ascertain the stereochemistry	126
Table 4.1. Reaction condition evaluation.	153
Table 4.2. Substrate screen.	160
Table 5.1. Efforts to remove sulfonamide protecting group directly. ^a	184
Table 5.2. Attempts to install diphenyl onto methyl ester via Grignard reaction.	187
Table 5.3. Ester hydrolysis.	189
Table 5.4. Organocatalyzed Diels-Alder reaction condition screen.	191
Table 5.5. Preliminary attempts of using 5.8a,b as organocatalysts for aldol reactions. ^a	192
Table 5.6. Asymmetric dihydroxylation.	195
Table 5.7. Organocatalyzed diethylzinc addition to benzaldehyde using 5.58a,b. ^a	200

List of abbreviations

Ac	acetyl
ACE	Asymmetric Catalyst Evaluation
AD	asymmetric dihydroxylation
Aux	auxiliary
BINOL	1,1'-bi-2-naphthol
Bn	benzyl
Boc	<i>tert</i> -butyloxycarbonyl
bs	broad singlet
Bz	benzoyl
CAM	ceric ammonium molybdate
Cbz	carboxybenzyl
coll	2,3,5-collidine
COSY	correlation spectroscopy
CPU	central processing unit
CSA	10-camphorsulfonic acid
Cy	cyclohexyl
d	doublet
DABCO	1,4-diazabicyclo[2.2.2]octane
DAIB	(dimethylamino)isoborneol
DFT	density functional theory
DIB	[diacetoxyiodo]benzene
DMAP	4-dimethylaminopyridine
DMF	dimethyl formamide
DMSO	dimethyl sulfoxide
dppf	1,1'-bis(diphenylphosphino)ferrocene
dr	diastereomeric ratio
ee	enantiomeric excess
er	enantiomeric ratio
es	enantiospecificity
ESI-QTOF	electrospray ionization quadrupole/time-of-flight

Et	ethyl
EtOAc	ethyl acetate
EWG	electron withdrawing group
FTIR	Fourier transformed infrared spectroscopy
HFIP	hexafluoro-2-propanol
HMBC	heteronuclear multiple bond correlation spectroscopy
HMPTA	hexamethylphosphoramide
HPLC	high performance liquid chromatography
HRMS	high resolution mass spectrometry
HSQC	heteronuclear single quantum correlation spectroscopy
HTIB	[hydroxy(tosyloxy)iodo]benzene
ⁱ Pr	<i>iso</i> -propyl
IR	infrared
J	coupling constant
LAH	lithium aluminum hydride
LB	Lewis base
LDA	lithium diisopropylamide
LiHMDS	lithium bis(trimethylsilyl)amide
LUMO	lowest unoccupied molecular orbital
m	multiplet
Me	methyl
MM	molecular mechanics
MOM	methyl methyl ether
MS	molecular sieves
Ms	mesyl
NaHMDS	sodium bis(trimethylsilyl)amide
NBP	<i>N</i> -bromophthalimide
NBS	<i>N</i> -bromosuccinimide
ⁿ Bu	<i>n</i> -butyl
NCS	<i>N</i> -chlorosuccinimide
NIS	<i>N</i> -iodosuccinimide

NMO	<i>N</i> -methylmorpholine <i>N</i> -oxide
NMR	nuclear magnetic resonance
NOE	nuclear Overhauser effect
NOESY	nuclear Overhauser effect spectroscopy
ⁿ Pr	<i>n</i> -propyl
Ns	nosyl
PCM	polarizable continuum model
PES	potential energy surface
PG	protecting group
Piv	trimethylacetyl (pivaloyl)
PMB	<i>para</i> -methoxybenzyl
Pro	proline
PTSA	<i>para</i> -toluenesulfonic acid
Pyr	pyridine
q	quartet
rt	room temperature
s	singlet
t	triplet
TBABr	tetrabutylammonium bromide
TBACl	tetrabutylammonium chloride
TBAF	tetrabutylammonium fluoride
TBAI	tetrabutylammonium iodide
TBCO	2,4,4,6-tetrabromo-2,5-cyclohexadienone
TBDPS	<i>tert</i> -butyldiphenylsilyl
TBS	<i>tert</i> -butylsilyl
^t Bu	<i>tert</i> -butyl
Teoc	2-trimethylsilylethyl carbamate
Tf	triflate
TFA	trifluoroacetic acid
THF	tetrahydrofuran
TLC	thin layer chromatography

TMS	trimethylsilyl
TS	transition state
Ts	tosyl

Contribution(s) of authors

This thesis contains 6 original chapters. Chapters 2 and 3 are published material. Chapters 1 and 4 are drafts which we plan on submitting for publication.

Professor Nicolas Moitessier, as my supervisor, is a co-author and contributor on all the articles presented here.

Chapter 1: I reviewed the field of synthesis of small & medium sized heterocycles by haliranium-mediated cyclization.

Chapter 2: I made most of the molecules presented in this chapter with the assistance of undergraduate student Michael Cueto. Synthesis and characterization of four compounds presented was done by Dr. Sylvestre Toumieux and some preliminary work on the synthetic method was done by Dr. Sylvestre Toumieux and Dr. Rana Bilbeisi.

Chapter 3: I strategically planned the substrate scope to investigate the mechanism. I synthesized, characterized and assigned the structure of all the compounds in this chapter. Any computational work presented was carried out by Dr. Joshua Pottel.

Chapter 4: I synthesized and characterized all of the compounds in this chapter. I strategically planned the substrate scope to investigate the mechanism. Any crystal structures presented were obtained by Igor Huskic. Any computational mechanistic studies presented were carried out by Anna Tomberg.

Chapter 5: I made most of the molecules presented in this chapter. Preliminary investigations into methods of sulfonamide deprotection were aided significantly by Jonathan O'Mondays. Any X-ray crystal structures presented were done by Igor Huskic. The aldol catalysis presented was

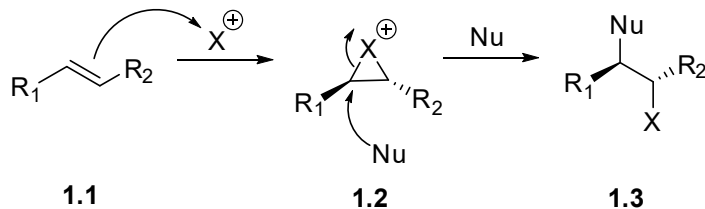
done by Tazkia Hassan as part of an undergraduate honours project. Calculations done using ACE were performed by Professor Nicolas Moitessier and Mihai Burai Patrascu.

Chapter 6: I wrote the conclusion and future perspective.

Chapter 1 Synthesis of small & medium sized heterocycles by haliranium-mediated cyclization

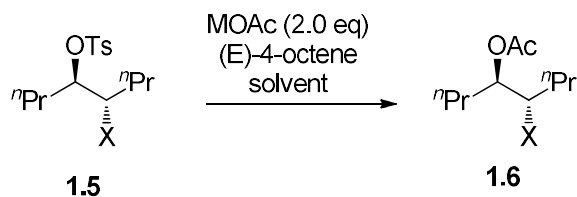
1.1 Halofunctionalization

Halofunctionalizations of olefins, whereby a haliranium ion is formed from an electrophilic halogen source and an olefin, then subsequently opened by nucleophilic attack, is a simple reaction and one of the oldest, most well-known in the synthetic chemist's toolbox, being used for more than 150 years.¹ The first mechanism involving a haliranium ion was proposed by Roberts and Kimball in 1937² and haliranium ions based on chlorine, bromine and iodine were first characterized by Olah *et al.* in 1967.³ Scheme 1.1 shows the generally accepted mechanism of electrophilic halofunctionalization of alkenes: a 3-membered haliranium ion is formed between the alkene and the electrophilic halogen source followed by a stereospecific attack of a nucleophile in an S_N2 manner to give diastereomeric products with the halide and the newly introduced nucleophile in an *anti*-relationship. This mechanism is also representative of other ring openings that do not feature a halogen, such as acid catalyzed epoxide opening or seleniranium ion opening.



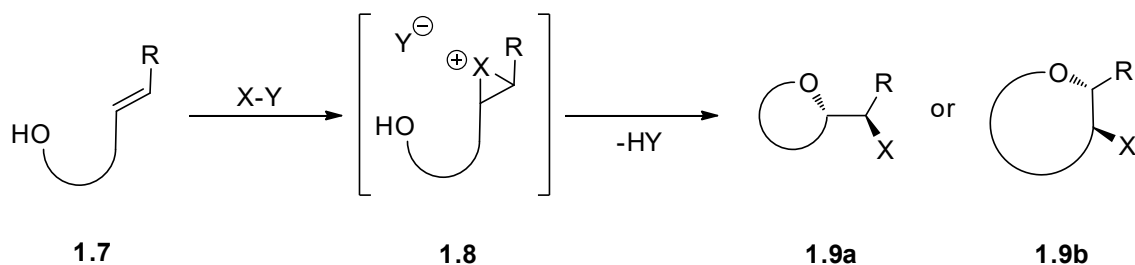
Scheme 1.1. Generally accepted mechanism of halofunctionalization

For clarity, some nomenclature will be covered here at the onset of this review. Hypercoordinate group 17 cations are called halonium ions; however, the special case of cyclic halonium ions falls under the nomenclature of ring compounds, meaning that 3-membered halonium ions, the focus of this review, are termed haliranium ions. On the other hand, hypocoordinate group 17 cations are referred to as halenium ions (Figure 1.1).

Table 1.1. Enantiospecificity of acetolysis

Entry	X	M	Eq. of (<i>E</i>)-4-octene	Solvent	es (%)
1	Br	Na	0	HFIP	100
2	Br	Na	1	HFIP	28
3	Br	ⁿ Bu ₄ N	1	HFIP	81
4	Cl	ⁿ Bu ₄ N	1	HFIP/CH ₂ Cl ₂	100

Halofunctionalization of alkenes affords materials such as halolactones, halolactams, haloethers, haloamines, halohydrins or dihalides that are either themselves useful (such as bioactive or natural products) or are intermediates with good handles for additional functionalization. The importance of such reactivity is highlighted by the thousands of naturally occurring organohalogen compounds that are the result of one or more halocyclization reaction.¹⁸ The entire chemical space of this reactivity is obviously outside the scope of this thesis. Specifically, the process of halocycloetherification will be discussed herein whereby a haliranium ion, formed from an electrophilic halogen and an olefin, is attacked intramolecularly by a pendent alcohol to make small to medium sized heterocycles, specifically 3- to 6-membered rings (Scheme 1.3). The literature will be presented based on the size of the ring that is being formed and the mode of cyclization. The review will not be exhaustive but rather representative examples will be presented that were important contributions to the field for their synthetic utility or the scientific insight they provided. The discussion involving the formation of 7-membered rings will not be included here but rather in the introduction of Chapter 3.



Scheme 1.3. Intramolecular halocycloetherification

1.2 Baldwin's rules

When one thinks of intramolecular cyclization, the first thought is of Baldwin's rules.¹⁹ The rules, presented in Table 1.2, classify ring closure and its subsequent naming into three categories: 1) the number of atoms in the newly formed ring, 2) *endo* or *exo* depending on if the bond breaking during the reaction is internal or external to the newly formed ring, respectively, and 3) *tet*, *trig* or *dig* depending on if the hybridization of the atom being attacked is sp^3 , sp^2 or sp , respectively. For example, as can be seen in Figure 1.2, if the alcohol of **1.10** attacks the olefin it will form a 5-membered ring, the remaining sigma bond of the olefin will be part of the newly formed ring and the hybridization at the olefin is sp^2 so this cyclization is *5-endo-trig* (**1.11**, Figure 1.2, red). If the alcohol attacks the carbonyl it will still form a 5-membered ring, the carbonyl bond is outside of the newly formed ring and the hybridization at the carbonyl is sp^2 so this cyclization is *5-exo-trig* (**1.12**, Figure 1.2, blue). Baldwin's rules tell us that *5-exo-trig* is favoured over *5-endo-trig* and indeed, under simple conditions, one would expect see significant or even exclusive preference for **1.12**.²⁰

Table 1.2. Baldwin's Rules

	3		4		5		6		7	
	<i>Exo</i>	<i>Endo</i>								
Tet	✓		✓		✓	✗	✓	✗	✓	✗
Trig	✓	✗	✓	✗	✓	✗	✓	✓	✓	✓
Dig	✗	✓	✗	✓	✓	✓	✓	✓	✓	✓

Check mark = favoured; X = disfavoured

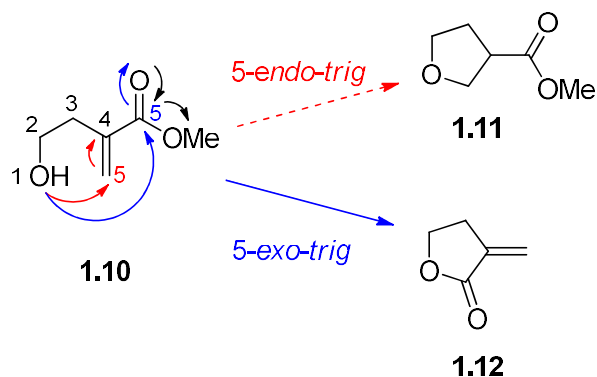
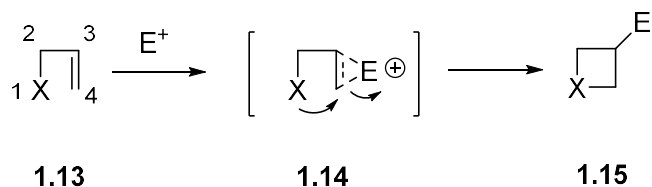


Figure 1.2. Baldwin's rules for ring closure.

The problem with Baldwin's rules, and particularly the naming system that accompanies them, is that they tend to be ambiguous when haliranium ions are involved, or really when any non-acyclic substrate undergoes a cyclization reaction.



Scheme 1.4. Hypothetical depiction of a 4-endo-trig cyclization.

Let us consider the hypothetical, formally 4-endo-trig cyclization depicted in Scheme 1.4. This reaction is mediated by an electrophilic halogen (or other electrophilic reagent) forming a haliranium ion from the olefin. The hybridization of the atom being attacked is now not strictly an sp^2 atom but is more sp^3 -like so does this cyclization follow the rules for *trig* or *tet* cyclization? Additionally, the bond being broken during the formation of the ring is now the $C4-E^+$ σ -bond, not the olefin π -bond, which would already be broken from formation of the haliranium ion. This $C4-E^+$ bond is *exo* to the newly formed ring so is this cyclization considered a 4-*exo-tet* or a 4-*endo-trig*? What if X cyclized onto C3 instead of C4? The bond breaking would now be either $C3-E^+$ when considering the intermediate structure or the olefin bond when considering the overall reaction. Would that cyclization be considered 3-*exo-tet* or 3-*exo-trig*? If cyclization to the 3-membered ring was competitive with 4-membered ring formation, the rules to be considered may not be as straight forward as 4-*endo-trig* vs 3-*exo-trig* as one would expect looking at the overall formal transformation.

The problem becomes even more confusing when starting from an already cyclic structure such as **1.16**. Under halogenating conditions, a haliranium ion forms, causing an ambiguity in the hybridization of the atoms being attacked by the intramolecular nucleophile. Additionally, when considering the newly formed bridged bicycles, it's unclear which type of reaction occurred. In the instance of **1.18a**, was the cyclization 5-*exo* or 5-*endo*? Similarly, in **1.18b**, would the cyclization be 4-*exo* or 6-*endo*?

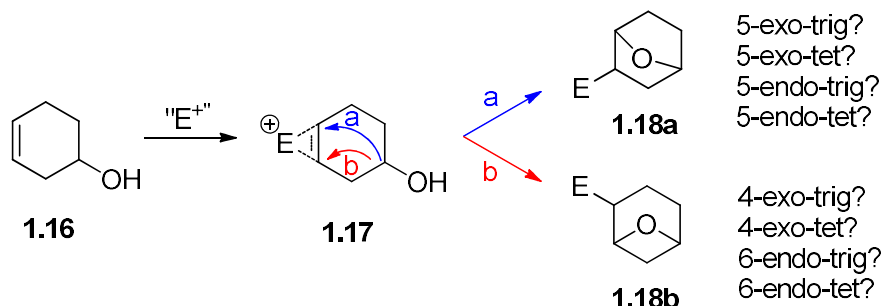


Figure 1.3. Ambiguity of naming system accompanying the cyclization of a cyclic precursor (1.16) to give bridged bicycles (1.18a and 1.18b).

This inherent confusion associated with such a naming system is still an unsolved problem. To clarify this inconsistency, in the literature review of halocycloetherification reactions that follows, reactions will be divided into the size of the rings formed and also into *exo* and *endo* modes of cyclization as they would be *formally* defined overall. In cases that have no obvious formal definition, the classification of the mode of cyclization will be clearly identified.

1.3 Intramolecular halocycloetherification

While the following review will be divided based on ring size and cyclization mode, there will not be distinctions made between reactions that are chloro-, bromo- or iodocycloetherification reactions, rather the presentation will be more or less chronological within each section. It is worth noting here that to the best of our knowledge, while there is some excellent work on asymmetric fluorocycloetherifications in the literature, it has been shown that mechanistically they do not go through a fluoriranium ion and so they will not be included here.²¹⁻²³ In fact, to the best of our knowledge to date, the existence of a 3-membered fluoriranium was confirmed in the gas phase by a neutral product analysis of a mass spectrometry experiment that conclusively showed fluorine shifts.²⁴ No other cyclic fluoronium ions had been observed until 2013 and even then, they were

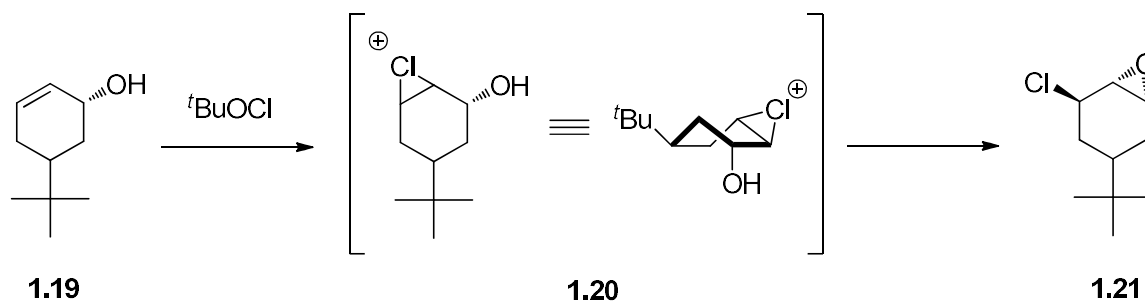
very short-lived entities and were reported in 5- or 6-membered rings, not the much more strained 3-membered ring.^{25,26}

The presence of chlorocycloetherification in the literature is also relatively less common, although there are some examples that will be highlighted in the sections below. The majority of the work presented will focus on bromo- and iodocycloetherifications.

1.3.1 3-*exo* halocycloetherification

Reports of 3-*exo* halocycloetherifications are chiefly absent in the literature. Some early reports of this type of cyclization were either very low-yielding or were side products in other reactions.^{27,28}

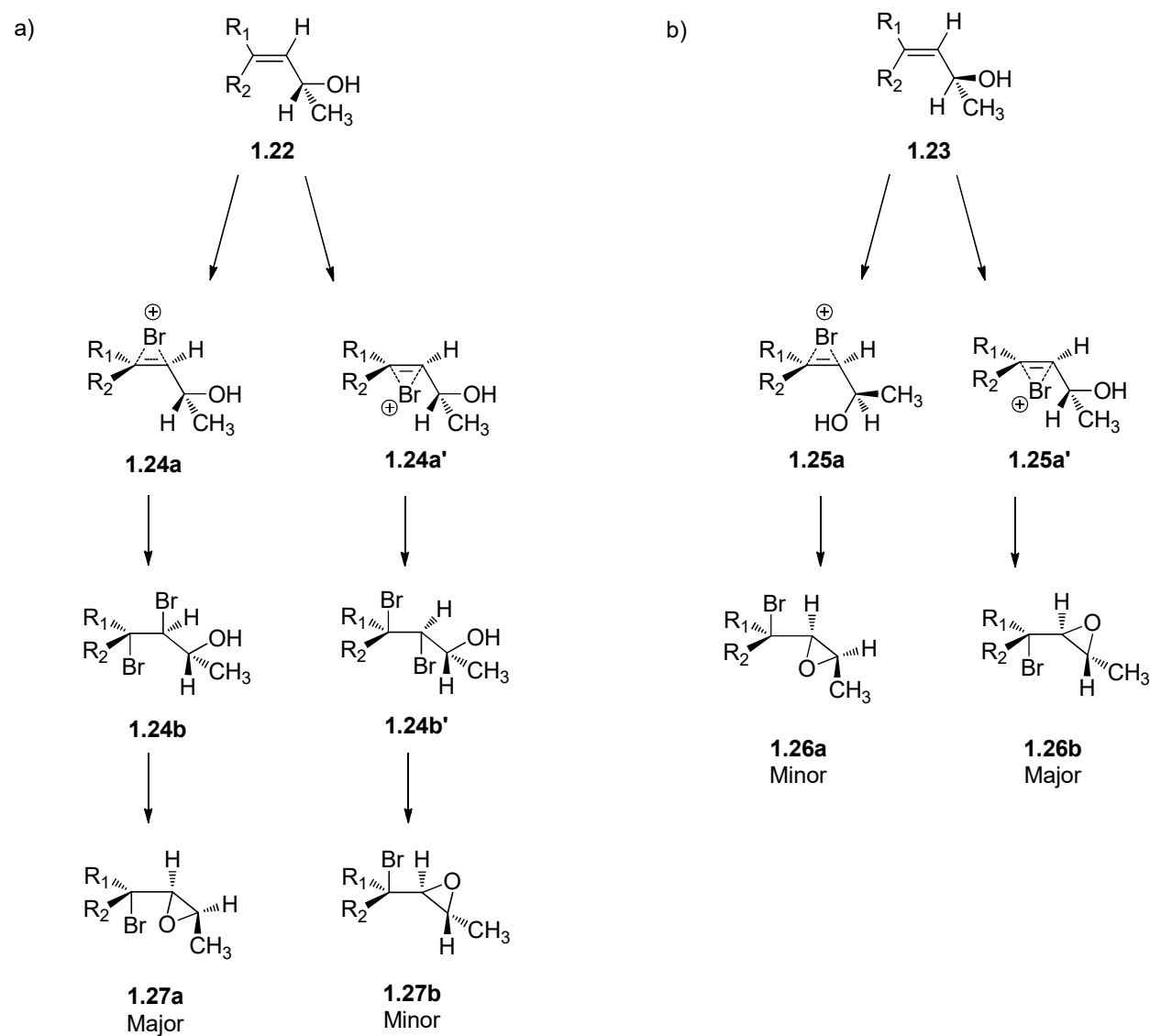
To the best of our knowledge, the first report that investigated this cyclization to any extent was from Ganem in 1976.²⁹ He reported the stereospecific synthesis of haloepoxides from 2-cycloalkenols through a haliranium intermediate under conditions where the electrophile has a non-nucleophilic counterion. He proposed that the intermediate haliranium must adopt an unfavourable boat conformation to undergo *trans*-diaxial ring opening (Scheme 1.5).



Scheme 1.5. 3-*exo-trig* chlorocycloetherification of 2-cycloalkenols via a boat-like transition state.

In 1981, Midland and Halterman reported what appeared to be a formally 3-*exo-trig* cyclization.³⁰ They investigated the mechanism of this reaction by reasoning the stereochemistry of the bromoepoxide products they obtained relative to the geometry of the starting olefin. If the reaction went only through formation of the dibromide species followed by $\text{S}_{\text{N}}2$ displacement of proximal bromide by alcohol, then a (*Z*)-olefin would give an (*E*)-epoxide and an (*E*)-olefin would give a (*Z*)-epoxide (Scheme 1.6a). Alternatively, if the mechanism were to go through direct attack of the alcohol onto the bromiranium ion, then both olefins would give (*E*)-epoxides that would

only differ at the stereochemistry of the bromide center (Scheme 1.6b). They concluded through experiment that direct attack of the bromiranium was the mechanism of action.

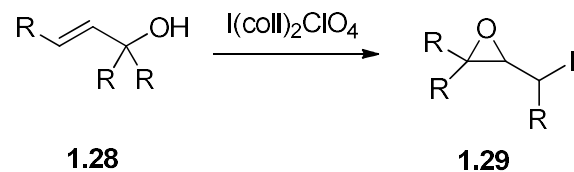


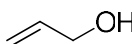
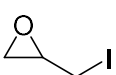
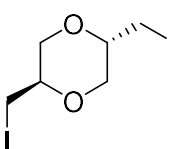
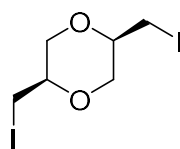
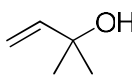
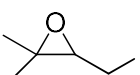
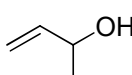
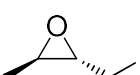
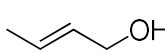
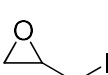
Scheme 1.6. Stereochemical differences in bromoepoxides formed through a) dibromination- S_N2 sequence reaction and b) direct epoxidation from bromiranium ion. (*E*)-olefin: $R_1 = \text{CH}_3$, $R_2 = \text{H}$; (*Z*)-olefin: $R_1 = \text{H}$, $R_2 = \text{CH}_3$.

The field was expanded upon in 1988 by Schauble and coworkers when they reported halocycloetherifications to make a variety of different size rings, arguably the most interesting of which was the synthesis of oxiranes and oxetanes (oxetanes will be discussed in Section 1.3.3).³¹ They only reported four examples of oxirane synthesis (Table 1.3). The cyclization of

unsubstituted allyl alcohol was accompanied by the formation of dioxanes (**1.30a**, **1.30a'**), likely from an equivalent of allyl alcohol trapping the reactive iodonium intermediate.

Table 1.3. Iodocycloetherification of allyl alcohols with $I(\text{coll})_2\text{ClO}_4$.

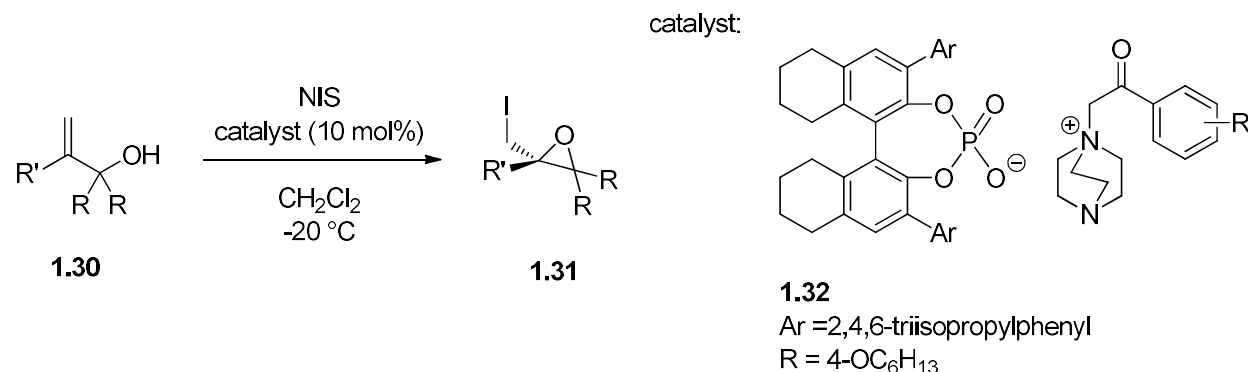


Entry	Allyl Alcohol	Iodoether Product
1	 1.28a	 1.29a 32%  1.29a' 12%  1.29a'' 12%
2	 1.28b	 1.29b 68%
3	 1.28c	 1.29c  1.29c' 71% combined yield (76:24)
4	 1.28d	 1.29d

One of the most recent important breakthroughs in this field was published in 2015 by Xie *et al.* when they reported the first enantioselective 3-*exo-trig* iodocycloetherification reaction.³² They used chiral phosphate and DABCO-derived quaternary ammonium ion pair organocatalysis, albeit their substrate scope utilized both geminal substitution alpha to the reactive alcohol and an aryl on the internal position of the olefin to stabilize cationic charge and favour reactivity at that position. Additionally, this methodology suffered from long reaction times, requiring anywhere

from 21 to 134 h to go to completion. Despite these drawbacks, this reaction proceeded with excellent yields and enantioselectivities with good tolerance to steric and electronic factors in suitable substrates (Table 1.4). This report represents a major step forward in the field of asymmetric catalytic halofunctionalization of olefins to make oxiranes.

Table 1.4. Substrate variation in the enantioselective 3-*exo* iodocycloetherification of allyl alcohols.



Entry	R	R'	Yield ^a	%ee ^b
1	Ph	Me	99	94
2	4-Me-C ₆ H ₄	Me	95	93
3	3-F-C ₆ H ₄	Me	32	86
4	Ph	-(CH ₂) ₄ -	99	97
5	3-Me-C ₆ H ₄	-(CH ₂) ₄ -	84	95
6	3-F-C ₆ H ₄	-(CH ₂) ₄ -	81	96.5
7	Ph	H	41	63
8	Cy	Me	71	37

^a Isolated yields; ^b Determined by chiral HPLC.

1.3.2 3-*endo* halocycloetherification

There are no examples of 3-*endo* cyclization reported in the literature. This is because the required trajectory of 109° (Bürgi–Dunitz angle) is not possible (Figure 1.4).

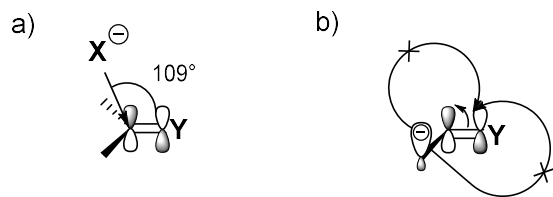
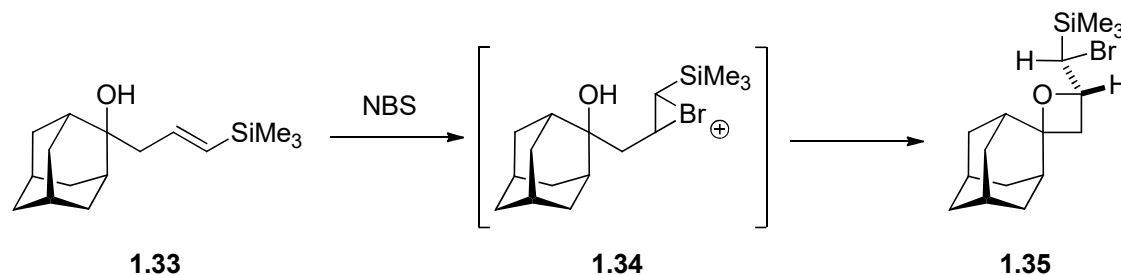


Figure 1.4. a) Bürgi-Dunitz angle of attack of nucleophiles onto olefins required for *trig* cyclizations and b) intramolecular cyclization unable to attack at the correct angle.

1.3.3 4-*exo* halocycloetherification

Oxetanes, 4-membered cyclic ethers, are interesting motifs that can be found in some synthetic and natural products and more intriguingly, also represent a synthetic handle to other heterocyclic compounds through ring expansion and ring opening chemistry, making oxetanes significant motifs to synthesize efficiently.³³

One of the earliest reports of 4-*exo* halocycloetherification was published in 1980 by Ehlinger and Magnus.³⁴ Rather than obtaining the desired 5-*endo* cyclic tetrahydrofuran product, they obtained oxetane **1.35** by a 4-*exo* cyclization (Scheme 1.7). This is the only example they reported and they did not discuss it in any detail.



Scheme 1.7. Oxetane synthesis by 4-*exo* halocycloetherification.

The report of Schauble and coworkers was mentioned above in the context of 3-*exo* cycloetherification reactions.³¹ In the same report, they also synthesized several oxetanes starting from homoallylic alcohols (**1.36**), either because of gem-dialkyl substitution alpha to the alcohol favouring the reactive conformation (Table 1.5, entry 1,3) or because substitution at C3 was enough to render the charge distribution such that C3 was more electrophilic and thereby favouring

oxetane formation (Table 1.5, entry 2). In the case of homoallylic alcohol where both of these phenomena were absent (**1.36d**), the 5-*endo* cyclization was competitive (Table 1.5, entry 4).

Table 1.5. 4-*exo-trig* iodocycloetherification of homoallylic alcohols with I(coll)₂ClO₄ to synthesize oxetanes as reported by Schauble *et al.*

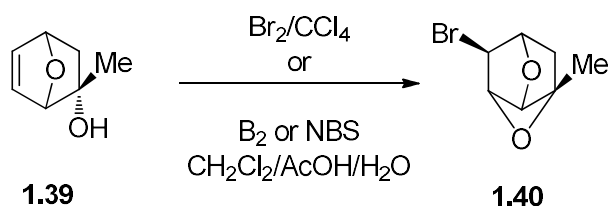
1.36 **1.37**

Entry	Homoallyl Alcohol	Oxetane Product	
1	 1.36a	 1.37a 62%	
2	 1.36b	 1.37b 67%	
3	 1.36c	 1.37c 64%	
4 ^a	 1.36d	 1.37d	 1.38d

^a Inseparable mixture of isomers, 1:1 mole ratio by ¹H NMR.

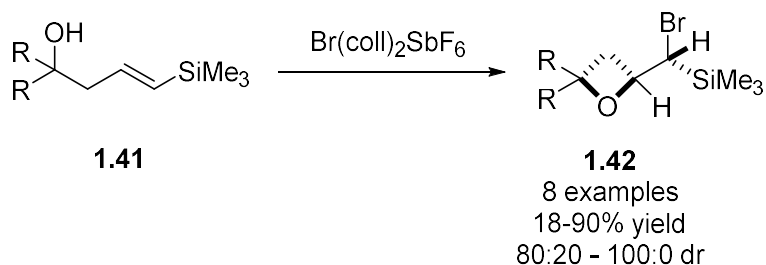
Viso and coworkers also reported a single example of 4-*exo* oxetane formation via bromocycloetherification in a 1989 report where they were examining the differences in reactivity

between norbornene and oxanorbornene, specifically the higher propensity that oxanorbornene has for undergoing intramolecular cyclization reactions with various electrophiles (Scheme 1.8).³⁵



Scheme 1.8. 4-*exo-trig* bromocycloetherification of oxanorbornene derivative **1.39** to synthesize oxetane **1.40**.

A report by Rousseau and coworkers looked into synthesizing oxetanes by 4-*exo* halocycloetherification.³⁶ They had previously reported making oxetanes by 4-*endo* halocycloetherification (will be discussed in Section 1.3.4) and rationalized that the *exo* cyclization should be more facile. They reasoned that vinyl silyl groups on homoallylic alcohols would promote 4-*exo* cyclization via the β -silicon effect and synthesized several oxetane compounds in good yield and diastereoselectivity (Scheme 1.9). They made no mention of 5-*endo* cyclization being competitive.



Scheme 1.9. Oxetane formation through silicon-directed 4-*exo* bromocycloetherification.

The Galatsis group had several publications discussing the formation of oxetanes and tetrahydrofurans via 4-*exo* and 5-*endo* iodocycloetherification, respectively.³⁷⁻³⁹ They reported a deconjugative aldol-cyclization sequence reaction, first in a diastereoselective manner³⁸ and later in an enantioselective fashion using a chiral auxiliary.³⁹ They originally rationalized the stereochemical outcome as simply avoiding $A^{1,3}$ strain (Figure 1.5a,c) however, when employing an unsubstituted olefin substrate, the major product does exhibit minimal $A^{1,3}$ strain so they

adjusted their hypothesis to include possible 1,3-transannular interactions between the iodomethyl and R groups in the developing oxetane ring (Figure 1.5b).

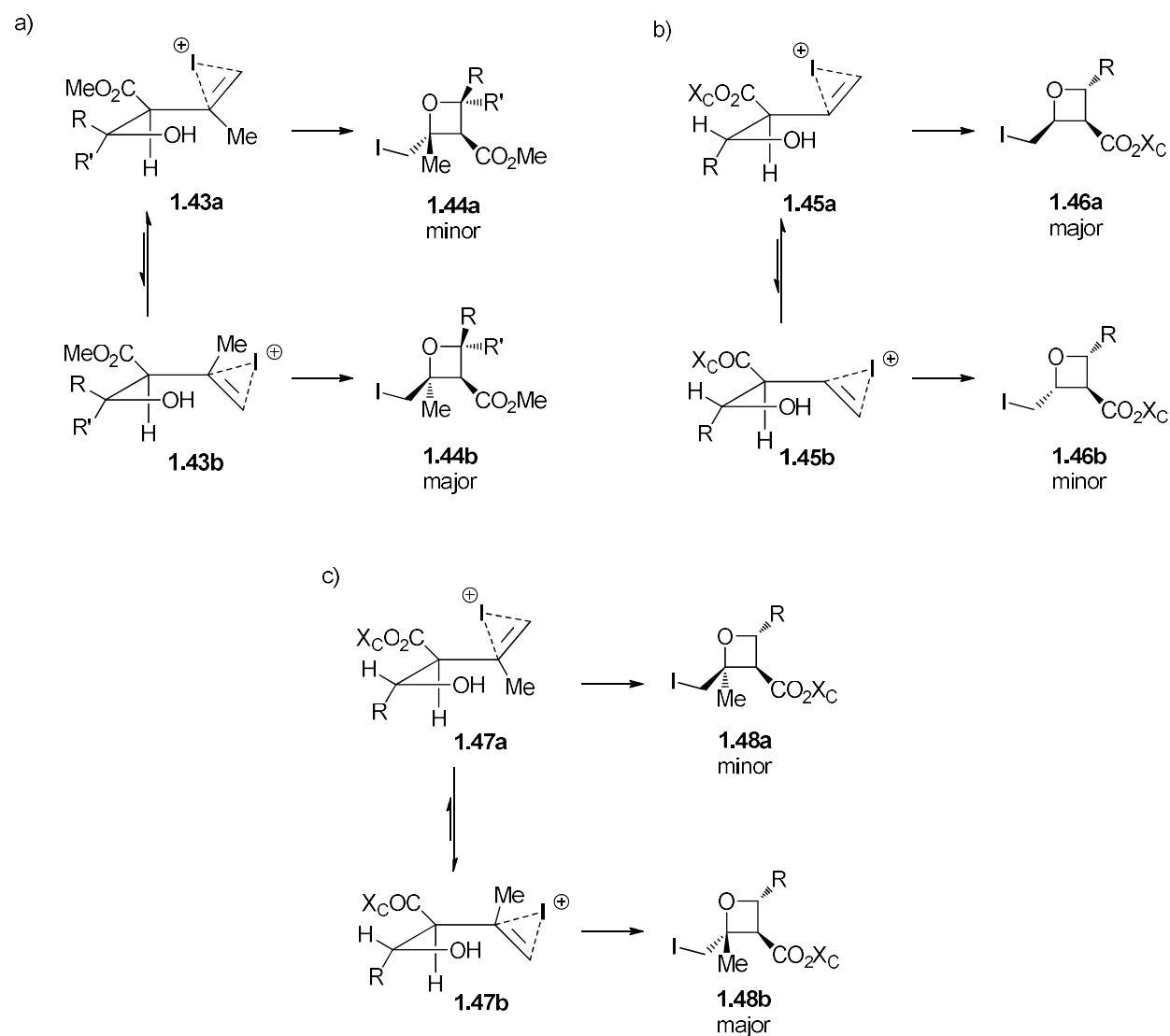
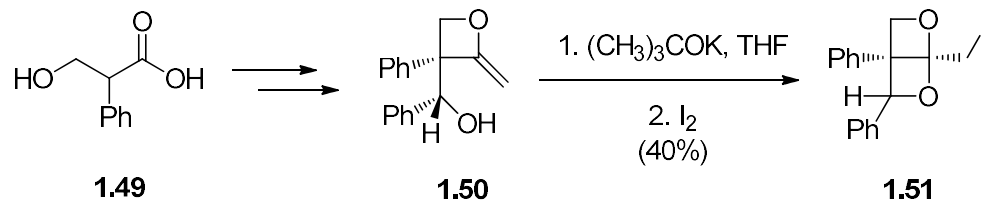


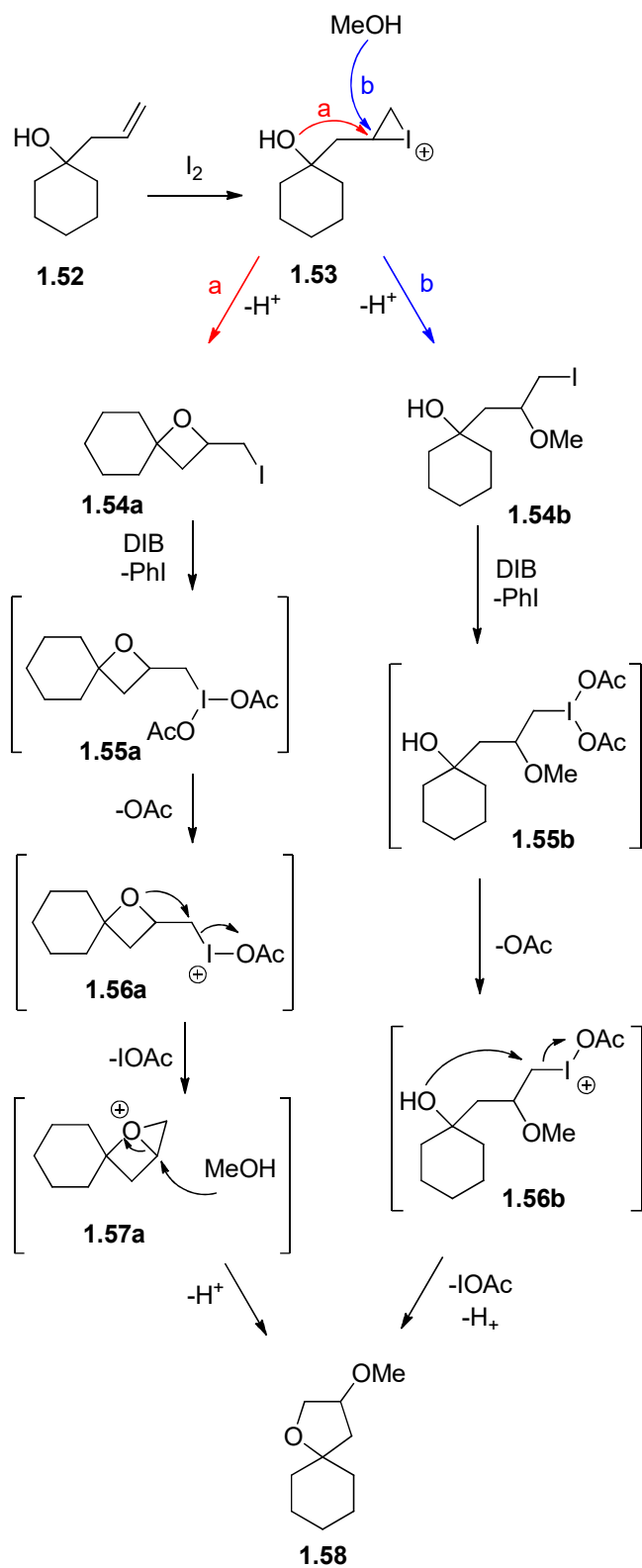
Figure 1.5. Stereochemical model of 4-*exo-trig* iodocycloetherification to make oxetanes in a) a diastereoselective manner and b,c) an enantioselective manner; X_C = Evans auxiliary.

Howell *et al.* published an interesting report in 1999 on the unprecedented synthesis of [2.2.0] fused ketals.⁴⁰ Unfortunately they only present a single example in their report (Scheme 1.10) but this methodology could be of interest in the synthesis of both [*n*.3] spiroketals and [*n*.2.0] fused ketals.



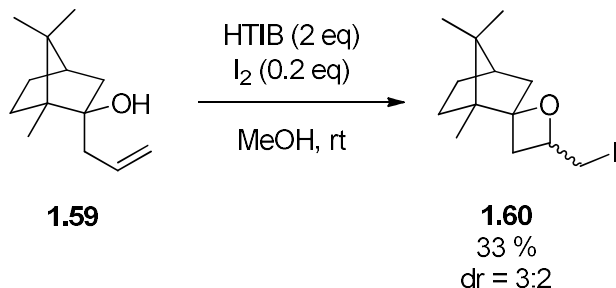
Scheme 1.10. Synthesis of [2.2.0] fused ketal by iodocycloetherification.

Vasconcelos, Silva and Giannis reported an interesting reaction that is overall a *5-endo-trig* cyclization but that goes through two mechanistic pathways, both of which have isolable intermediates and both of which convert after some time to the *5-endo* product **1.58** (Scheme 1.11).⁴¹ One of the intermediates, **1.54b**, is formed from the intermolecular reaction of solvent opening the iodonium. Subsequent oxidation with I(III) gave a good acetoxyiodonium leaving group (**1.55b**) that the alcohol then displaced via a simple S_N2 reaction (**1.56b**) to yield **1.58**. More interesting is the isolable oxetane intermediate **1.54a** formed via *4-exo* cyclization, a product previously reported by Schauble (Table 1.5, entry 3). This compound also underwent iodine oxidation by I(III) (**1.55a**), followed by displacement by the oxetane oxygen to give strained [2.1.0]spirocycle **1.57a** which is easily opened by solvent to relieve ring strain and give the formally *5-endo* product **1.58**.



Scheme 1.11. Competing a) 4-*exo* cyclization and b) iodonium opening mechanisms to give **1.58**.

While most of the substrates they tested continued on the reaction path to the tetrahydrofuran, they did discover one isborneol derivative that awarded only spirooxetane **1.60**, albeit in low yield and poor diastereoselectivity (Scheme 1.12).

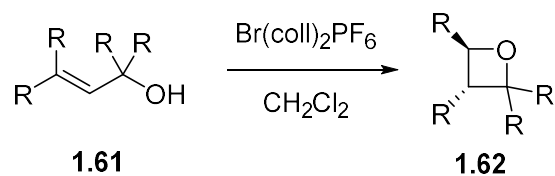


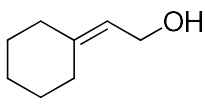
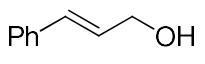
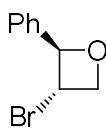
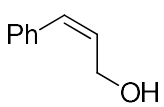
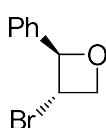
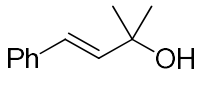
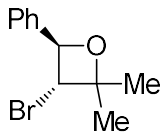
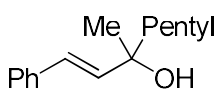
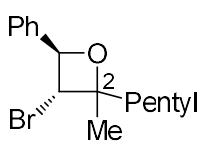
Scheme 1.12. 4-*exo-trig* cyclization of **1.59** with I₂/HTIB to give oxetane **1.60**.

1.3.4 4-*endo* halocycloetherification

The formation of oxetanes by 4-*endo* haloetherification has not been widely reported in the literature.

Rousseau and coworkers reported the synthesis of oxetanes via bromocycloetherification of cinnamyl alcohols.^{42,43} The only substrates that were well susceptible to this methodology however were substrates that were both 1,1-disubstituted and bearing an aryl group on the distal end of the olefin (Table 1.6). Substrates that did not have substitution alpha to the alcohol would still form oxetanes but in poor yield and those that lacked the distal aryl group did not form any 4-*endo* product (Table 1.6, entry 1). The aryl group was likely necessary because the mechanism goes through a carbocationic intermediate that is stabilized by the aryl group. Interestingly, the same stereochemistry is obtained in the product from the starting materials with either *Z* or *E* olefin geometry, indicating the cyclization operates under thermodynamic control (Table 1.6, entry 2,3).

Table 1.6. Reaction of cinnamyl alcohols with Br(coll)₂PF₆ to make oxetanes.

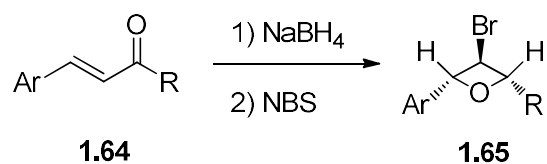
Entry	Alcohol	Product	Yield
1	 1.61a	 1.63a	49
2	 1.61b	 1.62b	36
3	 1.61c	 1.62b	36
4	 1.61d	 1.62d	78
5 ^a	 1.61e	 1.62e	88

^a Mixture of diastereomers at C2

Following up this report, Chang and coworkers reported the 4-*endo* bromocycloetherification of allyl alcohols derived from an aldol condensation reaction followed by a one-pot reduction-cyclization sequence to make oxetanes in 3 steps.⁴⁴ They determined that the stereochemistry of the products was in a *trans-trans* relationship at the contiguous C2-C3-C4

chiral centers. The substrate scope of this reaction was not well explored but it seemed that R was tolerant to both alkyl and aryl substituents while, although Ar had to be an aryl substituent, it appeared to be tolerant to both electron donating and withdrawing effects and heterocycles (Table 1.7).

Table 1.7. Synthesis of oxetanes by 4-*endo-trig* bromocycloetherification.^a



Entry	Product	Yield (%)	Entry	Product	Yield (%)
1	 1.65a	78	5	 1.65e	69
2	 1.65b	76	6	 1.65f	92
3	 1.65c	72	7	 1.65g	91
4	 1.65d	70	8	 1.65h	92

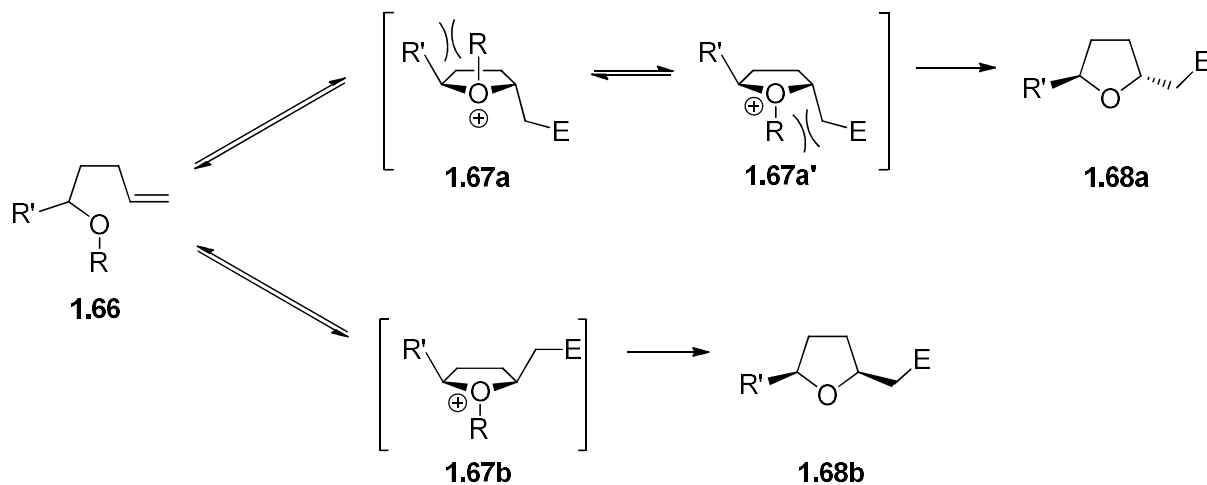
^a Conditions: **1.64** (1.0 mmol), NaBH₄ (2.0 mmol), MeOH/THF (v/v: 1/1, 10 mL), rt, 1 h, and NBS (1.0 mmol), 0 °C, 1 h; ^b Determined by ¹H NMR.

1.3.5 5-*exo* halocycloetherification

5-*exo* halocycloetherifications are by far the most common type of halocycloetherification reaction in the literature, as it is a particularly effective method of making polysubstituted tetrahydrofurans in a regio- and often stereoselective manner, either through substrate control or by catalyst control. This field is easily large enough that an entire review could be written on only this type of cyclization and so in this section, only a small subset of the literature will be reviewed that were either important contributions to the field for their synthetic utility or the scientific insight they provided and the focus will be on the more interesting catalytic asymmetric variants.

1.3.5.1 Diastereoselective Halocycloetherification

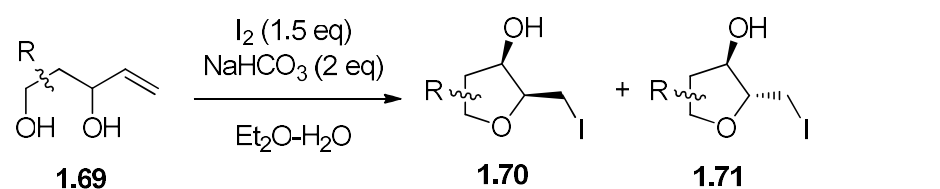
Some of the seminal work done in the field was from the group of Bartlett. His most important contribution to the field was the discovery that free homoallylic alcohols cyclize to give *trans*-2,5-disubstituted tetrahydrofurans predominantly but the *cis*-2,5-disubstituted tetrahydrofuran can be readily obtained from the corresponding ether.⁴⁵ It can be seen in Scheme 1.13 that if $R \neq H$, then there will be significant steric interactions between $-R'$ (**1.67a**) or $-CH_2E$ (**1.67a'**) in the transition state, and will therefore preferentially adopt **1.67b**, leading to the *cis*-2,5-disubstituted isomer, **1.68b**. Alternatively, if $R = H$, then the steric interactions are much less significant and so the major isomer obtained is the *trans*-2,5-disubstituted isomer **1.68a**. Also significant are the electronic effects of R: if loss of R from the oxonium intermediate is rapid, there may not be enough time for equilibration between **1.67a**, **1.67a'** and **1.67b**, thereby reducing the extent of thermodynamic control; if loss of R is slow, side reactions may become a concern.

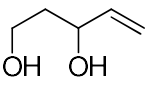
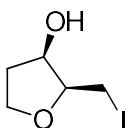
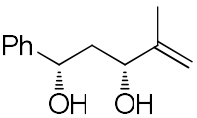
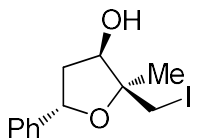
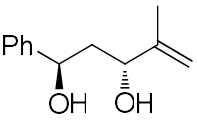
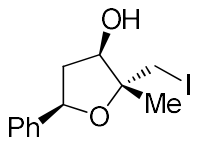
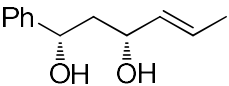
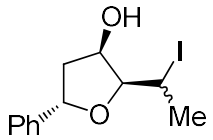


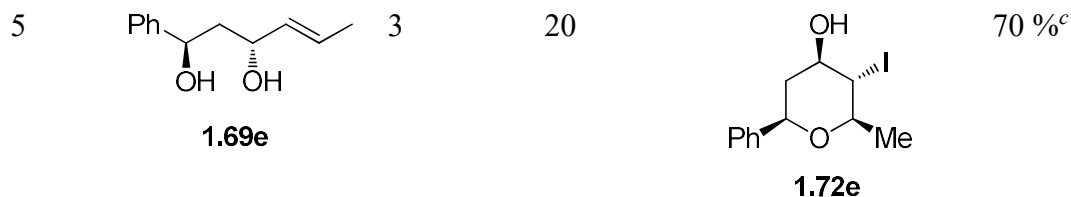
Scheme 1.13. Stereochemical course of 5-*exo* halocycloetherification.

Another early report of iodocycloetherification came in 1985 from Yoshida's group on their efforts to make substituted tetrahydrofurans in a stereocontrolled manner.⁴⁶ They report the synthesis of a variety of *cis*-2-iodomethyl-3-hydroxytetrahydrofurans through a 5-*exo* iodocycloetherification reaction in high yields and selectivities (Table 1.8). Interestingly, they observed only one case that 6-*endo* cyclization was competitive, likely due to the product having all the substituents in favorable equatorial positions (Table 1.8, entry 5). They observed a single instance where the *trans*-2,3 isomer was favored over the *cis*-2,3 isomer however they offer no explanation of possible reasons for this stereochemical outcome (Table 1.8, entry 3).

Table 1.8. Iodocycloetherifications of 4-penten-1,3-diols.

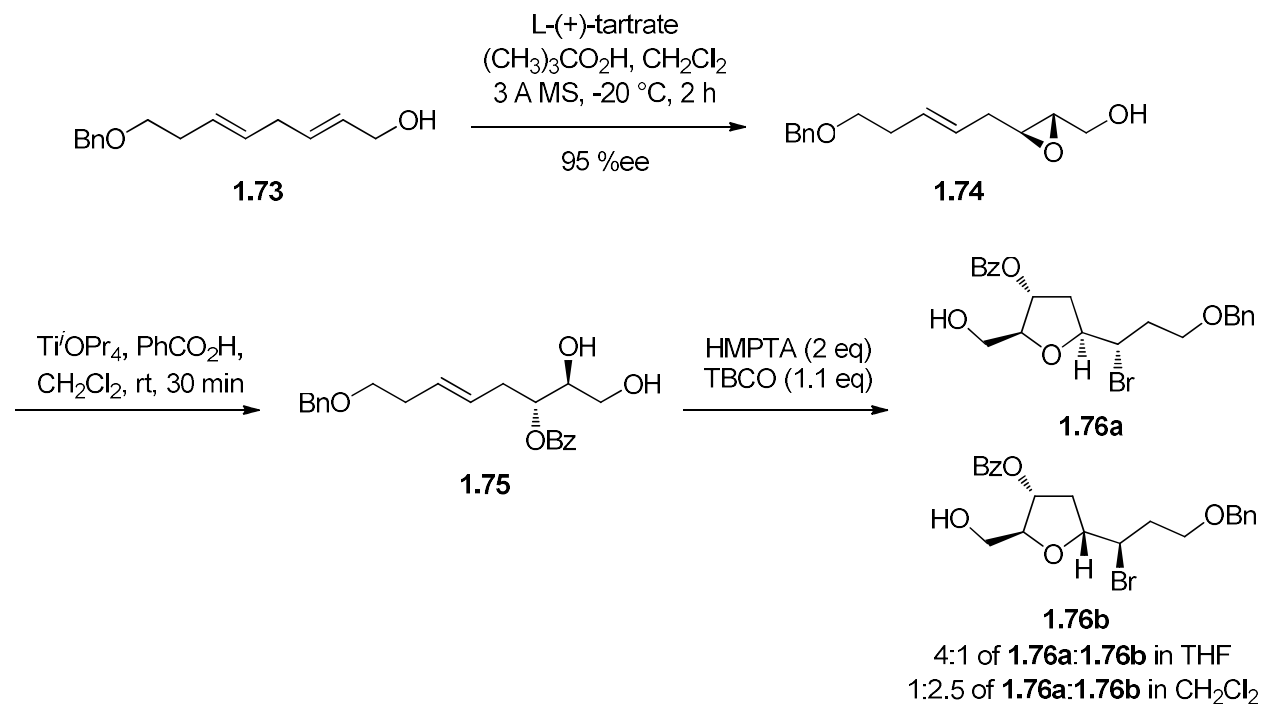


Entry	Starting Material	Time (h)	Temp (°C)	Major Product	Yield (1.70:1.71) ^a
1	 1.69a	3	0	 1.70a	87 % (95:5)
2	 1.69b	0.5	0	 1.70b	93 % (98:2)
3	 1.69c	3	20	 1.71c	94 % (39:61) ^b
4	 1.69d	10	0	 1.70d	79 % (93:7)



^a Product ratio was determined by ¹H and ¹³C spectra and/or HPLC; ^b Yield was based on 80 % conversion; ^c Also isolated 12 % of 5-*exo* tetrahydrofuran products (**1.70**:**1.71** = 95:5).

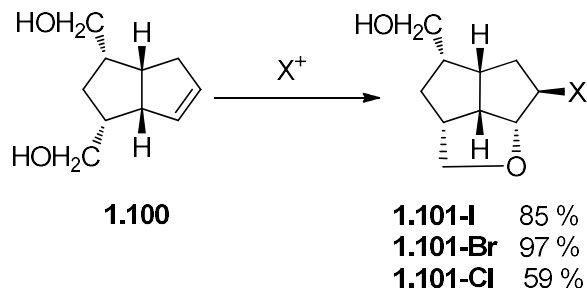
Martin and coworkers described the synthesis of polysubstituted tetrahydrofurans starting from diene **1.73**.⁴⁷ Using L-(+)-diethyl tartrate, asymmetric epoxidation occurred in more than 95 %ee to give **1.74**. This was then subjected to Ti(O^{*i*}Pr)₄ assisted opening with benzoic acid to give **1.75** and finally was treated with HMPTA and TBCO to yield **1.76a** and **1.76b**. Significantly, depending on the solvent used, the ratio of the products could be easily manipulated (Scheme 1.14).



Scheme 1.14. Enantiomeric synthesis of polysubstituted tetrahydrofurans.

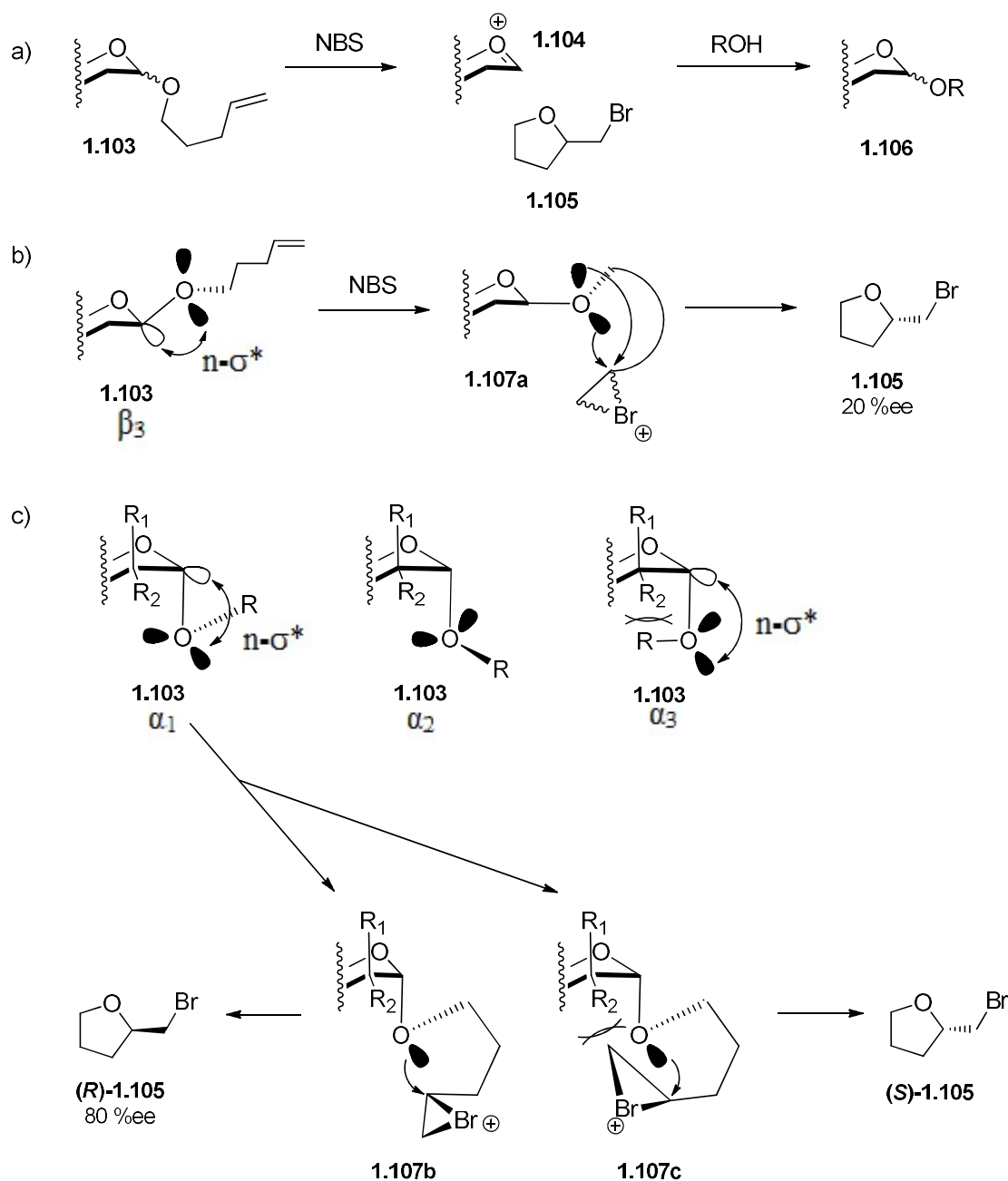
An example of substrate control can be seen in Tănase and co-workers report of a regioselective reaction of 1,3-dihydroxymethyl hexahydropentalene skeletons with several different electrophilic halogen sources.⁴⁸ Haloetherification with all halogen sources gave the same regioselectivity, with the hydroxymethyl group closer to the double bond being the reactive group.

While iodonium and bromiranium ions gave excellent yields, the chloriranium ion was less reactive and suffered from a lower yield; all the haliranium ions gave a single enantiomer (Scheme 1.15).



Scheme 1.15. Synthesis of pentalenofurane compounds by haloetherification.

In the late 1980s and early 1990s, Fraser-Reid and co-workers were focused on *n*-pentenylglycosides and utilizing the resulting oxocarbenium ions in glycosidation and hydrolysis reactions (Scheme 1.16a).⁴⁹ The authors realized that the 5-*exo* halocycloetherification byproduct of the reactions were synthetically useful halomethyltetrahydrofurans (**1.105**) and that the use of carbohydrate precursors could lead to enantioselectivity in the tetrahydrofuran products.⁵⁰ Indeed, starting with **α -1.103**, the authors obtained (***R***)-**1.105** in 80 %ee and starting with **β -1.103**, they obtained (***S***)-**1.105** in 20 %ee. They rationalized the difference in selectivity by examining the assumed reactive ground state rotamers. For **β -1.103**, the β_3 rotamer is $n\text{-}\sigma^*$ stabilized leading to little facial selectivity in the formation of the bromiranium ion or the nucleophilic attack of the diastereotopic lone pairs of the attacking oxygen and hence only 20 %ee was observed in the product (Scheme 1.16b). On the other hand, looking closely at **α -1.103** ground state rotamers, while both α_1 and α_3 have $n\text{-}\sigma^*$ interactions, α_3 suffers from steric interactions with R substituents in glucose-derived carbohydrates (Scheme 1.16c). Therefore, α_1 is the most stable ground state rotamer. Similar to the β_3 rotamer of **β -1.103**, there is no high diastereoselectivity for the formation of the bromiranium ion. There is however only one lone pair on the nucleophilic oxygen that is poised to attack and due to steric interactions destabilizing intermediate **1.107c**, high selectivity is observed for (***R***)-**1.105**. Interestingly, this behaviour was limited to *n*-pentenylglycosides; *n*-hexenylglycosides gave exclusively bromohydrin products.



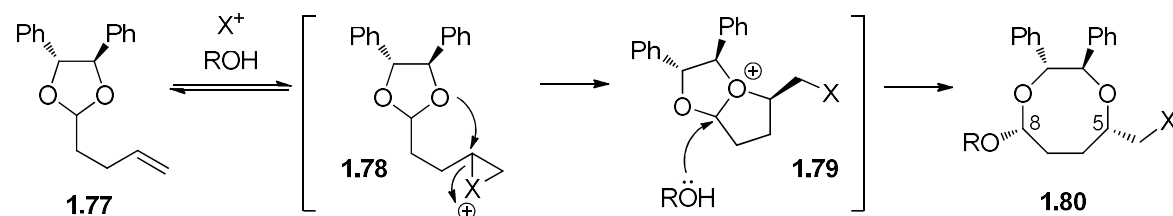
Scheme 1.16. Formation of bromomethyltetrahydrofuran through 5-*exo* bromocycloetherification of *n*-pentenylglycosides.

The Fujioka group developed the concept of “chiral auxiliary multiple-use methodology”.⁵¹ While it is generally recognized that enantioselective synthesis using asymmetric catalysis is more efficient than diastereoselective synthesis, there is more than just a single reaction to consider when focusing on the synthesis of complex natural products. Regiochemistry, stereochemistry and protection and deprotection of functional groups must all be considered. They suggested that in

certain cases, when a single chiral auxiliary can be used to control reactions at several different steps of a synthesis, then diastereoselective synthesis becomes competitive or even more efficient than enantioselective catalysis.

In 1996, Fujioka and coworkers reported using C_2 -symmetric ene acetals to make chiral 1,4-diols.⁵² Acetal **1.77** acted first as a nucleophile to attack a haliranium ion (**1.78**) to form bicyclic cationic intermediate **1.79** followed by the acetal acting as an electrophile in a one-pot operation that installs two remote stereocenters concurrently. The authors were able to make 8-membered acetals that led to 1,4-diols (Table 1.9, entry 1,2) with good selectivity for the (5*S*,8*R*)-acetal. Notably, when the hydrobenzoin acetal of 5-hexenal was subjected to an electrophilic halogen source in alcohol, only intermolecular haloetherification was observed thereby showing selectivity for 5-*exo* cyclization exclusively when 5-membered acetals were used (Table 1.9, entry 3).

Table 1.9. Acetal expansion via halofunctionalization to make chiral 1,4-diols.



Entry	X^+	R	Solvent	Temperature	Yield (%)	Selectivity ^a
1	NBS	Me	CH_2Cl_2	-78 °C - rt	95	74:8:18:0 ^b
2	$I(coll)_2ClO_4$	$MeO(CH_2)_2$	CH_2Cl_2	-78 °C - rt	90	86:2:11:1 ^b
3 ^c	$I(coll)_2ClO_4$	$MeO(CH_2)_2$	CH_2Cl_2	-78 °C - rt	0 ^d	

^a Determined by 1H NMR studies and chiral HPLC analysis; ^b (5*S*,8*R*) : (5*S*,8*S*) : (5*R*,8*R*) : (5*R*,8*S*);

^c 5-hexenal was used instead of 4-pental; ^d Only intermolecular haloetherification was observed.

The stereoselectivity of the above reaction is outlined in Figure 1.6 where it can be seen that the *cis*-fused ring systems were the most stable intermediates and the reaction proceeded through an S_N2 -type attack of alcohol onto a bicyclic oxonium ion. Interestingly, despite being higher in energy, **1.82a** was the intermediate that led to the observed product. This was rationalized as the halomethyl sterically interacting with the anion species on the convex side of the oxonium ion not being accounted for in the calculations.

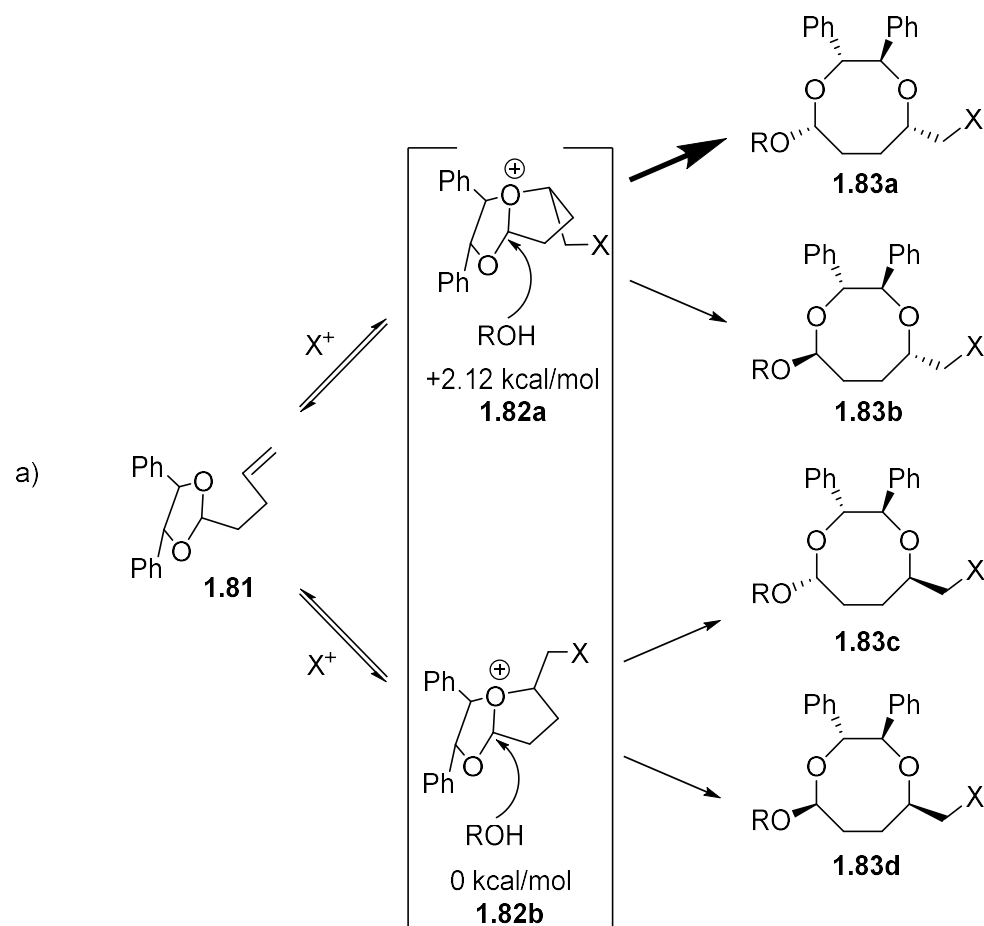
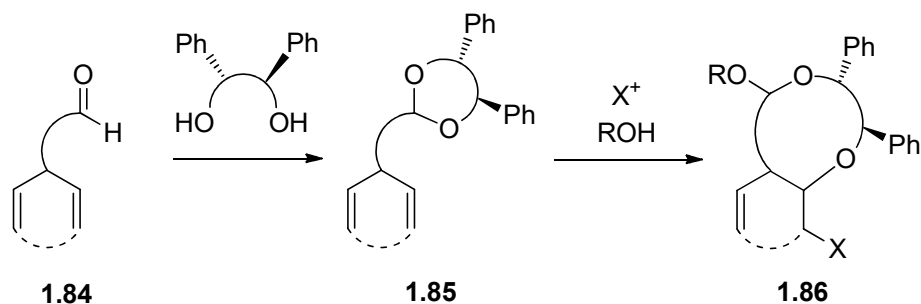


Figure 1.6. Explanation of observed stereochemistry selectivity presented in Table 1.9.

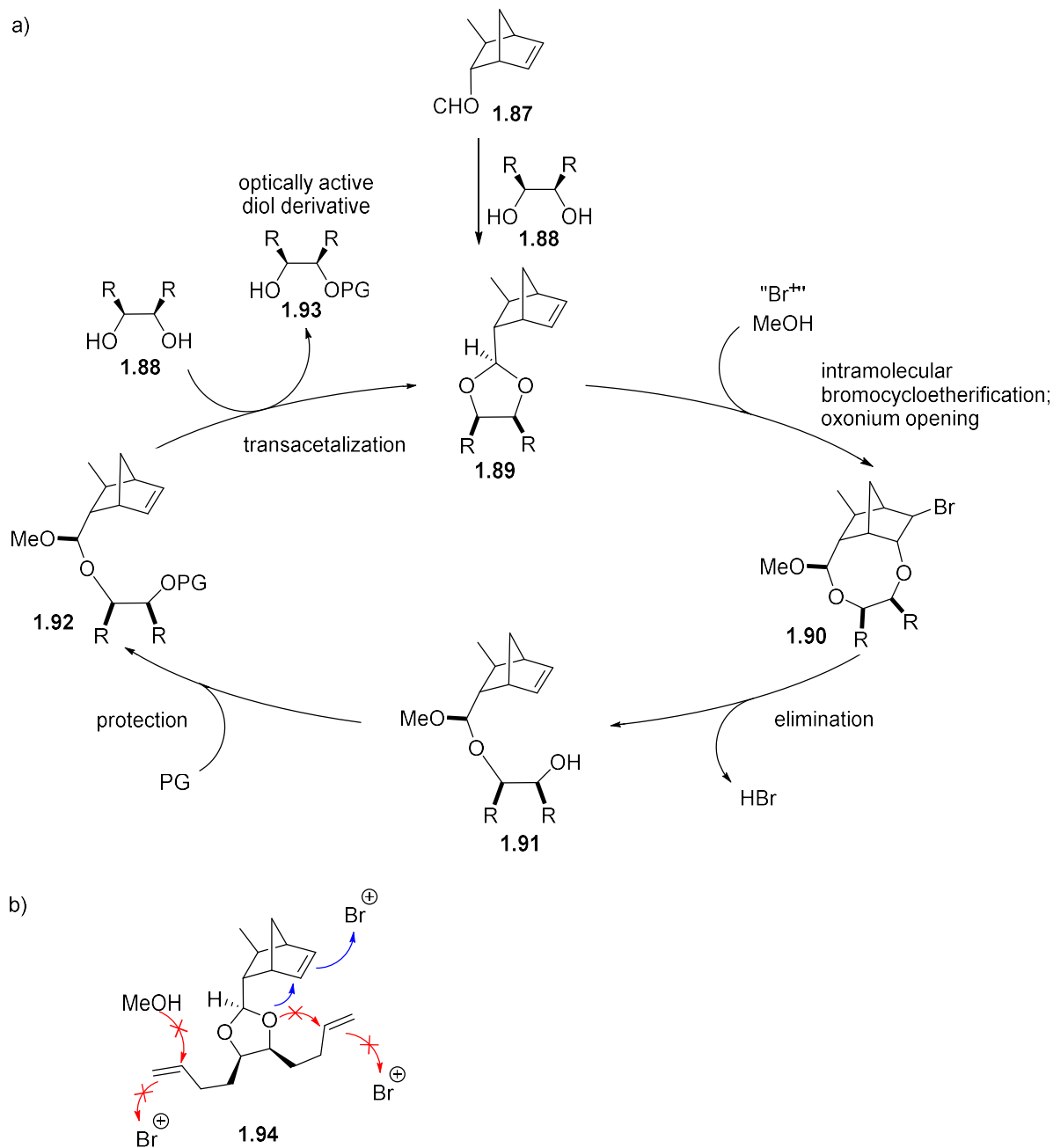
Fujioka expanded this intramolecular acetal haloetherification to reactions with cyclic and acyclic dienes such that discrimination between prochiral dienes was possible (Scheme 1.17).⁵³⁻⁵⁵



Scheme 1.17. Discrimination of cyclic and acyclic prochiral dienes.

Using similar methodology, the Fujioka group catalytically desymmetrized asymmetric *meso*-1,2-, 1,3- and 1,4-diols using norborene derived aldehydes to make ene acetals. Acetal **1.89** was subjected to bromocycloetherification conditions in methanol to give **1.90**. After elimination

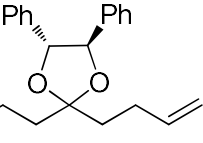
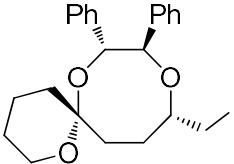
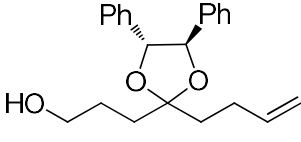
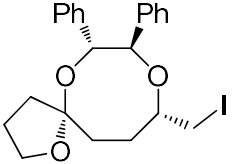
(**1.91**), protection of the free secondary alcohol (**1.92**) and transacetalization with another molecule of the asymmetric *meso*-diol (**1.88**), desymmetrized diol derivative **1.93** was obtained (Scheme 1.18a).⁵⁶⁻⁵⁸ Worth noting from their study was that even *meso*-diols bearing pendent olefin functionality that could react in a 5-*exo* manner with the acetal, such as **1.94**, reacted selectively with the bromiranium formed on the methyl norbornene unit (Scheme 1.18b).



Scheme 1.18. a) Catalytic cycle of desymmetrizing *meso*-diols using norbornene derived aldehydes; b) olefin selectivity of haloetherification reaction.

Finally, the Fujioka group expanded their work to intramolecular iodocycloetherification of ene ketals to synthesize spiroketals, functional groups that are very common in many natural products (Table 1.10).⁵⁹

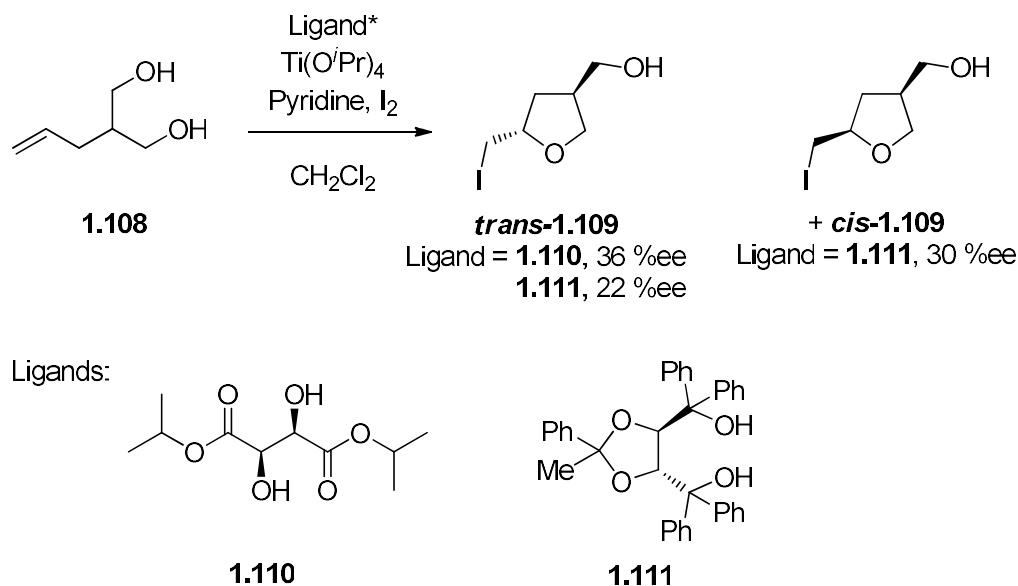
Table 1.10. Iodocycloetherification of ene ketals.

Entry	Ene Ketal	I ⁺ source	Temp	Product	Yield (%) ^a	dr ^b
1		I ₂	rt		nd ^c	-
2		NIS	rt		58	2:1
3		I(coll) ₂ PF ₆	rt		84	3.4:1
4	1.95a	I(coll) ₂ PF ₆	-40 °C	1.96a	84	4.3:1
5		I(coll) ₂ PF ₆	-40 °C		61	nd ^c
	1.95b			1.96b		

^a Total isolated yield of two isomers; ^b Diastereomeric ratio (dr) of the major isomer and the other isomer at the spirocenter; ^c Not determined.

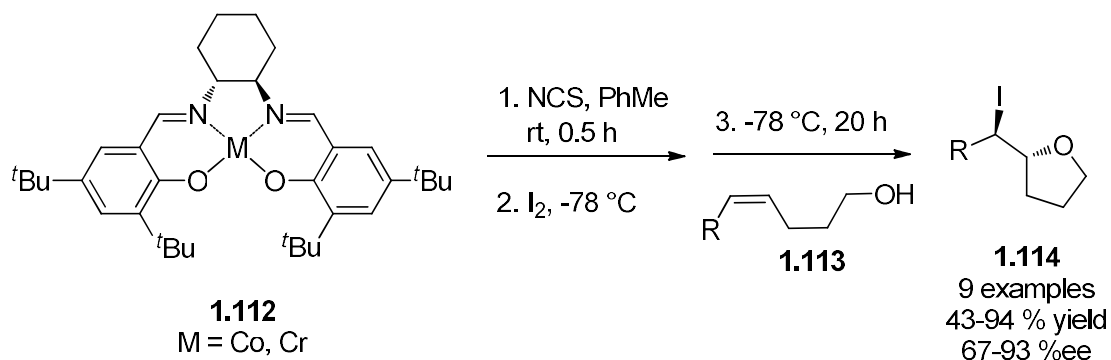
Denmark followed up on his studies on the absolute configurational stability of haliranium ions discussed in Chapter 1.1, reporting later in 2010 on the presence of Lewis bases on bromo- and iodocycloetherification reactions.¹⁶ The regioselectivity of the reactions was determined primarily by the substrate structure, where conjugated (*E*)-alkenes were highly *endo* selective and conjugated (*Z*)-alkenes and non-conjugated alkenes were *exo* selective (Table 1.11). However, the influence of the catalytic Lewis base on the cyclization selectivity suggests that the catalyst must be present in the product-determining transition structure. This implied that if the Lewis base used was chiral, then the reaction could be rendered enantioselective. Denmark did not test any chiral Lewis bases in this report to prove this conclusively but did later report an asymmetric variant that will be discussed below in Chapter 1.3.5.2.

cis:trans = 1:5.4), they were able to induce low levels of enantioselectivity, depending on the chiral ligand used (Scheme 1.19).



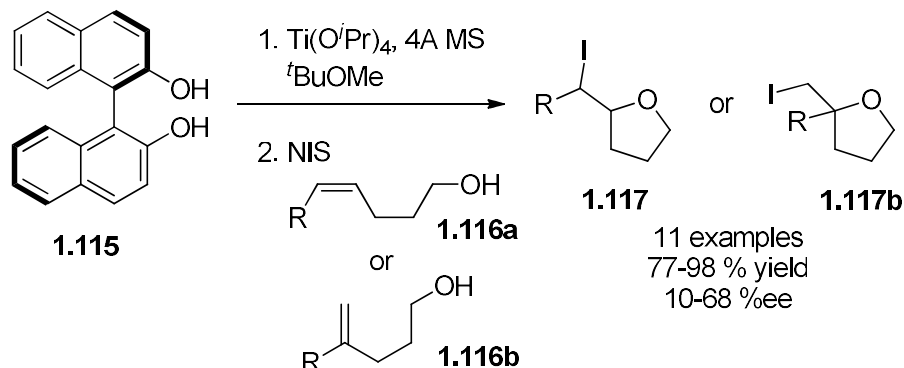
Scheme 1.19. Desymmetrization of symmetric alkenediols via Ti-catalyzed iodocycloetherification.

In a 2003 report of catalytic enantioselective iodocycloetherification from Kang and coworkers, the authors used chiral salen-Co complexes to cyclize a variety of γ -hydroxy-*cis*-alkenes (**1.113**) with excellent yields and good selectivity.⁶¹ This method involved premixing I_2 with the salen-metal complex and NCS additive, done in toluene to suppress any background reaction, and subsequent addition of the hydroxyalkene to give **1.114** in up to 90 %ee, depending on the steric demand of the substrate (Scheme 1.20). In a subsequent 2008 report, they tested various other metal-salen complexes and found comparable or better yields and selectivities when they employed salen- $\text{Cr}^{\text{III}}\text{Cl}$ at 10 mol% catalyst loading rather than the 30 mol% required of salen-Co complexes.⁶²



Scheme 1.20. Iodocycloetherification of γ -hydroxy-*cis*-alkenes using salen-metal complexes and NCS.

In 2004, Kang employed BINOL-Ti(IV) complexes to catalyze intramolecular iodocycloetherification of γ -hydroxyalkenes.^{63,64} The authors found BINOL itself, rather than derivatives, worked most efficiently and were able to cyclize 1,2- and 1,1-disubstituted γ -hydroxyalkenes (**1.116a** and **1.116b**, respectively) in good to excellent yield with enantioselectivity ranging from 10-68 %ee (Scheme 1.21).

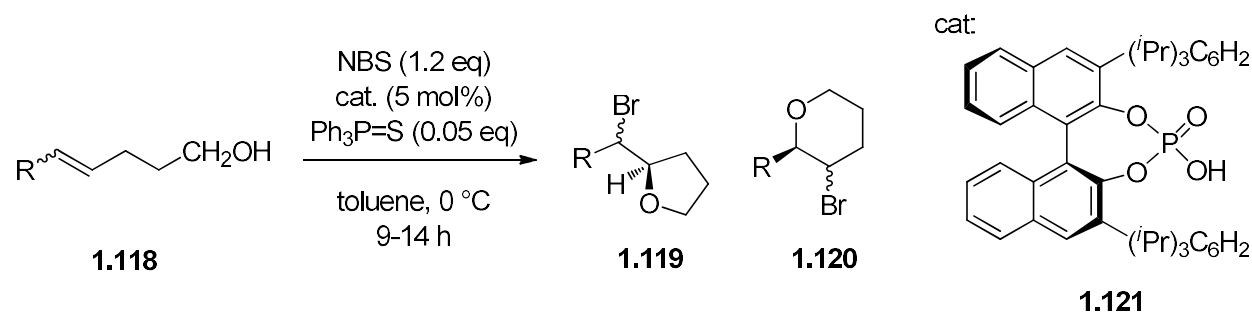


Scheme 1.21. Asymmetric iodocycloetherification of γ -hydroxyalkenes in the presence of (*R*)-BINOL-Ti(IV) complex.

Denmark reported in 2012 that Lewis base/chiral Brønsted acid cooperative catalysis yielded bromocycloetherification products in good enantioselectivities.⁶⁵ While no enantioinduction was observed when employing chiral catalysts containing Lewis basic nitrogen functional groups, Denmark realized that a more efficient method of enantioinduction was through a chiral ion pair to the bromiranium, particularly to ensure that the association be carried through an olefin-to-olefin transfer. This transfer is hindered by ion pairing as well since the coordination sphere of the bromiranium would be more saturated and less sterically available. With that in mind, they

designed a system such that the conjugate base of a sufficiently strong Brønsted acid could replace the succinimide as the bromiranium counterion. If the Brønsted acid was chiral, it influenced the stereochemistry of the reaction. A summary of their results is presented Table 1.12. (*E*)-alkenes have an inherent preference for 6-*endo* cyclization that the catalyst system was not able to overcome however the use of toluene rather than CHCl_3 did seem to bias the system (Table 1.12, entry 1, 2). The Brønsted acid alone pushed the ratio to a modest 48:52, which could be pushed further in the presence of electron withdrawing substituents on the aryl ring, although at a cost to the enantiomeric ratio obtained for the 5-*exo* product (Table 1.12, entry 1,4). Alternatively, (*Z*)-alkenes had a significant preference for 5-*exo* cyclization and the cooperative catalytic system saw these substrates react with good selectivity (Table 1.12, entries 5-7). The selectivity of the 6-*endo* product seemed to be irrelevant of the starting olefin geometry or the catalyst system.

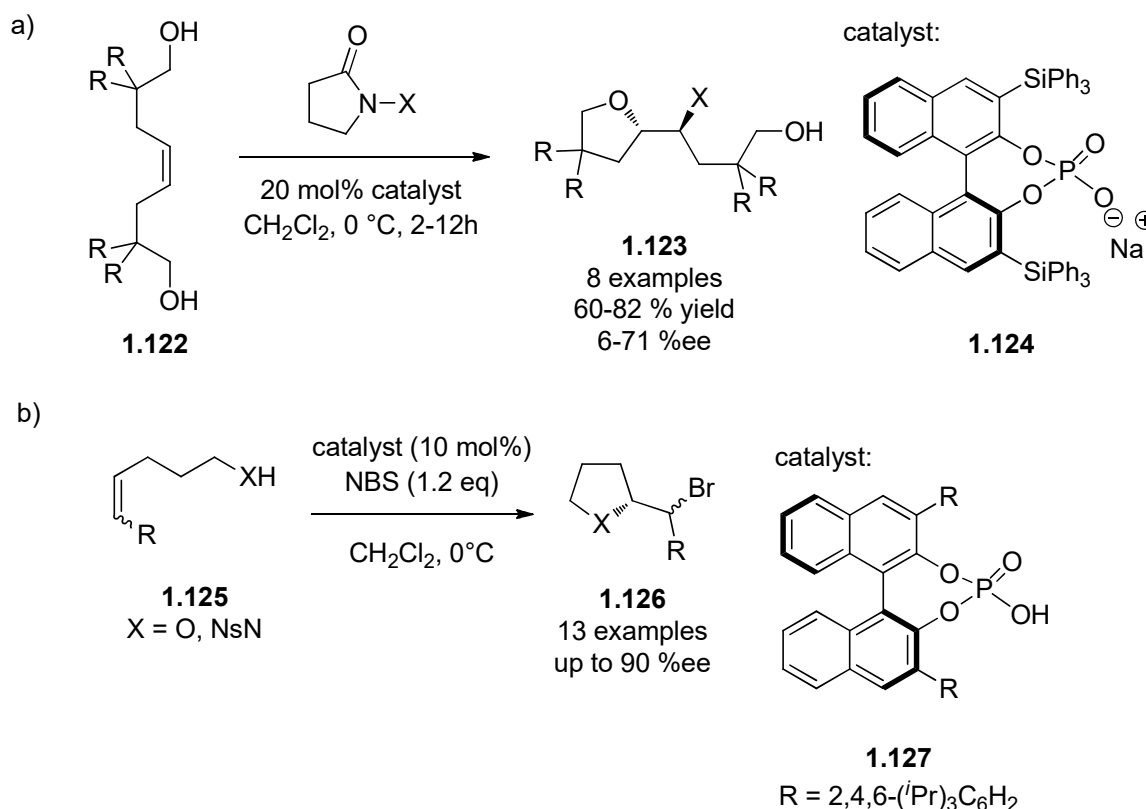
Table 1.12. Bromocycloetherification using Lewis base/chiral Brønsted acid cooperative catalysis



Entry	R	Ratio (1.119:1.120) ^b	er (1.119)	er (1.120)	Yield (%) ^c
1	(<i>E</i>)-C ₆ H ₅	48:52	97:3	57:43	83
2 ^d	(<i>E</i>)-C ₆ H ₅	3:97	56:44	51:49	90
3	(<i>E</i>)-4-CH ₃ -C ₆ H ₄	37:63	97:3	65:35	95
4	(<i>E</i>)-4-CF ₃ -C ₆ H ₄	86:14	85:15	65:35	55
5	(<i>Z</i>)-C ₆ H ₅	> 95:5	91:9	nd ^e	77
6	(<i>Z</i>)-4-CH ₃ -C ₆ H ₄	90:10	94:6	65:35	73
7	(<i>Z</i>)-4-FC ₆ H ₄	98:2	90:10	60:40	78

^a Reactions run on 0.1 mmol of substrate and 0.025 M and 0 °C ^b Determined by ¹H NMR of crude; ^c Combined yield after chromatography, all reactions run on 0.1 mmol of substrate; ^d Reaction run in CHCl₃; ^e Not determined

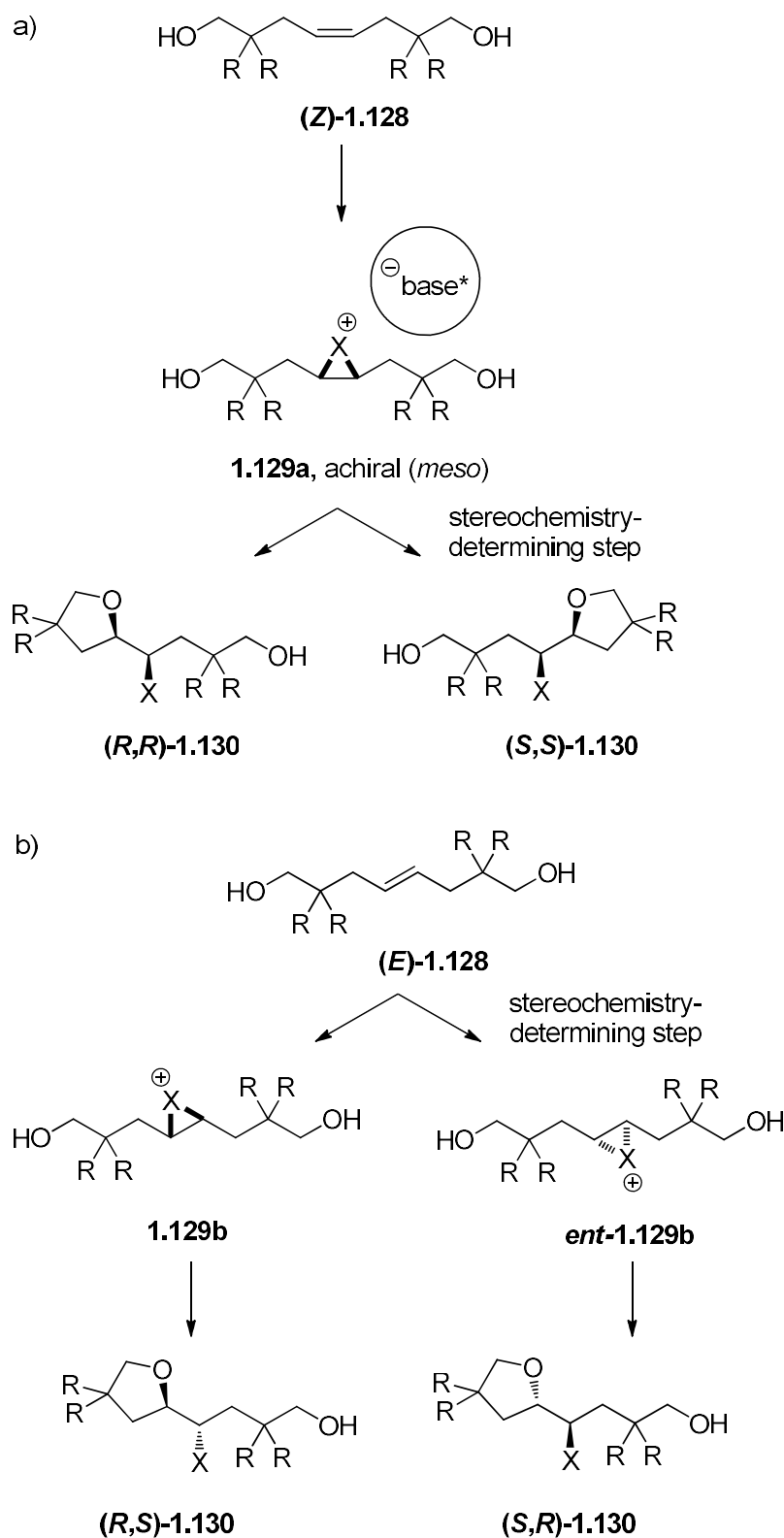
Others have also used this strategy of employing chiral phosphoric acids to render halocycloetherification reactions catalytically enantioselective. Hennecke and co-workers reported using *N*-haloamides with catalytic sodium salts of chiral phosphoric acids to desymmetrize *meso*-haliranium ions made *in situ* from symmetric ene-diol systems (Scheme 1.22a).⁶⁶ They leave room for improvement however as their yields were good (60-82 %) but their selectivities ranged from 6-71 %ee. Shi reported a similar reaction that, while not a desymmetrization, did use a chiral phosphoric acid catalyst and the reaction proceeded with up to 90 %ee (Scheme 1.22b).⁶⁷



Scheme 1.22. Chiral phosphoric acid catalysts to make asymmetric haliranium ions as reported by a) Hennecke and b) Shi.

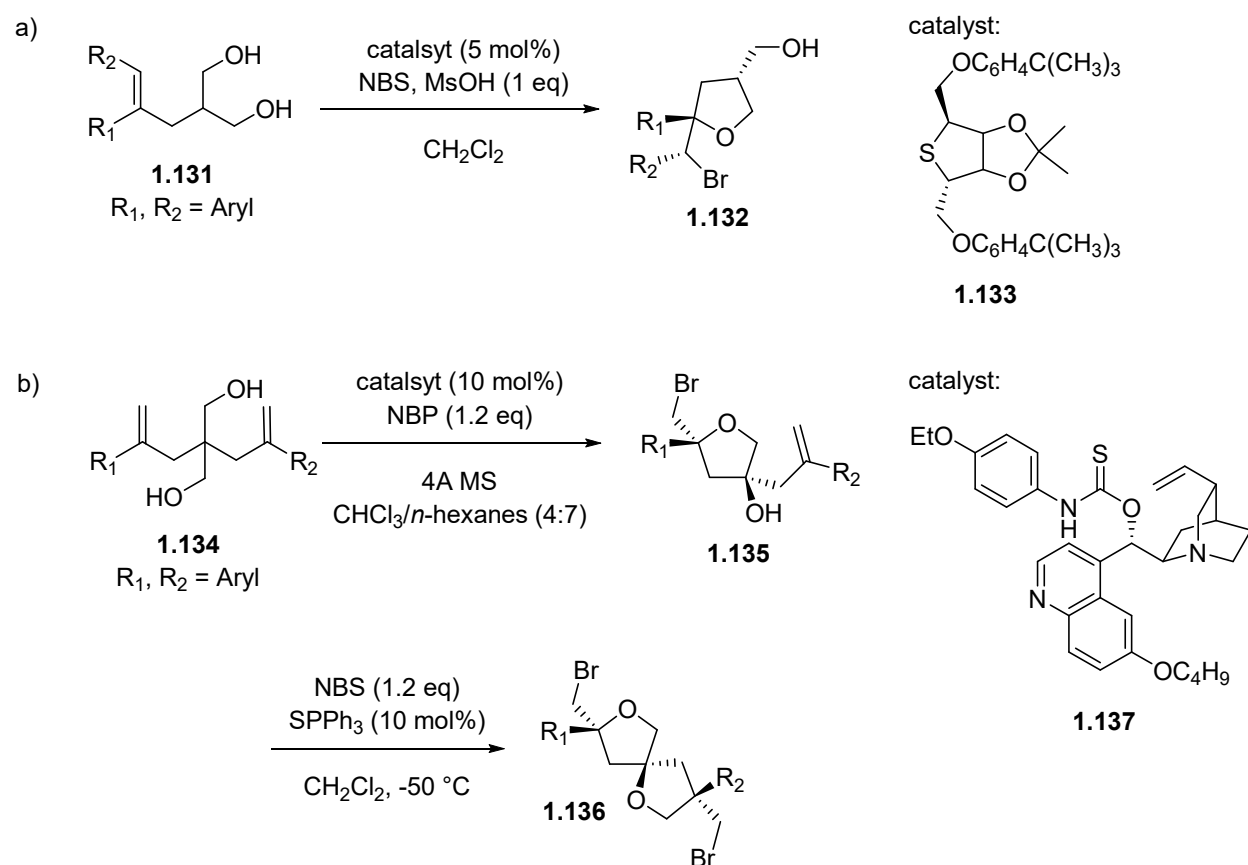
Hennecke subsequently reported a study on the enantioselective halocycloetherification of symmetric alkenediols and alkenols using chiral BINOL phosphate catalysts.⁶⁸ They realized the importance of the configuration of the double bond in regards to the stereochemical consequences

of the resultant haliranium ion: if the olefin is *Z*-configured, the haliranium ion will be a *meso* compound and the stereochemistry will not be set until the cyclization occurs; if the olefin is *E*-configured, electrophilic halogenation will lead to a chiral, C_2 symmetric haliranium ion and the cyclization of either alcohol group would lead to the same enantiomer of the product, indicating that the stereochemistry is set at the formation of the haliranium ion (Scheme 1.23). While the authors were able to show that depending on the substrate, the choice of BINOL phosphate catalyst was important and could exhibit remarkably different selectivities, their results were too preliminary to draw irrefutable conclusions regarding possible transition states of the reaction. Investigations that are more thorough are needed but this study is good evidence that a feature as simple as olefin geometry can drastically affect the mechanism of a reaction in the context of catalytic asymmetric halocycloetherification. The authors extended this hypothesis to suggest that it could be possible halolactonization also undergoes different catalytic mechanisms than halocycloetherification due to the reactivity and selectivity differences of catalytic systems when used with alkenoic acids compared to alkenols.



Scheme 1.23. Stereochemical consequences of a) (*Z*)-configuration and b) (*E*)-configuration olefin geometry on the halocycloetherification of symmetric alkenediols.

Recently Yeung and coworkers reported several examples of asymmetric catalytic haloetherification reactions. They reported an enantio- and diastereoselective bromocycloetherification-desymmetrization of olefinic 1,3-diols (**1.131**) using NBS and C_2 -symmetric sulfide catalysts (**1.133**)^{69,70} or thiourea-quinidine derived catalysts (**1.137**).⁷¹ They constructed tetrahydrofurans with up to three stereogenic centers (**1.132**, Scheme 1.24a) and spirocyclic tetrahydrofurans (**1.136**, Scheme 1.24b) in excellent yields (73-99 %) and stereoselectivities (dr >99:1, er up to 97.5:2.5). The reaction proceeded through a 5-*exo* selective cyclization and no competition of the 6-*endo* cyclization was observed even when aromatic substituents were in the R_2 position.



Scheme 1.24. Desymmetrization of olefinic 1,3-diols using a) C_2 -symmetric sulfide catalysts and b) quinidine derived catalyst.

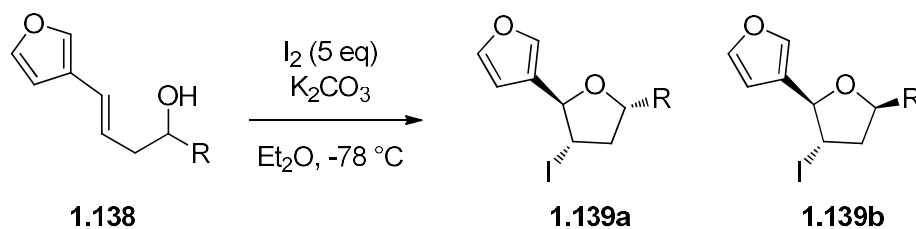
1.3.6 5-*endo* halocycloetherification

Despite the inherent favourability of *exo* over *endo* cyclization, many 5-*endo* halocycloetherifications reported in the literature arise from conditions where 4-*exo* cyclization

appears as though it would be favoured, a phenomenon that is very counterintuitive when considering Baldwin's rules. Some of these examples are discussed below.

The work of Kang *et al.* was discussed thoroughly in Chapter 1.3.5 in regards to their efforts in catalytic asymmetric 5-*exo* halocycloetherification reactions. They also published some early work on the diastereoselective synthesis of substituted tetrahydrofurans by 5-*endo* iodocycloetherification.⁷² They synthesized several *trans*-2,5-disubstituted tetrahydrofurans in good to excellent yields and from 14:1 to 65:1 *cis:trans* isomeric ratio. They electronically biased the system to favour 5-*endo* cyclization by placing an aromatic furanyl group at the distal end of the olefin and they explained their stereoselectivity as the substrate adopting a conformation in the transition state that would minimize 1,3-diaxial interactions.

Table 1.13. Diastereoselective 5-*endo* iodocycloetherification to make *trans*-2,5-disubstituted tetrahydrofurans.^a

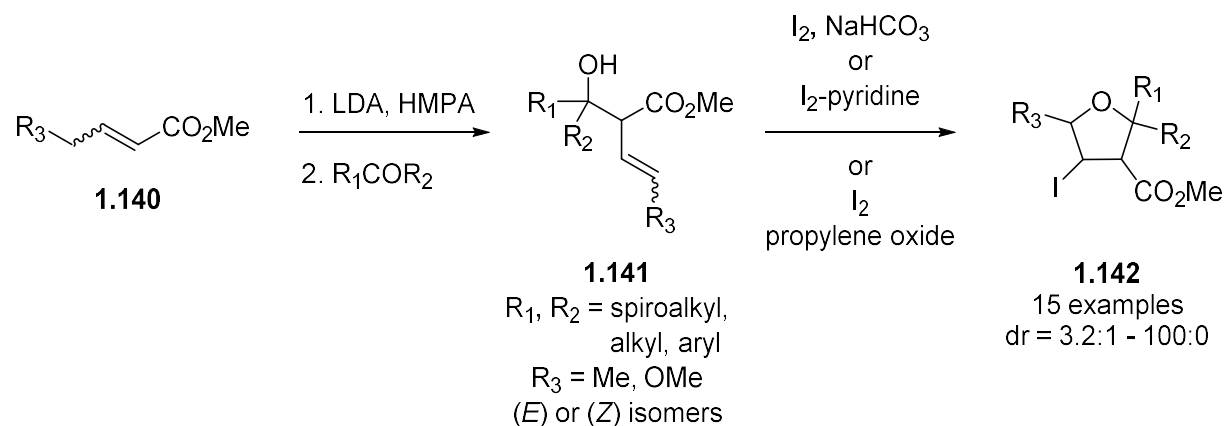


Entry	R	Yield (%)	Isomeric Ratio (1.139a : 1.139b)
1	CH ₂ OTBDPS	86	16.5:1
2	CH ₂ OCPPh ₃	86	27.5:1
3 ^b	CH ₂ OCO ^t Bu	92	16.5:1
4	Me	84	14:1
5	Et	90	20:1
6	^t Pr	87	65:1

^a Substrate **1.138** in Et₂O were added dropwise to I₂ solution; ^b The reaction temperature was maintained at -78 °C for 6 hours and then raised to rt over 2 hours.

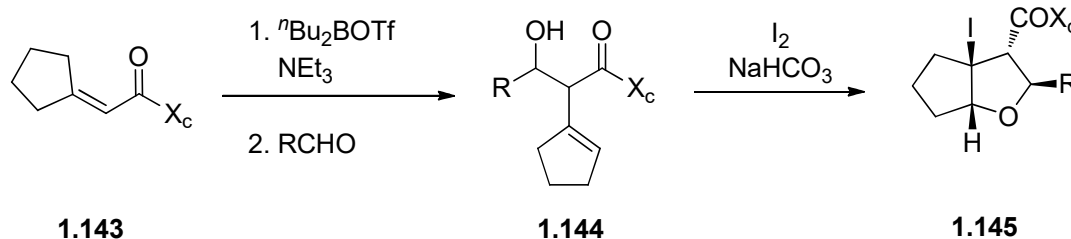
The work of the Galatsis group was mentioned earlier in the context of 4-*exo* iodocycloetherification but they have also reported examples of 5-*endo* iodocycloetherification to

make substituted tetrahydrofurans.³⁷ Using the same deconjugative aldol methodology on slightly modified substrates to include substitution at the distal end of the olefin rather than the proximal end, they altered the selectivity of the reaction to favor 5-*endo* iodocycloetherification over 4-*exo* (Scheme 1.25). Additionally, they identified conditions that would both increase selectivity and yields and lessen yields of de-iodo compounds by using organic bases to increase solubility in the organic layer of these biphasic reactions, thereby better controlling the presence of acid responsible for de-iodo compounds.⁷³



Scheme 1.25. Deconjugative aldol-iodocycloetherification sequence reaction to make polysubstituted tetrahydrofurans.

While Galatsis and coworkers had some success using chiral auxiliaries to synthesize oxetanes in an enantioselective fashion, their results using chiral auxiliaries to make enantioenriched tetrahydrofurans were somewhat more restricted.³⁹ Contrary to their results using simple methyl esters, the incorporation of a chiral auxiliary rendered the conversion of double bond geometry incomplete in the deconjugative aldol step of the reaction when using acyclic substituents, thereby leading to a mixture of diastereomers after the subsequent iodocycloetherification reaction. The use of a cyclic substituent led to a single enantiomer since the olefin geometry was necessarily restricted to a single isomer (Table 1.14).

Table 1.14. Enantioselective 5-endo iodocycloetherification using Evans auxiliary. ^a

Entry	R	Yield (%)
1	Me	83
2	Et	81
3	<i>i</i> Pr	61
4	Ph	83

^a Xc = Evans auxiliary

Barton and Lipshutz reported the stereochemical outcomes of halocycloetherification to make tetrahydrofurans in a 5-*endo* fashion.⁷⁴ As part of their efforts to synthesize tetronasin (**1.146**, Figure 1.7), they examined the effects of reacting different electrophiles with homoallylic alcohol derivatives with particular stereochemistry. The results are summarized in Figure 1.8. They found that when reacting *cis*-(*E*)-**1.147** with I₂ as a source of iodonium, they observed the formally *syn* addition across the double bond. Similarly, a *syn* addition was observed when reacting *cis*-(*Z*)-**1.147** and I₂ but the product was epimeric at the iodine substituent because the electrophile was attacked from the opposite face of the alkene. Contrastingly, when PhSeCl was used as the electrophile with *cis*-(*E*)-**1.147** or *cis*-(*Z*)-**1.147**, the expected *anti* addition occurred across the double bond, again with the difference between the products being that they were epimeric at the selenium substituent. Similar results were obtained when the starting materials were *trans*-(*E*)-**1.147** and *trans*-(*Z*)-**1.147** except that the face of attack on the electrophile was opposite and thereby effected the stereochemical outcome at the newly formed ether centers.

Importantly, these results have been contested by other groups as will be discussed below and have since been declared to be incorrect due to misassignment of the stereochemistry of the products.⁷⁵ As one of the seminal papers in the field, this mistake is well worth noting.

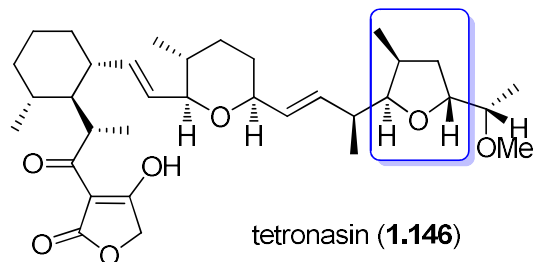


Figure 1.7. Structure of tetronasin (**1.146**) with the tetrahydrofuran portion of interest highlighted in blue.

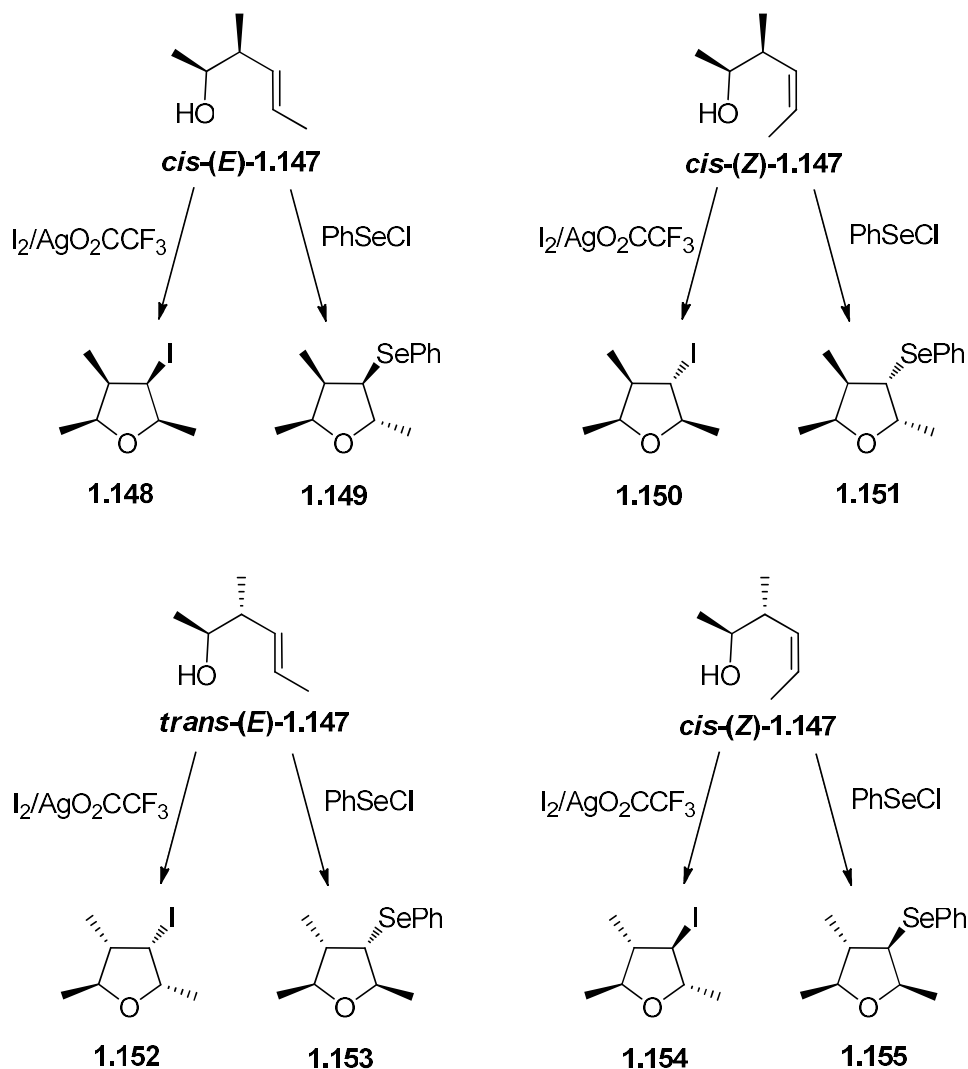
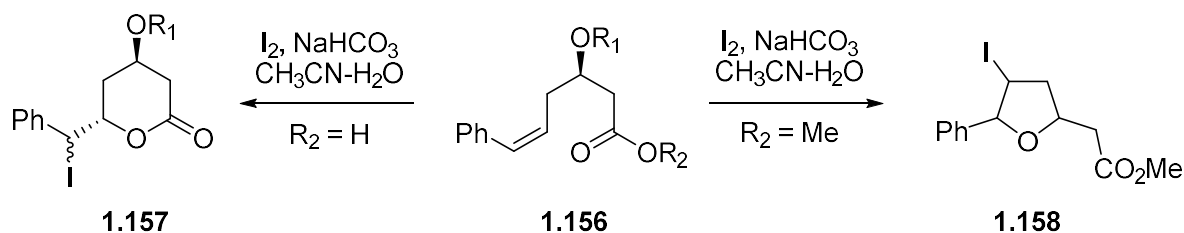


Figure 1.8. Incorrect stereochemical outcome of the 5-*endo* cyclizations of *cis*-(*E*)-**1.147**, *cis*-(*Z*)-**1.147**, *trans*-(*E*)-**1.147** and *trans*-(*Z*)-**1.147** mediated by I^+ and $PhSe^+$, as misassigned by Barton and Lipshutz.

In initial reports from the Knight group, the authors reported observing the formation of a small amount of side product in addition to expected product, **1.157**.⁷⁶⁻⁷⁸ Rather than simply disregard this undesired product, Knight and coworkers further examined the side product with the intention of being able to eliminate it from the reaction once its structure and mechanism of formation were known. The product was determined to be tetrahydrofuran derivative **1.158** that arose from the unexpected 5-*endo* iodocycloetherification of **1.156** being competitive with the 6-*exo* lactonization (Scheme 1.26).



Scheme 1.26. Competition between 6-*exo* lactonization and 5-*endo* etherification, $\text{R}_1 = \text{H}, \text{SiR}_3$.

Intrigued by the lack of literature reports of such methods of making tetrahydrofurans, the authors looked closer at this reaction and found that when the free carboxylic acid was used, 5-*endo* cyclization was only observed when the distal end of the olefin was stabilized by an aryl ring. This limitation could be easily overcome by blocking the competitive lactonization by using esters in place of acids. Additionally, homoallylic alcohol derivatives that lacked an ester group were more susceptible to halohydrin formation since they lacked the extra stabilization in the transition state that the ester provided (Figure 1.9) and it was found that 5-*endo* cyclization could be favoured by simply performing the reaction with anhydrous solvent.

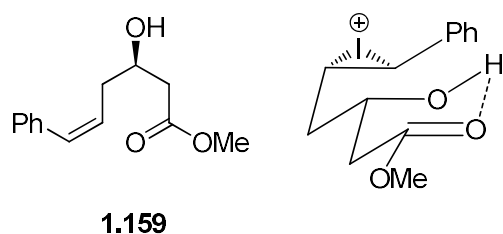
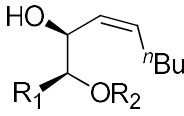
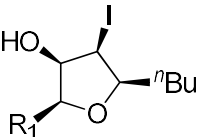
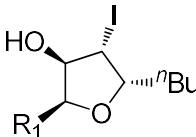
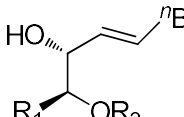
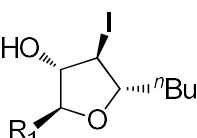
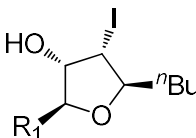
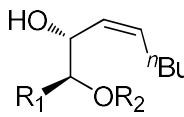
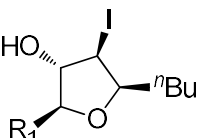
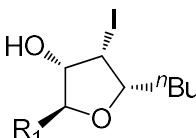


Figure 1.9. Transition state of 1.159 showing the stabilization provided by the ester group that makes the reaction less susceptible to intermolecular attack of water to form halohydrins.

	 <i>cis</i>-(Z)-1.160	Ph	H	 1.161b	 1.162b	64	51:49
3	 <i>trans</i>-(E)-1.160	Me	Bn	 1.161c	 1.162c	66	91:9
		Me	H			77	75:25
		Ph	H			75	67:33
4	 <i>trans</i>-(Z)-1.160	Me	Bn	 1.161d	 1.162d	66	91:9
		Me	H			97	97:3
		Ph	H			92	92:8

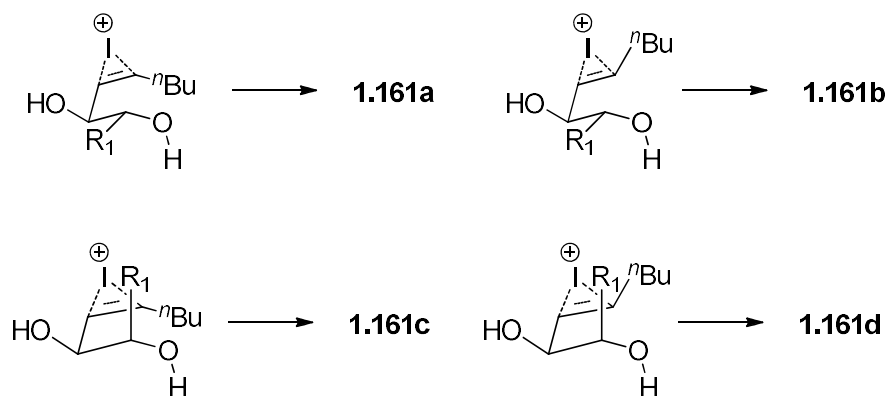
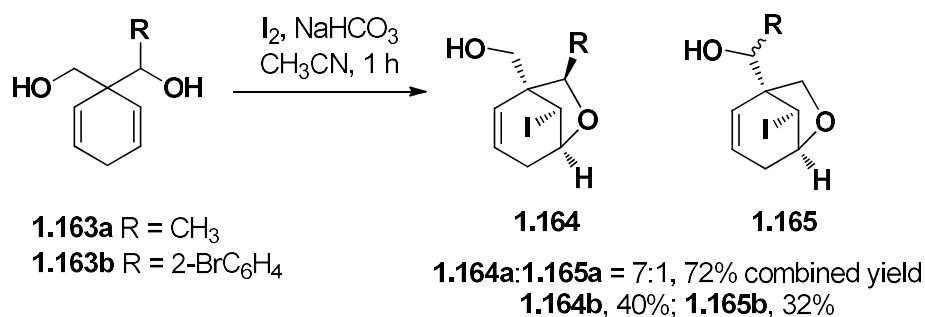


Figure 1.10. Proposed transition state for 5-*endo* iodocycloetherification of transformations shown in Table 1.15.

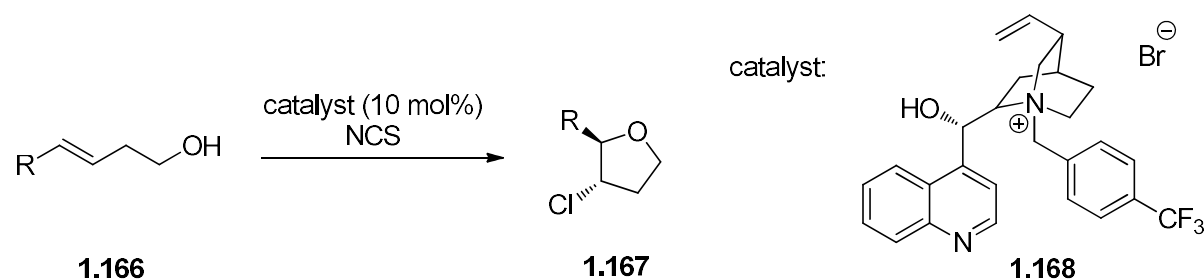
A report from Elliott and coworkers described the desymmetrization of cyclohexadienes via a 5-*endo* iodocycloetherification (Scheme 1.27).⁸⁰ Using substrates **1.163a** and **1.163b**, in which either of the alcohols can react in a 5-*endo* manner, they observed a 7:1 regioselectivity for secondary alcohol attack when R was an alkyl and a much more modest 1.25:1 regioselectivity when R was an aryl. This is difficult to attribute to nucleophilicity parameters and was thought to perhaps arise from conformational effects. However, in both cases only a single stereoisomer was obtained.



Scheme 1.27. 5-endo iodocycloetherification of 1.163a and 1.163b.

Despite progress being made in the area of catalytic asymmetric *5-exo* halocycloetherification, little has been reported for the *5-endo* mode of cyclization. As such, a report from Sun and coworkers was particularly important in 2013.⁸¹ They successfully employed quaternary ammonium salts derived from cinchonine as organocatalysts for the asymmetric chlorocycloetherification of homoallylic alcohol derivatives. They screened 13 catalysts and counterion combinations and after optimization, discovered that **1.168** worked best. Upon screening a substrate scope, good to excellent yields were observed along with moderate to excellent enantioselectivity (Table 1.16). Some limitations to this work include difficult to predict selectivity as no patterns based on steric or electronic effects seem immediately evident and that aliphatic homoallylic alcohols do not perform well under these conditions, giving poor yields and low enantioselectivity. Nevertheless, this is a significant contribution to the field as both a rare example of chlorocycloetherification and as a catalytic enantioselective variant of this transformation.

Table 1.16. Scope of catalytic asymmetric 5-endo chlorocycloetherification of homoallylic alcohols.



Entry ^a	R	Yield ^b	ee (%) ^c
1	Ph	85	95
2	4-Me-Ph	78	86
3	4-OH-Ph	80	63
4	4-OMe-Ph	90	61
5	2-Cl-Ph	85	95
6	4-Cl-Ph	80	96
7	2,4-di-Cl-Ph	87	52
8	4-F-Ph	83	70
9	4-Br-Ph	82	75
10	4-CF ₃ -Ph	75	92
11	3-NO ₂ -Ph	92	96
12	Cy	56	11

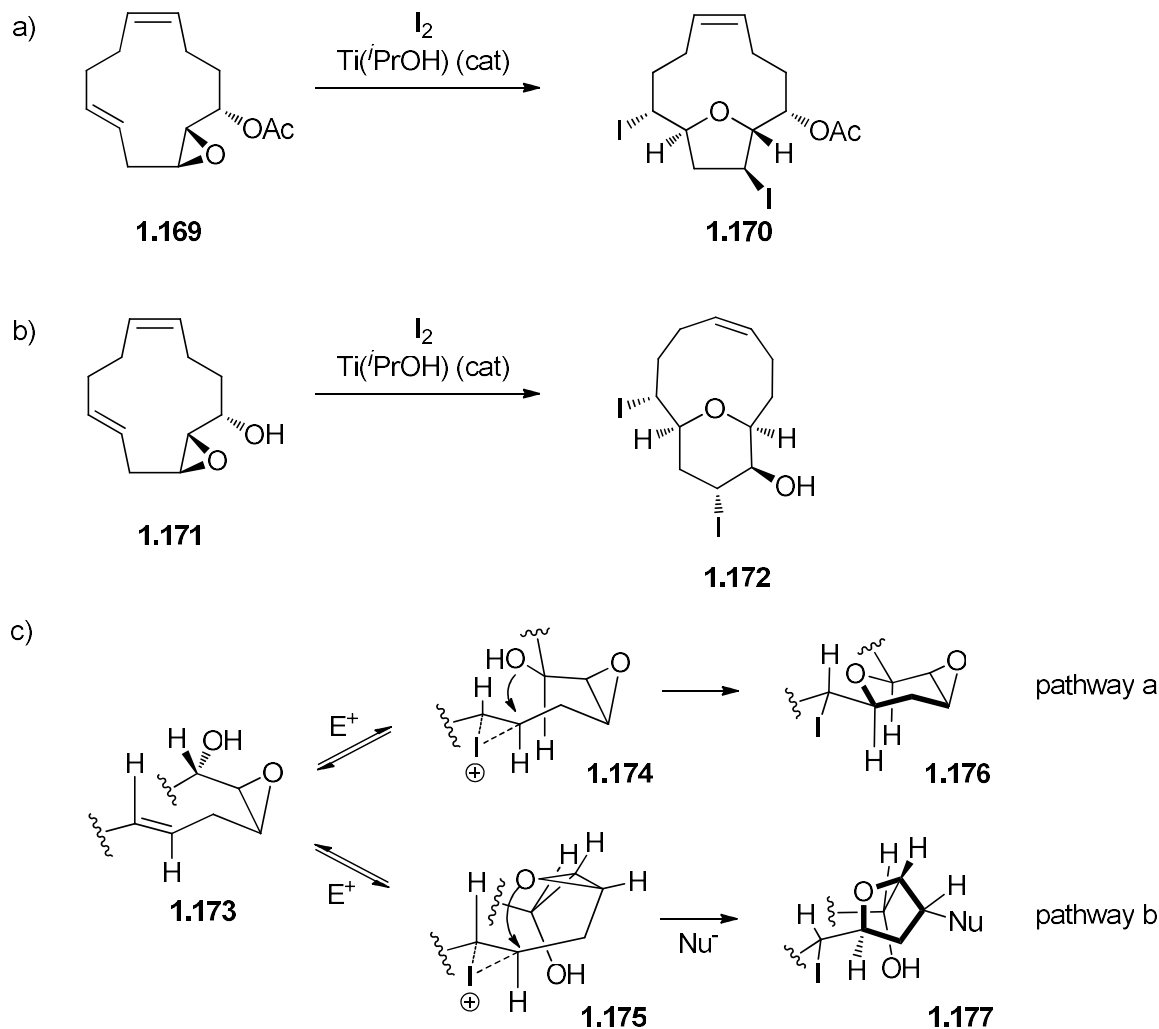
^a **1.166** (0.20 mmol), NCS (0.24 mmol), TsNH₂ (0.10 mmol), catalyst (10 mol%), THF (1 mL), -20 °C, under argon, 12 h; ^b Isolated yields; ^c Determined by chiral HPLC analysis.

1.3.7 6-*exo* halocycloetherification

To preface this section, we reported a synthesis of morpholines via a diastereoselective 6-*exo* bromocycloetherification reaction. This will be discussed in detail in Chapter 2 and Chapter 3.

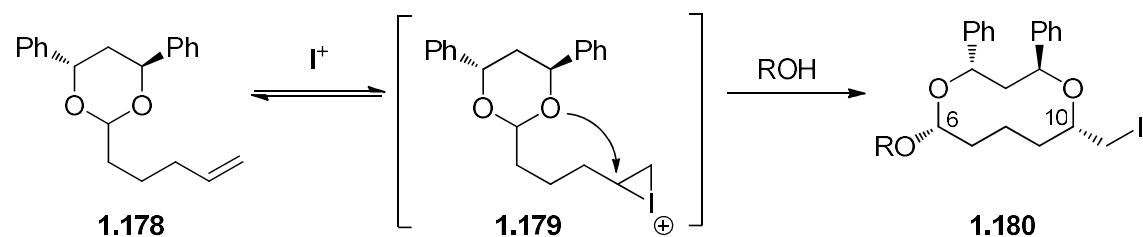
There are few reports in the literature that are detailed studies of the reactivity, regioselectivity and stereoselectivity of 6-*exo* halocycloetherifications. While the few that do exist will be discussed below, the most common occurrence of these reactions is them being utilized in the synthesis of natural products or biologically important molecules. A thorough review of these reactions would simply not be interesting and so a limited subset of examples will be presented herein.

A study published in 1989 from the Martín group showed their efforts towards 5-*exo* and 6-*exo* iodocycloetherifications to make tetrahydrofurans and tetrahydropyrans, respectively, in their studies toward microalga polyether macrolides.⁸² They showed that the selectivity can be manipulated in an interesting way: when **1.169** was subjected to iodocycloetherification conditions, the epoxide attacked the iodonium to form the *trans*-2,5-tetrahydrofuran **1.170** via a 5-*exo* cyclization (Scheme 1.28a); when the alcohol was unprotected as in **1.171**, exclusively the *cis*-2,6-tetrahydropyran **1.172** was formed by a 6-*exo* cyclization, with no competition from the epoxide (Scheme 1.28b). In both cases, the formation of halohydrins was competitive and isolated in about 30 % yield. The stereochemistry of these reactions is outlined in Scheme 1.28c. The chair conformation adopted by **1.147** to avoid 1,3-diaxial interactions led to the *cis*-2,6-disubstituted **1.176** (pathway a) while the boat-like conformation adopted by **1.175** led to the *trans*-2,5-disubstituted **1.177** (pathway b).



Scheme 1.28. a) Formation of *trans*-2,5-disubstituted tetrahydrofuran via 5-*exo* iodocycloetherification, b) formation of *cis*-2,6-disubstituted tetrahydropyran via 6-*exo* iodocycloetherification and c) the stereochemical explanation of those cyclizations.

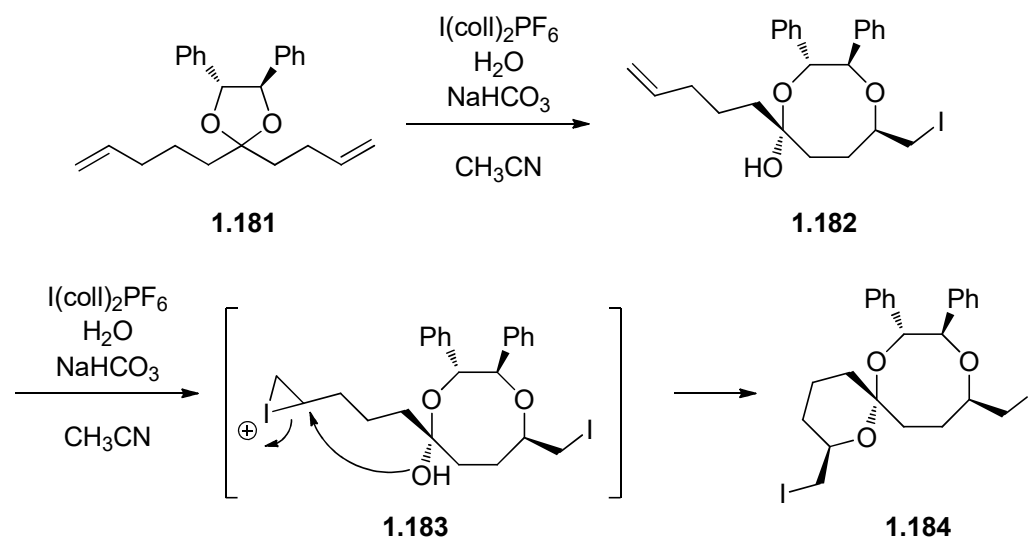
Fujioka and coworkers published a plethora of reports mentioned above in Chapter 1.3.5.1 on the use of ene acetals in intramolecular haloetherification reactions. While the vast majority of their results showed exclusively 5-*exo* selectivity, they reported two specific instances of 6-*exo* selectivity. The first instance was in their seminal paper in 1996 where under the circumstance of using the ene acetal **1.178**, derived from 1,3-diphenyl-1,3-propanediol and 5-hexenal, to make 1,5-diols upon removal of the propanediol protecting group. They did not explore any substrate scope for this reaction but did report that it works using several different sources of iodonium (Table 1.17).

Table 1.17. Acetal expansion via halofunctionalization to make chiral 1,4-diols.

Entry	I ⁺	R	Solvent	Temperature	Yield (%)	Selectivity ^{a,b}
1	I(coll) ₂ ClO ₄	MeO(CH ₂) ₂	CH ₂ Cl ₂	-78 °C – rt	57	76:4:18:2
2	I(coll) ₂ PF ₆	MeO(CH ₂) ₂	CH ₃ CN	-20 °C – rt	85	80:6:12:2
3	NIS	MeO(CH ₂) ₂	CH ₃ CN	-20 °C – rt	41	72:12:15:1

^a Determined by ¹H NMR studies and chiral HPLC analysis; ^b (6*R*,10*S*):(6*R*,10*R*):(6*S*,10*S*):(6*S*,10*R*).

The other report of 6-*exo* iodocycloetherification from Fujioka was in fact a double iodocycloetherification shown in Scheme 1.29. The first iodocycloetherification took place in the typical 5-*exo* fashion that Fujioka normally reports but upon water opening the resulting oxonium, the subsequently formed hemiacetal **1.182**, with tertiary alcohol and second pendent olefin, underwent a second iodocycloetherification reaction, this time in a 6-*exo* fashion to yield **1.184**.

**Scheme 1.29. Formation of spiroketals through a 5-*exo*-6-*exo* double iodocycloetherification sequence.**

Díez Martín *et al.* published studies examining the stereoselectivity of iodocycloetherification to make 2,2,6,6-tetrasubstituted tetrahydropyrans as part of their efforts of synthesizing a variety of natural products that feature such polysubstituted tetrahydropyran motifs in their skeletons such as usneidone E (Figure 1.11. **1.185**).^{83,84} Starting from **1.186**, the 6-*exo* cyclized product was made in a stereoselective manner. Unfortunately, the authors did not examine any substrate scope but they did examine the stereoselectivity which is outlined in Scheme 1.30. *Trans*-**1.186** gave **1.188a** and **1.188b** in a 93:7 ratio while *cis*-**1.186** gave **1.188c** and **1.188d** with almost no selectivity in a ratio of 9:10. This was explained by both the inductive effects of the preference of C1-oxygenated acyclic alkenes for the eclipsed conformation as well as steric effects in the transition state. Considering these effects, transition state **1.187a** is more favourable than **1.187b** for *trans*-**1.186** while for *cis*-**1.186**, the transition states **1.187c** and **1.187d** have comparable energies due to interactions of the alcohol and benzyloxy groups.

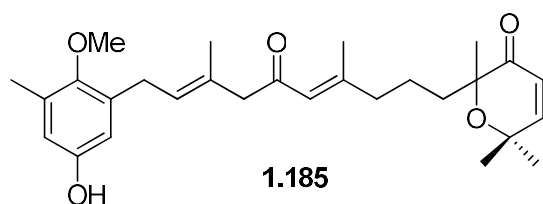
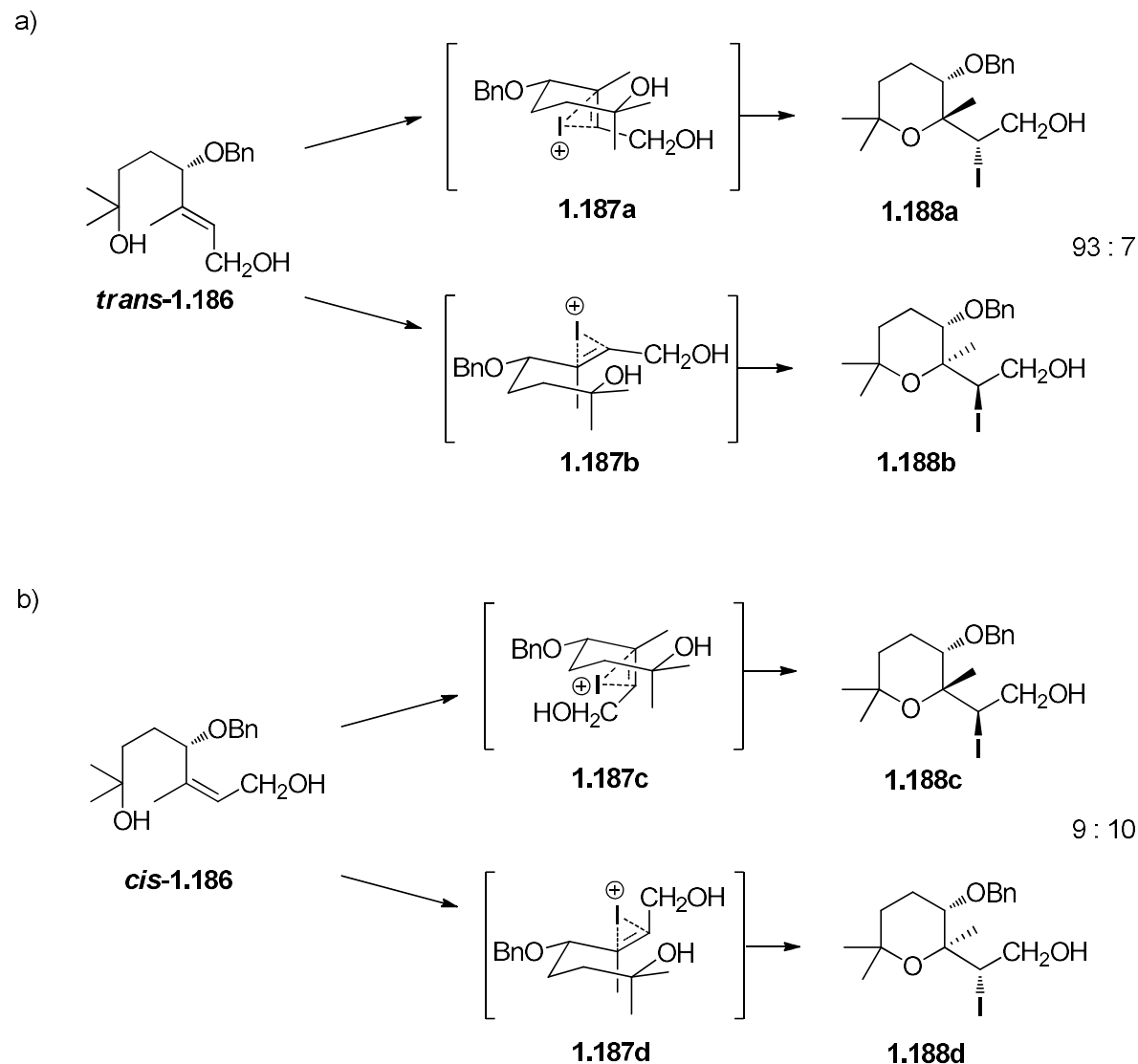


Figure 1.11. Structure of natural product usneidone E (1.185).

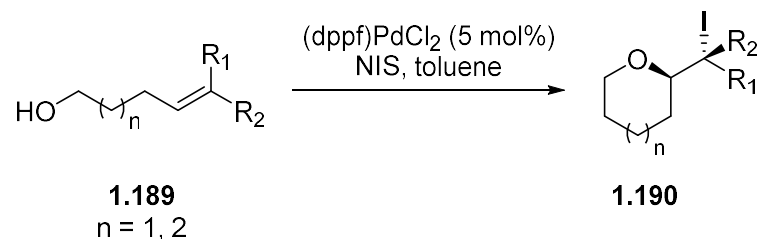


Scheme 1.30. Transition states and selectivity of iodocycloetherification of *trans*-1.186 and *cis*-1.186.

A fascinating study from the Morgan group explored using diphosphine palladium(II) complexes as catalysts for the iodocycloetherification of unactivated alkenes, with the goal of eventually developing a catalytic asymmetric version using chiral phosphines.⁸⁵ To suppress the rapid background rate of reaction, the reaction was run in toluene. After screening a variety of Pd(II) complexes, the most active was (dppf)PdCl₂. As they were expressly trying to cyclize unactivated alkenes, the only substrates tested to cyclize in a 6-*exo* fashion to give tetrahydropyrans were substrates containing either terminal olefin or alkyl substituted olefins. No

activated, aryl substituted olefins were tested in this study. All of the substrates underwent iodocycloetherification in good yields and excellent diastereoselectivity.

Table 1.18. Substrate effect on Pd(II)-catalyzed iodocycloetherification.

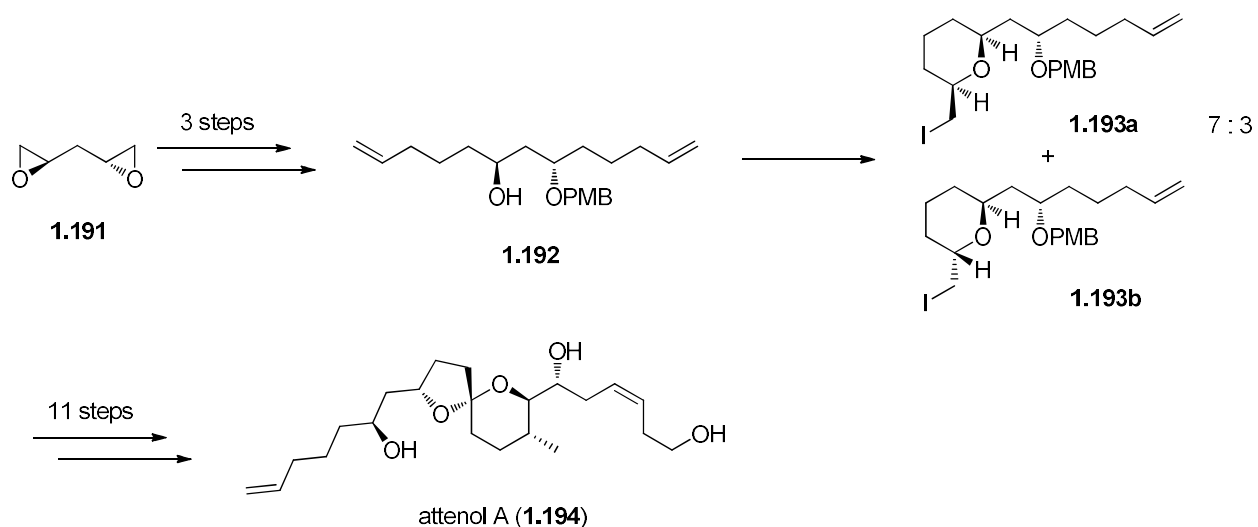


Entry	Alkene	Product	dr	Yield (%)
1	 1.189a	 1.190a	-	55
2	 1.189b	 1.190b	>20:1	61
3	 1.189c	 1.190c	>20:1	67

Tetrahydropyrans are quite common in natural products and bioactive molecules. Some examples of using 6-*exo* halocycloetherification, specifically the mild and most commonly used iodocycloetherification reaction, will be highlighted next.

Eustache and coworkers published a report on the synthesis of attenol A (**1.194**) that utilized a 6-*exo* iodocycloetherification reaction.⁸⁶ Attenol A is a densely functionalized asymmetric molecule that poses significant challenges to organic chemists. The authors used the 6-*exo* iodocycloetherification reaction for a rare purpose: the protection of a 5-alken-1-ol fragment. Of concern was the sensitivity of the primary iodide in the rest of the synthesis but fortunately, it was untouched until subjected to conditions specific to its removal to reveal the original 5-alken-1-ol

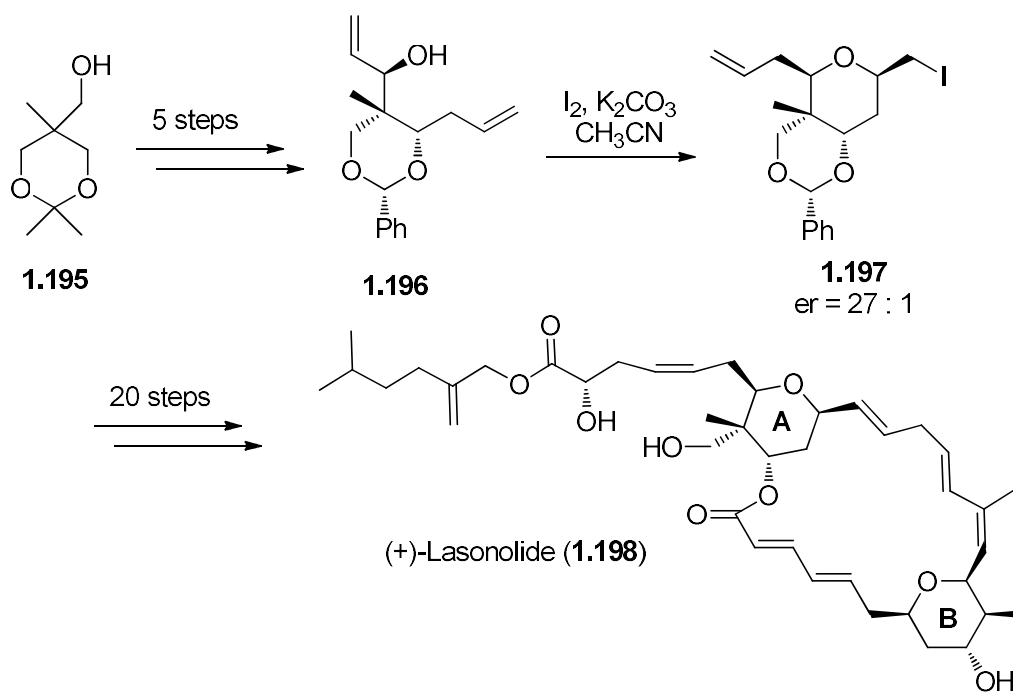
group. While the iodocycloetherification did go with moderate selectivity (7:3), as it was removed later, this was inconsequential. The abbreviated synthesis can be seen in Scheme 1.31.



Scheme 1.31. Synthesis of attenol A (1.194) using 6-*exo* iodocycloetherification as a protecting group for a 5-alken-1-ol fragment.

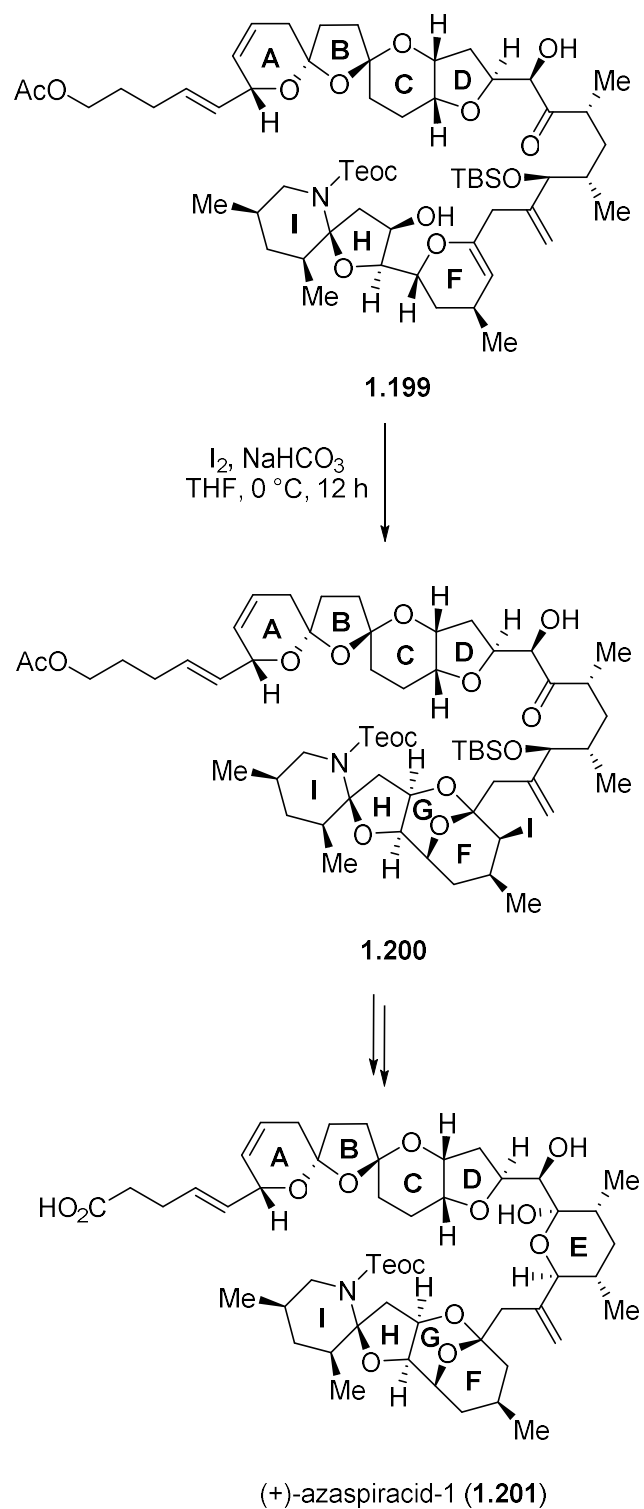
Kang *et al.* published the total synthesis of (+)-Lasonolide (**1.198**), a natural product isolated from the Caribbean marine sponge *Forcepia* sp. that is interesting for its antitumor activity against A-549 human lung carcinoma cells as well as its cell adhesion inhibition properties in cell assays to detect signal transduction agents.^{87,88} They used 6-*exo* iodocycloetherification to make the *cis*-2,6-disubstituted tetrahydropyran A-ring, **1.197** in an excellent 27:1 enantiomeric ratio. As

can be seen in Scheme 1.32, iodocycloetherification was used early in the synthesis that had a longest linear sequence of 26 steps and yielded the natural product in 7.4 % overall yield.



Scheme 1.32. Substrate-controlled enantioselective 6-*exo* iodocycloetherification reaction to make the A-ring in the total synthesis of (+)-Lasonolide (1.198).

The final example that will be presented here is Nicolaou and coworkers total synthesis and structural elucidation of azaspiracid-1 (**1.201**), leading to its final and correct structural assignment.⁸⁹ Through some degradation studies of the notorious marine biotoxin, they were able to identify the structure of the EFGHI domain, partly by using 6-*exo* iodocycloetherification to assemble the G-ring (**1.200**). Amazingly, this reaction could also be used very late in the total synthesis, as it was mild enough to not disturb any of the other functionality or stereochemistry in the molecule (Scheme 1.33).

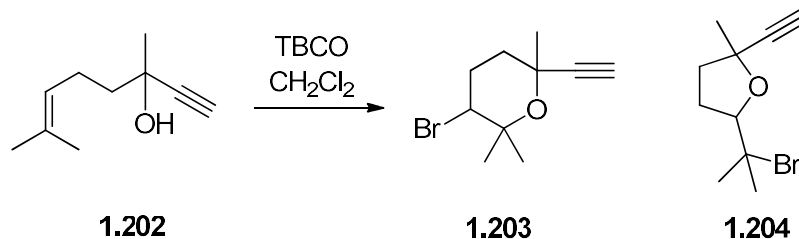


Scheme 1.33. Nicolaou's total synthesis of (+)-azaspiracid-1 (1.201) utilizing a 6-exo iodocycloetherification at a late stage in the synthesis.

1.3.8 6-endo halocycloetherification

Similar to 6-*exo* halocycloetherification, there are also only a few studies on the reactivity, regioselectivity and stereoselectivity of 6-*endo* halocycloetherification, yet there are several examples of this reactivity being employed in the synthesis of bioactive molecules and natural products. The studies that do exist will be discussed below and some of the applications of this reactivity will be highlighted herein.

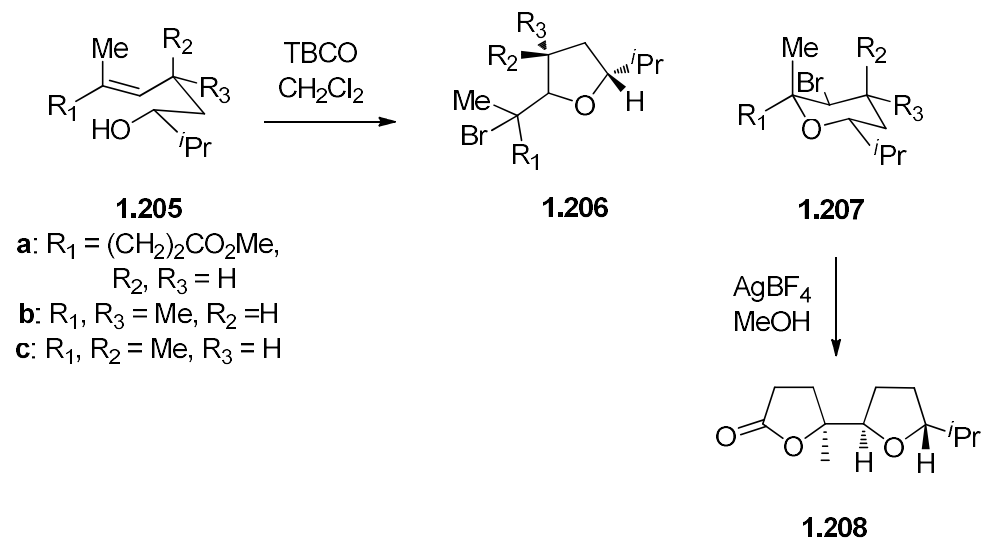
An early report of using bromocycloetherification in the literature came from Kato and coworkers in 1976 in regards to their efforts in cyclizing polyenes.⁹⁰ They discovered that when employing brominating agent 2,4,4,6-tetrabromocyclohexadienone (TBCO) with polyene **1.202**, they obtained a 6-*endo*-cyclized tetrahydropyran, **1.203**, and 5-*exo*-cyclized tetrahydrofuran, **1.204**, in a 4:1 mixture of regioisomers (Scheme 1.34). Interestingly, TBCO seemed to be inert to the acetylenic bond of **1.202**, indicating its utility as a regioselective brominating agent in polyunsaturated compounds containing alkynes. Additionally, it seemed to possess complimentary reactivity to NBS, which yielded tetrahydrofuran **1.204** as the major product.⁹¹



Scheme 1.34. 6-*endo* bromocycloetherification of polyenes using TBCO.

In 1984, the Bartlett group published a paper that focused on making *trans*-2,5-disubstituted tetrahydrofurans.⁹² Rather than making them directly through a 5-*endo* or 5-*exo* cyclization, they took advantage of the more readily attainable 1,3 relative asymmetric induction that 6-membered rings offer and instead made tetrahydropyrans in a diastereoselective fashion and then subsequently performed a ring contraction, preserving the stereochemistry, to give the tetrahydrofuran. For example, using substrate **1.205a**, the 6-*endo* bromocycloetherification worked excellently, giving **1.207a** in 78 % yield and >95 % diastereoselectivity. This was then successfully stereospecifically contracted to the tetrahydrofuran, **1.208a**, using silver tetrafluoroborate in methanol. An interesting example in this report is **1.205b**, which provided 88 % of **1.207b** and 11 % of **1.206b** upon bromocycloetherification, explained by the lack of 1,3-

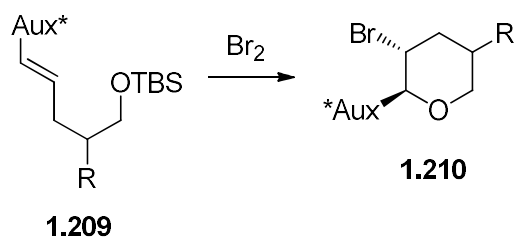
diaxial interactions in the transition state. In contrast, **1.205c** gives exclusively **1.206c** as a 2:1 diastereomeric mixture, showing clearly that Markovnikov selectivity is not enough to override 1,3-diaxial interactions when determining the regioselectivity (Scheme 1.35).



Scheme 1.35. Diastereoselective 6-*endo* synthesis of tetrahydropyrans and subsequent stereospecific ring contraction to *trans*-2,5-disubstituted tetrahydrofurans.

A study in 2007 from Hsung and coworkers showed that they could achieve enantioselective halocycloetherification of enamides using chiral auxiliaries.⁹³ They tested several different chiral auxiliaries including Evans' (Table 1.19, entry 1-4), Seebach's (Table 1.19, entry 5), Close's (Table 1.19, entry 6) and Sibi's (Table 1.19, entry 7) and found that the latter gave the best stereoselectivity. They also showed that they could synthesize larger ring systems with this methodology, including 7-, 8- and 10-membered cyclic ethers, although the yields start to drop off drastically in the latter case. These larger-ring systems will be discussed further in Chapter 3.

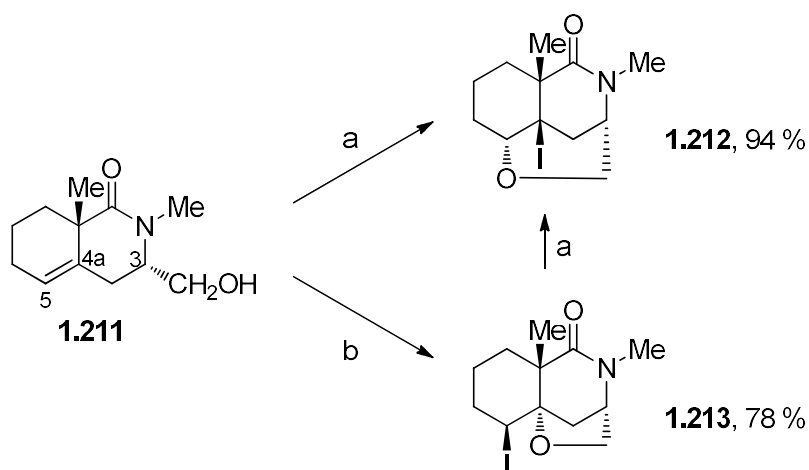
Table 1.19. Effects of chiral auxiliaries on the stereoselectivity of 6-endo bromocycloetherification of enamides.



Entry ^a	Product	Yield (%) ^b [er]	Entry	Product	Yield (%) ^b [er]
1	 1.210a	87 [2.8:1]	5	 1.210e	92 [7.7:1]
2	 1.210b	91 [3:1]	6	 1.210f	63 [5.8:1]
3	 1.210c	83 [7.4:1]	7	 1.210g	90 [9:1]
4	 1.210d	72 [2.8:1] ^c			

^a Conditions: At -78 °C in toluene or CH₂Cl₂, added Br₂ [0.5 M in CH₂Cl₂] and stirred from -78 °C to rt over 0.5-2 h.; ^b Isolated yields; ^c Diastereomeric ratio, not enantiomeric ratio.

In efforts to show the value of introducing a stereodirecting group in the C3 position of **1.211** to influence the functionalization of the C4a-C5 olefin, Schultz *et al.* demonstrated the stereoselective functionalization of the double bond by iodocycloetherification and that the regioselectivity could be manipulated by running the reaction under kinetic or thermodynamic conditions.⁹⁴ Under thermodynamic control, they obtained iodotetrahydropyran **1.212** and under kinetic control they obtained iodotetrahydrofuran **1.213**. Additionally, the kinetic product could be converted to the thermodynamic product upon treatment with thermodynamic conditions (Scheme 1.36).



Scheme 1.36. Kinetic and thermodynamic control of iodocycloetherification. Conditions: a) I₂, THF, H₂O, 25 °C, 96 h; b) NIS, CH₂Cl₂, NaHCO₃, 0 °C, 3 h.

Waal A is a natural product derived from the fermentation broth of *Myceliophthora lutea* TF-0409 that shows a broad spectrum of activity against several cultured tumor cell lines including adriamycin-resistant HL-60 cells.⁹⁵ Upon close inspection of the spectroscopic data of waal A, Gao and Snider noticed some inconsistencies with the proposed structure (**1.214**).⁹⁶ They suggested a revised ring system (**1.215**) that was also supported by spectroscopic similarities with the closely related compounds TAN-2483A (**1.216**) and TAN-2483B (**1.217**) (Figure 1.12). Using a stereoselective 6-*endo* iodocycloetherification, they were able to synthesize **1.218** and confirm by comparing spectral data that **1.218** is the correct structure of waal A (Scheme 1.37). They encountered difficulties cyclizing the desired isomer using traditional I₂, NaHCO₃ conditions, while iodocycloetherification of the undesired isomer went in 70 % yield under the same conditions. They postulated that the desired cyclization would have to occur through the

disfavoured π -complex **1.223b** with the hydrogen eclipsed by the double bond and the undesired cyclization would occur through the favoured π -complex **1.223a** with the alcohol eclipsed by the double bond. They overcame this problem by simply using a stronger iodinating agent, bis(*sym*-collidine)IPF₆. In same article, the authors also used this methodology to synthesize other related natural products, massarilactone B (**1.219**) and fusidilactone B (**1.220**) (Figure 1.12).

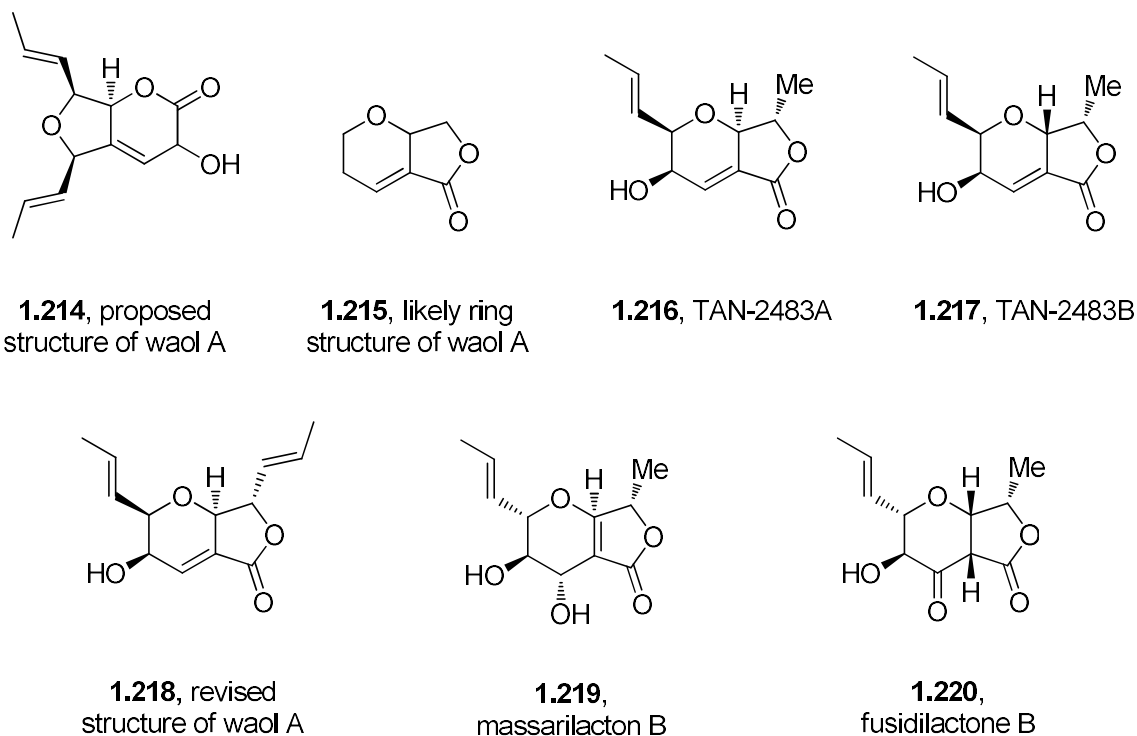
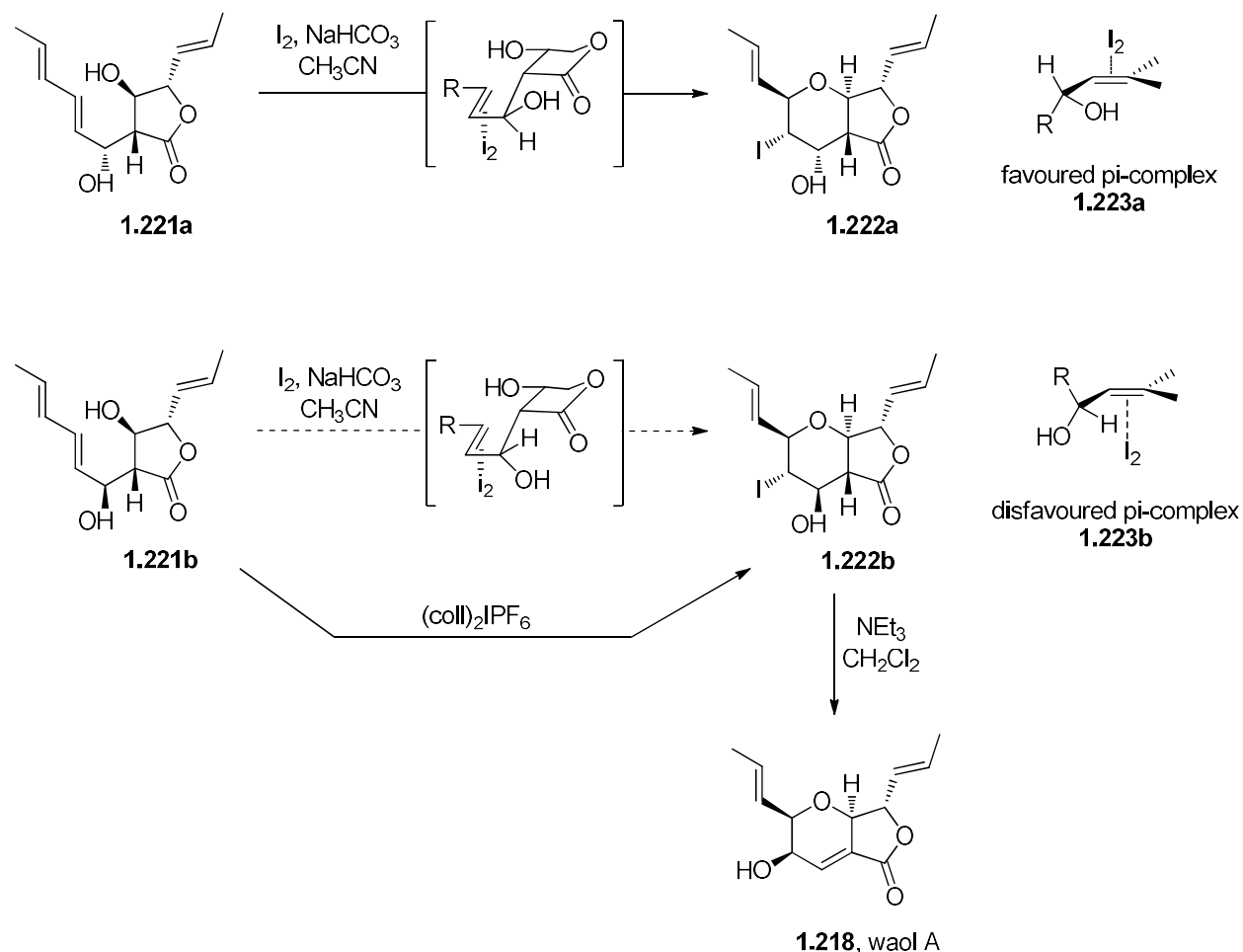
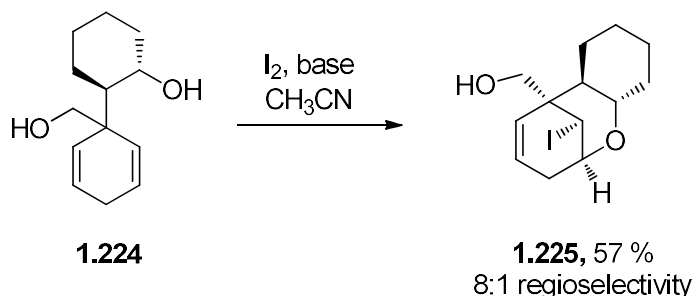


Figure 1.12. Proposed structure of waol A (**1.214**), structures of TAN-2483A (**1.216**) and TAN-2483B (**1.217**), revised structure of waol A (**1.218**) and structures of massarilactone B (**1.219**) and fusidilactone B (**1.220**).



Scheme 1.37. Stereoselective 6-*endo* iodocycloetherification in the synthesis and efforts towards the confirmation of the revised structure of woal A (1.218).

In a report previously mentioned in Chapter 1.3.6 where Elliott and coworkers reported desymmetrization of cyclohexadienes via a 5-*endo* iodocycloetherification (Scheme 1.27), they also reported desymmetrization of the cyclohexadienes with alcohols on ethylene or propylene linkers containing the presence of chiral centers on the backbone chain of the pendent alcohol to induce diastereoselectivity.⁸⁰ While they reported obtaining not exclusively the 5-*exo* products but also minor amounts of the 6-*endo* product when an ethylene chain was used, they in fact were able to identify a particular substrate, **1.224**, which favoured the formation of the 6-*endo* product to give complex tricyclic ring system **1.225**, although only in moderate yield (Scheme 1.38). When a propylene chain was used, they saw preference for the 6-*exo* product but also obtained 10 % yield of the 7-*endo* product. This example will be discussed further in Chapter 3.



Scheme 1.38. Synthesis of a tricyclic ring structure via 6-*endo* iodocycloetherification.

1.4 Conclusion and Perspective

In this chapter, the prevalence of halocycloetherification reactions in the literature has been highlighted, organized by the size of the ring formed (3-membered to 6-membered rings) and the mode of cyclization (*endo* or *exo*). The focus was on reports that were the most scientifically insightful, synthetically important or utilized these versatile reactions in the syntheses of natural products or bioactive molecules.

While fluorocycloetherifications that proceed through fluoriranium ions are chiefly lacking in the literature and chlorocycloetherifications are still relatively rare, bromo- and iodocycloetherification are very common reactions because these halogens are much more reactive than their fluoro- and chloro- counterparts and have therefore been the focus of much of the research done in the field. Despite the inherent difficulties associated with the racemization of brom- and iodiraniums via olefin-to-olefin transfer, there has been a lot of work in the development of highly regio- and diastereo- or enantioselective halocycloetherifications. Interestingly, there has even been significant progress made in the catalytic enantioselective variations of these halocycloetherification reactions, most notably those examples highlighted in Chapter 1.3.5.2. While there is still a lot of room for work in this field, these studies have laid the ground work for scientists going forward.

The importance of these reactions can be easily recognized by the number of organohalogen containing natural products that exist, the interesting motifs that can be synthesized via halocycloetherification reactions, and the synthetic handles that halogens provide when synthesizing natural products and biologically relevant molecules. Expanding this reactivity into fluorocycloetherification with predictable regio- and stereoselectivity would also mark a great step

forward in this field due to the marked number of pharmaceuticals containing fluorine and the likely increasing number of such compounds.^{97,98}

1.5 References

- (1) Reynolds, J. W. *Q. J. Chem. Soc.* **1851**, 3, 111.
- (2) Roberts, I.; Kimball, G. E. *J. Am. Chem. Soc.* **1937**, 59, 947.
- (3) Olah, G. A.; Bollinger, J. M. *J. Am. Chem. Soc.* **1967**, 89, 4744.
- (4) Terashima, S.; Jew, S.-s. *Tetrahedron Lett.* **1977**, 18, 1005.
- (5) Jew, S. s.; Terashima, S.; Koga, K. *Tetrahedron* **1979**, 35, 2337.
- (6) Jew, S. S.; Terashima, S.; Koga, K. *Tetrahedron* **1979**, 35, 2345.
- (7) Grossman, R. B.; Trupp, R. J. *Can. J. Chem.* **1998**, 76, 1233.
- (8) Haas, J.; Piguel, S.; Wirth, T. *Org. Lett.* **2002**, 4, 297.
- (9) Lucas, H. J.; Gould, C. W. *J. Am. Chem. Soc.* **1941**, 63, 2541.
- (10) Winstein, S.; Seymour, D. *J. Am. Chem. Soc.* **1946**, 68, 119.
- (11) Bennet, A. J.; Brown, R. S.; McClung, R. E. D.; Klobukowski, M.; Aarts, G. H. M.; Santarsiero, B. D.; Bellucci, G.; Bianchini, R. *J. Am. Chem. Soc.* **1991**, 113, 8532.
- (12) Brown, R. S.; Nagorski, R. W.; Bennet, A. J.; McClung, R. E. D.; Aarts, G. H. M.; Klobukowski, M.; McDonald, R.; Santarsiero, B. D. *J. Am. Chem. Soc.* **1994**, 116, 2448.
- (13) Neverov, A. A.; Brown, R. S. *J. Org. Chem.* **1996**, 61, 962.
- (14) Brown, R. S. *Acc. Chem. Res.* **1997**, 30, 131.
- (15) Neverov, A. A.; Brown, R. S. *J. Org. Chem.* **1998**, 63, 5977.
- (16) Denmark, S. E.; Burk, M. T. *Proc. Natl. Acad. Sci. U. S. A.* **2010**, 107, 20655.
- (17) Denmark, S. E.; Burk, M. T.; Hoover, A. J. *J. Am. Chem. Soc.* **2010**, 132, 1232.
- (18) Gribble, G. W. *Acc. Chem. Res.* **1998**, 31, 141.
- (19) Baldwin, J. E. *J. Chem. Soc., Chem. Commun.* **1976**, 734.
- (20) Nicponski, D. R. *Tetrahedron Lett.* **2014**, 55, 2075.
- (21) Lourie, L. F.; Serguchev, Y. A.; Ponomarenko, M. V.; Rusanov, E. B.; Vovk, M. V.; Ignat'ev, N. V. *Tetrahedron* **2013**, 69, 833.
- (22) Lozano, O.; Blessley, G.; Martinez del Campo, T.; Thompson, A. L.; Giuffredi, G. T.; Bettati, M.; Walker, M.; Borman, R.; Gouverneur, V. *Angew. Chem. Int. Ed.* **2011**, 50, 8105.
- (23) Wolstenhulme, J. R.; Gouverneur, V. *Acc. Chem. Res.* **2014**, 47, 3560.
- (24) Nguyen, V.; Cheng, X.; Morton, T. H. *J. Am. Chem. Soc.* **1992**, 114, 7127.

- (25) Struble, M. D.; Scerba, M. T.; Siegler, M.; Lectka, T. *Science* **2013**, *340*, 57.
- (26) Struble, M. D.; Holl, M. G.; Scerba, M. T.; Siegler, M. A.; Lectka, T. *J. Am. Chem. Soc.* **2015**, *137*, 11476.
- (27) Diner, U. E.; Worsley, M.; Lown, J. W. *J. Chem. Soc. C* **1971**, 3131.
- (28) Winstein, S.; Goodman, L. *J. Am. Chem. Soc.* **1954**, *76*, 4368.
- (29) Ganem, B. *J. Am. Chem. Soc.* **1976**, *98*, 858.
- (30) Midland, M. M.; Halterman, R. L. *J. Org. Chem.* **1981**, *46*, 1227.
- (31) Evans, R. D.; Magee, J. W.; Schauble, J. H. *Synthesis* **1988**, *11*, 862.
- (32) Shen, Z.; Pan, X.; Lai, Y.; Hu, J.; Wan, X.; Li, X.; Zhang, H.; Xie, W. *Chem. Sci.* **2015**, *6*, 6986.
- (33) Malapit, C. A.; Howell, A. R. *J. Org. Chem.* **2015**, *80*, 8489.
- (34) Ehlinger, E.; Magnus, P. *J. Am. Chem. Soc.* **1980**, *102*, 5004.
- (35) Arjona, O.; de la Pradilla, R. F.; Plumet, J.; Viso, A. *Tetrahedron* **1989**, *45*, 4565.
- (36) Rofoo, M.; Roux, M.-C.; Rousseau, G. *Tetrahedron Lett.* **2001**, *42*, 2481.
- (37) Galatsis, P.; Millan, S. D.; Nechala, P.; Ferguson, G. *J. Org. Chem.* **1994**, *59*, 6643.
- (38) Galatsis, P.; Parks, D. J. *Tetrahedron Lett.* **1994**, *35*, 6611.
- (39) Galatsis, P.; Millan, S. D.; Ferguson, G. *J. Org. Chem.* **1997**, *62*, 5048.
- (40) Wang, G.; Wang, Y.; Arcari, J. T.; Howell, A. R.; Rheingold, A. L.; Concolino, T. *Tetrahedron Lett.* **1999**, *40*, 7051.
- (41) Vasconcelos, R. S.; Silva, L. F.; Giannis, A. *J. Org. Chem.* **2011**, *76*, 1499.
- (42) Albert, S.; Robin, S.; Rousseau, G. *Tetrahedron Lett.* **2001**, *42*, 2477.
- (43) Homsí, F.; Rousseau, G. *J. Org. Chem.* **1999**, *64*, 81.
- (44) Chang, M.-Y.; Tsai, C.-Y.; Wu, M.-H. *Tetrahedron* **2013**, *69*, 6364.
- (45) Rychnovsky, S. D.; Bartlett, P. A. *J. Am. Chem. Soc.* **1981**, *103*, 3963.
- (46) Tamaru, Y.; Kawamura, S.-i.; Yoshida, Z.-i. *Tetrahedron Lett.* **1985**, *26*, 2885.
- (47) Tonn, C. E.; Palazon, J. M.; Ruizperez, C.; Rodriguez, M. L.; Martin, V. S. *Tetrahedron Lett.* **1988**, *29*, 3149.
- (48) Tănase, C. I.; Drăghici, C.; Shova, S.; Cojocar, A.; Maganu, M.; Munteanu, C. V. A.; Cocu, F. *Tetrahedron* **2015**, *71*, 6852.
- (49) Mootoo, D. R.; Date, V.; Fraser-Reid, B. *J. Am. Chem. Soc.* **1988**, *110*, 2662.
- (50) Llera, J. M.; Lopez, J. C.; Fraser-Reid, B. *J. Org. Chem.* **1990**, *55*, 2997.

- (51) Fujioka, H.; Ohba, Y.; Nakahara, K.; Takatsuji, M.; Murai, K.; Ito, M.; Kita, Y. *Org. Lett.* **2007**, *9*, 5605.
- (52) Fujioka, H.; Kitagawa, H.; Nagatomi, Y.; Kita, Y. *J. Org. Chem.* **1996**, *61*, 7309.
- (53) Fujioka, H.; Kotoku, N.; Sawama, Y.; Kitagawa, H.; Ohba, Y.; Wang, T.-L.; Nagatomi, Y.; Kita, Y. *Chem. Pharm. Bull.* **2005**, *53*, 952.
- (54) Fujioka, H.; Ohba, Y.; Hirose, H.; Murai, K.; Kita, Y. *Angew. Chem. Int. Ed.* **2005**, *44*, 734.
- (55) Fujioka, H.; Ohba, Y.; Hirose, H.; Nakahara, K.; Murai, K.; Kita, Y. *Tetrahedron* **2008**, *64*, 4233.
- (56) Fujioka, H.; Nagatomi, Y.; Kotoku, N.; Kitagawa, H.; Kita, Y. *Tetrahedron* **2000**, *56*, 10141.
- (57) Fujioka, H.; Fujita, T.; Kotoku, N.; Ohba, Y.; Nagatomi, Y.; Hiramatsu, A.; Kita, Y. *Chem. Eur. J.* **2004**, *10*, 5386.
- (58) Fujioka, H.; Kotoku, N.; Nagatomi, Y.; Kita, Y. *Tetrahedron Lett.* **2000**, *41*, 1829.
- (59) Fujioka, H.; Nakahara, K.; Hirose, H.; Hirano, K.; Oki, T.; Kita, Y. *Chem. Commun.* **2011**, *47*, 1060.
- (60) Kitagawa, O.; Hanano, T.; Tanabe, K.; Shiro, M.; Taguchi, T. *J. Chem. Soc., Chem. Commun.* **1992**, 1005.
- (61) Kang, S. H.; Lee, S. B.; Park, C. M. *J. Am. Chem. Soc.* **2003**, *125*, 15748.
- (62) Kwon, H. Y.; Park, C. M.; Lee, S. B.; Youn, J.-H.; Kang, S. H. *Chem. Eur. J.* **2008**, *14*, 1023.
- (63) Kang, S. H.; Park, C. M.; Lee, S. B.; Kim, M. *Synlett* **2004**, *2004*, 1279.
- (64) Kang, S.-H.; Park, C.-M.; Lee, S.-B. *Bull. Korean Chem. Soc.* **2004**, *25*, 1615.
- (65) Denmark, S. E.; Burk, M. T. *Org. Lett.* **2012**, *14*, 256.
- (66) Hennecke, U.; Müller, C. H.; Fröhlich, R. *Org. Lett.* **2011**, *13*, 860.
- (67) Huang, D.; Wang, H.; Xue, F.; Guan, H.; Li, L.; Peng, X.; Shi, Y. *Org. Lett.* **2011**, *13*, 6350.
- (68) Müller, C. H.; Rösner, C.; Hennecke, U. *Chem. Asian J.* **2014**, *9*, 2162.
- (69) Ke, Z.; Tan, C. K.; Chen, F.; Yeung, Y. Y. *J. Am. Chem. Soc.* **2014**, *136*, 5627.
- (70) Ke, Z. H.; Tan, C. K.; Liu, Y.; Lee, K. G. Z.; Yeung, Y. Y. *Tetrahedron* **2016**, *72*, 2683.
- (71) Tay, D. W.; Leung, G. Y. C.; Yeung, Y.-Y. *Angew. Chem. Int. Ed.* **2014**, *53*, 5161.

- (72) Ho Kang, S.; Bae Lee, S. *Tetrahedron Lett.* **1993**, *34*, 1955.
- (73) Galatsis, P.; Manwell, J. J. *Tetrahedron Lett.* **1995**, *36*, 8179.
- (74) Lipshutz, B. H.; Barton, J. C. *J. Am. Chem. Soc.* **1992**, *114*, 1084.
- (75) Barks, J. M.; Knight, D. W.; Seaman, C. J.; Weingarten, G. G. *Tetrahedron Lett.* **1994**, *35*, 7259.
- (76) B. Bedford, S.; E. Bell, K.; Bennett, F.; J. Hayes, C.; W. Knight, D.; E. Shaw, D. *J. Chem. Soc., Perkin Trans. 1* **1999**, 2143.
- (77) Bennett, F.; Bedford, S. B.; Bell, K. E.; Fenton, G.; Knight, D. W.; Shaw, D. *Tetrahedron Lett.* **1992**, *33*, 6507.
- (78) Bedford, S. B.; Bell, K. E.; Fenton, G.; Hayes, C. J.; Knight, D. W.; Shaw, D. *Tetrahedron Lett.* **1992**, *33*, 6511.
- (79) Bew, S. P.; Barks, J. M.; Knight, D. W.; Middleton, R. J. *Tetrahedron Lett.* **2000**, *41*, 4447.
- (80) Butters, M.; Elliott, M. C.; Hill-Cousins, J.; Paine, J. S.; Walker, J. K. E. *Org. Lett.* **2007**, *9*, 3635.
- (81) Zeng, X.; Miao, C.; Wang, S.; Xia, C.; Sun, W. *Chem. Commun.* **2013**, *49*, 2418.
- (82) Zárraga, M.; Rodríguez, M. L.; Ruiz-Pérez, C.; Martín, J. D. *Tetrahedron Lett.* **1989**, *30*, 3725.
- (83) Díez Martín, D.; Marcos, I. S.; Basabe, P.; Romero, R. E.; Moro, R. F.; Lumeras, W.; Rodríguez, L.; Urones, J. G. *Synthesis* **2001**, *2001*, 1013.
- (84) Díez, D.; Núñez, M. G.; Moro, R. F.; Lumeras, W.; Marcos, I. S.; Basabe, P.; Urones, J. G. *Synlett* **2006**, *2006*, 939.
- (85) Doroski, T. A.; Cox, M. R.; Morgan, J. B. *Tetrahedron Lett.* **2009**, *50*, 5162.
- (86) Van de Weghe, P.; Aoun, D.; Boiteau, J.-G.; Eustache, J. *Org. Lett.* **2002**, *4*, 4105.
- (87) Horton, P. A.; Koehn, F. E.; Longley, R. E.; McConnell, O. J. *J. Am. Chem. Soc.* **1994**, *116*, 6015.
- (88) Kang, S. H.; Kang, S. Y.; Kim, C. M.; Choi, H. W.; Jun, H. S.; Lee, B. M.; Park, C. M.; Jeong, J. W. *Angew. Chem. Int. Ed.* **2003**, *42*, 4779.
- (89) Nicolaou, K. C.; Koftis, T. V.; Vyskocil, S.; Petrovic, G.; Tang, W.; Frederick, M. O.; Chen, D. Y. K.; Li, Y.; Ling, T.; Yamada, Y. M. A. *J. Am. Chem. Soc.* **2006**, *128*, 2859.
- (90) Kato, T.; Ichinose, I.; Hosogai, T.; Kitahara, Y. *Chem. Lett.* **1976**, 1187.
- (91) Demole, E.; Enggist, P. *Helv. Chim. Acta* **1971**, *54*, 456.

- (92) Ting, P. C.; Bartlett, P. A. *J. Am. Chem. Soc.* **1984**, *106*, 2668.
- (93) Ko, C.; Hsung, R. P.; Al-Rashid, Z. F.; Feltenberger, J. B.; Lu, T.; Yang, J.-H.; Wei, Y.; Zifcsak, C. A. *Org. Lett.* **2007**, *9*, 4459.
- (94) Schultz, A. G.; Guzi, T. J.; Larsson, E.; Rahm, R.; Thakkar, K.; Bidlack, J. M. *J. Org. Chem.* **1998**, *63*, 7795.
- (95) Nozawa, O.; Okazaki, T.; Sakai, N.; Komurasaki, T.; Hanada, K.; Morimoto, S.; Chen, Z.-X.; He, B.-M.; Mizoue, K. *J. Antibiot.* **1995**, *48*, 113.
- (96) Gao, X.; Snider, B. B. *J. Org. Chem.* **2004**, *69*, 5517.
- (97) Wang, J.; Sánchez-Roselló, M.; Aceña, J. L.; del Pozo, C.; Sorochinsky, A. E.; Fustero, S.; Soloshonok, V. A.; Liu, H. *Chem. Rev.* **2014**, *114*, 2432.
- (98) Müller, K.; Faeh, C.; Diederich, F. *Science* **2007**, *317*, 1881.

Chapter 2 Synthesis of chiral polysubstituted oxazepanes and morpholines

2.1 Preface

The significance of halocycloetherification in synthesis was demonstrated in Chapter 1. Studying the literature closely revealed that there is a need for efficient synthetic approaches of making morpholines and oxazepanes, motifs that are common in natural products and bioactive molecules.

A general synthetic route for the synthesis of *N*-sulfonamide protected oxazepanes and morpholines is presented in this chapter. This route was designed to give access to both heterocycles through regioselective reactions: morpholine derivatives through 6-*exo* cyclization and oxazepane derivatives through 7-*endo* cyclization. Conditions were also examined. Any optimization done in the R6 position of **2.35** other than the nosyl protecting group was done by Rana Bilbeisi in the Moitessier lab. Synthesis and characterization of compounds **2.39a**, **2.39d**, **2.39e** and **2.39i** were completed before I joined the Moitessier lab by either Rana Bilbeisi or Dr. Sylvestre Toumieux.

2.2 Introduction

Molecular scaffolds such as mono- and bicyclic structures are of utmost interest in medicinal chemistry and more specifically in the preparation of geometrically constrained peptidomimetics or in the preparation of a focused library where the scaffolds contain orthogonally protected functionalizable groups. Thus a number of potent enzyme inhibitors¹⁻³ and receptor antagonists^{4,5} built around (bi)cyclic scaffolds have been reported. In parallel, a number of scaffolds inducing turns observed in proteins or peptides have been developed.^{6,7} However, the number of readily available scaffolds remains limited or their lengthy synthesis remains to be improved. As a result, developing synthetic strategies to prepare molecular scaffolds is an active field.⁸⁻¹¹

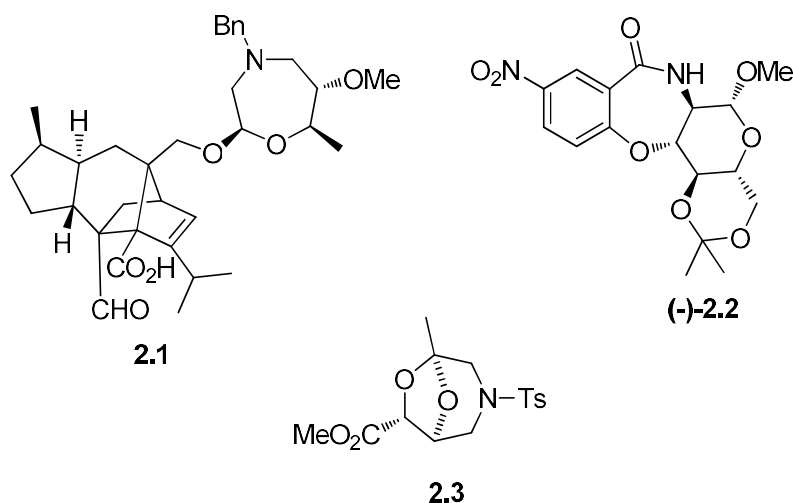
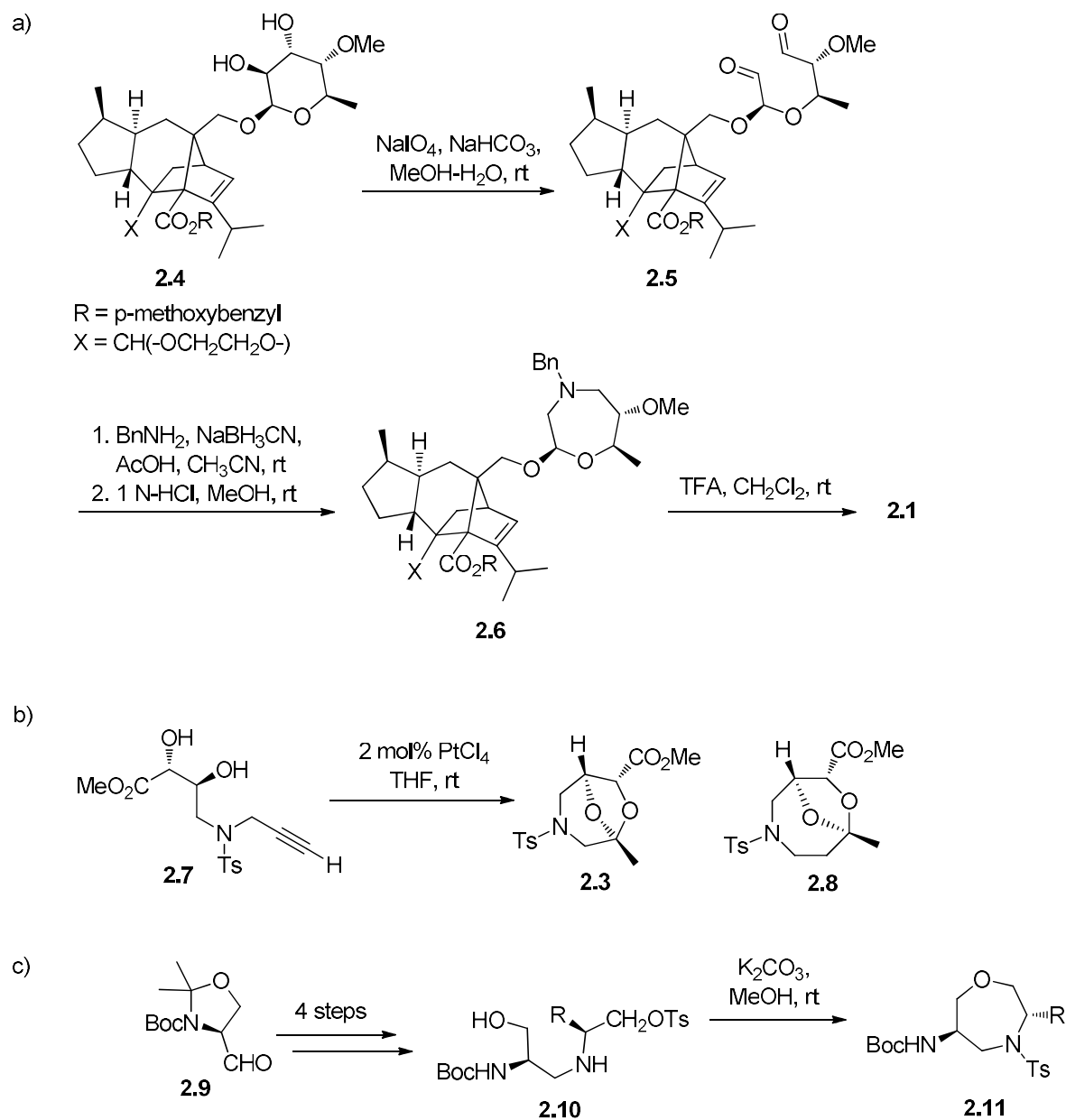


Figure 2.1. Reported synthetic oxazepanes.

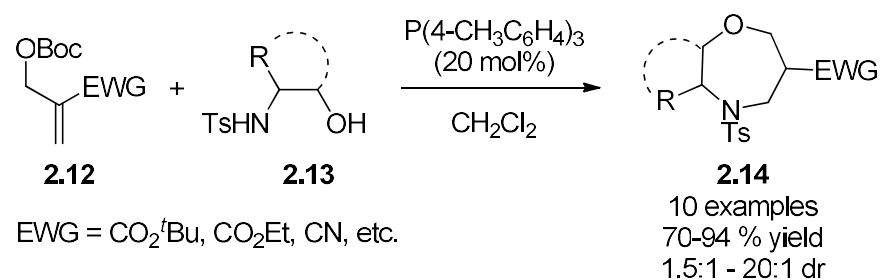
Despite the discovery of bioactive oxazepane derivatives such as antifungal **2.1**¹² and many reports on synthesis of oxazepinones (e.g., **2.2**¹³),¹⁴⁻¹⁶ very little attention has been devoted to the synthesis of polysubstituted chiral oxazepane derivatives. In addition, most of these reports focused on benzoxazepines.^{17,18} In fact, an exhaustive search of the literature revealed that very few syntheses of chiral polysubstituted oxazepanes have been reported. For example, Machetti and co-workers¹⁹ then Ley *et al.*²⁰ have reported efficient methods to prepare bridged oxazepanes around acetal functional groups (**2.3**, Figure 2.1).



Scheme 2.1. a) Synthesis of oxazepanes by ring expansion as reported by Kaneko, *et al.*, b) platinum-catalyzed synthesis of fused bicyclic oxazepane containing acetals as reported by Diéguez-Vásquez, *et al.* and c) synthesis of 1,4-oxazepanes from Garner aldehydes as reported by Panda, *et al.*

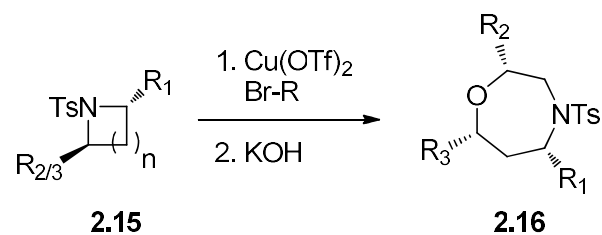
In fact, most of the reported syntheses of oxazepanes rely on acetalization of ketones, intramolecular opening of epoxides or ring expansion¹² (e.g., from carbohydrates^{21,22}) as can be seen in Scheme 2.1a. A few other methods catalyzed by transition metals have been reported such as the palladium-catalyzed cyclization of allenols²³ and platinum-catalyzed cyclization of 6-

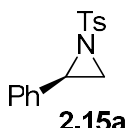
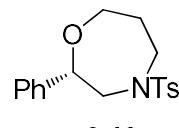
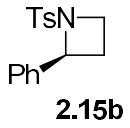
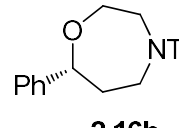
heptyne-1,2-diols (Scheme 2.1b).²⁰ Panda and co-workers reported a route to 1,4-oxazepanes starting from Garner aldehydes (Scheme 2.1c).²⁴ In 2012, He and co-workers reported a phosphine-triggered tandem annulation reaction between Morita-Baylis-Hillman carbonates and β -amino alcohols as well as other dinucleophiles to synthesize 1,4-oxazepanes and other 1,4-diheteroatom 7-membered rings (Scheme 2.2).²⁵ Ghorai and coworkers reported in 2009 a one-pot Cu-catalyzed ring-opening, cyclization sequence for making 1,4-oxazepanes.²⁶ They were able to get variability in the substitution pattern of the oxazepane based on the size of the starting ring and the length of the carbon chain of the haloalcohol (Table 2.1).



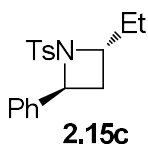
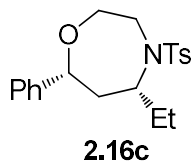
Scheme 2.2. Synthesis of 1,4-oxazepanes **2.14** from carbonates **2.12** and dinucleophiles **2.13**.

Table 2.1. One-pot synthesis of 1,4-oxazepanes via ring-opening of aziridines and azetidines.



Entry	Starting Material	Haloalcohol ^a	Major Product	Yield (%) ^b	ee (%) ^c
1	 2.15a	Br(CH ₂) ₃ OH	 2.16a	87	86
2	 2.15b	Br(CH ₂) ₂ OH	 2.16b	62	56

3

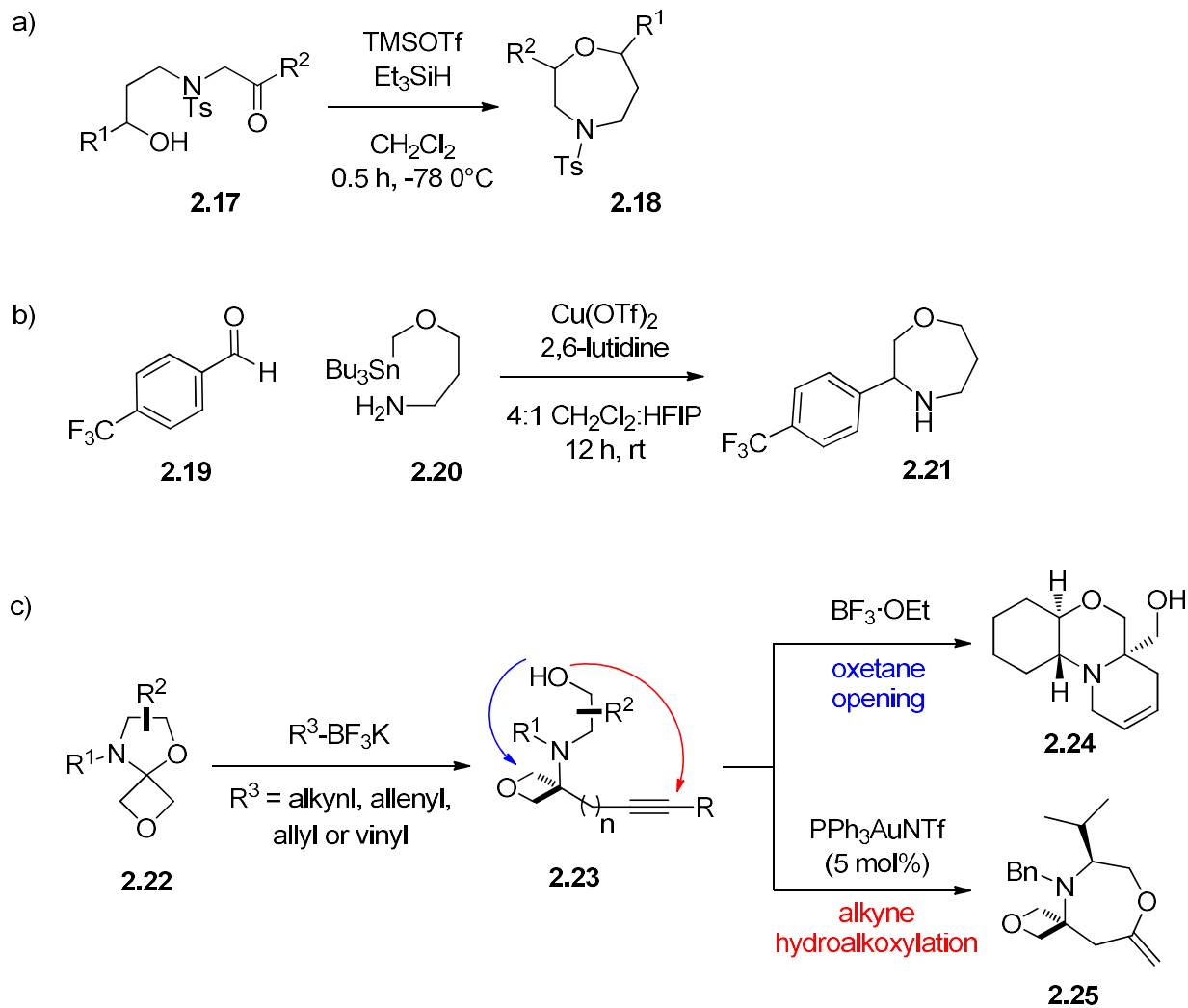
Br(CH₂)₂OH

70

99

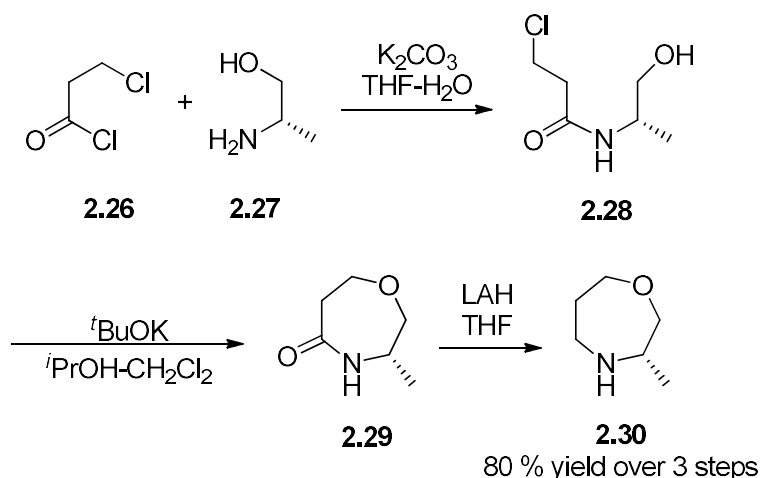
^a In all cases, the alcohol served as the solvent; ^b Yield of isolated product after purification by column chromatography; ^c Determined by chiral HPLC.

Following our report in 2013²⁷, there were several reports on the synthesis of chiral polysubstituted 1,4-oxazepanes. Gharpure and Prasad reported a method of stereoselectively synthesizing *cis*-disubstituted 1,4-oxazepanes **2.18** via the reductive etherification of sulfonamide containing keto alcohols **2.17** under Lewis acidic conditions.²⁸ Their method was also expandable to mono- and tri-substituted oxazepanes. They attribute the excellent observed stereoselectivity to the cyclic oxonium intermediate preferring a chair-like conformation rather than a twisted-boat like conformation, thereby placing all the substituents in pseudo-equatorial positions and avoiding significant 1,3-diaxial interaction. This forces the incoming nucleophile to attack in an axial direction (Scheme 2.3a). A notable publication by Bode and co-workers reported the synthesis of several diheteroatom 6-, 7-, 8- and 9-membered rings by a copper (II)-catalyzed reaction between aldehydes such as **2.19** and “SnAP” (Sn amino protocol) reagents such as **2.20**.^{29,30} They report mono- and *cis*-disubstituted fully saturated, N-unprotected 1,4-oxazepanes (e.g. **2.21**) in moderate to good yields (43-86 %) and diastereoselectivities of >10:1 (Scheme 2.3b). A report by Brady and Carreira uses 3-oxetanone-derived *N,O*-acetals **2.22** to make 3-amino oxetanes **2.23** by a nucleophilic addition of alkyne potassium trifluoroborates. Depending on the conditions used in the next step, they were able to make morpholines **2.24** via Lewis acid promoted oxetane opening or oxazepanes **2.25** via a Au-catalyzed 7-*exo-dig* hydroalkoxylation (Scheme 2.3c).³¹



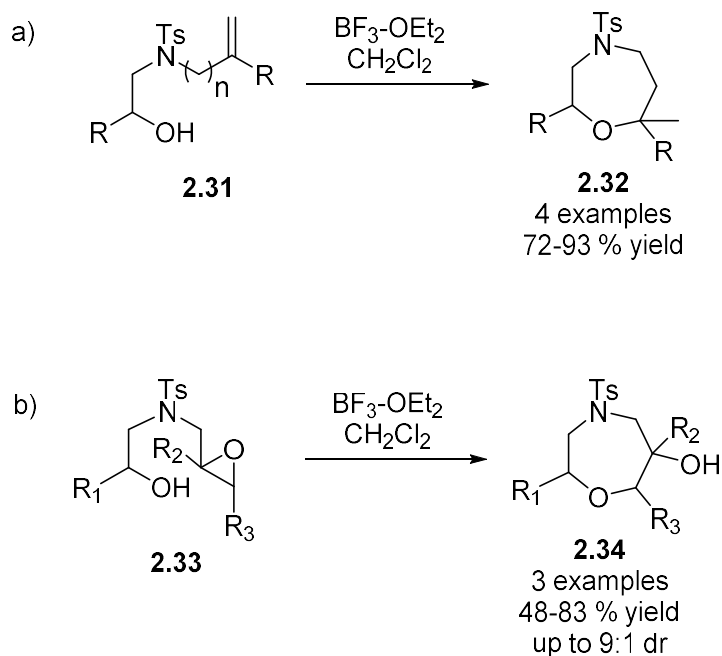
Scheme 2.3. Synthesis of chiral substituted oxazepanes from 1) Gharpure and Prasad, b) Bode and coworkers and c) Brady and Carrera.

In 2014, Mahajan and coworkers reported the synthesis of substituted morpholines by a sequence of coupling, cyclization and reduction reactions.³² In this report, they made a single 1,4-oxazepane (**2.30**), the synthesis of which can be seen in Scheme 2.4.



Scheme 2.4. Synthesis of **2.30** via a coupling, cyclization, reduction sequence of reactions.

In recent reports from Saikia and coworkers, they demonstrated that they could form 1,4-oxazepanes via Lewis-acid mediated intramolecular C-O bond formation starting from either nitrogen-tethered alkenols (Scheme 2.5a) or nitrogen-tethered oxiranols (Scheme 2.5b).^{33,34} Using $\text{BF}_3 \cdot \text{OEt}_2$, they were able to obtain oxazepanes in moderate to excellent yields (48 – 93 %). Intriguingly, isomeric alkenols **2.31** and **2.32** cyclize through 7-*endo* and 7-*exo* modes, respectively, to both give oxazepanes under the same conditions. While the authors do note this, they offer no explanation for this selectivity.



Scheme 2.5. Lewis acid mediated synthesis of 1,4-oxazepanes from a) alkenols and b)

oxiranols.

As part of a medicinal chemistry program aiming to develop constrained enzyme inhibitors in a green fashion,³⁵ we developed a method to efficiently prepare polysubstituted oxazepanes, with some improvements upon the above-mentioned existing methods. This chapter presents our efforts to develop an efficient and expedient synthetic route to chiral oxazepanes. Additional computations and mechanistic experiments were carried out to investigate the factors controlling the stereo- and regioselectivity of the key cyclization and will be presented in detail in Chapter 3.

2.3 Results and Discussion

2.3.1 Design of synthetic strategy

Prior to the development of this synthetic methodology, we set stringent criteria we wished to fulfill, considering that these molecular scaffolds should be easy to access and use by medicinal chemists and/or to be applicable to large scale drug synthesis.³⁶ First the synthesis should not exceed 3 to 4 steps and should be scalable. Second, the obtained cyclic scaffold should bear functionalizable groups. These first two criteria are essential for applicability to medicinal chemistry programs where diversification will follow. Third, it should not use toxic reagents (e.g. metal catalysts). Fourth, it should start from inexpensive, commercially available materials. Fifth, stereogenic centers should be formed in a controlled manner or taken from the chiral pool. This is a critical issue as poor stereoselectivity renders the synthesis and isolation difficult. Sixth, atom economy should be considered (i.e. neither chiral auxiliaries nor excessive protection/deprotection steps). Finally, the number of tedious and non-green purifications should be limited. More specifically, simple workups requiring quantitative conversion or crystallization would be preferred over chromatography of complex mixtures. After extensive investigations, we developed the strategy outlined in Figure 2.2.

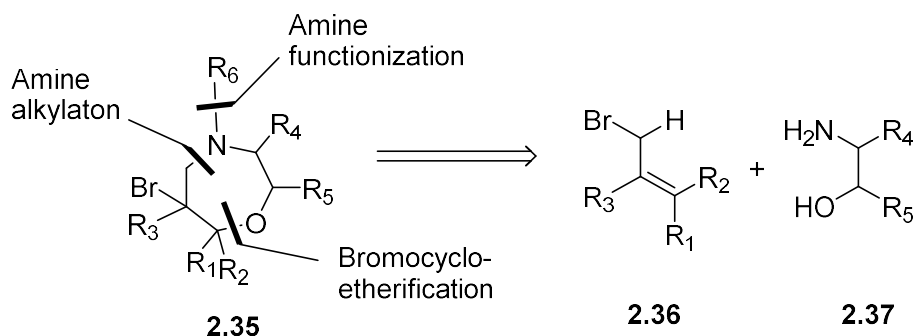
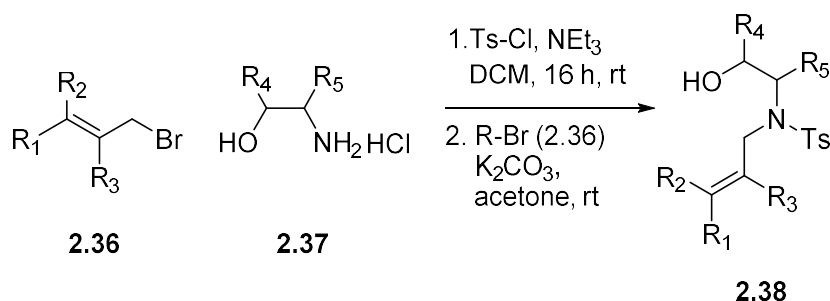


Figure 2.2. General synthetic strategy.

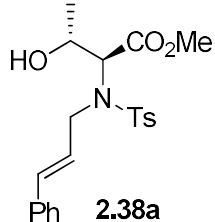
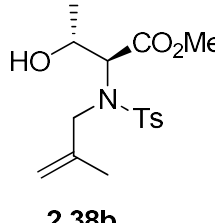
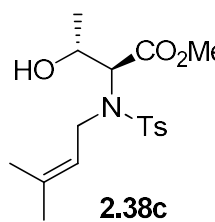
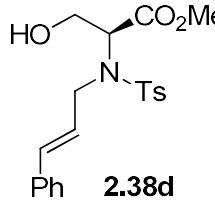
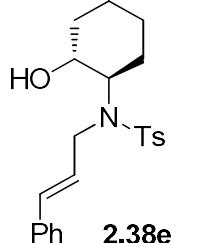
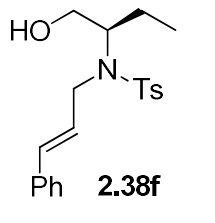
2.3.2 Preparation of unsaturated alcohols

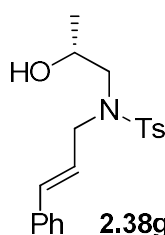
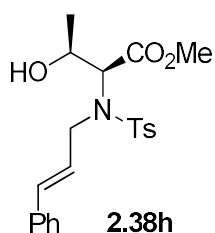
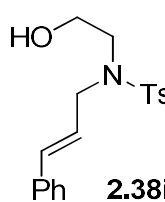
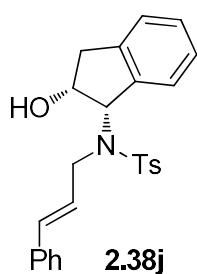
With this approach, the first or first two stereocenters bearing R_4 and R_5 are borrowed from the chiral pool, ensuring that the final molecule will be enantiopure. The other stereocenters will be introduced through substrate induction. Throughout the process, the alcohol will not be protected, thus reducing the number of steps and chemicals to be used (hence the waste) as compared to existing methods.³⁷ Although, this strategy may look straightforward, many issues had to be addressed. The first hurdle we met was the formation of the intermediate unsaturated amino alcohol that will be the substrate for the halo-etherification cyclization. After extensive optimization³⁸, the acyclic compounds were made following the strategy outlined in Table 2.2. Other approaches such as reductive amination followed by further amine functionalization proved less successful.

Table 2.2. *N*-Ts protection and alkylation.



Entry	R-Br	R ¹ / R ² / R ³	AA ^a	R ⁴ / R ⁵	Prod.	Yield (%) ^b
-------	------	--	-----------------	---------------------------------	-------	------------------------

1	2.36a	Ph / H / H	2.37a	Me / CO ₂ Me	 2.38a	90
2	2.36b	H / H / Me	2.37a	Me / CO ₂ Me	 2.38b	30
3	2.36c	Me / Me / H	2.37a	Me / CO ₂ Me	 2.38c	98
4	2.36a	Ph / H / H	2.37b	H / CO ₂ Me	 2.38d	39
5	2.36a	Ph / H / H	2.37c	<i>trans</i> -c-Hex	 2.38e	84
6	2.36a	Ph / H / H	2.37d	H / Et	 2.38f	51

7	2.36a	Ph / H / H	2.37e	Me / H	 2.38g	46
8	2.36a	Ph / H / H	2.37f	Me / CO ₂ Me ^c	 2.38h	67
9	2.36a	Ph / H / H	2.37g	H / H	 2.38i	62
10	2.36a	Ph / H / H	2.37h	<i>cis</i> -ind ^d	 2.38j	84

^a Amino alcohol; ^b Over two steps; ^c Allo-threonine methyl ester; ^d *Cis*-indanolamine.

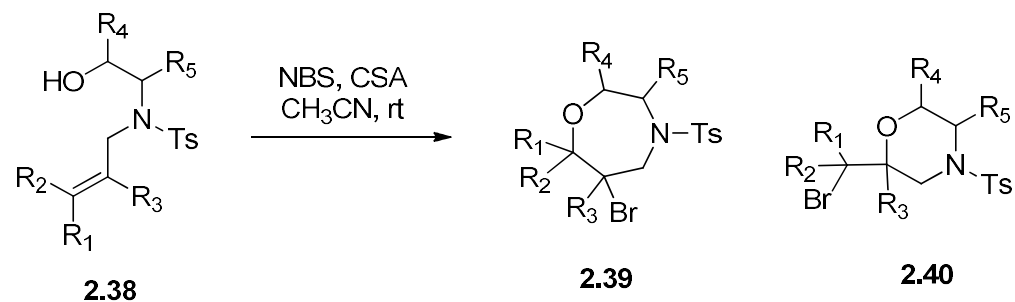
Thus, threonine methyl ester (**2.37a**), serine methyl ester (**2.37b**) and another six highly diverse amino alcohols (**2.37c** - **2.37h**) were reacted sequentially with tosyl chloride then cinnamyl bromide (**2.36a**) or other allyl bromides (**2.36b**, **2.36c**), affording the corresponding secondary amines, **2.38a** – **2.38j**, in reasonable to excellent yields. This approach did not require any protection of the primary alcohol.

2.3.3 Key Cyclization

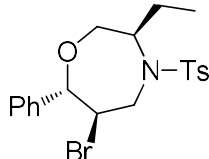
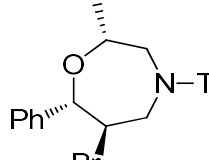
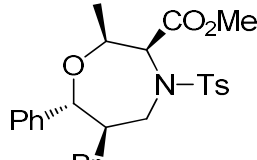
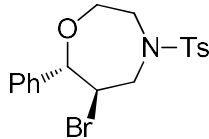
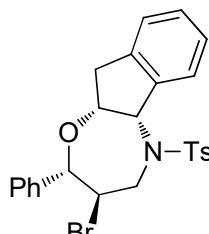
With this set of substrates in hand, the key cyclization was carried out. Throughout the course of the cyclization reaction, one can expect the formation of oxazepanes through a *7-endo* cyclization or morpholines through a *6-exo* cyclization. In addition, two stereogenic centers were formed, leading to eight potential regio- and stereoisomers. In order to develop an efficient method,

one has to significantly reduce this number of possible isomers. These efforts will be discussed further in Chapter 3.

Table 2.3. Oxazepanes by haloetherification of *N*-Ts protected derivatives.



Entry	Product ^a	Yield (%)	2.39:2.40	dr ^b
1	 2.39a	95	> 20 : 1	1.3 : 1
2	 2.40b	77	> 1 : 20	2.0 : 1
3	 2.39c	37	> 20 : 1	1.5 : 1
4	 2.39d	69	> 20 : 1	2.0 : 1
5	 2.39e	83	> 20 : 1	1.1 : 1

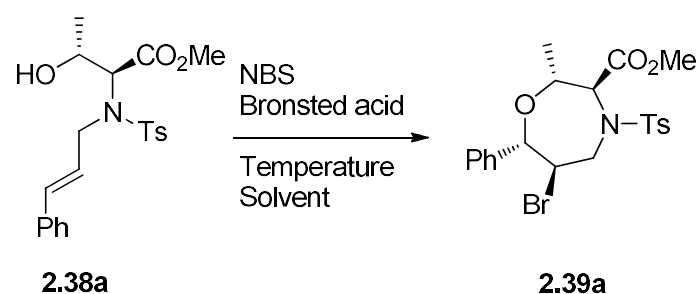
6		2.39f	> 99	> 20 : 1	2.0 : 1
7		2.39g	80	> 20 : 1	1.5 : 1
8		2.39h	78	> 20 : 1	1.4 : 1
9		2.39i	99	> 20:1	-
10		2.39j	85	> 20 : 1	1.5 : 1

^a Major diastereomer shown; ^b As determined by ¹H NMR of the crude product; when possible, the ester peak was used for comparisons, otherwise aromatic peaks of the tosyl protecting group were used.

The cyclic oxazepane (**2.39**) and morpholine (**2.40**) products were obtained in good to excellent yields (69 - >99 %) and excellent regioselectivities, with all cases showing only a single regioisomer by NMR. The low yield of **2.39c** (Table 2.3, entry 3) was thought to perhaps be a steric issue. Although the cyclization was successful, the observed stereoselectivities were low (up to 2.0:1) and called for further optimization. The solvent, temperature and additives were subsequently optimized (Table 2.4). For instance, the use of several different solvents showed excellent conversions although a wide variety of diastereoselectivities, with DMF and THF exhibiting the best results for both conversion and selectivity (Table 2.4, entry 4, 16). For ease of

utility, we opted to use THF for further experiments. We were pleased to see that rather than a stoichiometric amount, the use of a catalytic amount of a Brønsted acid such as CSA activating the brominating reagent retained the significantly improved diastereomeric ratio (Table 2.4, entry 18). Cooling the reaction temperature showed increased diastereoselectivity below 0 °C (Table 2.4, entry 1-3). However, running reactions at lower temperature reduces the applicability of this methodology to larger scales or large libraries, which would violate the criteria we outlined previously in Chapter 2.3.1. With these optimized conditions (NBS, THF, catalytic (±)-CSA, 0 °C), a variety of oxazepanes were obtainable.

Table 2.4. Condition optimization.



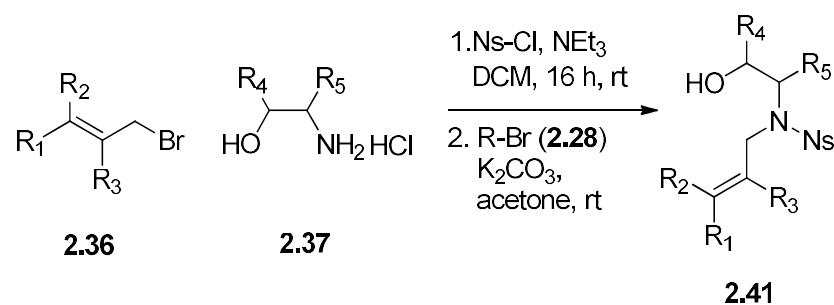
Entry	Solvent	Temperature	Brønsted Acid	Conversion (%) ^a	dr ^a
1	CH ₃ CN	0 °C	(±)-CSA	100	2.1 : 1
2	CH ₃ CN	-20 °C	(±)-CSA	97	3.4 : 1
3	CH ₃ CN	-78 °C	(±)-CSA	97	4.0 : 1
4	DMF	0 °C	(±)-CSA	100	> 20 : 1
5	CH ₂ Cl ₂	0 °C	(±)-CSA	100	1.9 : 1
6	THF	0 °C	(±)-CSA	100	8.6 : 1
7	MeOH	0 °C	(±)-CSA	74	3.1 : 1
8	EtOH	0 °C	(±)-CSA	100	7.7 : 1
9	ⁱ PrOH	0 °C	(±)-CSA	47	14.3 : 1
10	EtOAc	0 °C	(±)-CSA	61	4.4 : 1
11	CHCl ₃	0 °C	(±)-CSA	95	2.9 : 1

12	Acetone	0 °C	(±)-CSA	96	1.2 : 1
13	1,4-dioxane	0 °C	(±)-CSA	0	-
14	Benzene	0 °C	(±)-CSA	95	7.1 : 1
15	Toluene	0 °C	(±)-CSA	96	7.3 : 1
16	THF	0 °C	(+)-CSA	66	11.5 : 1
17	THF	0 °C	(-)-CSA	63	10.0 : 1
18	THF	0 °C	(±)-CSA ^b	51	10.0 : 1

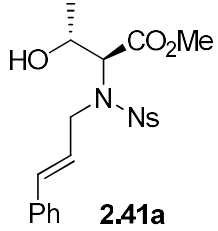
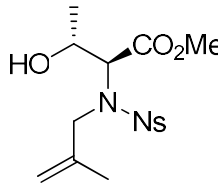
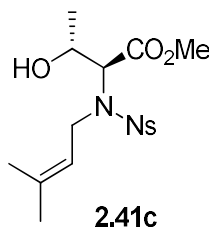
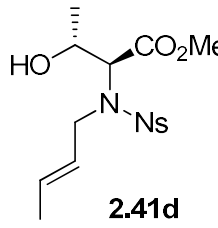
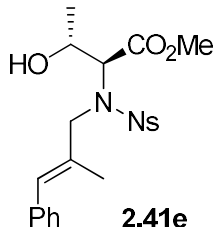
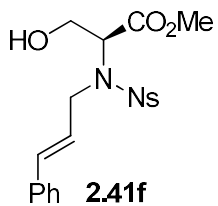
^a As determined by NMR of the crude mixtures; ^b 10 mol %

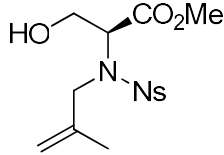
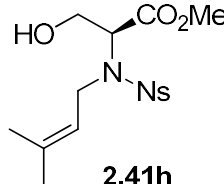
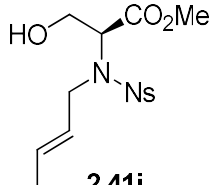
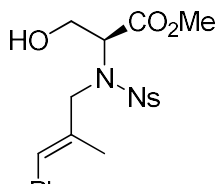
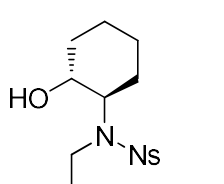
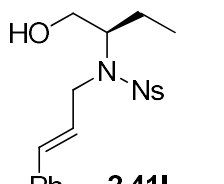
We next optimized the cyclization conditions and the selection of the group attached to the ring nitrogen (R^6 in Figure 2.2) which turned out to be critical. Preliminary investigations with non-functionalized secondary amines ($R^6 = H$) led to poor yielding cyclization and bromination of the nitrogen while the use of carbamates ($R^6 = Boc, Cbz$) led to the formation of oxazolidinones, as reported by Guindon and co-workers.³⁹ The use of other protecting groups ($R^6 = Bn, Me$) also led to poor yields (<60 %). Fortunately, sulfonamide protecting groups like tosyl ($R^6 = Ts$) and even more so, nosyl ($R^6 = Ns$) led to higher yields during the alkylation step to afford **2.41** (e.g. Table 2.5, entry 1) and also gave the desired cyclized products **2.42** and **2.43** with unexpectedly improved stereoselectivities (e.g. Table 2.6, entry 1).

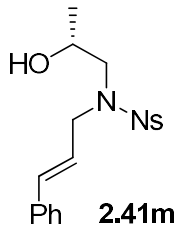
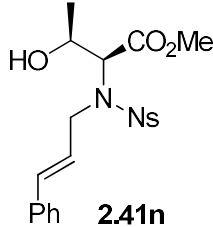
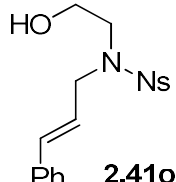
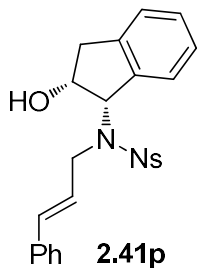
Table 2.5. N-Ns protection and alkylation.



Entry	R-Br	R ¹ / R ² / R ³	AA ^a	R ⁴ / R ⁵	Product	Yield (%) ^b
-------	------	--	-----------------	---------------------------------	---------	------------------------

1	2.36a	Ph / H / H	2.37a	Me / CO ₂ Me	 2.41a	> 99
2 ^c	2.36b	H / H / Me	2.37a	Me / CO ₂ Me	 2.41b	74
3	2.36c	Me / Me / H	2.37a	Me / CO ₂ Me	 2.41c	> 99
4	2.36d	Me / H / H	2.37a	Me / CO ₂ Me	 2.41d	> 99
5	2.36e	Ph / H / Me	2.37a	Me / CO ₂ Me	 2.41e	> 99
6	2.36a	Ph / H / H	2.37b	H / CO ₂ Me	 2.41f	79

7	2.36b	H / H / Me	2.37b	H / CO ₂ Me		42
					2.41g	
8	2.36c	Me / Me / H	2.37b	H / CO ₂ Me		97
					2.41h	
9	2.36d	Me / H / H	2.37b	H / CO ₂ Me		36
					2.41i	
10	2.36e	Ph / H / Me	2.37b	H / CO ₂ Me		38
					2.41j	
11	2.36a	Ph / H / H	2.37c	<i>trans</i> -c-Hex		>99
					2.41k	
12	2.36a	Ph / H / H	2.37d	H / Et		53
					2.41l	

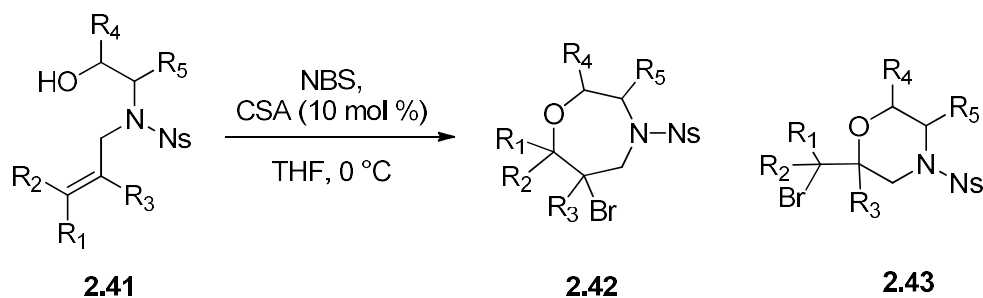
13	2.36a	Ph / H / H	2.37e	Me / H	 2.41m	91
14	2.36a	Ph / H / H	2.37f	Me / CO ₂ Me ^d	 2.41n	> 99
15	2.36a	Ph / H / H	2.37g	H / H	 2.41o	93
16	2.36a	Ph / H / H	2.37h	<i>cis</i> -ind ^e	 2.41p	94

^a Amino alcohol; ^b Over two steps; ^c Step 2 included 1.1 equivalents of TBAI additive; ^d Allo-threonine methyl ester; ^e *Cis*-indanolamine.

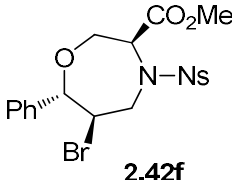
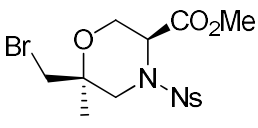
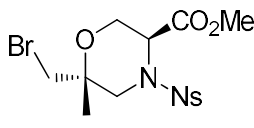
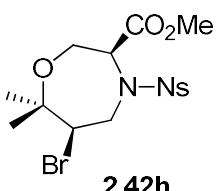
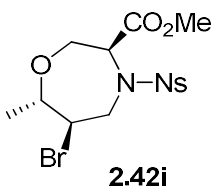
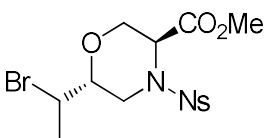
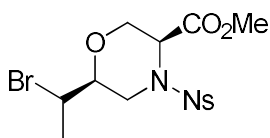
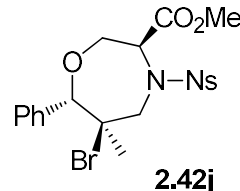
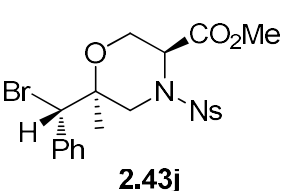
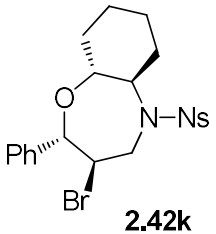
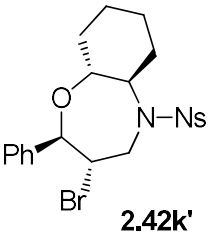
With the additional optimization of R⁶ = Ns in hand, we synthesized a library of acyclic precursors starting from the same amino alcohols we examined in Table 2.2 (**2.37a-h**) along with already examined allyl bromide derivatives (**2.36a-c**) as well as crotyl bromide (**2.36d**) and 2-methyl cinnamyl bromide (**2.36e**). With the exception of serine derivatives (**2.41f,g,i,j**) which exhibited lower yields, most compounds were isolated in good to excellent yields (53 - >99 %) regardless of any obvious steric or electronic effects of amino alcohol **2.37** or allyl bromide **2.36**.

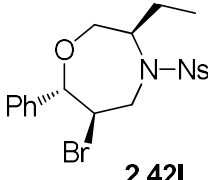
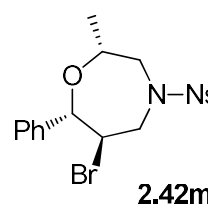
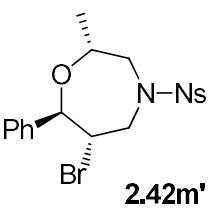
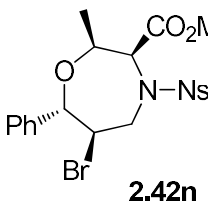
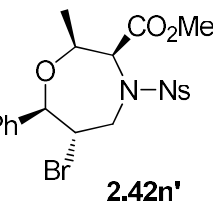
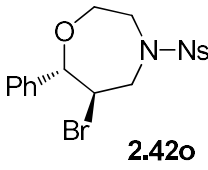
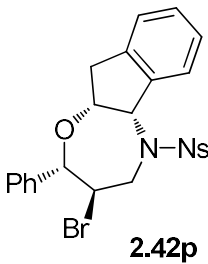
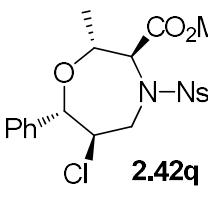
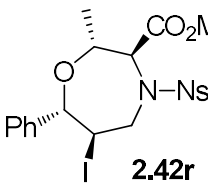
At this stage, the optimal conditions and nitrogen protecting group were applied to the reaction (Table 2.6).

Table 2.6. Oxazepanes by haloetherification of *N*-Ns protected derivatives.



Entry	Product ^a	Yield (%)	2.44 : 2.45	dr ^b
1	 2.42a	72	> 20 : 1	> 20 : 1
2	 2.43b	99	> 1 : 20	1.7 : 1
	 2.43b'			
3	 2.42c	61	> 20 : 1	> 20 : 1
4	 2.42d	> 99	2.9 : 1	> 20 : 1
	 2.43d			
5	 2.42e	59	1.5 : 1	> 20 : 1
	 2.43e			

6	 2.42f	94	> 20 : 1	> 20 : 1	
7	 2.43g	 2.43g'	77	> 1 : 20	1.7 : 1
8	 2.42h	> 99	> 20 : 1	> 20 : 1	
9	 2.42i	57	1.6 : 1	> 20 : 1	
	 2.43i	 2.43i'		1.2 : 1	
10	 2.42j	 2.43j	42	1.8 : 1	> 20 : 1
11	 2.42k	 2.42k'	73	> 20 : 1	2.0 : 1

12	 2.42l	> 99	> 20 : 1	> 20 : 1	
13	 2.42m	 2.42m'	78	> 20 : 1	1.2 : 1
14	 2.42n	 2.42n'	42	> 20 : 1	2.1 : 1
15	 2.42o	> 99	> 20 : 1	-	
16	 2.42p	98	> 20 : 1	> 20 : 1	
17 ^c	 2.42q	18	> 20 : 1	> 20 : 1	
18 ^d	 2.42r	58	> 20 : 1	> 20 : 1	

^a As determined by NMR for the major isomer; ^b Product is a mixture of enantiomers; ^c Electrophilic halogenating agent was NCS; ^d Electrophilic halogenating agent was NIS.

The bromocycloetherification proceeded with good to excellent yields (42 - >99 %) although the chloro- and iodocycloetherification yields were poor and moderate, respectively, however both proceeded with excellent diastereoselectivity (Table 2.6, entry 17, 18). Most of the cyclizations went with excellent regioselectivity: acyclic derivatives featuring a cinnamyl, 2-methyl allyl or 3-methylcrotyl appendage all proceeded with excellent regioselectivity, yielding only a single regioisomers in each case (Table 2.6, entry 1-3,6-8,11-18); acyclic derivatives that featured a crotyl or 2-methyl cinnamyl appendage had poor regioselectivity, ranging from 1.5:1 - 2.9:1 (Table 2.6, entry 3,4,9,10). Formation of morpholine products seemed to be less selective than formation of oxazepanes, with morpholine products being obtained with drs ranging from 1.2:1 - 1.7:1 (Table 2.6, entry 2,7,9). There were no obvious trends in the substitution of the starting amino alcohols, with drs ranging from >20:1 - 1.2:1. As the optimization supported, there was an improvement in diastereoselectivity of many oxazepanes with R⁶ = Ns instead of Ts (**2.42a,c,f,l,p**) while other selectivities were relatively similar (**2.43b**, **2.42k,m,n**). The reason for this is still unclear. The regioselectivity and stereoselectivity of the key cyclization step will be discussed in further detail in Chapter 3.

2.4 Conclusions

We have developed a strategy enabling the synthesis of chiral polysubstituted oxazepanes and morpholines with excellent yields and regio- and diastereoselectivity that allows the introduction of diversity points in the final products. Starting from enantiopure amino alcohols and suitably substituted allyl bromides, the method was conducted in only three steps: *N*-sulfonamide protection, *N*-alkylation and haloetherification cyclization. The strategy relies on the use of the chiral pool to introduce up to two stereogenic centers and a key stereo- and regioselective haloetherification to introduce up to two other stereogenic centers.

The *N*-protecting group had little effect on the yields and no effect on the regioselectivity but did have drastic effects on the stereoselectivity, with more electron-withdrawing *N*-Ns derivatives exhibiting significantly higher stereoselectivities, with dr for oxazepanes reaching >20:1 in many cases (an improvement over *N*-Ts derivatives which showed a range of 1:1 in many cases, to 14.3:1, depending on the conditions used). Yields ranged from 42 % to quantitative.

2.5 Experimental

2.5.1 General considerations and procedures

All commercially available reagents were used without further purification, unless otherwise stated. Chemical shift (δ) are reported in parts per million (ppm) relative to CDCl_3 (7.26 ppm for ^1H and 77.160 ppm for ^{13}C). ^1H and ^{13}C NMR assignments were confirmed by 2D COSY, HSQC HMBC and NOESY experiments recorded using 400 MHz and 500 MHz spectrometers. Chromatography was performed on silica gel 60 (230-240 mesh). Visualization was performed by UV or by development using ceric ammonium molybdate. Mass spectra were obtained from the McGill University mass spectral facilities. A Perkin Elmer Spectrum One FT-IR spectrometer was used to collect spectra of the samples at resolution of 4 cm^{-1} and 32 scans. HRMS were obtained by ESI-QTOF on a Bruker Maxis Impact mass spectrometer. Optical rotations were measured at the wavelength 589 nm (sodium D line).

General procedure for N-alkylation of N-protected amino alcohols. To a suspension of threonine-methyl ester hydrochloride salt **2.37a** (200 mg, 1.18 mmol) in CH_2Cl_2 (40 mL), NEt_3 (330 mL, 2.36 mmol) was added via syringe and stirred for 0.5 h. The flask was then chilled to $0\text{ }^\circ\text{C}$ and solid nosyl chloride (288 mg, 1.30 mmol) was added and the resulting mixture was left to warm slowly to rt and stir for 16 h. The mixture was washed with water (3 x 100 mL) and the organic layers were combined and dried over Na_2SO_4 , filtered and concentrated under reduced pressure to obtain (2S,3R)-methyl 3-hydroxy-2-(4-nitrophenylsulfonamido)butanoate. The product was used in subsequent experiments without further purification. (2S,3R)-methyl 3-hydroxy-2-(4-nitrophenylsulfonamido)butanoate (260 mg, 0.82 mmol) was dissolved in acetone (40 mL) and a large excess of solid K_2CO_3 (>10 eq.) was added. Solid cinnamyl bromide **2.36a** (200 mg, 1.01 mmol) was added and the mixture was stirred at rt for 16 h. The mixture was concentrated under reduced pressure and the resulting residue was partitioned between CH_2Cl_2 (50 mL) and water (50 mL). The organic layer was dried over Na_2SO_4 , filtered and concentrated under reduced pressure. The crude was purified by column chromatography on silica gel (eluent system: 7:3 Hexanes:EtOAc) to obtain **2.41a**.

General procedure for cyclization of N-sulfonamide protected amino alcohols. 2.41a (284 mg, 0.65 mmol) was dissolved in THF (10 mL). Solid (\pm)-CSA (15 mg, 0.065 mmol) was added followed by solid NBS (128 mg, 0.72 mmol). The mixture was cooled to $0\text{ }^\circ\text{C}$ and stirred

for 12 h. The mixture was then allowed to warm slowly to rt and was stirred for an additional 5 h. The mixture is diluted with NaHCO₃ (25 mL) and extracted with EtOAc (3 x 25 mL). The combined organic layers were dried over Na₂SO₄, filtered and concentrated under reduced pressure. The crude mixture was purified by column chromatography on silica gel (eluent system: 8:2 Hexanes:EtOAc) to obtain **2.42a**.

2.5.2 Experimental data

(2S,3R)-methyl 2-(N-cinnamyl-4-methylphenylsulfonamido)-3-hydroxybutanoate (2.38a): white solid; MP = 88 - 90 °C; 90 % isolated yield; $[\alpha]_D^{22} = -57.3$ (*c* 1.00, CHCl₃); $R_f = 0.19$, (1:99 MeOH:CH₂Cl₂); IR (film, cm⁻¹) 3531.3, 1737.7, 1335.3, 1153.2, 731.0; ¹H NMR (400 MHz, CDCl₃) δ 7.73 (d, *J* = 8.4 Hz, 2H), 7.26 (m, 7H), 6.48 (d, *J* = 16.0 Hz, 1H), 6.20 (m, 1H), 4.49 (d, *J* = 5.6 Hz, 1H), 4.36 (br s, 1H), 4.19 (ddd, *J* = 7.2, 16.0, 23.6 Hz, 2H), 3.49 (s, 3H), 2.56 (br s, 1H), 2.39 (s, 3H), 1.28 (d, *J* = 6.4 Hz, 3H); ¹³C NMR (75 MHz, CDCl₃) δ 170.2, 143.6, 136.8, 136.2, 133.4, 129.4, 128.5, 127.9, 127.7, 126.5, 125.9, 66.9, 64.6, 52.1, 49.0, 21.5, 19.9; HRMS (M + H) for C₂₁H₂₅NO₅SH, calcd: 404.15317, found: 404.15253.

(2S,3R)-methyl 3-hydroxy-2-(4-methyl-N-(2-methylallyl)phenylsulfonamido)butanoate (2.38b): colourless oil; 30 % isolated yield; $[\alpha]_D^{22} = -44.5$ ° (*c* 1.30, CHCl₃); $R_f = 0.23$ (1:99 MeOH: CH₂Cl₂); IR (film, cm⁻¹) 3526.6, 1738.7, 1338.2, 1156.1, 1091.3, 814.8, 661.3; ¹H NMR (400 MHz, CDCl₃) δ 7.71 (d, *J* = 8.1 Hz, 2H), 7.29 (d, *J* = 8.1 Hz, 2H), 5.06 (s, 1H), 4.97 (s, 1H), 4.22 (s, 2H), 3.98 (s, 2H), 3.44 (s, 3H), 2.42 (s, 3H), 1.73 (s, 3H), 1.24 (d, *J* = 5.8 Hz, 3H); ¹³C NMR (75 MHz, CDCl₃) δ 223.0, 169.7, 143.7, 142.2, 136.2, 129.3, 127.8, 114.5, 66.3, 65.4, 52.7, 51.8, 21.5, 20.3, 20.0 19.9; HRMS (M + H) for C₁₆H₂₃NO₅SH, calcd: 342.13752, found: 342.13643.

(2S,3R)-methyl 3-hydroxy-2-(4-methyl-N-(3-methylbut-2-en-1-yl)phenylsulfonamido)butanoate (2.38c): colourless oil; 98 % isolated yield; $[\alpha]_D^{22} = -91.8$ ° (*c* 0.55, CHCl₃); $R_f = 0.42$ (7:3 Hex:EtOAc); IR (film, cm⁻¹) 3529.9, 2978.8, 1738.1, 1335.9, 1090.4, 667.9; ¹H NMR (400 MHz, CDCl₃) δ 7.71 (d, *J* = 8.1 Hz, 2H), 7.28 (d, *J* = 8.1 Hz, 2H), 5.23 (m, 1H), 4.40 (d, *J* = 6.6 Hz, 1H), 4.20 (m, 1H), 4.01 (d, *J* = 7.5 Hz, 2H), 3.52 (s, 3H), 2.42 (s, 3H), 1.68 (s, 3H), 1.62 (s, 3H), 1.27 (d, *J* = 6.3 Hz, 3H); ¹³C NMR (75 MHz, CDCl₃) δ 170.2, 143.4, 136.5, 129.3, 127.6, 121.0, 66.4, 64.7, 51.9, 44.3, 25.8, 21.5, 19.7, 17.8; HRMS (M + H) for C₁₇H₂₅NO₅SH, calcd: 356.15317, found: 356.15214.

(S)-methyl 2-(N-cinnamyl-4-methylphenylsulfonamido)-3-hydroxypropanoate (2.38d): colourless oil; 39 % isolated yield; $[\alpha]^{22}_{\text{D}} = -28.9^{\circ}$ (*c* 1.00, CHCl₃); $R_f = 0.14$ (7:3 Hex:EtOAc); IR (film, cm⁻¹) 3524.9, 1737.9, 1334.0, 1153.7, 908.9, 727.0; ¹H NMR (400 MHz, CDCl₃) δ 7.76 (d, *J* = 8.4 Hz, 2H), 7.26 (m, 7H), 6.48 (d, *J* = 16.2 Hz, 1H), 6.12 (dt, *J* = 8.1, 16.2 Hz, 1H), 4.66 (t, *J* = 4.0 Hz, 1H), 4.02 (m, 4H), 3.57 (s, 3H), 2.41 (s, 3H); ¹³C NMR (75 MHz, CDCl₃) δ 170.3, 143.7, 137.0, 136.1, 133.6, 129.6, 128.6, 128.0, 127.6, 126.5, 125.1, 61.3, 60.9, 52.4, 48.9, 21.5; HRMS (M + H) for C₂₀H₂₃NO₅SH, calcd: 390.13752, found: 390.13645.

N-cinnamyl-N-((1R,2R)-2-hydroxycyclohexyl)-4-methylbenzenesulfonamide (2.38e): white solid; MP = 121 - 123 °C; 84 % isolated yield; $[\alpha]^{22}_{\text{D}} = +10.4^{\circ}$ (*c* 1.10, CHCl₃); $R_f = 0.52$ (7:3 Hex:EtOAc); IR (film, cm⁻¹) 3529.6, 1330.7, 1092.6, 735.1, 661.3; ¹H NMR (300 MHz, CDCl₃) δ 17.74 (d, *J* = 8.0 Hz, 2H), 7.29 (m, 7H), 6.53 (d, *J* = 16.0 Hz, 1H), 6.15 (m, 1H), 4.06 (m, 2H), 3.53 (m, 2H), 2.41 (s, 3H), 2.31 (s, 1H), 2.10 (m, 1H), 1.66 (m, 2H), 1.48 (m, 2H), 1.22 (m, 3H); ¹³C NMR (75 MHz, CDCl₃) δ 143.4, 138.0, 136.2, 132.9, 129.7, 128.6, 127.9, 127.2, 126.5, 70.1, 64.1, 46.2, 34.4, 29.3, 25.4, 24.0, 21.6; HRMS (M + H) for C₂₂H₂₇NO₃SH, calcd: 386.17899, found: 386.17774.

(R)-N-cinnamyl-N-(1-hydroxybutan-2-yl)-4-methylbenzenesulfonamide (2.38f): white solid; MP = 70 - 72 °C; 51 % isolated yield; $[\alpha]^{22}_{\text{D}} = +30.4^{\circ}$ (*c* 1.20, CHCl₃); $R_f = 0.31$ (7:3 Hex:EtOAc); IR (film, cm⁻¹) 3519.0, 1330.7, 1092.6, 657.9; ¹H NMR (400 MHz, CDCl₃) δ 7.75 (d, *J* = 8.4 Hz, 2H), 7.27 (m, 7H), 6.51 (d, *J* = 16.0 Hz, 1H), 6.17 (m, 1H), 3.85 (m, 2H), 3.62 (t, *J* = 6.4 Hz, 2H), 2.41 (s, 3H), 2.28 (br s, 1H), 1.46 (m, 2H), 0.73 (t, *J* = 7.6 Hz, 3H); ¹³C NMR (75 MHz, CDCl₃) δ 143.3, 138.0, 136.2, 132.7, 129.6, 128.6, 127.9, 127.3, 126.6, 126.5, 63.5, 61.9, 46.0, 22.3, 21.5, 11.1; HRMS (M + H) for C₂₀H₂₅NO₃SH, calcd: 360.16334, found: 360.16239.

(R)-N-cinnamyl-N-(2-hydroxypropyl)-4-methylbenzenesulfonamide (2.38g): colourless oil; 46 % isolated yield; $[\alpha]^{22}_{\text{D}} = +11.9^{\circ}$ (*c* 1.15, CHCl₃); $R_f = 0.31$ (7:3 Hex:EtOAc); IR (film, cm⁻¹) 3529.8, 1334.9, 1089.5, 736.4; ¹H NMR (400 MHz, CDCl₃) δ 7.74 (d, *J* = 8.4 Hz, 2H), 7.25 (m, 7H), 6.43 (d, *J* = 15.6 Hz, 1H), 5.94 (dt, *J* = 6.8, 15.6 Hz, 1H), 4.02 (m, 3H), 3.10 (m, 2H), 2.66 (br s, 1H), 2.41 (s, 3H), 1.15 (d, *J* = 6.0 Hz, 3H); ¹³C NMR (75 MHz, CDCl₃) δ 143.7, 136.3, 135.9, 134.3, 129.8, 127.4, 126.4, 123.7, 66.2, 55.1, 52.1, 21.5, 20.5; HRMS (M + H) for C₁₉H₂₃NO₃SH, calcd: 346.14769, found: 346.14652.

(2*S*,3*S*)-methyl 2-(*N*-cinnamyl-4-methylphenylsulfonamido)-3-hydroxybutanoate (2.38h): colourless oil; 67 % isolated yield; $[\alpha]_D^{22} = -31.3^\circ$ (*c* 1.05, CHCl₃); $R_f = 0.25$ (7:3 Hex:EtOAc); IR (film, cm⁻¹) 3518.6, 1739.2, 1340.2, 1090.3, 743.7; ¹H NMR (400 MHz, CDCl₃) δ 7.74 (d, *J* = 8.4 Hz, 2H), 7.27 (m, 7H), 6.44 (d, *J* = 15.9 Hz, 1H), 6.07 (dt, *J* = 6.6, 15.9 Hz, 1H), 4.31 (m, 2H), 4.00 (ddd, *J* = 1.2, 6.3, 9.3 Hz, 2H), 3.49 (s, 3H), 2.42 (s, 3H), 1.30 (d, *J* = 6.0 Hz, 3H); ¹³C NMR (75 MHz, CDCl₃) δ 171.5, 143.6, 137.1, 136.0, 134.0, 129.4, 128.6, 128.1, 127.7, 126.5, 124.8, 66.9, 64.3, 52.2, 49.3, 21.5, 19.9; HRMS (M + H) for C₂₁H₂₅NO₅SH, calcd: 404.15317, found: 404.15233.

***N*-cinnamyl-*N*-(2-hydroxyethyl)-4-methylbenzenesulfonamide (2.38i):** white solid; MP = 54-58 °C; 62 % isolated yield; $R_f = 0.15$ (7:3 Hex:EtOAc); IR (film, cm⁻¹) 3518.4, 1332.0, 1153.3, 814.5, 719.5 v; ¹H NMR (400 MHz, CDCl₃) δ 7.74 (d, *J* = 8.4 Hz, 2H), 7.28 (m, 7H), 6.45 (d, *J* = 16.0 Hz, 1H), 5.98 (dt, *J* = 6.4, 16.0 Hz, 1H), 4.02 (dd, *J* = 0.8, 6.8 Hz, 2H), 3.75 (t, *J* = 5.2 Hz, 2H), 3.29 (t, *J* = 5.6 Hz, 2H), 2.43 (s, 3H); ¹³C NMR (75 MHz, CDCl₃) δ 143.7, 136.3, 136.0, 134.2, 128.6, 127.3, 126.5, 123.8, 61.2, 51.7, 49.7, 21.5; HRMS (M + H) for C₁₈H₂₁NO₃SH, calcd: 332.13204, found: 332.13094.

***N*-cinnamyl-*N*-((1*R*,2*S*)-2-hydroxy-2,3-dihydro-1*H*-inden-1-yl)-4-methylbenzenesulfonamide (2.38j):** colourless oil; 84 % isolated yield; $[\alpha]_D^{22} = -74.9^\circ$ (*c* 1.05, CHCl₃); $R_f = 0.58$ (7:3 Hex:EtOAc); IR (film, cm⁻¹) 3518.0, 1333.8, 1094.1, 815.3, 740.0; ¹H NMR (400 MHz, CDCl₃) δ 7.82 (d, *J* = 8.0 Hz, 2H), 7.32 (d, *J* = 8.0 Hz, 2H), 7.22 (m, 8H), 7.06 (t, *J* = 6.8 Hz, 1H), 6.58 (d, *J* = 7.6 Hz, 1H), 6.03 (m, 1H), 5.20 (d, *J* = 6.8 Hz, 1H), 4.68 (dq, *J* = 3.6, 7.6 Hz, 1H), 3.85 (m, 2H), 3.21 (dd, *J* = 7.2, 16.4 Hz, 1H), 2.93 (dd, *J* = 6.0, 16.8 Hz, 1H), 2.45 (s, 3H); ¹³C NMR (75 MHz, CDCl₃) δ 143.7, 141.4, 137.5, 137.0, 136.4, 132.8, 129.8, 129.2, 128.5, 127.7, 127.4, 126.9, 126.5, 126.3, 125.8, 125.5, 72.3, 64.8, 48.5, 39.5, 21.6; HRMS (M + H) for C₂₅H₂₅NO₃SH, calcd: 420.16334, found: 420.16206.

(2*S*,3*R*)-methyl 2-(*N*-cinnamyl-4-nitrophenylsulfonamido)-3-hydroxybutanoate (2.41a): colourless oil; >99 % isolated yield; $[\alpha]_D^{22} = -57.9^\circ$ (*c* 0.50, CHCl₃); $R_f = 0.48$ (6:4 Hex:EtOAc); IR (film, cm⁻¹) 3540.7, 1741.3, 1530.0, 1311.1, 1162.3, 742.7; ¹H NMR (300 MHz, CDCl₃) δ 8.27 (d, *J* = 9.0 Hz, 2H), 8.02 (d, *J* = 9.0 Hz, 2H), 7.30 (m, 5H), 6.51 (d, *J* = 15.9 Hz, 1H), 6.11 (ddd, *J* = 6.3, 7.8, 15.9 Hz, 1H), 4.59 (d, *J* = 5.7 Hz, 1H), 4.47 (sextet, *J* = 6 Hz, 1H), 4.23 (ddq, *J* = 1.5, 6.3, 15.9 Hz, 2H), 4.16 (dd, *J* = 0.9, 7.8 Hz, 1H), 3.59 (s, 3H), 1.35 (d, *J* = 6.3

Hz, 3H); ^{13}C NMR (75 MHz, CDCl_3) δ 169.9, 146.0, 135.8, 134.4, 129.0, 128.7, 128.3, 126.7, 126.4, 124.7, 123.9, 67.2, 65.0, 52.5, 49.7, 20.1; HRMS (M + Na) for $\text{C}_{20}\text{H}_{22}\text{N}_2\text{O}_7\text{SNa}$, calcd: 457.10454, found: 457.10383.

(2*S*,3*R*)-methyl 3-hydroxy-2-(*N*-(2-methylallyl)-4-nitrophenylsulfonamido)butanoate (2.41b): colourless oil; 74 % isolated yield; $[\alpha]_D^{22} = -45.2^\circ$ (*c* 1.55, CHCl_3); $R_f = 0.26$ (7:3 Hex:EtOAc); IR (film, cm^{-1}) 3545.8, 1739.3, 1529.5, 1309.5, 1161.4, 1090.3, 855.9, 734.7; ^1H NMR (300 MHz, CDCl_3) δ 8.34 (d, $J = 8.7$ Hz, 2H), 8.04 (d, $J = 8.7$ Hz, 2H), 5.03 (s, 1H), 4.99 (s, 1H), 4.32 (m, 2H), 3.99 (br s, 2H), 3.53 (s, 3H), 1.70 (s, 3H), 1.29 (d, $J = 6.0$ Hz, 3H); ^{13}C NMR (75 MHz, CDCl_3) δ 169.4, 150.0, 145.2, 141.2, 129.1, 123.9, 115.5, 66.4, 65.5, 53.3, 52.2, 20.3; HRMS (M + Na) for $\text{C}_{15}\text{H}_{20}\text{N}_2\text{O}_7\text{SNa}$, calcd: 395.08889, found: 395.08907.

(2*S*,3*R*)-methyl 3-hydroxy-2-(*N*-(3-methylbut-2-en-1-yl)-4-nitrophenylsulfonamido)butanoate (2.41c): colourless oil; >99 % isolated yield; $[\alpha]_D^{22} = -58.8^\circ$ (*c* 1.35, CHCl_3); $R_f = 0.53$ (6:4 Hex:EtOAc); IR (film, cm^{-1}) 3538.0, 1740.3, 1530.1, 1310.8, 1162.7, 1090.2, 855.3, 759.6; ^1H NMR (300 MHz, CDCl_3) δ 8.33 (d, $J = 9.0$ Hz, 2H), 8.02 (d, $J = 9.3$ Hz, 2H), 5.14 (m, 1H), 4.49 (d, $J = 6.0$ Hz, 1H), 4.32 (q, $J = 6.3$ Hz, 1H), 4.06 (d, $J = 6.9$ Hz, 2H), 3.59 (s, 3H), 2.31 (d, $J = 4.8$ Hz, 1H), 1.67 (s, 3H), 1.64 (s, 3H), 1.32 (d, $J = 6.3$ Hz, 3H); ^{13}C NMR (75 MHz, CDCl_3) δ 169.9, 149.9, 146.1, 137.3, 128.9, 123.8, 120.1, 66.7, 64.9, 52.3, 45.1, 25.8, 20.0, 17.8; HRMS (M + Na) for $\text{C}_{16}\text{H}_{22}\text{N}_2\text{O}_7\text{SNa}$, calcd: 409.10454, found: 409.10374.

(2*S*,3*R*)-methyl 2-(*N*-((*E*)-but-2-en-1-yl)-4-nitrophenylsulfonamido)-3-hydroxybutanoate (2.41d): colourless oil; >99 % isolated yield; $[\alpha]_D^{22} = -40.7^\circ$ (*c* 0.85, CHCl_3); $R_f = 0.54$ (6:4 Hex:EtOAc); IR (film, cm^{-1}) 3538.1, 1740.7, 1530.4, 1311.4, 1163.5, 734.6; ^1H NMR (300 MHz, CDCl_3) δ 8.33 (d, $J = 8.8$ Hz, 2H), 8.01 (d, $J = 9.2$ Hz, 2H), 5.66 (m, 1H), 5.44 (qt, $J = 1.6, 7.6$ Hz, 1H), 4.47 (d, $J = 5.6$ Hz, 1H), 4.36 (q, $J = 6.0$ Hz, 1H), 3.97 (dq, $J = 6.3, 17.4$ Hz, 2H), 3.56 (s, 3H), 1.63 (dd, $J = 1.2, 6.4$ Hz, 3H), 1.30 (d, $J = 6.0$ Hz, 3H); ^{13}C NMR (75 MHz, CDCl_3) δ 169.8, 145.9, 131.2, 129.0, 128.9, 126.6, 123.8, 66.7, 64.8, 52.2, 49.2, 19.9, 17.6; HRMS (M + Na) for $\text{C}_{15}\text{H}_{20}\text{N}_2\text{O}_7\text{SNa}$, calcd: 395.08889, found: 395.08819.

(2*S*,3*R*)-methyl 3-hydroxy-2-(*N*-((*Z*)-2-methyl-3-phenylallyl)-4-nitrophenylsulfonamido)butanoate (2.41e): colourless oil; >99 % isolated yield; $[\alpha]_D^{22} = -63.4^\circ$ (*c* 1.10, CHCl_3); $R_f = 0.62$ (6:4 Hex:EtOAc); IR (film, cm^{-1}) 3544.1, 1740.5, 1530.5, 1310.7, 1162.9, 733.0; ^1H NMR (300 MHz, CDCl_3) δ 8.31 (d, $J = 9.0$ Hz, 2H), 8.03 (d, $J = 9.0$ Hz, 2H),

7.34 (m, 3H), 7.18 (m, 2H), 6.49 (s, 1H), 4.42 (t, $J = 7.2$ Hz, 2H), 4.14 (s, 2H), 3.58 (s, 3H), 2.41 (d, $J = 4.5$ Hz, 1H), 1.75 (s, 3H), 1.32 (d, $J = 69.0$ Hz, 3H); ^{13}C NMR (75 MHz, CDCl_3) δ 169.5, 149.9, 145.7, 136.5, 132.8, 130.7, 129.2, 128.8, 128.3, 127.1, 123.8, 66.3, 65.4, 56.0, 52.3, 20.6, 16.0; HRMS (M + Na) for $\text{C}_{21}\text{H}_{24}\text{N}_2\text{O}_7\text{SNa}$, calcd: 471.12019, found: 471.11926.

(S)-methyl 2-(N-cinnamyl-4-nitrophenylsulfonamido)-3-hydroxypropanoate (2.41f): white solid; MP = 116 - 118 °C; 79 % isolated yield; $[\alpha]_{\text{D}}^{22} = +6.7^\circ$ (c 0.55, CHCl_3); $R_f = 0.39$ (6:4 Hex:EtOAc); IR (film, cm^{-1}) 3543.1, 1740.2, 1530.1, 1311.7, 1162.4, 741.4; ^1H NMR (300 MHz, CDCl_3) δ 8.31 (d, $J = 9.0$ Hz, 2H), 8.07 (d, $J = 9.0$ Hz, 2H), 7.31 (m, 5H), 6.53 (d, $J = 15.9$ Hz, 1H), 6.09 (ddd, $J = 6.6, 7.2, 22.5$ Hz, 1H), 4.76 (dd, $J = 5.7, 7.2$ Hz, 1H), 4.17 (m, 2H), 4.02 (ddd, $J = 1.2, 7.2, 15.9$ Hz, 2H), 3.64 (s, 3H); ^{13}C NMR (75 MHz, CDCl_3) δ 169.6, 146.0, 145.9, 135.6, 134.5, 128.9, 128.7, 128.4, 126.5, 124.1, 124.0, 61.4, 61.3, 52.7, 49.2; HRMS (M + Na) for $\text{C}_{19}\text{H}_{20}\text{N}_2\text{O}_7\text{SNa}$, calcd: 443.08889, found: 443.08873.

(S)-methyl 3-hydroxy-2-(N-(2-methylallyl)-4-nitrophenylsulfonamido)propanoate (2.41g): colourless oil; 42 % isolated yield; $[\alpha]_{\text{D}}^{22} = +2.4^\circ$ (c 0.55, CHCl_3); $R_f = 0.59$ (6:4 Hex:EtOAc); IR (film, cm^{-1}) 3545.6, 1736.5, 1530.9, 1311.4, 1163.5, 736.9; ^1H NMR (300 MHz, CDCl_3) δ 8.36 (d, $J = 9.0$ Hz, 2H), 8.05 (d, $J = 9.0$ Hz, 2H), 5.02 (s, 1H), 4.98 (s, 1H), 4.52 (t, $J = 6.0$ Hz, 1H), 4.14 (dd, $J = 5.7, 11.7$ Hz, 1H), 3.95 (m, 2H), 3.74 (d, $J = 16.2$ Hz, 1H), 3.63 (s, 3H), 1.70 (s, 3H); ^{13}C NMR (75 MHz, CDCl_3) δ 169.5, 145.4, 140.9, 129.0, 124.4, 124.0, 115.2, 61.6, 61.5, 53.6, 52.5, 20.0; HRMS (M + Na) for $\text{C}_{14}\text{H}_{18}\text{N}_2\text{O}_7\text{SNa}$, calcd: 381.07324, found: 381.07260.

(S)-methyl 3-hydroxy-2-(N-(3-methylbut-2-en-1-yl)-4-nitrophenylsulfonamido)propanoate (2.41h): colourless oil; 97 % isolated yield; $[\alpha]_{\text{D}}^{22} = 3.2^\circ$ (c 1.05, CHCl_3); $R_f = 0.41$ (6:4 Hex:EtOAc); IR (film, cm^{-1}) 3548.7, 1736.2, 1530.1, 1311.0, 1162.1, 855.1, 743.7; ^1H NMR (300 MHz, CDCl_3) δ 8.4 (d, $J = 9.0$ Hz, 2H), 8.05 (d, $J = 9.0$ Hz, 2H), 5.10 (dt, $J = 1.5, 7.8$ Hz, 1H), 4.66 (t, $J = 7.2$ Hz, 1H), 4.08 (m, 1H), 3.97 (m, 1H), 3.86 (m, 2H), 3.65 (s, 3H), 1.67 (s, 3H), 1.62 (s, 3H); ^{13}C NMR (75 MHz, CDCl_3) δ 169.8, 146.1, 138.0, 128.8, 124.0, 119.4, 61.3, 61.2, 52.5, 44.8, 25.7, 17.8; HRMS (M + Na) for $\text{C}_{15}\text{H}_{20}\text{N}_2\text{O}_7\text{SNa}$, calcd: 395.08889, found: 395.08796.

(S,E)-methyl 2-(N-(but-2-en-1-yl)-4-nitrophenylsulfonamido)-3-hydroxypropanoate (2.41i): colourless oil; 36 % isolated yield; $[\alpha]_{\text{D}}^{22} = -4.9^\circ$ (c 0.90, CHCl_3); $R_f = 0.42$ (6:4 Hex:EtOAc); IR (film, cm^{-1}) 3547.0, 1736.5, 1530.4, 1311.5, 1163.1, 741.5; ^1H NMR (300 MHz,

CDCl₃) δ 8.35 (d, J = 9.0 Hz, 2H), 8.05 (d, J = 9.0 Hz, 2H), 5.67 (m, 1H), 5.41 (m, 1H), 4.66 (t, J = 6.9 Hz, 1H), 4.10 (dd, J = 5.7, 11.7 Hz, 1H), 3.92 (m, 2H), 3.78 (m, 1H), 3.64 (s, 3H), 2.23 (br s, 1H), 1.66 (d, J = 6.6 Hz, 3H); ¹³C NMR (75 MHz, CDCl₃) δ 169.7, 145.9, 131.5, 128.8, 126.0, 124.1, 124.0, 61.2, 61.1, 52.5, 49.0, 17.7; HRMS (M + Na) for C₁₄H₁₈N₂O₇SNa, calcd: 381.07324, found: 381.07244.

(S,Z)-methyl 3-hydroxy-2-(N-(2-methyl-3-phenylallyl)-4-nitrophenylsulfonamido)propanoate (2.41j): white solid; MP = 113 - 116 °C; 38 % isolated yield; $[\alpha]^{22}_{\text{D}} = -10.2^\circ$ (c 0.50, CHCl₃); $R_f = 0.52$ (6:4 Hex:EtOAc); IR (film, cm⁻¹) 3548.9, 1736.2, 1530.3, 1311.3, 1162.3, 743.0; ¹H NMR (300 MHz, CDCl₃) δ 8.35 (d, J = 9.0 Hz, 2H), 8.08 (d, J = 9.0 Hz, 2H), 7.34 (m, 3H), 7.19 (m, 2H), 6.45 (s, 1H), 4.59 (t, J = 6.6 Hz, 1H), 4.15 (m, 2H), 3.93 (m, 2H), 3.64 (s, 3H), 1.81 (d, J = 1.2 Hz, 3H); ¹³C NMR (75 MHz, CDCl₃) δ 169.6, 150.0, 145.6, 136.4, 132.6, 130.3, 129.0, 128.8, 128.3, 127.2, 124.0, 61.4, 61.2, 56.0, 52.6, 15.8; HRMS (M + Na) for C₂₀H₂₂N₂O₇SNa, calcd: 457.10454, found: 457.10355.

N-cinnamyl-N-((1R,2R)-2-hydroxycyclohexyl)-4-nitrobenzenesulfonamide (2.41k): white solid; MP = 147 - 149 °C; >99 % isolated yield; $[\alpha]^{22}_{\text{D}} = +8.8^\circ$ (c 0.50, CHCl₃); $R_f = 0.61$ (6:4 Hex:EtOAc); IR (film, cm⁻¹) 3548.6, 1528.0, 1347.8, 1162.5, 685.3; ¹H NMR (300 MHz, CDCl₃) δ 8.19 (d, J = 8.7 Hz, 2H), 7.97 (d, J = 8.7 Hz, 2H), 7.25 (m, 5H), 6.50 (d, J = 15.9 Hz, 1H), 6.01 (dt, J = 6.9, 15.9 Hz, 1H), 4.04 (m, 2H), 3.54 (m, 2H), 2.05 (br s, 1H), 1.80 (d, J = 2.7 Hz, 1H), 1.61 (m, 3H), 1.19 (m, 4H); ¹³C NMR (75 MHz, CDCl₃) δ 147.1, 135.8, 133.7, 128.7, 128.6, 128.2, 126.7, 126.4, 125.5, 124.0, 70.1, 64.5, 46.4, 35.0, 30.4, 25.3, 24.0; HRMS (M + Na) for C₂₁H₂₄N₂O₅SNa, calcd: 439.13036, found: 439.13042.

(R)-N-cinnamyl-N-(1-hydroxybutan-2-yl)-4-nitrobenzenesulfonamide (2.41l): colourless oil; 53 % isolated yield; $[\alpha]^{22}_{\text{D}} = 234.8^\circ$ (c 0.45, CHCl₃); $R_f = 0.56$ (6:4 Hex:EtOAc); IR (film, cm⁻¹) 3537.4, 1527.2, 1346.9, 1157.8, 854.3, 691.7; ¹H NMR (300 MHz, CDCl₃) δ 8.24 (d, J = 8.7 Hz, 2H), 8.04 (d, J = 8.7 Hz, 2H), 7.27 (m, 5H), 6.54 (d, J = 15.9 Hz, 1H), 6.07 (dt, J = 6.6, 15.9 Hz, 1H), 4.11 (dd, J = 6.9, 15.9 Hz, 1H), 3.96 (m, 2H), 3.65 (d, 6.3 Hz, 2H), 1.52 (m, 2H), 0.82 (t, J = 7.5 Hz, 3H); ¹³C NMR (75 MHz, CDCl₃) δ 149.7, 147.1, 135.8, 133.7, 128.7, 128.6, 128.2, 126.4, 125.4, 124.0, 63.3, 62.4, 46.1, 22.6, 11.1; HRMS (M + Na) for C₁₉H₂₂N₂O₅SNa, calcd: 413.11471, found: 413.11482.

(R)-N-cinnamyl-N-(2-hydroxypropyl)-4-nitrobenzenesulfonamide (2.41m): white solid; MP = 87 - 90 °C; 91 % isolated yield; $[\alpha]_D^{22} = +32.3^\circ$ (*c* 0.60, CHCl₃); $R_f = 0.53$ (6:4 Hex:EtOAc); IR (film, cm⁻¹) 3541.7, 1529.3, 1310.9, 1161.0 740.9; ¹H NMR (300 MHz, CDCl₃) δ 8.33 (d, *J* = 9.0 Hz, 2H), 8.05 (d, *J* = 9.0 Hz, 2H), 7.30 (m, 5H), 6.49 (d, *J* = 15.9 Hz, 1H), 5.95 (dt, *J* = 6.9, 15.9 Hz, 1H), 4.14 (dd, *J* = 7.5, 14.1 Hz, 3H), 3.19 (m, 2H), 2.24 (br s, 1H), 1.19 (d, *J* = 6.3 Hz, 3H); ¹³C NMR (75 MHz, CDCl₃) δ 145.7, 135.9, 135.6, 135.0, 128.7, 128.6, 128.4, 126.4, 124.3, 122.7, 66.4, 54.8, 51.8, 20.8; HRMS (M + Na) for C₁₈H₂₀N₂O₅SNa, calcd: 399.09906, found: 399.09867.

(2S,3S)-methyl 2-(N-cinnamyl-4-nitrophenylsulfonamido)-3-hydroxybutanoate (2.41n): colourless oil; >99 % isolated yield; $[\alpha]_D^{22} = -30.8^\circ$ (*c* 0.90, CHCl₃); $R_f = 0.47$ (6:4 Hex:EtOAc); IR (film, cm⁻¹) 3537.4, 1740.0, 1530.6, 1311.5, 1164.7, 743.4; ¹H NMR (300 MHz, CDCl₃) δ 8.31 (d, *J* = 9.0 Hz, 2H), 8.04 (d, *J* = 9.0 Hz, 2H), 7.33 (m, 5H), 6.35 (d, *J* = 15.9 Hz, 1H), 5.84 (ddd, *J* = 6.6, 7.8, 15.9 Hz, 1H), 4.22 (m, 2H), 4.02 (dd, *J* = 0.9, 7.5 Hz, 1H), 3.90 (ddq, *J* = 1.2, 7.5, 18.3 Hz, 2H), 3.39 (s, 3H), 1.21 (d, *J* = 6 Hz, 3H); ¹³C NMR (75 MHz, CDCl₃) δ 170.6, 150.0, 145.9, 135.5, 134.9, 128.9, 128.7, 128.4, 126.4, 123.9, 123.5, 67.0, 64.7, 52.4, 49.5, 20.0; HRMS (M + Na) for C₂₀H₂₂N₂O₇SNa, calcd: 457.10454, found: 457.10427.

N-cinnamyl-N-(2-hydroxyethyl)-4-nitrobenzenesulfonamide (2.41o): white solid; MP = 85 - 87 °C; 93 % isolated yield; $R_f = 0.35$ (6:4 Hex:EtOAc); IR (film, cm⁻¹) 3536.9, 1528.5, 1348.0, 1159.9, 965.2, 692.0; ¹H NMR (300 MHz, CDCl₃) δ 8.35 (d, *J* = 9.0 Hz, 2H), 8.06 (d, *J* = 9.0 Hz, 2H), 7.28 (m, 5H), 6.51 (dd, *J* = 0.9, 15.9 Hz, 1H), 6.00, (ddt, *J* = 0.9, 6.9, 15.9 Hz, 1H), 4.11 (d, *J* = 6.6 Hz, 2H), 3.81 (q, *J* = 5.4 Hz, 2H), 3.41 (t, *J* = 5.4 Hz, 2H); ¹³C NMR (75 MHz, CDCl₃) δ 145.6, 135.5, 135.0, 128.7, 128.5, 128.4, 126.4, 124.4, 122.8, 61.0, 51.5, 49.6; HRMS (M + Na) for C₁₇H₁₈N₂O₅SNa, calcd: 385.08341, found: 385.08321.

N-cinnamyl-N-(2-hydroxy-2,3-dihydro-1H-inden-1-yl)-4-nitrobenzenesulfonamide (2.41p): colourless oil; 94 % isolated yield; $[\alpha]_D^{22} = 75.5^\circ$ (*c* 1.40, CHCl₃); $R_f = 0.66$ (6:4 Hex:EtOAc); IR (film, cm⁻¹) 3538.1, 1529.3, 1344.4, 1162.4, 1094.8, 692.5; ¹H NMR (300 MHz, CDCl₃) δ 8.33 (d, *J* = 9.0 Hz, 2H), 8.06 (d, *J* = 9.0 Hz, 2H), 7.25 (m, 9H), 6.19 (d, *J* = 15.9 Hz, 1H), 5.89 (ddd, *J* = 6.0, 7.8, 15.9 Hz, 1H), 4.73 (dq, *J* = 4.2, 7.2 Hz, 1H), 4.16 (d, *J* = 7.5 Hz, 1H), 3.93 (dq, *J* = 8.1, 15.9 Hz, 2H), 3.27 (dd, *J* = 7.5, 16.8 Hz, 1H), 2.97 (dd, *J* = 4.0, 16.8 Hz, 1H), 2.49 (d, *J* = 2.4 Hz, 1H); ¹³C NMR (75 MHz, CDCl₃) δ 146.9, 141.2, 136.6, 136.0, 133.9, 129.6,

128.6, 128.5, 128.1, 127.3, 126.7, 126.4, 125.7, 125.5, 125.1, 124.3, 72.3, 65.3, 49.1, 39.7; HRMS (M + Na) for C₂₄H₂₂N₂O₅SNa, calcd: 473.11471, found: 473.11453.

(2R,3S)-methyl 6-bromo-2-methyl-7-phenyl-4-tosyl-1,4-oxazepane-3-carboxylate (2.39a): Major Diastereomer: colourless oil; 11 % isolated yield; R_f = 0.40 (7:3 Hex:EtOAc); IR (film, cm⁻¹) 2923.6, 1740.3, 1454.5, 1355.6, 1157.1, 1090.9, 1009.3, 699.4; ¹H NMR (300 MHz, CDCl₃) δ 7.73 (d, J = 6.3 Hz, 2H), 7.31-7.35 (m, 5H), 7.20-7.22 (m, 2H), 4.49 (d, J = 7.2 Hz, 1H), 4.37 (d, J = 7.8 Hz, 1H), 4.32 (dd, J = 2.7, 11.7 Hz, 1H), 4.06-4.13 (m, 1H), 3.94 (dd, J = 4.5, 7.2 Hz, 1H), 3.89 (dd, J = 8.7, 11.7 Hz, 1H), 3.55 (s, 3H), 2.46 (s, 3H), 1.32 (d, J = 4.5 Hz, 3H); ¹³C NMR (75 MHz, CDCl₃) δ 170.9, 143.8, 139.4, 137.3, 129.8, 128.6, 128.2, 127.4, 127.1, 90.0, 64.6, 52.3, 51.8, 50.1, 21.6, 20.3; HRMS (M + Na) for C₂₁H₂₄BrNO₅SNa, calcd: 504.04563, found: 504.04422. **Minor Diastereomer:** colourless oil; 63 % isolated yield; R_f = 0.34 (7:3 Hex:EtOAc); IR (film, cm⁻¹) 2923.6, 2853.0, 1745.4, 1455.8, 1340.9, 1219.8, 1159.0, 1091.7, 699.8; ¹H NMR (300 MHz, CDCl₃) δ 7.77 (d, J = 6.3 Hz, 2H), 7.30-7.34 (m, 7H), 4.89 (d, J = 6.9 Hz, 1H), 4.72 (dq, J = 2.4, 5.1 Hz, 1H), 4.42 (d, J = 2.7 Hz, 1H), 4.30-4.35 (m, 1H), 4.24 (dd, J = 3.3, 11.7 Hz, 1H), 4.05 (dd, J = 3.9, 11.7 Hz, 1H), 3.62 (s, 3H), 2.45 (s, 3H), 1.46 (d, J = 5.1 Hz, 3H); ¹³C NMR (75 MHz, CDCl₃) δ 166.9, 141.4, 167.6, 133.5, 127.1, 127.0, 126.0, 125.2, 124.3, 75.7, 70.5, 63.0, 50.5, 50.0, 49.7, 19.0; HRMS (M + Na) for C₂₁H₂₄BrNO₅SNa, calcd: 504.04563, found: 504.04463.

(2R,3S)-methyl 6-(bromomethyl)-2,6-dimethyl-4-tosylmorpholine-3-carboxylate (2.40b): characterized from a 2.0:1 mixture of diastereomers; colourless oil; 77 % isolated yield, R_f = 0.43 (7:3 Hex:EtOAc); IR (film, cm⁻¹) 2983.0, 1743.3, 1348.0, 1126.5, 1091.2, 1039.7, 816.2, 663.5; ¹H NMR (300 MHz, CDCl₃) δ 7.69 (d, J = 6.3 Hz, 2H), 7.33-7.37 (m, 2H), 3.93-3.99 (m, 1H), 3.79 (d, J = 8.1 Hz, 0.5H), 3.76 (s, 1H), 3.71 (s, 2H), 3.55 (d, J = 9.3 Hz, 0.5H), 3.44 (dd, J = 4.8, 8.4 Hz, 1H), 3.37 (d, J = 9.6 Hz, 0.5H), 3.21 (s, 1H), 3.17 (d, J = 6.9 Hz, 0.5H), 2.99 (d, J = 9.9 Hz, 0.5H), 2.60 (d, J = 9.3 Hz, 0.5H), 2.44 (s, 1H), 2.43 (s, 2H), 1.39 (s, 2H), 1.24 (s, 1H), 1.18 (d, J = 4.5 Hz, 2H), 1.14 (d, J = 4.5 Hz, 1H); ¹³C NMR (75 MHz, CDCl₃) δ 170.0, 169.7, 144.4, 144.2, 133.7, 132.3, 129.8, 129.7, 128.2, 127.9, 74.1, 72.6, 67.7, 67.6, 63.7, 63.6, 52.7, 52.6, 52.5, 49.8, 48.4, 38.5, 35.6, 24.4, 21.6, 20.2, 18.6, 18.3; HRMS (M + K) for C₁₆H₂₂BrNO₅SK, calcd: 458.0034, found: 458.0008.

(2R,3S)-methyl 6-bromo-2,7,7-trimethyl-4-tosyl-1,4-oxazepane-3-carboxylate (2.39c): characterized from a 1.5:1 mixture of diastereomers; colourless oil; 47 % isolated yield; $R_f = 0.36$ (7:3 Hex:EtOAc); IR (film, cm^{-1}) 2981.7, 1739.8, 1351.8, 1334.0, 1195.9, 1089.8, 957.1, 771.2, 662.8; ^1H NMR (300 MHz, CDCl_3) δ 7.68 (d, $J = 6.0$ Hz, 0.5H), 7.64 (d, $J = 6.3$ Hz, 1.5H), 7.27-7.29 (m, 2H), 4.41 (d, $J = 5.1$ Hz, 0.5H), 4.26 (d, $J = 7.2$ Hz, 1H), 4.03 (m, 0.5H), 3.85-3.93 (m, 2H), 3.73 (dd, $J = 8.7, 12.0$ Hz, 1H), 3.63 (s, 1H), 3.47 (s, 2H), 2.40 (s, 3H), 1.30-1.34 (m, 6H), 1.20-1.25 (m, 3H); ^{13}C NMR (75 MHz, CDCl_3) δ 171.4, 171.1, 143.7, 143.6, 137.1, 135.9, 129.6, 129.5, 127.6, 127.0, 78.3, 78.0, 67.6, 66.8, 64.4, 63.9, 56.0, 52.5, 52.1, 51.7, 48.5, 48.1, 29.8, 24.9, 23.4, 23.2, 21.6, 21.5, 20.7, 19.8; HRMS (2 M + K) for $2[\text{C}_{17}\text{H}_{24}\text{BrNO}_5\text{S}]\text{K}$, calcd: 905.0749, found: 905.0760.

(3S)-methyl 6-bromo-7-phenyl-4-tosyl-1,4-oxazepane-3-carboxylate (2.39d): characterized from a 2.0:1 mixture of diastereomers; colourless oil; 69 % isolated yield; $R_f = 0.29$ (7:3 Hex:EtOAc); IR (film, cm^{-1}) 3033.1, 2954.0, 1747.3, 1338.4, 1195.3, 1099.8, 1090.6, 1023.7, 757.5, 700.1, 662.2; ^1H NMR (300 MHz, CDCl_3) δ 7.77-7.80 (m, 2H), 7.30-7.37 (m, 5H), 7.17-7.19 (m, 1H), 4.99 (dd, $J = 5.1, 7.8$ Hz, 1H), 4.69 (t, $J = 1.8$ Hz, 0.5H), 4.62 (d, $J = 6.0$ Hz, 0.5H), 4.54 (dd, $J = 1.8, 10.2$ Hz, 0.5H), 4.50 (dd, $J = 5.1, 9.9$ Hz, 1H), 4.30-4.37 (m, 1.5H), 4.02-4.09 (m, 1H), 3.96 (dd, $J = 4.8, 11.7$ Hz, 0.5H), 3.75 (dd, $J = 8.7, 12.0$ Hz, 1H), 3.71 (s, 1H), 3.69 (dd, $J = 8.1, 9.9$ Hz, 0.5H), 3.63 (s, 2H), 2.47 (s, 2H), 2.44 (s, 1H); ^{13}C NMR (75 MHz, CDCl_3) δ 169.8, 169.8, 144.0, 139.8, 138.8, 137.2, 136.1, 129.8, 129.7, 128.8, 128.6, 128.5, 128.4, 127.6, 127.3, 127.3, 126.7, 90.6, 88.9, 70.8, 69.8, 61.0, 59.2, 53.7, 52.7, 52.6, 52.5, 52.5, 50.8, 50.2, 49.7, 21.6; HRMS (M + K) for $\text{C}_{20}\text{H}_{22}\text{BrNO}_5\text{SK}$, calcd: 506.0034, found: 506.0008.

(5aR,9aR)-3-bromo-2-phenyl-5-tosyldecahydrobenzo[b][1,4]oxazepine (2.39e): Major Diastereomer: colourless oil; 24 % isolated yield; $R_f = 0.16$ (1:1 CH_2Cl_2 :Toluene); IR (film, cm^{-1}) 2927.1, 2856.8, 1454.8, 1328.3, 1130.0, 1101.4, 761.8, 728.6; ^1H NMR (300 MHz, CDCl_3) δ 7.76 (d, $J = 6.3$ Hz, 2H), 7.26-7.35 (m, 7H), 4.63 (d, $J = 7.2$ Hz, 1H), 4.33 (m, 2H), 4.07 (dt, $J = 3.0, 8.7$ Hz, 1H), 3.31 (dd, $J = 7.8, 10.8$ Hz, 1H), 3.19 (dt, $J = 2.4, 8.7$ Hz, 1H), 2.44 (s, 3H), 2.14 (dq, $J = 2.7, 9.3$ Hz, 1H), 1.91 (t, $J = 11.4$ Hz, 2H), 1.75 (t, $J = 9.6$ Hz, 2H), 1.45 (dq, $J = 2.7, 9.3$ Hz, 1H), 1.32 (tq, $J = 2.7, 9.9$ Hz, 1H), 1.20 (tt, $J = 2.7, 9.6$ Hz, 2H); ^{13}C NMR (75 MHz, CDCl_3) δ 143.2, 141.0, 139.7, 129.7, 128.3, 128.2, 127.2, 126.7, 78.9, 77.7, 67.6, 58.2, 51.6, 31.4, 30.3, 26.2, 24.5, 21.5; HRMS (M + Na) for $\text{C}_{22}\text{H}_{26}\text{BrNO}_3\text{SNa}$, calcd: 486.07145, found: 486.07080.
Minor Diastereomer: colourless oil; 14 % isolated yield; $R_f = 0.24$ (1:1 CH_2Cl_2 :Toluene); IR

(film, cm^{-1}) 2937.8, 2860.5, 1335.9, 1180.0, 1087.2, 1000.0, 872.6, 776.6, 659.0; ^1H NMR (300 MHz, CDCl_3) δ 7.84 (d, $J = 6.3$ Hz, 2H), 7.38 (d, $J = 6.0$ Hz, 2H), 7.24 (m, 3H), 6.90 (dd, $J = 1.2, 6.0$ Hz, 2H), 4.31 (m, 2H), 3.78 (m, 2H), 3.63 (dd, $J = 9.0, 12.0$ Hz, 1H), 3.39 (dt, $J = 3.0, 7.8$ Hz, 1H), 2.49 (s, 3H), 2.14 (d, $J = 5.4$ Hz, 1H), 2.01 (d, $J = 9.3$ Hz, 1H), 1.71-1.79 (m, 2H), 1.25-1.49 (m, 4H); ^{13}C NMR (75 MHz, CDCl_3) δ 143.5, 139.7, 139.0, 130.0, 128.4, 128.1, 127.3, 127.2, 88.4, 82.4, 63.3, 51.4, 48.6, 33.9, 32.4, 24.8, 24.7, 21.6; HRMS ($\text{M} + \text{Na}$) for $\text{C}_{22}\text{H}_{26}\text{BrNO}_3\text{SNa}$, calcd: 486.07145, found: 486.07201

(3R)-6-bromo-3-ethyl-7-phenyl-4-tosyl-1,4-oxazepane (2.39f): characterized from a 2.0:1 mixture of diastereomers; colourless oil; >99 % isolated yield; $R_f = 0.61$ (7:3 Hex:EtOAc); IR (film, cm^{-1}) 3033.3, 2968.4, 2877.5, 1455.0, 1337.4, 1095.9, 1040.0, 760.87, 699.5; ^1H NMR (300 MHz, CDCl_3) δ 7.84 (d, $J = 6.3$ Hz, 1.5H), 7.81 (d, $J = 6.3$ Hz, 0.5H), 7.38 (d, $J = 6.0$ Hz, 1.5H), 7.33-7.35 (m, 2H), 7.22-7.26 (m, 1.5H), 6.85 (dd, $J = 1.2, 6.0$ Hz, 2H), 5.54 (d, $J = 6.9$ Hz, 0.5H), 4.38 (dd, $J = 2.4, 11.7$ Hz, 1H), 4.22-4.30 (m, 2H), 4.18 (d, $J = 7.5$ Hz, 1H), 3.93-4.00 (m, 1H), 3.77-3.84 (m, 1H), 3.70 (dd, $J = 2.4, 9.3$ Hz, 0.5H), 3.51 (dd, $J = 9.0, 12.0$ Hz, 1H), 3.36 (dd, $J = 9.9, 11.7$ Hz, 1H), 2.50 (s, 2H), 2.45 (s, 1H), 0.94 (t, $J = 5.7$ Hz, 2H), 0.79 (t, $J = 5.7$ Hz, 1H); ^{13}C NMR (75 MHz, CDCl_3) δ 143.5, 140.0, 139.3, 139.2, 137.5, 130.0, 129.7, 128.5, 128.4, 128.1, 127.5, 127.3, 127.1, 126.9, 90.5, 88.6, 73.9, 73.0, 60.2, 58.7, 54.2, 50.2, 49.0, 58.4, 31.6, 24.7, 22.7, 22.3, 21.6, 14.1, 10.9, 10.1; HRMS ($\text{M} + \text{Na}$) for $\text{C}_{20}\text{H}_{24}\text{BrNO}_3\text{SNa}$, calcd: 460.05525, found: 460.05520.

(2R)-6-bromo-2-methyl-7-phenyl-4-tosyl-1,4-oxazepane (2.39g): Major Diastereomer: colourless oil; 43 % isolated yield; $R_f = 0.63$ (7:3 Hex:EtOAc); IR (film, cm^{-1}) 2925.9, 1450.7, 1340.6, 1159.4, 1087.8, 699.4; ^1H NMR (400 MHz, CDCl_3) δ 7.71 (d, $J = 8.4$ Hz, 2H), 7.36 (m, 7H), 4.81 (d, $J = 9.2$ Hz, 1H), 4.37 (dt, $J = 3.6, 10.0$ Hz, 1H), 4.31 (ddd, $J = 1.2, 3.2, 14.0$ Hz, 1H), 3.93-3.98 (m, 1H), 3.82 (ddd, $J = 1.2, 3.2, 14.0$ Hz, 1H), 3.29 (dd, $J = 10.0, 14.0$ Hz, 1H), 2.69 (dd, $J = 10.0, 14.0$ Hz, 1H), 2.46 (s, 3H), 1.06 (d, $J = 6.4$ Hz, 3H); ^{13}C NMR (75 MHz, CDCl_3) δ 143.8, 138.9, 136.2, 129.9, 128.5, 128.4, 127.4, 127.0, 80.3, 71.0, 54.9, 54.7, 49.7, 21.5, 18.4; HRMS ($\text{M} + \text{H}$) for $\text{C}_{19}\text{H}_{22}\text{BrNO}_3\text{SH}$, calcd: 424.0567, found: 424.0558; **Minor Diastereomer:** colourless oil; 37 % isolated yield; $R_f = 0.56$ (7:3 Hex:EtOAc); IR (film, cm^{-1}) 2925.8, 1450.4, 1342.2, 1161.5, 1088.8, 771.6, 699.6; ^1H NMR (400 MHz, CDCl_3) δ 7.74 (d, $J = 8.4$ Hz, 2H), 7.32-7.37 (m, 7H), 4.60 (d, $J = 9.6$ Hz, 1H), 4.14 (ddd, $J = 4.0, 5.2, 9.6$ Hz, 1H), 3.93-3.97 (m, 1H), 3.91 (dd, $J = 0.8, 5.2$ Hz, 1H), 3.85 (dd, $J = 4.4, 15.2$ Hz, 1H), 3.57 (ddd, $J = 0.8, 3.2, 12.8$

Hz, 1H), 2.96 (dd, $J = 10.4, 12.8$ Hz, 1H), 2.46 (s, 3H), 1.17 (d, $J = 6.0$ Hz, 3H); ^{13}C NMR (75 MHz, CDCl_3) δ 143.7, 140.0, 135.8, 129.9, 128.3, 128.2, 127.3, 127.1, 87.6, 77.2, 56.7, 54.0, 53.9, 21.5, 19.5; HRMS (M + H) for $\text{C}_{19}\text{H}_{22}\text{BrNO}_3\text{SH}$, calcd: 424.0567, found: 424.0555.

(2*S*,3*S*)-methyl 6-bromo-2-methyl-7-phenyl-4-tosyl-1,4-oxazepane-3-carboxylate (2.39h): Major Diastereomer: colourless oil; 31 % isolated yield; $R_f = 0.29$ (8:2 Hex:EtOAc); IR (film, cm^{-1}) 2925.0, 1745.9, 1340.7, 1091.2, 1050.5, 902.2, 736.0; ^1H NMR (400 MHz, CDCl_3) δ 7.67 (d, $J = 8.0$ Hz, 2H), 7.31-7.45 (m, 7H), 4.97 (d, $J = 9.2$ Hz, 1H), 4.62 (d, $J = 1.6$ Hz, 1H), 4.54 (dt, $J = 2.4, 9.6$ Hz, 1H), 4.32 (m, 2H), 3.91 (dq, $J = 2.4, 5.2$ Hz, 1H), 3.54 (s, 3H), 2.44 (s, 3H), 1.09 (d, $J = 6.8$ Hz, 3H); ^{13}C NMR (75 MHz, CDCl_3) δ 168.6, 143.9, 136.6, 136.5, 129.8, 128.7, 128.6, 127.8, 127.0, 83.0, 73.2, 61.6, 51.9, 50.1, 47.8, 21.6, 19.7; HRMS (M + Na) for $\text{C}_{21}\text{H}_{24}\text{BrNO}_5\text{SNa}$, calcd: 504.04563, found: 504.04558. **Minor Diastereomer:** colourless oil; 16 % isolated yield; $R_f = 0.21$ (8:2 Hex:EtOAc); IR (film, cm^{-1}) 2950.8, 1744.1, 1343.6, 1219.4, 1160.3, 731.1; ^1H NMR (400 MHz, CDCl_3) δ 7.72 (d, $J = 8.0$ Hz, 2H), 7.32 (m, 7H), 4.70 (d, $J = 7.2$ Hz, 1H), 4.60 (dd, $J = 2.4, 15.2$ Hz, 1H), 4.52 (d, $J = 2.0$ Hz, 1H), 4.39 (dt, $J = 2.4, 7.2$ Hz, 1H), 4.33 (dq, $J = 2.4, 6.4$ Hz, 1H), 3.91 (dd, $J = 7.2, 15.2$ Hz, 1H), 3.64 (s, 3H), 2.44 (s, 3H), 1.30 (d, $J = 6.8$ Hz, 3H); ^{13}C NMR (75 MHz, CDCl_3) δ 169.3, 144.0, 140.4, 135.9, 129.7, 128.4, 127.5, 126.7, 87.9, 75.6, 69.6, 63.8, 54.7, 52.0, 49.3, 21.6, 19.6; HRMS (M + Na) for $\text{C}_{21}\text{H}_{24}\text{BrNO}_5\text{SNa}$, calcd: 504.04563, found: 504.04408

6-bromo-7-phenyl-4-tosyl-1,4-oxazepane (2.39i): white solid; MP = 93 - 94 °C; >99 % isolated yield; $R_f = 0.47$ (7:3 Hex:EtOAc); IR (film, cm^{-1}) 2923.3, 1713.8, 1337.7, 1158.0, 1088.3, 906.1, 771.9, 698.2; ^1H NMR (300 MHz, CDCl_3) δ 7.74 (d, $J = 8.4$ Hz, 2H), 7.27-7.37 (m, 7H), 4.50 (d, $J = 9.3$ Hz, 1H), 4.10-4.20 (m, 2H), 4.01 (dd, $J = 3.9, 15.3$ Hz, 1H), 3.71-3.81 (m, 2H), 3.40-5.56 (m, 2H), 2.46 (s, 3H); ^{13}C NMR (75 MHz, CDCl_3) δ 143.9, 139.5, 135.9, 130.0, 128.5, 128.4, 127.2, 127.1, 88.7, 53.1, 21.6; HRMS (M + Na) for $\text{C}_{18}\text{H}_{20}\text{BrNO}_3\text{SNa}$, calcd: 432.02450, found: 432.02502

(5*aS*,10*aR*)-3-bromo-2-phenyl-5-tosyl-3,4,5,5*a*,10,10*a*-hexahydro-2*H*-indeno[2,1-*b*][1,4]oxazepine (2.39j): Major Diastereomer: colourless oil; 18 % isolated yield; $R_f = 0.24$ (1:1 DMC:Toluene); IR (film, cm^{-1}) 2923.4, 1339.7, 1219.7, 1162.0, 1092.1, 1062.6, 911.0, 699.3, 673.0; ^1H NMR (300 MHz, CDCl_3) δ 8.02 (d, $J = 8.1$ Hz, 2H), 7.40 (d, $J = 7.8$ Hz, 2H), 7.25-7.30 (m, 5H), 7.15-7.20 (m, 3H), 6.76 (d, $J = 7.5$ Hz, 1H), 5.47 (d, $J = 3.9$ Hz, 1H), 4.63 (d, $J = 9.9$ Hz,

1H), 4.44-4.51 (m, 2H), 4.01 (dd, $J = 4.8, 10.2$ Hz, 1H), 3.89 (dd, $J = 5.1, 16.5$ Hz, 1H), 2.89-3.06 (m, 2H), 2.50 (s, 3H); ^{13}C NMR (75 MHz, CDCl_3) δ 141.3, 138.1, 136.6, 135.2, 134.3, 127.3, 125.8, 125.7, 125.6, 125.3, 124.8, 124.4, 122.9, 121.5, 81.9, 81.8, 64.2, 51.7, 45.9, 35.4, 19.0; HRMS ($\text{M} + \text{Na}$) for $\text{C}_{25}\text{H}_{24}\text{BrNO}_3\text{SNa}$, calcd: 520.05580, found: 520.05545. **Minor Diastereomer:** colourless oil; 45 % isolated yield; $R_f = 0.14$ (1:1 DMC:Toluene); IR (film, cm^{-1}) 2924.5, 1598.0, 1456.9, 1337.0, 1157.5, 1093.0, 998.9, 809.3, 698.9, 660.9; ^1H NMR (300 MHz, CDCl_3) δ 7.93 (d, $J = 8.4$ Hz, 2H), 7.42 (d, $J = 8.1$ Hz, 2H), 7.13-1.35 (m, 8H), 6.81 (d, $J = 7.5$ Hz, 1H), 5.75 (d, $J = 7.5$ Hz, 1H), 4.94 (dt, $J = 1.5, 7.8$ Hz, 1H), 4.31 (dd, $J = 4.2, 15.0$ Hz, 1H), 4.04-4.19 (m, 2H), 3.07-3.35 (m, 3H), 2.52 (s, 3H); ^{13}C NMR (75 MHz, CDCl_3) δ 141.3, 138.2, 138.1, 135.5, 134.8, 127.4, 126.6, 125.9, 125.8, 125.1, 124.6, 124.3, 122.5, 122.4, 77.3, 74.8, 62.0, 47.9, 46.5, 34.2, 19.1; HRMS ($\text{M} + \text{Na}$) for $\text{C}_{25}\text{H}_{24}\text{BrNO}_3\text{SNa}$, calcd: 520.05580, found: 520.05555.

(2R,3S,6R,7S)-methyl 6-bromo-2-methyl-4-((4-nitrophenyl)sulfonyl)-7-phenyl-1,4-oxazepane-3-carboxylate (2.42a): white solid; MP = 138 - 141 °C; 72 % isolated yield; $[\alpha]_{\text{D}}^{22} = -22.1$ (c 1.00, CHCl_3); $R_f = 0.55$ (7:3 Hex:EtOAc); IR (film, cm^{-1}) 2957.6, 1739.2, 1530.3, 1348.4, 1159.0, 1088.5, 1008.3, 699.0; ^1H NMR (300 MHz, CDCl_3) δ 8.40 (d, $J = 8.7$ Hz, 2H), 8.04 (d, $J = 8.7$ Hz, 2H), 7.31 (m, 5H), 4.53 (d, $J = 9.6$ Hz, 1H), 4.40 (d, $J = 10.2$ Hz, 1H), 4.27 (dd, $J = 3.6, 15.3$ Hz, 1H), 4.15 (dt, $J = 3.9, 11.4$ Hz, 1H), 3.92 (m, 2H), 3.57 (s, 3H), 1.37 (d, $J = 6.0$ Hz, 3H); ^{13}C NMR (75 MHz, CDCl_3) δ 170.3, 150.1, 145.5, 139.0, 128.8, 128.4, 128.3, 127.3, 124.4, 90.1, 77.5, 64.7, 52.5, 51.5, 50.5, 20.5; HRMS ($\text{M} + \text{Na}$) for $\text{C}_{20}\text{H}_{21}\text{BrN}_2\text{O}_7\text{SNa}$, calcd: 535.01505, found: 535.01620.

(2R,3S,6S)-methyl 6-(bromomethyl)-2,6-dimethyl-4-((4-nitrophenyl)sulfonyl)morpholine-3-carboxylate (2.43b): colourless oil; 94 % isolated yield; $[\alpha]_{\text{D}}^{22} = -74.7$ ° (c 0.15, CHCl_3); $R_f = 0.55$ (7:3 Hex:EtOAc); IR (film, cm^{-1}) 2926.4, 1743.6, 1532.1, 1350.8, 1165.3, 1089.8, 855.9, 737.9; ^1H NMR (300 MHz, CDCl_3) δ 8.41 (d, $J = 9.0$ Hz, 2H), 8.02 (d, $J = 8.7$ Hz, 2H), 3.98 (dd, $J = 6.0, 9.0$ Hz, 1H), 3.72 (s, 3H), 3.53-3.60 (m, 2H), 3.46 (d, $J = 10.2$ Hz, 1H), 3.00 (d, $J = 12.9$ Hz, 1H), 1.32 (s, 3H), 1.22 (d, $J = 6.3$ Hz, 3H); ^{13}C NMR (75 MHz, CDCl_3) δ 164.0, 142.8, 142.0, 129.2, 124.3, 73.3, 67.6, 63.2, 52.8, 49.0, 35.6, 24.3, 18.6; HRMS ($\text{M} + \text{H}$) for $\text{C}_{15}\text{H}_{19}\text{BrN}_2\text{O}_7\text{SH}$, calcd: 451.0169, found: 451.0170.

(2R,3S,6R)-methyl 6-(bromomethyl)-2,6-dimethyl-4-((4-nitrophenyl)sulfonyl)morpholine-3-carboxylate (2.43b'): characterized from a 1.7:1 mixture of diastereomers; yellow oil; $R_f = 0.48$ (7:3 Hex:EtOAc); IR (film, cm^{-1}) 3106.3, 1984.4, 2954.3, 1741.7, 1530.5, 1345.0, 1163.3, 911.6, 855.7, 819.3, 736.3; ^1H NMR (300 MHz, CDCl_3) δ 8.39 (m, 2H), 8.02 (d, $J = 8.7$ Hz, 2H), 3.93-4.00 (m, 1H), 3.75 (d, $J = 9.0$ Hz, 0.5H), 3.71 (s, 1.5H), 3.69 (s, 1.5H), 3.52-3.58 (m, 1.5H), 3.46 (d, $J = 10.8$ Hz, 0.5H), 3.37 (d, $J = 8.1$ Hz, 0.5H), 3.25 (s, 1H), 2.99 (d, $J = 12.9$ Hz, 0.5H), 1.36 (s, 1.5H), 1.31 (s, 1.5H), 1.26 (d, $J = 6.0$ Hz, 1.5H), 1.22 (d, $J = 6.0$ Hz, 1.5H); ^{13}C NMR (75 MHz, CDCl_3) δ 169.6, 169.4, 150.4, 150.3, 143.6, 142.8, 129.1, 128.9, 124.3, 74.7, 73.3, 67.6, 67.5, 63.3, 63.2, 52.8, 52.7, 49.0, 47.5, 37.9, 35.6, 24.3, 20.7, 19.0, 18.6; HRMS (M + H) for $\text{C}_{15}\text{H}_{19}\text{BrN}_2\text{O}_7\text{SH}$, calcd: 451.0169, found: 451.0173.

(2R,3S,6R)-methyl 6-bromo-2,7,7-trimethyl-4-((4-nitrophenyl)sulfonyl)-1,4-oxazepane-3-carboxylate (2.42c): white solid; MP = 119 - 122 °C; 61 % isolated yield; $[\alpha]^{22}_{\text{D}} = -35.0^\circ$ (c 0.60, CHCl_3); $R_f = 0.56$ (7:3 Hex:EtOAc); IR (film, cm^{-1}) 2982.7, 1739.6, 1531.3, 1349.6, 1157.7, 1088.4, 684.9; ^1H NMR (300 MHz, CDCl_3) δ 8.36 (d, $J = 9.0$ Hz, 2H), 7.98 (d, $J = 9.0$ Hz, 2H), 4.33 (d, $J = 9.9$ Hz, 1H), 4.05 (dd, $J = 1.8, 15.6$ Hz, 1H), 3.94 (m, 2H), 3.73 (dd, $J = 4.3, 15.6$ Hz, 1H), 3.52 (s, 3H), 1.39 (s, 3H), 1.36 (s, 3H), 1.26 (d, $J = 6.3$ Hz, 3H); ^{13}C NMR (75 MHz, CDCl_3) δ 170.8, 150.1, 145.5, 128.3, 124.3, 78.2, 67.6, 64.6, 55.6, 52.4, 48.5, 29.8, 20.9, 19.7; HRMS (M + Na) for $\text{C}_{16}\text{H}_{21}\text{BrN}_2\text{O}_7\text{SNa}$, calcd: 487.01505, found: 487.01370.

(2R,3S,6R,7S)-methyl 6-bromo-2,7-dimethyl-4-((4-nitrophenyl)sulfonyl)-1,4-oxazepane-3-carboxylate (2.42d): colourless oil; 66 % isolated yield; $[\alpha]^{22}_{\text{D}} = -29.3^\circ$ (c 0.90, CHCl_3); $R_f = 0.55$ (7:3 Hex:EtOAc); IR (film, cm^{-1}) 2926.6, 1739.4, 1530.8, 1348.2, 1160.9, 1089.9, 1024.5, 684.9; ^1H NMR (300 MHz, CDCl_3) δ 8.36 (d, $J = 9.0$ Hz, 2H), 7.98 (d, $J = 9.0$ Hz, 2H), 7.45 (m, 2H), 7.34 (m, 3H), 4.69 (s, 1H), 4.49 (d, $J = 15.3$ Hz, 1H), 4.42 (d, $J = 9.6$ Hz, 1H), 4.24 (d, $J = 15.6$ Hz, 1H), 3.88 (dt, $J = 6.0, 15.3$ Hz, 1H), 3.29 (s, 3H), 1.74 (s, 3H), 1.33 (d, $J = 6.3$ Hz, 3H); ^{13}C NMR (75 MHz, CDCl_3) δ 170.2, 150.1, 145.1, 137.2, 128.8, 128.7, 128.1, 127.3, 124.1, 92.7, 79.2, 66.9, 65.2, 56.9, 52.1, 22.8, 20.7; HRMS (M + Na) for $\text{C}_{15}\text{H}_{19}\text{BrN}_2\text{O}_7\text{SNa}$, calcd: 472.99940, found: 472.99854.

(2R,3S,6S)-methyl 6-((R)-1-bromoethyl)-2-methyl-4-((4-nitrophenyl)sulfonyl)morpholine-3-carboxylate (2.42d): colourless oil; 32 % isolated yield; $[\alpha]^{22}_{\text{D}} = -48.9^\circ$ (c 0.70, CHCl_3); $R_f = 0.47$ (7:3 Hex:EtOAc); IR (film, cm^{-1}) 3106.1, 2955.4, 1745.2,

1530.7, 1312.8, 1168.8, 995.4, 855.6, 762.8, 736.5; ^1H NMR (300 MHz, CDCl_3) δ 8.37 (d, $J = 8.7$ Hz, 2H), 7.96 (d, $J = 8.7$ Hz, 2H), 4.69 (q, $J = 6.9$ Hz, 1H), 4.35 (s, 1H), 3.93 (m, 2H), 3.75 (dd, $J = 3.0, 12.3$ Hz, 1H), 3.59 (s, 3H), 3.27 (t, $J = 13.2$ Hz, 1H), 1.65 (d, $J = 6.9$ Hz, 3H), 1.51 (d, $J = 6.6$ Hz, 3H); ^{13}C NMR (75 MHz, CDCl_3) δ 168.8, 150.1, 144.7, 128.5, 124.2, 70.5, 69.7, 58.4, 52.6, 47.7, 43.9, 21.2, 16.5; HRMS (M + Na) for $\text{C}_{15}\text{H}_{19}\text{BrN}_2\text{O}_7\text{SNa}$, calcd: 472.99940, found: 472.99850.

(2R,3S,6R,7S)-methyl 6-bromo-2,6-dimethyl-4-((4-nitrophenyl)sulfonyl)-7-phenyl-1,4-oxazepane-3-carboxylate (2.42e): white solid; MP = 213 - 217 °C; 39 % isolated yield; $[\alpha]_{\text{D}}^{22} = +17.1^\circ$ (c 0.50, CHCl_3); $R_f = 0.58$ (7:3 Hex:EtOAc); IR (film, cm^{-1}) 2926.4, 1740.5, 1531.3, 1344.5, 1161.1, 1023.5, 910.1, 701.8; ^1H NMR (300 MHz, CDCl_3) δ 8.36 (d, $J = 9.0$ Hz, 2H), 7.98 (d, $J = 9.0$ Hz, 2H), 7.34 (m, 3H), 7.45 (m, 2H), 4.69 (s, 1H), 4.49 (d, $J = 15.3$ Hz, 1H), 4.42 (d, $J = 9.6$ Hz, 1H), 4.24 (d, $J = 15.6$ Hz, 1H), 3.88 (dt, $J = 6.0, 15.3$ Hz, 1H), 3.29 (s, 3H), 1.74 (s, 3H), 1.33 (d, $J = 6.3$ Hz, 3H); ^{13}C NMR (75 MHz, CDCl_3) δ 170.2, 150.1, 145.1, 137.2, 128.8, 128.7, 128.1, 127.3, 124.1, 92.7, 79.2, 66.9, 65.2, 56.9, 52.1, 22.8, 20.7; HRMS (M + Na) for $\text{C}_{21}\text{H}_{23}\text{BrN}_2\text{O}_7\text{SNa}$, calcd: 549.03070, found: 549.03051

(2R,3S,6S)-methyl 6-((S)-bromo(phenyl)methyl)-2,6-dimethyl-4-((4-nitrophenyl)sulfonyl)morpholine-3-carboxylate (2.43e): colourless oil; 20 % isolated yield; $[\alpha]_{\text{D}}^{22} = -78.6^\circ$ (c 1.55, CHCl_3); $R_f = 0.48$ (7:3 Hex:EtOAc); IR (film, cm^{-1}) 3105.6, 2937.3, 1741.8, 1530.5, 1311.8, 1161.5, 1090.3, 1039.3, 852.7, 746.2, 736.6; ^1H NMR (300 MHz, CDCl_3) δ 8.37 (d, $J = 9.0$ Hz, 2H), 7.99 (d, $J = 8.7$ Hz, 2H), 7.33 (m, 5H), 5.04 (s, 1H), 4.12 (m, 2H), 3.75 (s, 2H), 3.59 (s, 3H), 1.27 (s, 3H), 1.25 (s, 3H); ^{13}C NMR (75 MHz, CDCl_3) δ 169.6, 150.1, 145.0, 136.6, 129.5, 128.6, 128.5, 128.0, 124.2, 77.9, 67.3, 62.3, 57.4, 52.5, 48.7, 21.3, 18.9; HRMS (M + H) for $\text{C}_{21}\text{H}_{23}\text{BrN}_2\text{O}_7\text{SH}$, calcd: 527.0482, found: 527.0458.

(3S,6R,7S)-methyl 6-bromo-4-((4-nitrophenyl)sulfonyl)-7-phenyl-1,4-oxazepane-3-carboxylate (2.42f): white solid; MP = 148 - 150 °C; 94 % isolated yield; $[\alpha]_{\text{D}}^{22} = -21.1^\circ$ (c 0.75, CHCl_3); $R_f = 0.45$ (7:3 Hex:EtOAc); IR (film, cm^{-1}) 2955.5, 1745.6, 1530.5, 1349.3, 1100.9, 739.0; ^1H NMR (300 MHz, CDCl_3) δ 8.40 (d, $J = 9.0$ Hz, 2H), 8.09 (d, $J = 9.0$ Hz, 2H), 7.28 (m, 2H), 7.36 (m, 3H), 5.06 (dd, $J = 7.2, 10.5$ Hz, 1H), 4.55 (dd, $J = 7.2, 13.2$ Hz, 1H), 4.37 (d, $J = 10.2$ Hz, 1H), 4.21 (m, 2H), 3.72 (m, 2H), 3.65 (s, 3H); ^{13}C NMR (75 MHz, CDCl_3) δ 169.3, 150.2, 145.3,

138.4, 129.0, 128.7, 128.5, 127.3, 124.4, 90.7, 69.6, 59.2, 52.7, 50.7, 50.1; HRMS (M + Na) for C₁₉H₁₉BrN₂O₇SNa, calcd: 520.99940, found: 521.00099.

(3S)-methyl 6-bromo-6-methyl-4-((4-nitrophenyl)sulfonyl)-1,4-oxazepane-3-carboxylate (2.43g): characterized from a 1.7:1 mixture of diastereomers; yellow oil; 77 % isolated yield; *R_f* = 0.40 (7:3 Hex:EtOAc); IR (film, cm⁻¹) 2956.0, 1745.4, 1529.9, 1348.9, 1162.6, 1090.9, 855.4, 768.8, 731.2; ¹H NMR (300 MHz, CDCl₃) δ 8.36 (d, *J* = 8.7 Hz, 2H), 7.95 (d, *J* = 8.7 Hz, 2H), 4.54-5.57 (m, 1H), 4.08-4.14 (m, 0.5H), 3.99 (dd, *J* = 4.2, 12.6 Hz, 1H), 3.85 (d, *J* = 11.1 Hz, 1H), 3.72 (d, *J* = 13.2 Hz, 1H), 3.62 (s, 2H), 3.59 (s, 1H), 3.46 (d, *J* = 11.4 Hz, 1H), 3.28 (m, 1.5H), 1.26 (s, 3H); ¹³C NMR (75 MHz, CDCl₃) δ 168.7, 168.6, 150.2, 150.1, 144.7, 144.5, 128.6, 128.5, 124.2, 124.1, 72.1, 71.4, 62.8, 62.3, 54.6, 54.2, 52.8, 52.7, 48.5, 47.4, 38.7, 33.8, 24.2, 17.9; HRMS (M + H) for C₁₄H₁₇BrN₂O₇SH, calcd: 437.0013, found: 436.9996.

(3S)-methyl 6-bromo-7,7-dimethyl-4-((4-nitrophenyl)sulfonyl)-1,4-oxazepane-3-carboxylate (2.42h): white solid; MP = 113 - 115 °C; >99 % isolated yield; [α]_D²² = -22.1 ° (*c* 0.95, CHCl₃); *R_f* = 0.44 (7:3 Hex:EtOAc); IR (film, cm⁻¹) 2957.2, 1747.0, 1530.3, 1349.0, 1158.2, 1088.0, 706.8; ¹H NMR (300 MHz, CDCl₃) δ 8.37 (d, *J* = 8.1 Hz, 2H), 8.03 (d, *J* = 8.1 Hz, 2H), 4.84 (t, *J* = 3.6 Hz, 1H), 4.11 (dd, *J* = 3.9, 13.2 Hz, 1H), 3.97 (m, 3H), 3.74 (dd, *J* = 10.2, 15.6 Hz, 1H), 3.66 (s, 3H), 1.37 (s, 3H), 1.30 (s, 3H); ¹³C NMR (75 MHz, CDCl₃) δ 169.1, 145.2, 128.7, 128.6, 124.3, 78.7, 63.9, 59.4, 54.9, 52.7, 48.9, 25.4, 24.0; HRMS (M + Na) for C₁₅H₁₉BrN₂O₇SNa, calcd: 472.99940, found: 472.99955.

(3S,6S,7R)-methyl 6-bromo-7-methyl-4-((4-nitrophenyl)sulfonyl)-1,4-oxazepane-3-carboxylate (2.42i): Colourless oil; 46 % isolated yield; [α]_D²² = -35.2 ° (*c* 1.65, CHCl₃); *R_f* = 0.42 (7:3 Hex:EtOAc); IR (film, cm⁻¹) 3106.8, 2925.4, 1745.2, 1530.3, 1313.8, 1160.9, 1103.9, 1089.8, 1008.2, 855.5, 738.7; ¹H NMR (300 MHz, CDCl₃) δ 8.37 (d, *J* = 8.7 Hz, 2H), 8.03 (d, *J* = 8.7 Hz, 2H), 4.93 (dd, *J* = 7.2, 10.2 Hz, 1H), 4.44 (dd, *J* = 6.6, 13.2 Hz, 1H), 4.10 (dd, *J* = 3.0, 15.6 Hz, 1H), 3.80 (m, 1H), 3.60 (s, 3H), 3.55 (m, 3H), 1.42 (d, *J* = 6.0 Hz, 3H); ¹³C NMR (75 MHz, CDCl₃) δ 169.3, 150.1, 145.3, 128.6, 124.2, 84.6, 68.9, 59.2, 52.6, 51.7, 59.9, 20.2; HRMS (M + H) for C₁₄H₁₇BrN₂O₇SH, calcd: 437.0013, found: 437.0002.

(3S)-methyl 6-(1-bromoethyl)-4-((4-nitrophenyl)sulfonyl)morpholine-3-carboxylate (2.43i): characterized from a 1.2:1 mixture of diastereomers; yellow oil; *R_f* = 0.35 (7:3 Hex:EtOAc); IR (film, cm⁻¹) 3106.5, 2956.1, 1745.2, 1530.4, 1349.2, 1104.0, 1090.0, 855.4, 773.4,

738.1; ^1H NMR (300 MHz, CDCl_3) δ 8.36 (d, $J = 8.7$ Hz, 2H), 7.94-8.04 (m, 2H), 4.93 (dd, $J = 6.9, 3.9$ Hz, 0.5H), 4.44 (dd, $J = 6.9, 13.2$ Hz, 1H), 4.10 (dd, $J = 2.7, 15.9$ Hz, 1H), 3.7-3.89 (m, 2H), 3.68 (s, 1H), 3.61 (s, 3H), 3.52-3.57 (m, 1.5H), 1.67-1.74 (m, 1H), 1.42 (d, $J = 6.0$ Hz, 2H); ^{13}C NMR (75 MHz, CDCl_3) δ 169.3, 168.6, 150.7, 150.2, 145.3, 144.8, 128.9, 128.6, 124.3, 124.2, 84.6, 79.2, 78.5, 77.2, 68.9, 59.2, 54.8, 54.7, 52.8, 52.6, 51.7, 49.9, 46.8, 46.8, 21.9, 20.2; HRMS (M + H) for $\text{C}_{14}\text{H}_{17}\text{BrN}_2\text{O}_7\text{SH}$, calcd: 437.0013, found: 436.9992.

(3*S*,6*R*,7*R*)-methyl 6-bromo-6-methyl-4-((4-nitrophenyl)sulfonyl)-7-phenyl-1,4-oxazepane-3-carboxylate (2.42j): colourless oil; 25 % isolated yield; $[\alpha]_{\text{D}}^{22} = +7.9^\circ$ (c 3.15, CHCl_3); $R_f = 0.66$ (7:3 Hex:EtOAc); IR (film, cm^{-1}) 3106.0, 2953.9, 1743.5, 1530.3, 1348.5, 1160.1, 1112.1 1021.6, 1011.5, 895.3, 855.1, 701.9; ^1H NMR (300 MHz, CDCl_3) δ 8.36 (d, $J = 9.0$ Hz, 2H), 7.99 (d, $J = 9.0$ Hz, 2H), 7.43 (m, 2H), 7.35 (m, 3H), 4.91 (dd, $J = 7.5, 10.8$ Hz, 1H), 4.59 (t, $J = 7.5$ Hz, 1H), 4.55 (d, $J = 7.5$ Hz, 1H), 4.53 (dd, $J = 0.9, 15.6$ Hz, 1H), 4.13 (d, $J = 15.6$ Hz, 1H), 3.64 (d, $J = 10.8$ Hz, 1H), 3.38 (s, 3H), 1.75 (s, 3H); ^{13}C NMR (75 MHz, CDCl_3) δ 169.2, 150.1, 145.3, 136.7, 128.8, 128.7, 128.3, 127.5, 124.1, 94.1, 71.8, 66.5, 59.6, 56.5, 52.4, 22.8; HRMS (M + NH_4) for $\text{C}_{20}\text{H}_{21}\text{BrN}_2\text{O}_7\text{SNH}_4$, calcd: 530.0591, found: 530.0567.

(3*S*)-methyl 6-(bromo(phenyl)methyl)-6-methyl-4-((4-nitrophenyl)sulfonyl)morpholine-3-carboxylate (2.43j): colourless oil; 17 % isolated yield; $[\alpha]_{\text{D}}^{22} = -9.8^\circ$ (c 1.50, CHCl_3); $R_f = 0.53$ (7:3 Hex:EtOAc); IR (film, cm^{-1}) 3106.0, 2953.7, 1746.9, 1530.5, 1311.9, 1164.3, 1089.3, 855.6, 759.4, 734.4; ^1H NMR (300 MHz, CDCl_3) δ 8.39 (d, $J = 8.7$ Hz, 2H), 7.57 (d, $J = 8.7$ Hz, 2H), 7.32-7.49 (m, 5H), 5.53 (s, 1H), 4.58 (d, $J = 3.9$ Hz, 1H), 4.31 (d, $J = 13.5$ Hz, 1H), 4.16 (dt, $J = 4.2, 12.3$ Hz, 1H), 4.01 (dd, $J = 1.5, 12.3$ Hz, 1H), 3.62 (s, 3H), 3.24 (d, $J = 13.2$ Hz, 1H), 1.46 (s, 3H); ^{13}C NMR (75 MHz, CDCl_3) δ 168.6, 150.2, 144.5, 136.9, 129.2, 128.9, 128.7, 128.3, 124.2, 75.9, 62.4, 54.6, 52.7, 52.5, 48.7, 21.8; HRMS (M + H) for $\text{C}_{20}\text{H}_{21}\text{BrN}_2\text{O}_7\text{SH}$, calcd: 513.0323, found: 513.0294.

(5*aR*,9*aR*)-3-bromo-5-((4-nitrophenyl)sulfonyl)-2-phenyldecahydrobenzo[*b*][1,4]oxazepine (2.42k): characterized from a 2.0:1 mixture of diastereomers: **Major Diastereomer**: colourless oil; 49 % isolated yield; $R_f = 0.78$ (7:3 Hex:EtOAc); IR (film, cm^{-1}) 2940, 1529.2, 1311.1, 1157.2, 1086.8, 1000.0, 728.2; ^1H NMR (300 MHz, CDCl_3) δ 8.42 (d, $J = 9.0$ Hz, 2H), 8.14 (d, $J = 9.0$ Hz, 2H), 7.26 (m, 3H), 6.95 (dd, $J = 1.8, 7.8$ Hz, 2H), 4.26 (m, 2H), 3.66 (m, 3H), 3.43 (dt, $J = 3.9, 10.8$ Hz, 1H), 2.05 (m, 2H), 1.79 (m,

2H), 1.36 (m, 4H); ^{13}C NMR (75 MHz, CDCl_3) δ 150.0, 147.4, 139.3, 128.7, 128.4, 128.2, 127.1, 124.7, 88.4, 82.3, 77.4, 77.0, 76.6, 63.7, 51.4, 48.8, 33.8, 32.0, 24.7, 24.6; HRMS (M + Na) for $\text{C}_{21}\text{H}_{23}\text{BrN}_2\text{O}_5\text{SNa}$, calcd: 517.04087, found: 517.04134. **Minor Diastereomer:** yellow oil; R_f = 0.67 (7:3 Hex:EtOAc); IR (film, cm^{-1}) 2940.2, 1530.0, 1348.7, 1219.7, 1158.7, 1088.4, 855.3, 772.4; ^1H NMR (300 MHz, CDCl_3) δ 8.43 (d, J = 9.0 Hz, 1H), 8.37 (d, J = 8.7 Hz, 1H), 8.14 (d, J = 9.0 Hz, 1H), 8.05 (d, J = 8.7 Hz, 1H), 7.30-7.35 (m, 3H), 6.95 (m, 1H), 4.66 (d, J = 9.6 Hz, 0.5H), 4.28-4.39 (M, 2H), 4.03-4.11 (M, 0.5H), 3.74-3.82 (m, 1H), 3.67 (m, 0.5H), 3.21-3.45 (br m, 2H), 2.05 (m, 1.5H), 1.74-1.82 (br m, 3H), 1.16-1.37 (br m, 4H); ^{13}C NMR (75 MHz, CDCl_3) δ ; HRMS (M + K) for $\text{C}_{21}\text{H}_{23}\text{BrN}_2\text{O}_5\text{SK}$, calcd: 533.0143, found: 533.0118.

(3R,6R,7S)-6-bromo-3-ethyl-4-((4-nitrophenyl)sulfonyl)-7-phenyl-1,4-oxazepane

(2.42l): colourless oil; >99 % isolated yield; $[\alpha]_D^{22} = +54.0^\circ$ (c 0.80, CHCl_3); R_f = 0.60 (7:3 Hex:EtOAc); IR (film, cm^{-1}) 2968.0, 1529.2, 1347.7, 1155.6, 1087.8, 907.8, 678.9; ^1H NMR (300 MHz, CDCl_3) δ 8.42 (d, J = 8.7 Hz, 2H), 8.14 (d, J = 8.7 Hz, 2H), 7.25 (m, 3H), 6.88 (d, J = 7.5 Hz, 2H), 4.38 (dd, J = 3.3, 13.2 Hz, 1H), 4.29 (m, 2H), 4.23 (d, J = 9.9 Hz, 1H), 3.81 (dt, J = 3.6, 10.2 Hz, 1H), 3.55 (dd, J = 12.0, 15.6 Hz, 1H), 3.39 (dd, J = 9.3, 12.0 Hz, 1H), 1.57 (br m, 2H), 0.93 (t, J = 9.0 Hz, 3H); ^{13}C NMR (75 MHz, CDCl_3) δ 150.0, 147.5, 138.8, 128.8, 128.6, 128.3, 126.8, 124.6, 90.5, 72.9, 59.1, 50.0, 48.5, 24.5, 10.1; HRMS (M + Na) for $\text{C}_{19}\text{H}_{21}\text{BrN}_2\text{O}_5\text{SNa}$, calcd: 491.02522, found: 491.02551.

(2R,6S,7R)-6-bromo-2-methyl-4-((4-nitrophenyl)sulfonyl)-7-phenyl-1,4-oxazepane

(2.42m): white solid; MP = 167 - 171 $^\circ\text{C}$; 47 % isolated yield; $[\alpha]_D^{22} = -29.4^\circ$ (c 0.85, CHCl_3); R_f = 0.62 (7:3 Hex:EtOAc); IR (film, cm^{-1}) 2926.7, 1530.0, 1311.3, 1163.6, 1087.0, 736.6; ^1H NMR (300 MHz, CDCl_3) δ 8.41 (d, J = 9.0 Hz, 2H), 8.03 (d, J = 9.0 Hz, 2H), 7.37 (m, 5H), 4.81 (d, J = 9.3 Hz, 1H), 4.35 (m, 2H), 3.99 (m, 1H), 3.85 (dd, J = 3.6, 14.1 Hz, 1H), 3.36 (dd, J = 9.6, 13.8 Hz, 1H), 2.78 (dd, J = 9.9, 13.8 Hz, 1H), 1.09 (d, J = 6.3 Hz, 3H); ^{13}C NMR (75 MHz, CDCl_3) δ 150.2, 145.1, 138.6, 138.5, 128.6, 128.2, 127.3, 124.6, 80.0, 71.1, 54.9, 54.8, 49.4, 18.2; HRMS (M + H) for $\text{C}_{18}\text{H}_{19}\text{BrN}_2\text{O}_5\text{SH}$, calcd: 454.0198, found: 454.0174.

(2R,6R,7S)-6-bromo-2-methyl-4-((4-nitrophenyl)sulfonyl)-7-phenyl-1,4-oxazepane

(2.42m'): characterized as a 1.2:1 mixture of diastereomers; yellow oil; R_f = 0.56 (7:3 Hex:EtOAc); IR (film, cm^{-1}) 3105.5, 2927.4, 1541.1, 1347.7, 1160.9, 1084.7, 907.1, 775.0, 731.3, 696.0; ^1H NMR (300 MHz, CDCl_3) δ 8.39-8.43 (m, 2H), 8.02-8.08 (m, 2H), 4.81 (d, J = 9.3 Hz,

0.7H), 4.59 (d, $J = 9.6$ Hz, 0.3H), 4.29-4.42 (m, 1.4H), 4.16 (m, 0.3H), 3.97-4.04 (M, 0.6H), 3.94 (d, $J = 5.1$ Hz, 0.7H), 3.85 (dd, $J = 3.6, 14.7$ Hz, 0.7H), 3.59 (dd, $J = 3.6, 12.6$ Hz, 0.3H). 3.37 (dd, $J = 9.9, 13.8$ Hz, 1H), 3.08 (dd, $J = 10.5, 12.6$ Hz, 0.3H), 2.78 (dd, $J = 10.2, 14.1$ Hz, 0.7H), 1.33-7.37 (m, 5H), 1.20 (d, $J = 6.3$ Hz, 1H), 1.09 (d, $J = 6.3$ Hz, 2H); ^{13}C NMR (75 MHz, CDCl_3) δ 150.2, 150.2, 145.1, 144.7, 139.6, 138.6, 128.6, 128.5, 128.4, 128.3, 128.2, 127.3, 127.0, 124.6, 87.8, 79.9, 71.1, 56.5, 54.9, 54.8, 53.8, 53.5, 49.5, 19.5, 18.2; HRMS (M + H) for $\text{C}_{18}\text{H}_{19}\text{BrN}_2\text{O}_5\text{SH}$, calcd: 454.0198, found: 454.0181.

(2*S*,3*S*,6*R*,7*S*)-methyl 6-bromo-2-methyl-4-((4-nitrophenyl)sulfonyl)-7-phenyl-1,4-oxazepane-3-carboxylate (2.42n): white solid; MP = 156 - 159 °C; 25 % isolated yield; $[\alpha]_{\text{D}}^{22} = -48.2^\circ$ (c 0.75, CHCl_3); $R_f = 0.66$ (7:3 Hex:EtOAc); IR (film, cm^{-1}) 2954.3, 1742.5, 1530.4, 1347.7, 1154.6, 1050.0, 901.8, 698.6; ^1H NMR (300 MHz, CDCl_3) δ 8.38 (d, $J = 9.0$ Hz, 2H), 7.98 (d, $J = 8.7$ Hz, 2H), 7.45 (m, 5H), 4.98 (d, $J = 9.6$ Hz, 1H), 4.64 (d, $J = 2.1$ Hz, 1H), 4.60 (dt, $J = 2.4, 9.6$ Hz, 1H), 4.30 (m, 2H), 3.97 (dq, $J = 2.1, 6.6$ Hz, 1H), 3.59 (s, 3H), 1.13 (d, $J = 6.6$ Hz, 3H); ^{13}C NMR (75 MHz, CDCl_3) δ 161.3, 145.0, 136.2, 128.9, 128.7, 128.6, 128.3, 127.8, 124.4, 83.0, 73.4, 62.0, 52.2, 50.5, 47.5, 19.8; HRMS (M + Na) for $\text{C}_{20}\text{H}_{21}\text{BrN}_2\text{O}_7\text{SNa}$, calcd: 535.01505, found: 535.01630.

(2*S*,3*S*,6*S*,7*R*)-methyl 6-bromo-2-methyl-4-((4-nitrophenyl)sulfonyl)-7-phenyl-1,4-oxazepane-3-carboxylate (2.42n'): white solid; MP = 174 - 177 °C; 17 % isolated yield; $[\alpha]_{\text{D}}^{22} = -29.2^\circ$ (c 0.65, CHCl_3); $R_f = 0.57$ (7:3 Hex:EtOAc); IR (film, cm^{-1}) 2953.6, 1743.2, 1531.3, 1311.0, 1166.0, 737.7; ^1H NMR (300 MHz, CDCl_3) δ 8.38 (d, $J = 9.0$ Hz, 2H), 8.03 (d, $J = 9.0$ Hz, 2H), 7.31 (m, 5H), 4.79 (d, $J = 6.6$ Hz, 1H), 4.60 (m, 2H), 4.44 (dq, $J = 2.4, 6.6$ Hz, 1H), 4.38 (dt, $J = 2.1, 6.6$ Hz, 1H), 4.01 (dd, $J = 6.9, 15.3$ Hz, 1H), 3.66 (s, 3H), 1.35 (d, $J = 6.9$ Hz, 3H); ^{13}C NMR (75 MHz, CDCl_3) δ 168.9, 144.8, 140.1, 128.7, 128.6, 128.5, 126.4, 124.4, 124.3, 87.8, 75.6, 64.1, 54.4, 52.2, 49.2, 19.6; HRMS (M + Na) for $\text{C}_{20}\text{H}_{21}\text{BrN}_2\text{O}_7\text{SNa}$, calcd: 535.01505, found: 535.01629.

6-bromo-4-((4-nitrophenyl)sulfonyl)-7-phenyl-1,4-oxazepane (2.42o): white solid; MP = 157 - 159 °C; >99 % isolated yield; $R_f = 0.42$ (7:3 Hex:EtOAc); IR (film, cm^{-1}) 2926.6, 1529.0, 1309.5, 1163.4, 1087.2, 1025.7, 855.0, 737.1; ^1H NMR (300 MHz, CDCl_3) δ 8.42 (d, $J = 9.0$ Hz, 2H), 8.07 (d, $J = 9.0$ Hz, 2H), 7.33 (m, 5H), 4.50 (d, $J = 9.3$ Hz, 1H), 4.19 (m, 2H), 4.09 (dd, $J = 3.9, 15.0$ Hz, 1H), 3.79 (m, 2H), 3.63 (dt, $J = 5.1, 10.8$ Hz, 1H), 3.46 (dt, $J = 2.7, 12.6$ Hz, 1H);

^{13}C NMR (75 MHz, CDCl_3) δ 150.2, 144.8, 139.1, 128.7, 128.5, 128.4, 127.0, 124.6, 88.8, 69.6, 53.3, 52.5, 50.1; HRMS (M + Na) for $\text{C}_{17}\text{H}_{17}\text{BrN}_2\text{O}_5\text{SNa}$, calcd: 462.99392, found: 462.99495.

(2*R*,3*S*,5*aS*,10*aR*)-3-bromo-5-((4-nitrophenyl)sulfonyl)-2-phenyl-3,4,5,5*a*,10,10*a*-hexahydro-2*H*-indeno[2,1-*b*][1,4]oxazepine (2.42*p*): white solid; MP = 158 - 161 °C; 98 % isolated yield; $[\alpha]_D^{22} = -45.2^\circ$ (c 0.55, CHCl_3); $R_f = 0.68$ (7:3 Hex:EtOAc); IR (near, cm^{-1}) 2935.5, 1529.9, 1349.0, 1164.1, 1090.9, 999.0, 906.9, 808.9, 678.9; ^1H NMR (300 MHz, CDCl_3) δ 8.47 (d, $J = 9.0$ Hz, 2H), 8.22 (d, $J = 9.0$ Hz, 2H), 7.30 (m, 6H), 7.10 (dd, $J = 1.5, 6.6$ Hz, 2H), 6.75 (d, $J = 7.5$ Hz, 1H), 5.73 (d, $J = 7.8$ Hz, 1H), 4.93 (t, $J = 7.5$ Hz, 1H), 4.26 (dd, $J = 4.2, 15.0$ Hz, 1H), 4.10 (dq, $J = 4.2, 10.8$ Hz, 1H), 4.03 (d, $J = 9.9$ Hz, 1H), 3.21 (m, 3H); ^{13}C NMR (75 MHz, CDCl_3) δ 146.7, 140.8, 140.3, 136.5, 129.6, 128.6, 128.5, 128.3, 128.0, 126.7, 125.2, 124.7, 124.6, 79.8, 77.3, 65.0, 49.9, 49.3, 36.7; HRMS (M + Na) for $\text{C}_{24}\text{H}_{21}\text{BrN}_2\text{O}_5\text{SNa}$, calcd: 551.02522, found: 551.02607.

(2*R*,3*S*,6*R*,7*S*)-methyl 6-chloro-2-methyl-4-((4-nitrophenyl)sulfonyl)-7-phenyl-1,4-oxazepane-3-carboxylate (2.42*q*): white solid; 18 % isolated yield; $[\alpha]_D^{22} = -29.55$ (c 1.52, CHCl_3); $R_f 0.47$ (7:3 Hexanes:EtOAc); MP: 153 – 155 °C; IR (film, cm^{-1}): 1728, 1530, 1360, 1348, 1159, 1089, 760, 746, 707, 684; ^1H NMR (400 MHz, CDCl_3) δ 8.41 (d, $J = 8.9$ Hz, 2H), 8.06 (d, $J = 9.0$ Hz, 2H), 7.37 (dd, $J = 5.0, 1.8$ Hz, 3H), 7.34 – 7.26 (m, 2H), 4.55 (dd, $J = 9.6, 0.7$ Hz, 1H), 4.30 (d, $J = 10.0$ Hz, 1H), 4.20 (ddd, $J = 15.5, 3.6, 0.7$ Hz, 1H), 4.10 (ddd, $J = 11.3, 10.0, 3.6$ Hz, 1H), 3.98 (dq, $J = 9.6, 6.1$ Hz, 1H), 3.83 (dd, $J = 15.5, 11.3$ Hz, 1H), 3.59 (s, 3H), 1.40 (d, $J = 6.1$ Hz, 3H); ^{13}C NMR (100 MHz, CDCl_3) δ 170.3, 150.2, 145.5, 138.9, 128.7, 128.4, 128.3, 127.3, 124.4, 89.9, 77.4, 64.7, 59.4, 52.5, 50.2, 20.6; HRMS: (M + K) for $\text{C}_{20}\text{H}_{21}\text{ClN}_2\text{O}_7\text{SK}$ calcd 507.03951, found 507.0366.

(2*R*,3*S*,6*R*,7*S*)-methyl 6-iodo-2-methyl-4-((4-nitrophenyl)sulfonyl)-7-phenyl-1,4-oxazepane-3-carboxylate (2.42*r*): yellow oil; 58 % isolated yield; $[\alpha]_D^{22} = +5.75$ (c 3.91, CHCl_3); $R_f 0.43$ (7:3 Hex:EtOAc); IR (film, cm^{-1}): 1737, 1530, 1348, 1159, 1088, 1006, 907, 729; ^1H NMR (400 MHz, CDCl_3) δ 8.39 (d, $J = 8.9$ Hz, 2H), 8.03 (d, $J = 8.9$ Hz, 2H), 7.33 (m, 3H), 7.30 – 7.21 (m, 2H), 4.54 (d, $J = 10.0$ Hz, 2H), 4.41 – 4.26 (m, 2H), 3.96 (m, 2H), 3.56 (s, 3H), 1.34 (d, $J = 6.1$ Hz, 3 H); ^{13}C NMR (100 MHz, CDCl_3) δ 170.3, 150.2, 145.6, 139.5, 128.8, 128.4, 128.3, 127.5, 124.4, 91.5, 77.0, 65.0, 52.5, 52.4, 33.3, 20.3; HRMS: (M + K)⁺ for $\text{C}_{20}\text{H}_{21}\text{IN}_2\text{O}_7\text{SK}$ calcd 598.97512, found 598.9724

2.6 References

- (1) Hanessian, S.; Auzzas, L. *Acc. Chem. Res.* **2008**, *41*, 1241.
- (2) Hanessian, S.; Moitessier, N. *Curr. Top. Med. Chem.* **2004**, *4*, 1269.
- (3) Sun, H.; Nikolovska-Coleska, Z.; Yang, C.-Y.; Qian, D.; Lu, J.; Qiu, S.; Bai, L.; Peng, Y.; Cai, Q.; Wang, S. *Acc. Chem. Res.* **2008**, *41*, 1264.
- (4) Moitessier, N.; Henry, C.; Aubert, N.; Chapleur, Y. *Tetrahedron Lett.* **2005**, *46*, 6191.
- (5) Moitessier, N.; Dufour, S.; Chrétien, F.; Thiery, J. P.; Maignet, B.; Chapleur, Y. *Bioorg. Med. Chem.* **2001**, *9*, 511.
- (6) Sacchetti, A.; Silvani, A.; Lesma, G.; Pilati, T. *J. Org. Chem.* **2011**, *76*, 833.
- (7) Proulx, C.; Lubell, W. D. *Org. Lett.* **2012**, *14*, 4552.
- (8) Liskamp, R. M. J.; Rijkers, D. T. S.; Kruijtzter, J. A. W.; Kemmink, J. *ChemBioChem* **2011**, *12*, 1626.
- (9) Ko, E.; Liu, J.; Perez, L. M.; Lu, G.; Schaefer, A.; Burgess, K. *J. Am. Chem. Soc.* **2011**, *133*, 462.
- (10) Ko, E.; Burgess, K. *Org. Lett.* **2011**, *13*, 980.
- (11) Ressurreicao, A. S. M.; Delatouche, R.; Gennari, C.; Piarulli, U. *Eur. J. Org. Chem.* **2011**, 217.
- (12) Kaneko, S.; Arai, M.; Uchida, T.; Harasaki, T.; Fukuoka, T.; Konosu, T. *Bioorg. Med. Chem. Lett.* **2002**, *12*, 1705.
- (13) Abrous, L.; Hynes, J.; Friedrich, S. R.; Smith, A. B.; Hirschmann, R. *Org. Lett.* **2001**, *3*, 1089.
- (14) Nakano, A.; Takahashi, K.; Ishihara, J.; Hatakeyama, S. *Org. Lett.* **2006**, *8*, 5357.
- (15) Kamimura, A.; Yamane, Y.; Yo, R.; Tanaka, T.; Uno, H. *J. Org. Chem.* **2014**, *79*, 7696.
- (16) Kaladevi, S.; Thirupathi, A.; Sridhar, J.; Muthusubramanian, S. *RSC Adv.* **2014**, *4*, 37526.
- (17) Mishra, J. K.; Panda, G. *J. Comb. Chem.* **2007**, *9*, 321.
- (18) Levai, A. *J. Heterocyclic Chem.* **2001**, *38*, 1011.
- (19) Machetti, F.; Bucelli, I.; Indiani, G.; Kappe, C. O.; Guarna, A. *J. Comb. Chem.* **2007**, *9*, 454.
- (20) Diéguez-Vázquez, A.; Tzschucke, C. C.; Lam, W. Y.; Ley, S. V. *Angew. Chem. Int. Ed.* **2008**, *47*, 209.
- (21) Clark, S. M.; Osborn, H. M. I. *Tetrahedron: Asymmetry* **2004**, *15*, 3643.

- (22) Burland, P. A.; Osborn, H. M.; Turkson, A. *Bioorg. Med. Chem.* **2011**, *19*, 5679.
- (23) Ohno, H.; Hamaguchi, H.; Ohata, M.; Kosaka, S.; Tanaka, T. *J. Am. Chem. Soc.* **2004**, *126*, 8744.
- (24) Das, S. K.; Srivastava, A. K.; Panda, G. *Tetrahedron Lett.* **2010**, *51*, 1483.
- (25) Zhou, R.; Wang, J.; Duan, C.; He, Z. *Org. Lett.* **2012**, *14*, 6134.
- (26) Ghorai, M. K.; Shukla, D.; Das, K. *J. Org. Chem.* **2009**, *74*, 7013.
- (27) Bezanson, M.; Pottel, J.; Bilbeisi, R.; Toumieux, S.; Cueto, M.; Moitessier, N. *J. Org. Chem.* **2013**, *78*, 872.
- (28) Gharpure, S. J.; Prasad, J. V. K. *Eur. J. Org. Chem.* **2013**, *2013*, 2076.
- (29) Vo, C. V.; Luescher, M. U.; Bode, J. W. *Nat. Chem.* **2014**, *6*, 310.
- (30) Geoghegan, K.; Bode, J. W. *Org. Lett.* **2015**, *17*, 1934.
- (31) Brady, P. B.; Carreira, E. M. *Org. Lett.* **2015**.
- (32) Mahajan, D.; Dugar, S.; Sharma, A.; Kuila, B.; Dwivedi, S.; Tripathi, V. *Synthesis* **2014**, *47*, 712.
- (33) Deka, M. J.; Indukuri, K.; Sultana, S.; Borah, M.; Saikia, A. K. *J. Org. Chem.* **2015**, *80*, 4349.
- (34) Ghosh, P.; Deka, M. J.; Saikia, A. K. *Tetrahedron* **2016**, *72*, 690.
- (35) Huot, M.; Moitessier, N. *Tetrahedron Lett.* **2010**, *51*, 2820.
- (36) Wender, P. A.; Verma, V. A.; Paxton, T. J.; Pillow, T. H. *Acc. Chem. Res.* **2008**, *41*, 40.
- (37) Ko, C.; Hsung, R. P.; Al-Rashid, Z. F.; Feltenberger, J. B.; Lu, T.; Yang, J.-H.; Wei, Y.; Zifcsak, C. A. *Org. Lett.* **2007**, *9*, 4459.
- (38) Bilbeisi, R., McGill University, 2008.
- (39) Guindon, Y.; Slassi, A.; Rancourt, J.; Bantle, G.; Bencheqroun, M.; Murtagh, L.; Ghire, E.; Jung, G. *J. Org. Chem.* **1995**, *60*, 288.

Chapter 3 Characterization & mechanistic study of the formation of regio- & stereoselective oxazepanes and morpholines

3.1 Preface

The synthesis, condition optimization and substrate scope of chiral poly-substituted oxazepane and morpholine derivatives was discussed in Chapter 2. Some of these heterocycles were formed regioselectively while others formed a mixture of regioisomers. Similarly, some compounds formed a single diastereomer in a stereoselective fashion while others formed as a mixture of diastereomers.

This chapter describes the investigation of the mechanism of formation of these oxazepane and morpholine derivatives, focusing on the key step of halocycloetherification. A variety of different starting materials were investigated to probe particular substituent effects on the regioselectivity and stereoselectivity of the reaction by chemical means. The stereoselectivity was additionally investigated by computational methods where chemical methods proved to not yield any useful information. Any computational work presented was carried out by Dr. Joshua Pottel in the Moitessier lab.

3.2 Introduction

Chapter 1 focused on halocycloetherification reactions to make 3- to 6- membered rings. This chapter focuses more heavily on the study of halocycloetherification, and specifically bromocycloetherification, to make morpholines and oxazepanes and explaining the regiochemistry and the relative and absolute stereochemistry of the products obtained in Chapter 2.

A literature review yields few examples of using halocycloetherification to make morpholines and oxazepanes. Those examples as well as some other halogen-mediated cyclization reactions will be introduced here. In addition, closely related selenocycloetherification reactions used to make these heterocycles will also be highlighted.

There are very few theoretical studies that have been done examining bromiranium ions and their symmetry. One study from Yamabe and Minato in 1993 did look at bromiranium ion intermediates in the bromination of olefins using a semi empirical method (PM3).¹ Not unexpectedly, they found that unsymmetric olefins adopted unsymmetric bromiraniums that favoured Markovnikov-type open forms. Less expectedly, they found that bromiraniums also typically exhibit asymmetry in olefins that are symmetrically substituted (Figure 3.1a). They account for this as being a feature of rapid equilibration via the symmetric transition state that they are unable to detect by computation (Figure 3.1b). The majority of the effects were based on simple sterics rather than electronics and they did not examine any competing effects such as unsymmetric alkenes that would offer two different tertiary carbocations or the effects of aryl substitution.

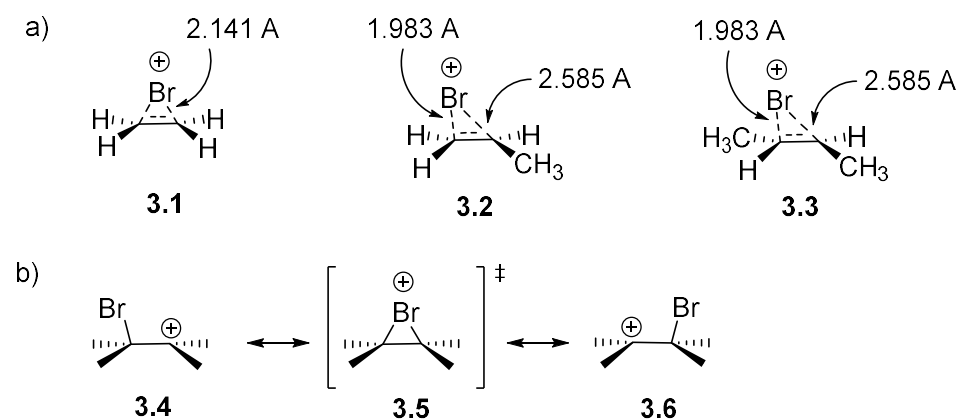
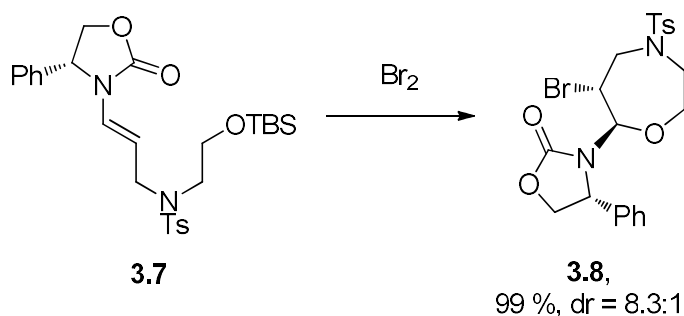


Figure 3.1. a) Symmetric bromiranium ion from symmetric olefin (3.1) and asymmetric bromiraniums from unsymmetric olefin (3.2) and symmetric olefin (3.3), bond lengths come from PM3-optimized geometries; b) Rapid equilibration of asymmetric β -halocarocations

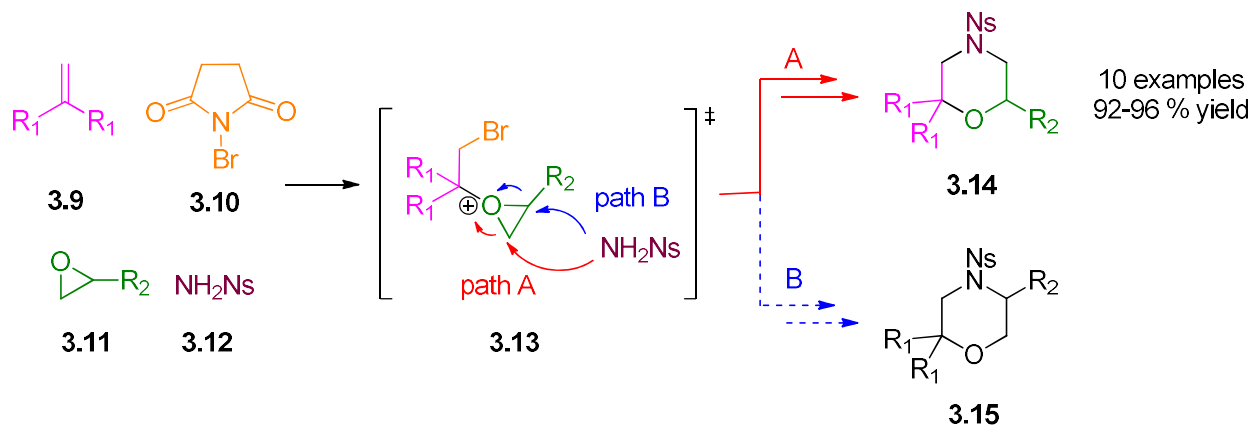
through the symmetric bromiranium ion.

A report that was mentioned in Chapter 1 from the Hsung group noted that they achieved stereoselective halocycloetherification of enamides made with chiral auxiliaries.² In this publication, they focused their efforts on synthesizing tetrahydropyrans via a 6-*endo* bromocycloetherification reaction. They were also able to extend this methodology to larger size rings including 7-, 8- and 10 membered rings. They reported a single example of forming one of these larger rings by a 7-*endo* bromocycloetherification to make 1,4-oxazepane derivative **3.8**. They synthesized **3.8** in excellent yield and good diastereoselectivity (Scheme 3.1). To the best of our knowledge, this is the only example in the literature that uses traditional halocycloetherification to prepare 1,4-oxazepanes other than our own report.³

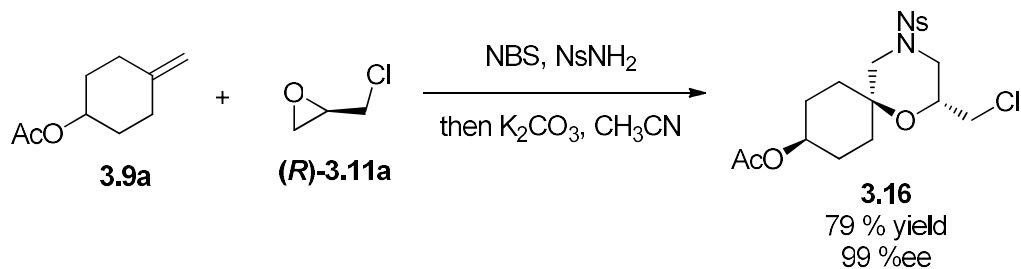


Scheme 3.1. Synthesis of 1,4-oxazepane 3.8 from a chiral enamine precursor.

While not strictly a halocycloetherification, Yeung and coworkers reported a multicomponent approach to synthesizing 2,2,6-trisubstituted morpholine derivatives that does involve a bromoetherification reaction.⁴ Using a 1,1-disubstituted olefin (**3.9**), a mono-substituted oxirane (**3.11**), an N-sulfonamide (**3.12**) and NBS (**3.10**) in either a two-step procedure or a one-pot reaction, they obtained morpholine products in good to excellent yield. The nucleophilic attack takes place exclusively at the least hindered carbon of the oxiranium (Scheme 3.2, pathway a). The only R groups tested on the 1,1-disubstituted olefin were alkyl groups with little variability in their electronics so conclusions about the broad applicability of this methodology cannot be made. Although not discussed, this geminal substitution may be required to position the bromide close enough to the sulfonamide for the S_N2 reaction to go at an appreciable rate. Notably, when using (*R*)-epichlorohydrin as the oxirane component, the reaction proceeded with an impressive 99 % ee and no other diastereomer obtained (Scheme 3.3).

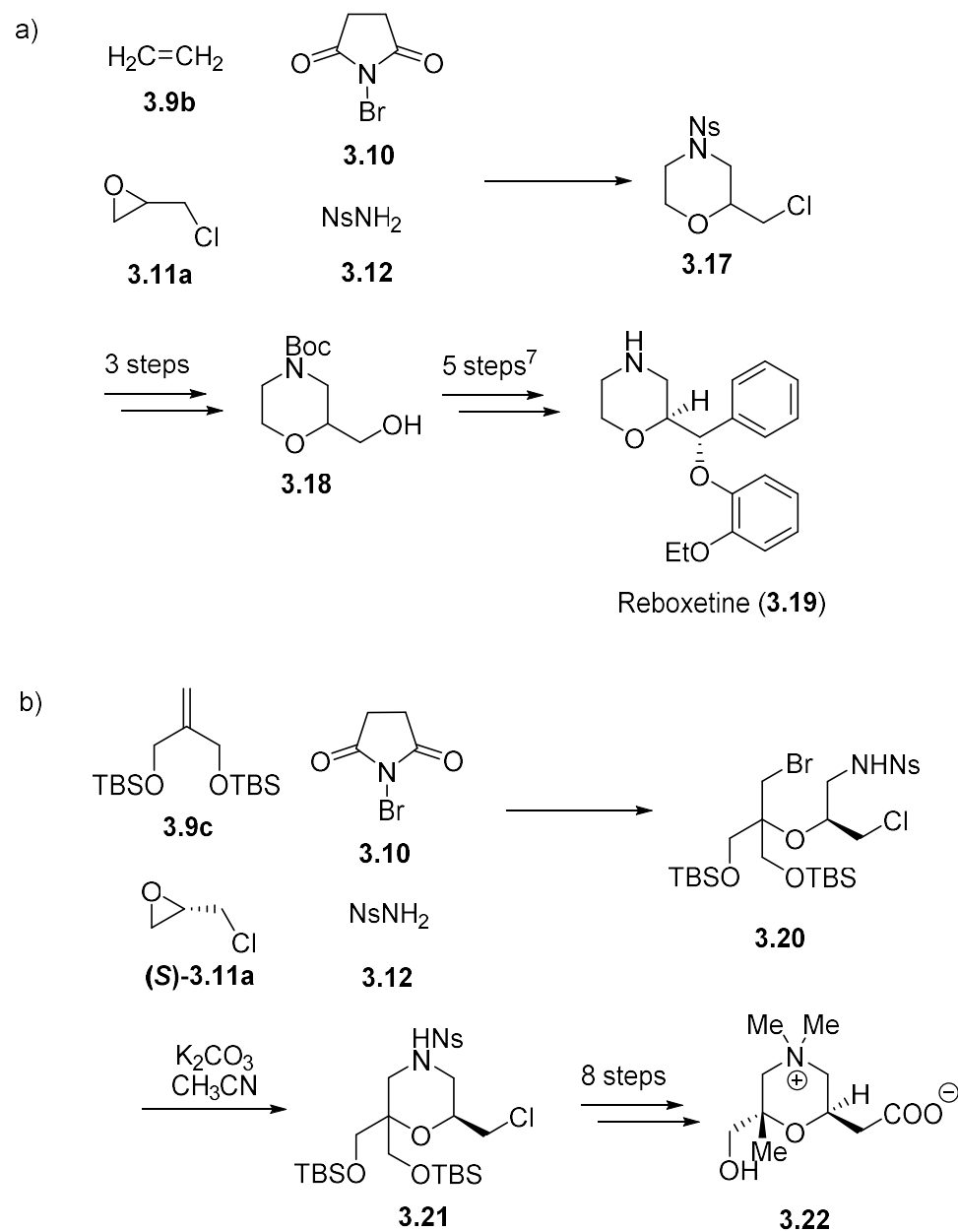


Scheme 3.2. Regioselectivity of aminoalkylation using monosubstituted epoxide.



Scheme 3.3. One-pot stereoselective synthesis of 3.18.

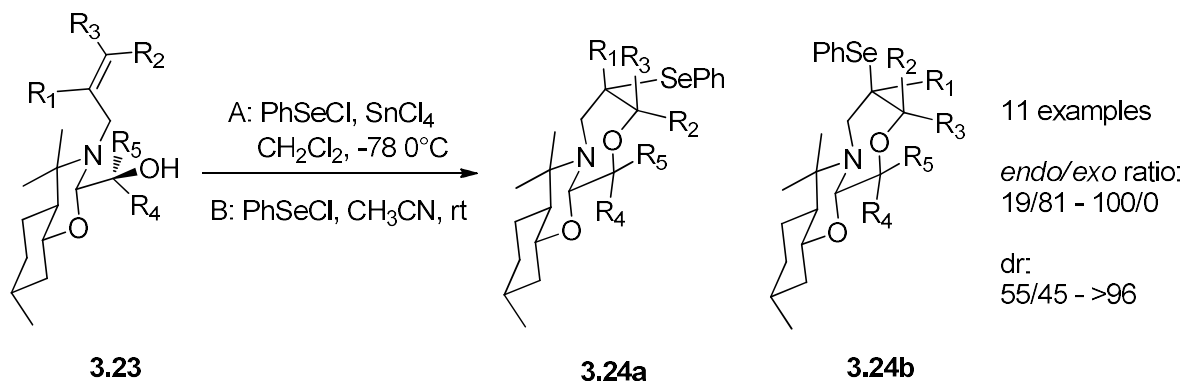
Using this NBS-induced electrophilic multicomponent methodology of making chiral morpholines, Yeung went on to show its utility in synthesizing a bioactive molecule, Reboxetine (**3.19**).⁵ Reboxetine is a norepinephrine reuptake inhibitor that is currently on the market (Pfizer) as the racemic mixture but it was recently discovered that the (+)-(*S,S*)-Reboxetine enantiomer is more active and therefore methods for preparing this drug in an asymmetric fashion are of interest.⁶ Employing their multicomponent methodology and simply modifying which enantiomer of epichlorohydrin they started with, both enantiomers of Reboxetine are readily accessible. The formal synthesis is shown in Scheme 3.4a.⁷ In the same publication, Yeung also reported the total synthesis of carnitine acetyltransferase inhibitor **3.22** (Scheme 3.4b).⁵



Scheme 3.4. Enantioselective synthesis of a) Reboxetine (3.19) and b) carnitine acetyltransferase inhibitor (3.22) using NBS-induced electrophilic multicomponent synthesis.

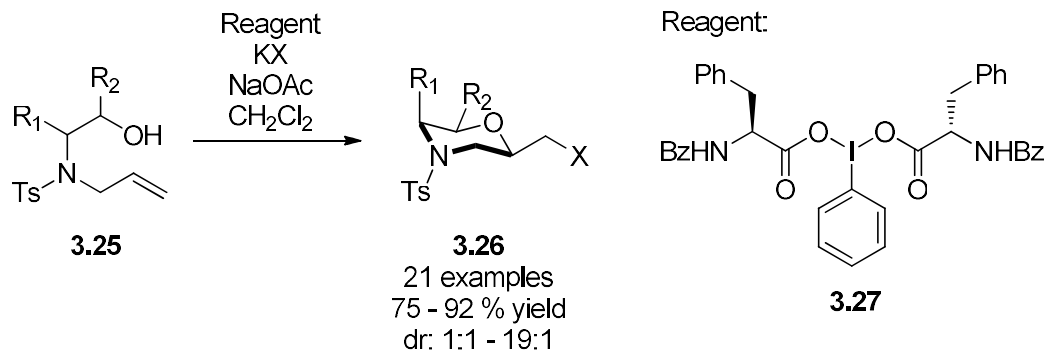
Nieto, Andrés and Pérez-Encabo reported a method for the preparation of chiral morpholines and chiral 1,4-oxazepanes in a diastereoselective manner starting from chiral perhydro-1,3-benzoxazines **3.23**.^{8,9} Upon treatment with benzene selenenyl chloride, the 7-endo oxazepane products were obtained with excellent regio- and diastereoselectivity depending on the conditions

used (Scheme 3.5). They could alter the regioselectivity of the reaction to make morpholines by simply manipulating the groups that were on the double bond so that the 6-*exo* cyclization could be favoured.



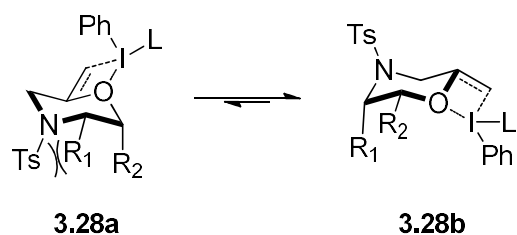
Scheme 3.5. Selenocycloetherification of perhydrobenzoxazines **3.23** induced by benzeneselenenyl chloride to make 1,4-oxazepanes **3.24a,b**. $R_1 = R_5 = \text{H}$, $R_2 = \text{CH}_3$ or H , $R_3 = \text{CH}_3$ or Ph , $R_4 = \text{H}$ or Ph .

Another example that is not strictly a halocycloetherification reaction but closely related was a 2015 report from Wang and coworkers. The authors used various amino acid derived hypervalent iodine complexes to increase the electrophilicity of an olefin, thereby activating it to intramolecular attack by a pendent alcohol to make 2,3,6-trisubstituted morpholines in a 6-*exo* fashion.¹⁰ They discovered that phenylalanine-derived iodine(III) provided the highest diastereoselectivity out of six different hypervalent iodine reagents tested. The R_2 substituent tolerated significant variability, proceeding in good yield with alkyl and aryl substituents and tolerated various electronic effects, including both electron donating and electron withdrawing groups (Scheme 3.6). The diastereoselectivity of the product seemed to rely on the R_1 substituent, with larger groups giving better selectivity by adopting an axial position to avoid torsional strain (Table 3.1). The major diastereomers isolated corresponded to the activated olefin adopting an equatorial position. They did not report any other heterocycles that could be made using this method.



Scheme 3.6. Hypervalent-iodine-mediated 6-*exo* cyclization to synthesize 2,3,6-trisubstituted morpholines.

Table 3.1. Rationale for diastereoselectivity.



Entry	R ₁	dr
1	Isobutyl	19 : 1
2	Isopropyl	9 : 1
3	Benzyl	4 : 1
4	Methyl	1.6 : 1

Despite being such a useful reaction, there are still some drawbacks to using halocycloetherification to make morpholines and, even more so, oxazepanes. There are very few examples that show regioselectivity for rings larger than 6-membered rings, and those that do typically see a drop off in reactivity. This is a limitation we have been able to overcome and have extended this methodology to 7-membered rings. The very few examples highlighted above and also notably, the lack of detailed studies regarding the stereochemical outcome of rings larger than 6-membered rings emphasizes that there is still a need for investigations into this field of electrophilic cyclizations. Additionally, the racemization of bromonium ions via olefin-to-olefin

transfer in competition with intermolecular nucleophilic attack presents difficulty when designing catalytic enantioselective halofunctionalization processes. As such, haloetherification reactions are still an active field of research.

3.3 Results and Discussion

3.3.1 Mechanism

Throughout the cyclization process presented in the previous chapter, many substrates formed a given stereo- and/or regioisomer preferentially. By examining these substrates closer, we probed both the scope of the reaction and further investigated the mechanism. As mentioned in Chapter 2, this reaction can potentially lead to a morpholine derivative through a 6-*exo-trig* cyclization or to an oxazepane through a 7-*endo-trig* cyclization (Figure 3.2a). In addition, the induction of two new stereocenters increases the amount of possible isomers to eight. Halocycloetherification, as will be discussed in more detail below, is believed to proceed through a haliranium ion (Figure 3.2b) and nucleophilic attack on a haliranium ion is a stereospecific addition, thereby reducing the number of potential isomers to four. The relative stereochemistry is set at this stage via transfer of stereochemistry from the olefin to the heterocycle. It is well established that scrambling of the stereochemistry may occur by halogen transfer to the alkene of another substrate molecule. Denmark has shown that this was a slow process that competed with intermolecular addition of alcohols¹¹ and that presence of a Lewis base shut down this undesired reaction and enabled asymmetric cyclization (Figure 3.2c).^{12,13} Both the intramolecular nature of our process and the presence of Lewis basic succinate originating from NBS should preclude the undesired isomerization.

We were originally expecting to generate morpholine derivatives from this developed methodology. We had to closely examine the spectroscopic data of the products to assess their regioselectivity and stereoselectivity correctly. Compounds **2.42j** and **2.43j** will be used as examples below to exhibit the process of analyzing the 2-D NMRs that were necessary to elucidate the structures.

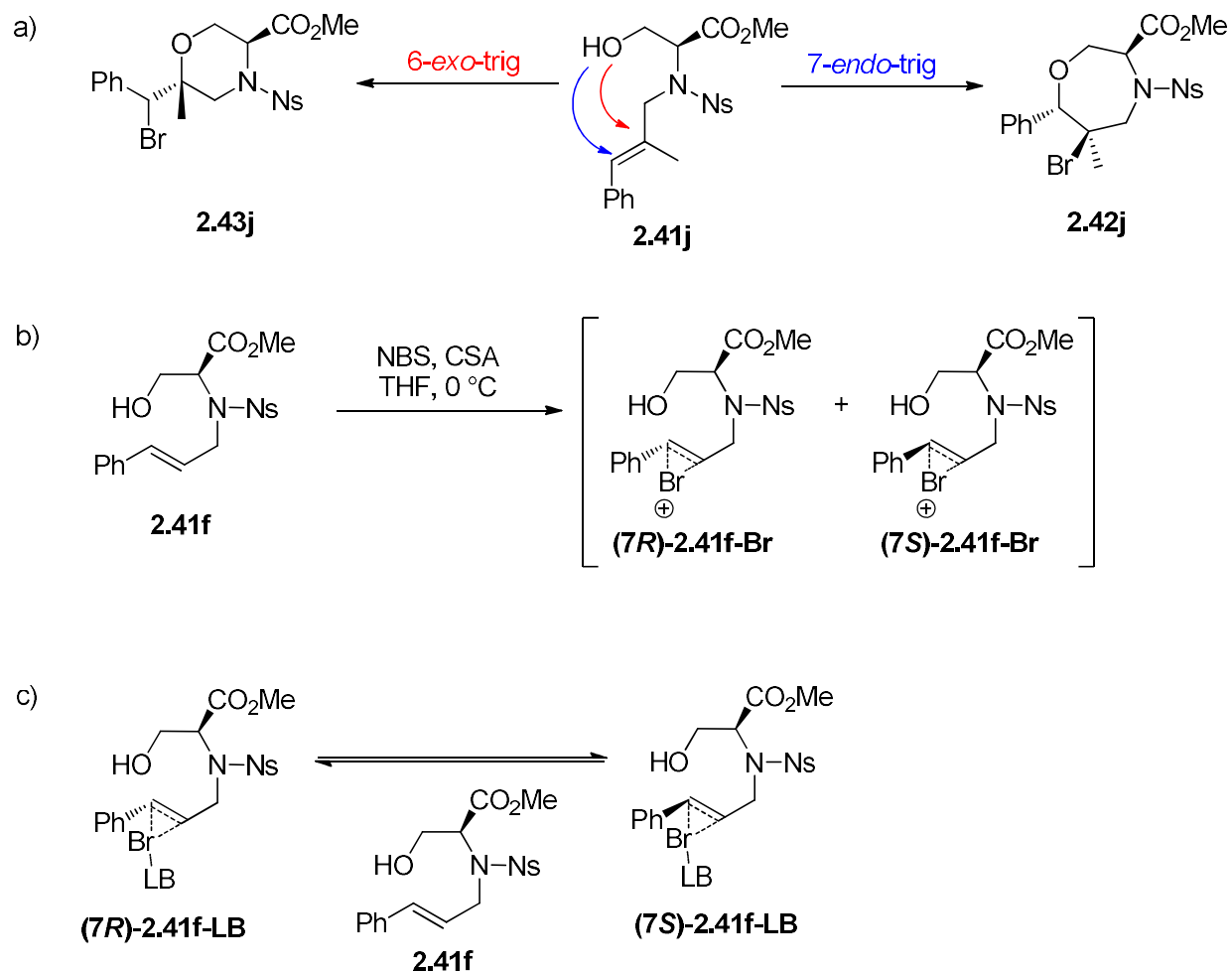


Figure 3.2 a) Example of selectivity observed depending on the alkene substituents; b) Formation of a bromonium ion; c) Stereochemistry scrambling from olefin-to-olefin transfer, LB = Lewis Base

3.3.2 Regiochemistry

Usually the first resource for rules regarding ring closure of acyclic compounds are Baldwin's rules (Table 3.2).¹⁴ However, Baldwin's rules allow both 6-*exo-trig* and 7-*endo-trig* cyclizations so this set of rules was not useful in this situation.

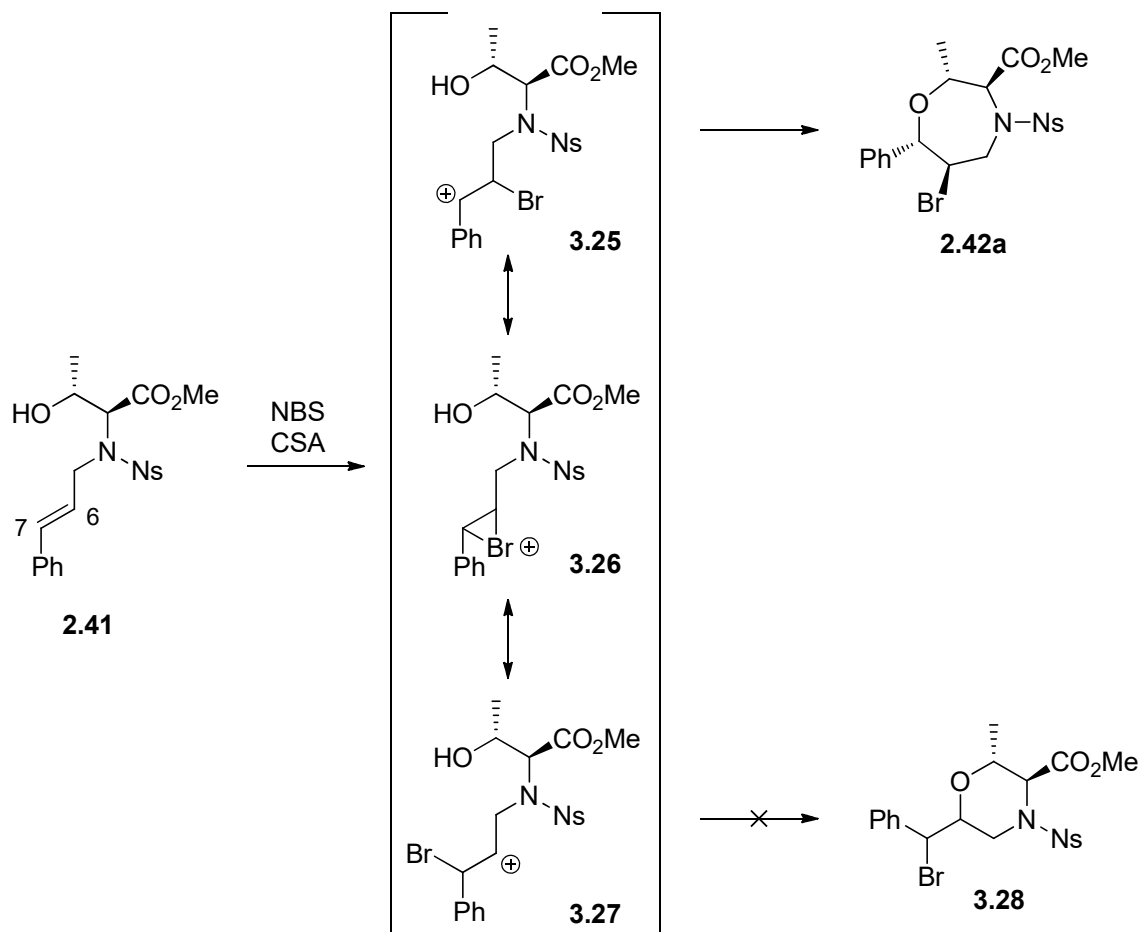
Table 3.2. Baldwin's rules

	3		4		5		6		7	
	<i>Exo</i>	<i>Endo</i>								
Tet	✓		✓		✓	✗	✓	✗	✓	✗
Trig	✓	✗	✓	✗	✓	✗	✓	✓	✓	✓
Dig	✗	✓	✗	✓	✓	✓	✓	✓	✓	✓

Check mark = favoured; X = disfavoured

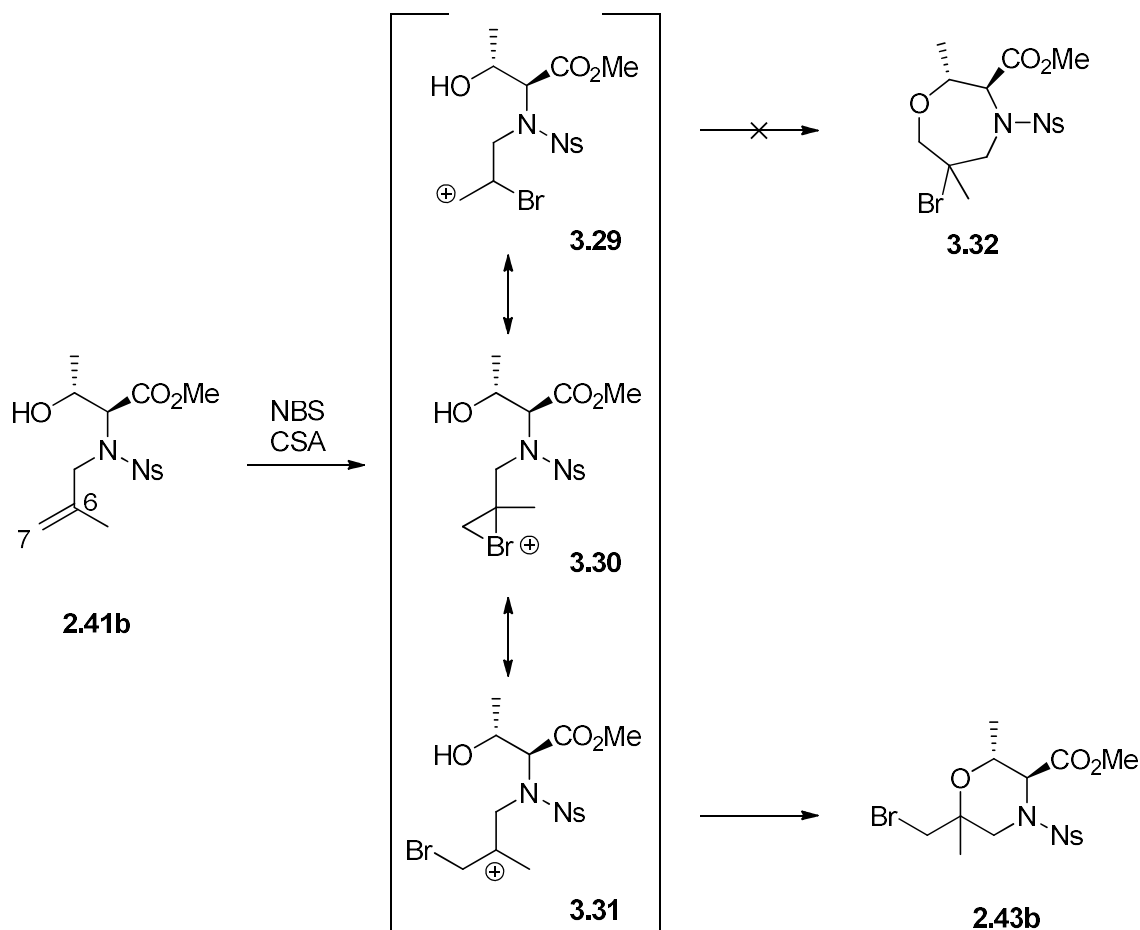
As Baldwin's rules were not applicable, we moved on to other possible explanations of the regiochemistry. While this work was in progress, haloetherification had been found to favour the 6-*endo* over the 5-*exo* and the 7-*endo* over the 6-*exo* cyclization when an aromatic or an enamine group can stabilize the developing positive charge of the adjacent carbon through conjugation.¹³ The presence of such groups controlled the regioselectivity by desymmetrizing the haliranium intermediate. If no such group was found, then the *exo* cyclization was competitive.

With this in mind, we looked closely at some representative examples of such instances. Scheme 3.7 shows the cyclization of **2.41a**. The electrophilic bromine from NBS formed a bromonium with the olefin, the extreme resonance structure of which could have the cation centered on the bromine atom (**3.26**), the benzylic carbocation (**3.25**) or the secondary carbocation (**3.27**). The most stable cation is the benzylic carbocation **3.1** and in this situation, one would expect to see 7-*endo* cyclization and indeed **2.42a** was the only regioisomer observed. In fact, in all compounds that featured such a cinnamyl appendage, the 7-*endo* cyclized product was the exclusive regioisomer.



Scheme 3.7. Regioselectivity of 2.42a.

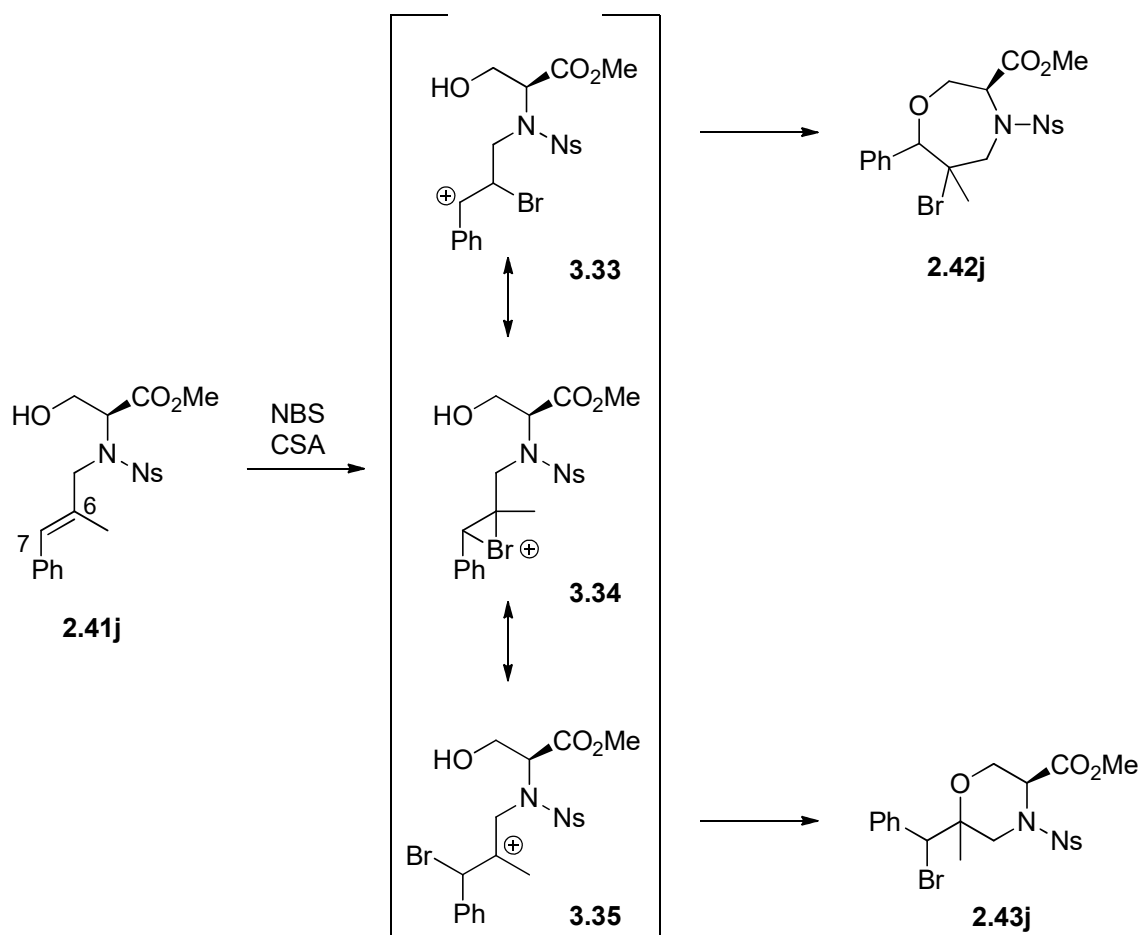
Along the same line, cyclization of **2.41b** also formed a bromonium, with extreme resonance structures having the cation centered on the bromine atom (**3.30**), the “primary carbocation” (**3.29**) or the tertiary carbocation (**3.31**) (Scheme 3.8). Since a primary carbocation is highly energetically disfavored, it was not surprising that the only regioisomer observed was the 6-*exo* cyclization product, **2.43b**.



Scheme 3.8. Regioselectivity of 2.43b.

The cases presented in Scheme 3.7 and Scheme 3.8 showed carbocations that had an obvious preference. The regioselectivity of the cyclization of **2.41j** was less obvious as the extreme resonance structures involve the cation centered on the bromine atom (**3.34**), the benzylic carbocation (**3.33**) or the tertiary carbocation (**3.35**) (Scheme 3.9). Both chemical intuition and computational results suggested a significant, if not exclusive, preference for the 7-*endo* cyclized product **2.42j**, as a benzylic carbocation is orders of magnitude more stable than a tertiary carbocation (5.33 kcal/mol, corresponding to a ratio of roughly 6400:1). However, experimentally both regioisomers **2.42j** and **2.43j** were observed with poor selectivity (< 2:1). The regioselectivity therefore cannot be driven just by the competition of stability between the tertiary carbocation and the benzylic-stabilized carbocation, implying that there was some entropic factor at play that was making the formation of the morpholine competitive.

As expected, the substitution on the starting amino alcohols **2.37** seems to have no effect on the regioselectivity of the cyclization.



Scheme 3.9. Competition of regioselectivity between **2.42j** and **2.43j**.

Experimentally, there was no characteristic shifts of any peaks in the ^1H NMR spectra that made assigning the regioselectivity obvious. In light of this, the most appropriate NMR technique to gain information on the regioselectivity was ^1H - ^{13}C HMBC NMR. Using the cyclization of **2.41j** as an example, the 7-*endo* cyclization to give **2.42j** would lead to a signal between C2 and H7 (Figure 3.3a) and/or between H2 and C7 (Figure 3.3b). Conversely, the 6-*exo* cyclization to give **2.43j** would lead to a signal between H2 and C6 (Figure 3.3c).

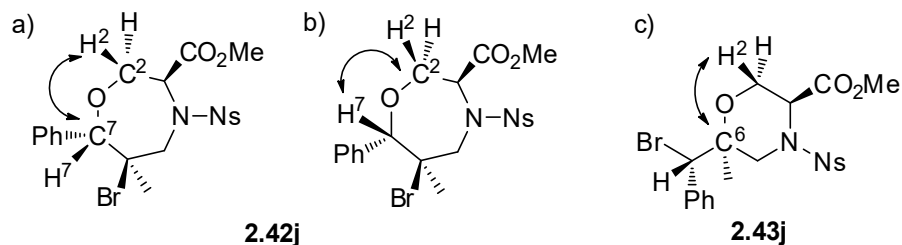


Figure 3.3. Expected signals in HMBC for 2.42j and 2.43j.

After assigning the peaks in the ^1H and ^{13}C NMR by thorough analysis of coupling constants, COSY and HSQC, we were able to analyze the HMBC NMRs. The HMBC spectrum of **2.42j** does show a signal between C2 and the multiplet at 4.58 ppm that includes H7, however since that multiplet also includes two other protons, this signal was not conclusive evidence that there was an interaction between C2 and H7 (Figure 3.4, red line). The spectrum showed a clear signal for an interaction between H2, at 3.62 ppm, with C7, a signal which could not appear in **2.43j**, thereby confirming the regiochemistry (Figure 3.4, blue line).

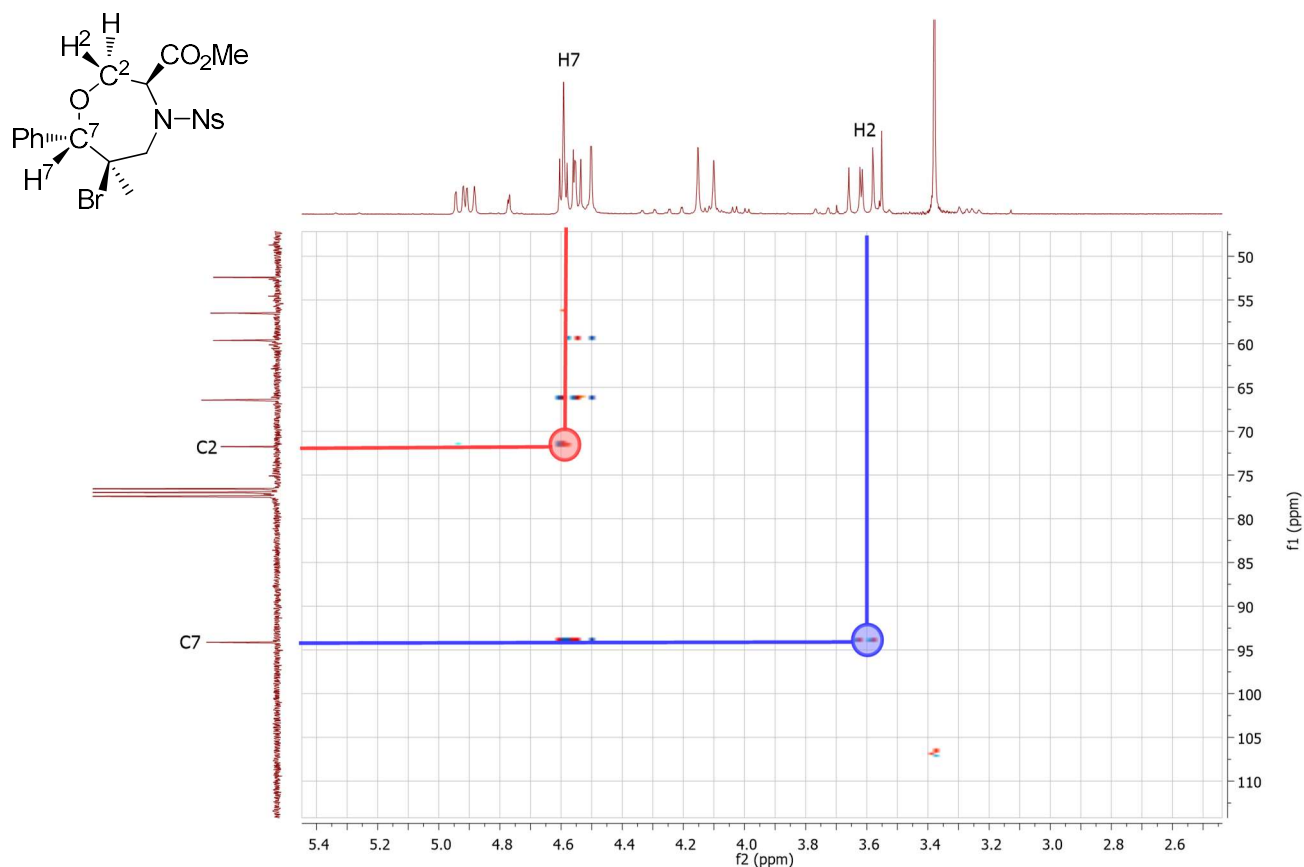


Figure 3.4. HMBC for 2.42j; the red line shows an inconclusive signal between C2 and what

may or may not be H7; the blue line shows a clear signal between H2 and C7, necessitating the regiochemistry shown.

The HMBC of **2.43j** (Figure 3.5) shows a clear signal between C6 and H2 indicating that the regioselectivity must be *6-exo-trig*.

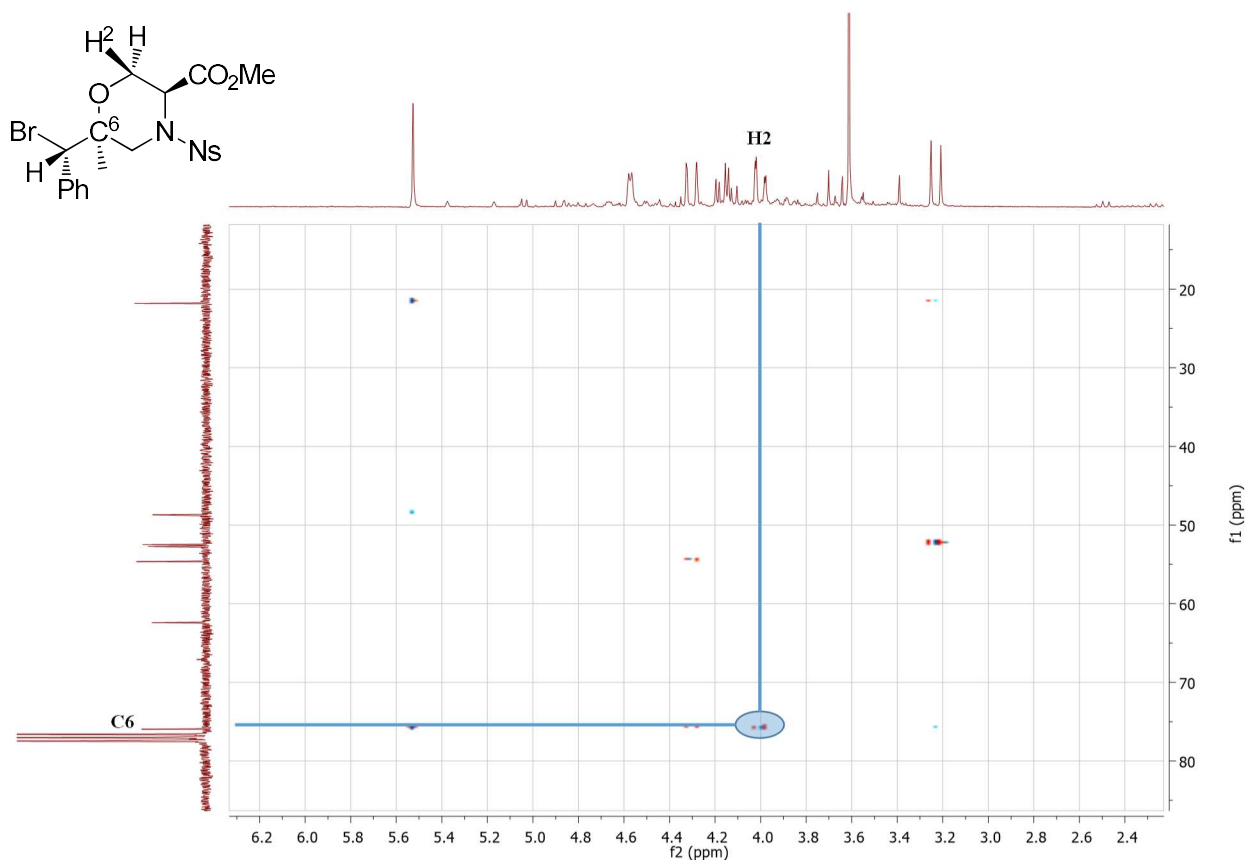


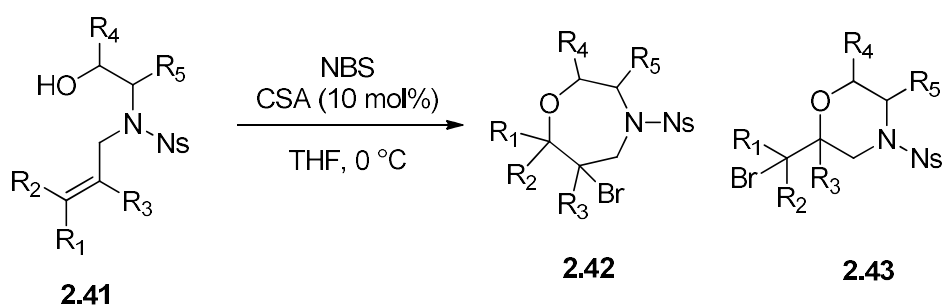
Figure 3.5. HMBC for **2.43j**; the blue line shows a clear signal between H2 and C6, necessitating the regiochemistry shown.

After analysis of the spectroscopic characterization of several compounds that exhibited *7-endo-trig* selectivity and/or *6-exo-trig* selectivity, we were pleased to see a trend in the ^{13}C NMR of oxazepanes and morpholines: regardless of the electronic effects of the substituents on the alkene, C7 of oxazepanes consistently showed up around 84-92 ppm, significantly downfield of the C7 shift of morpholines which were generally in the range of 47-57 ppm. This trend made assigning regioselectivity much simpler.

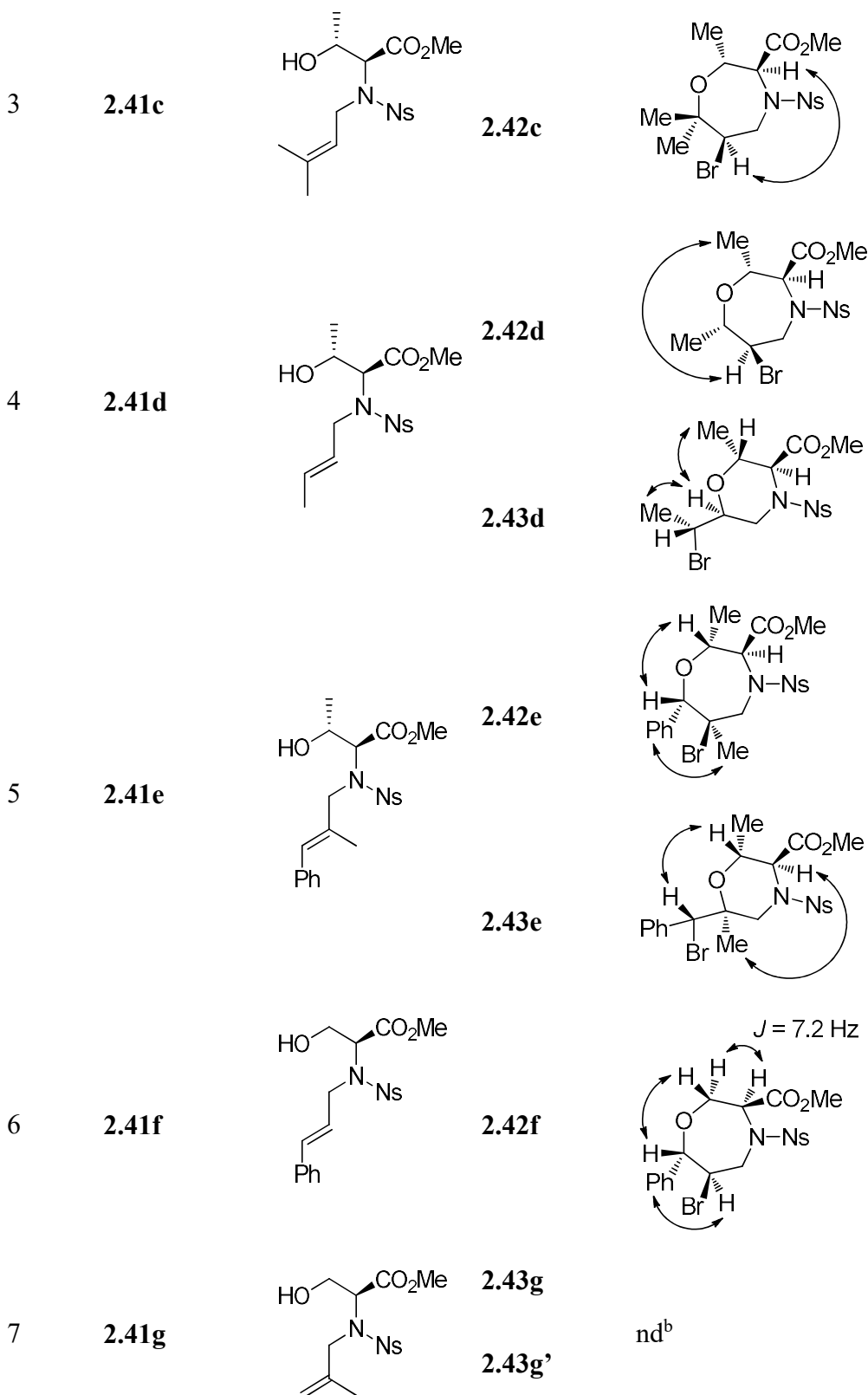
3.3.3 Stereochemistry

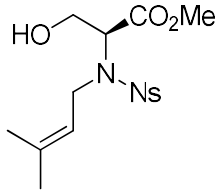
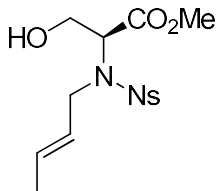
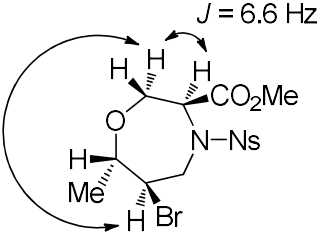
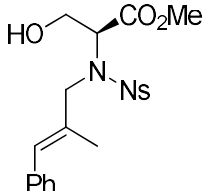
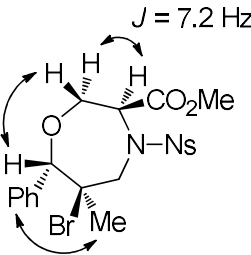
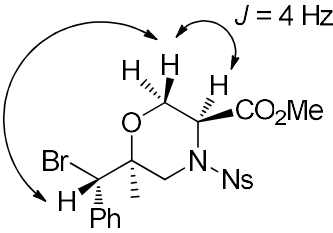
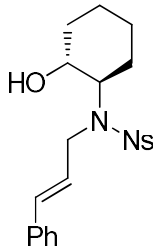
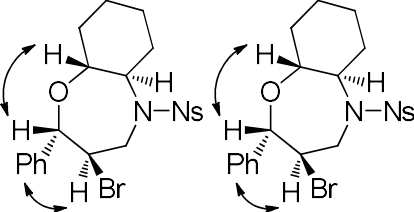
The stereochemistry of the observed isomers was determined by NOESY NMR experiments and when not possible by NMR, by analogy with similar substrates (Table 3.3). For additional information regarding the NOE interactions, please refer to the Supplementary Information in the scientific publication of this material.³ The structure of **2.42e** was also confirmed by X-ray crystal analysis (Figure 3.6). Details regarding the relative stereochemistry and diastereomeric preference will be discussed below in Sections 3.3.3.1 and 3.3.3.2, respectively.

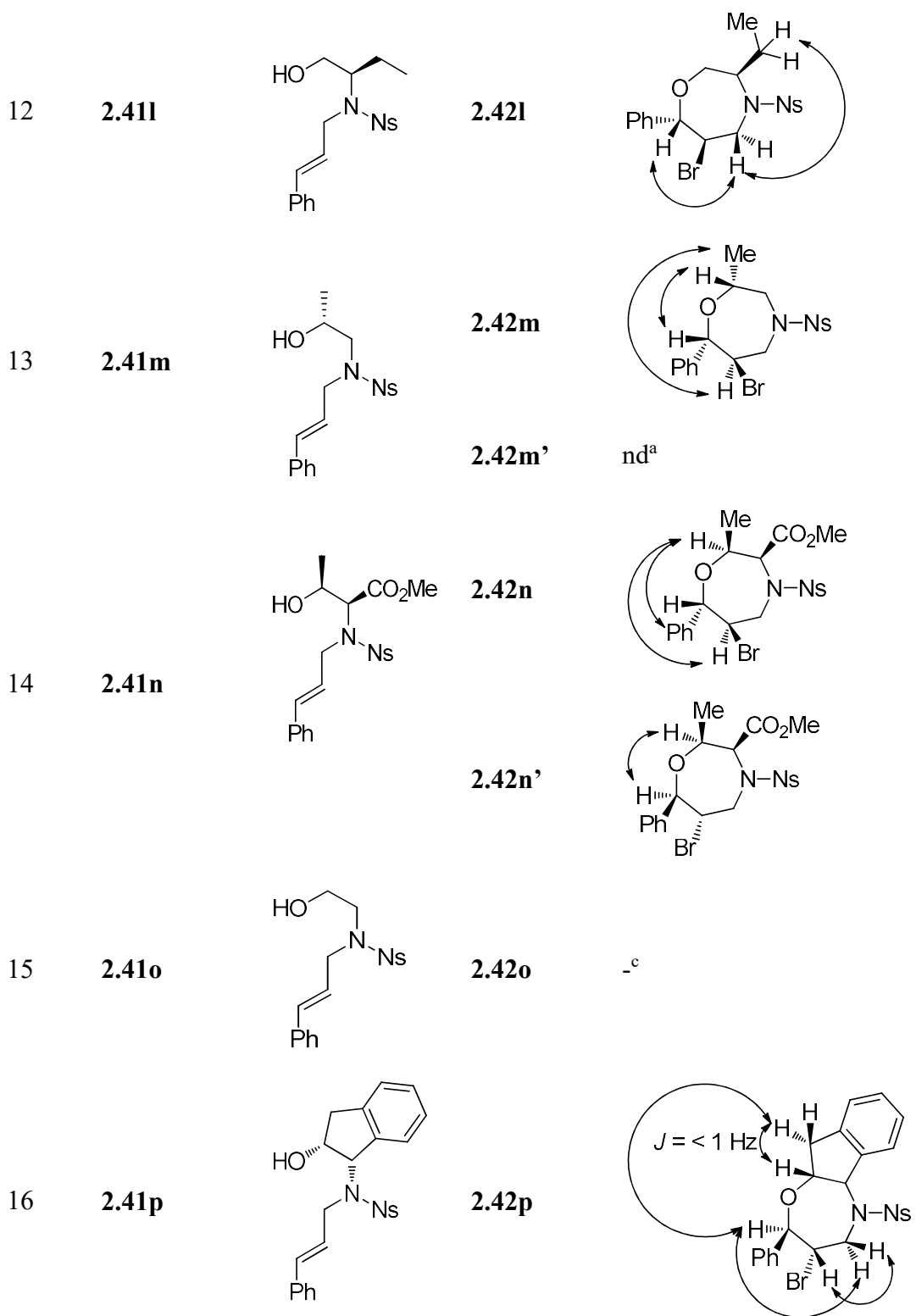
Table 3.3. NOESY signals used to ascertain the stereochemistry

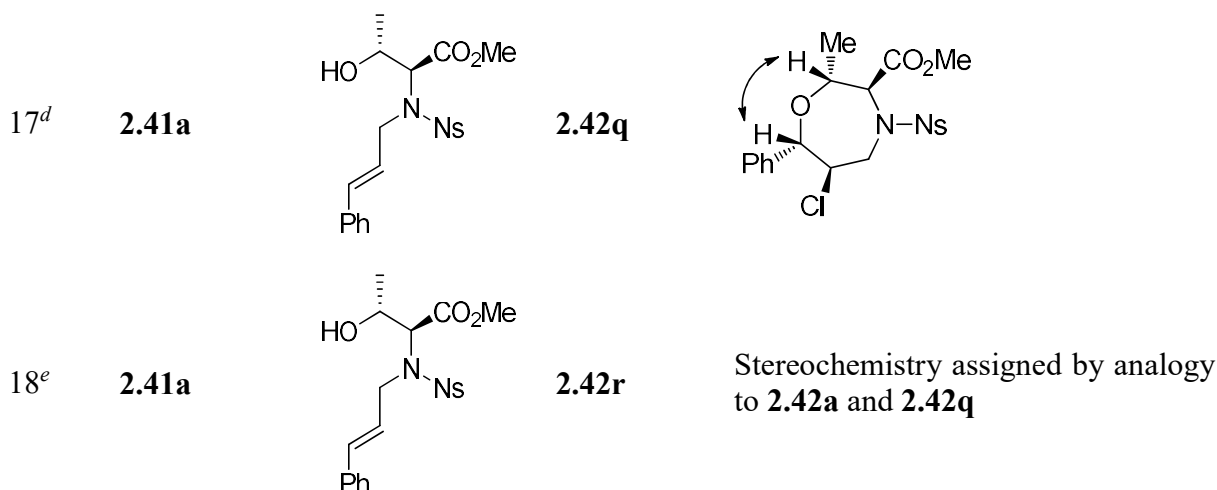


Entry	Starting Material	Product	NOEs
1	<p>2.41a</p>	<p>2.42a</p>	
2	<p>2.41b</p>	<p>2.43b</p>	
		<p>2.43b'</p>	<p>nd^a</p>



8	2.41h		2.42h	Stereochemistry assigned by analogy to 2.42c
9	2.41i		2.42i	
			2.43i	nd ^b
			2.43i'	
10	2.41j		2.42j	
			2.42j	
11	2.41k		2.42k	
			2.42k'	nd ^a





^a When a diastereomeric mixture of a single regioisomers was obtained, only one diastereomer was analyzed by NOESY and the other was assumed to have the inverted stereochemistry at the newly formed stereocenters, as shown in Table 3.3; ^b A roughly 1:1 inseparable mixture of diastereomers was obtained; ^c Product is a racemic mixture; ^d Electrophilic halogenating agent was NCS; ^e Electrophilic halogenating agent was NIS.



Figure 3.6. Solid-state molecular structure confirming the regiochemistry and stereochemistry of 2.42e.

3.3.3.1 Relative Stereochemistry

As mentioned in Chapter 3.3.1, haloetherification is believed to proceed through a haliranium ion (Figure 3.2b). Nucleophilic attack on a haliranium ion is a stereospecific addition, which reduces the potential number of isomers from eight to four.

For example, on **2.41a**, a hydrogen and the phenyl are *cis* to each other on the olefin. After the cyclization of **2.41a**, oxazepane **2.42a** has the hydrogen and phenyl *cis* to each other. This principle is true in all the tested cases: groups that are *cis* on the olefin are *cis* on the ring and groups that are *trans* on the olefin are *trans* on the ring. This means that the relative stereochemistry

of the product is set at the alkylation stage of the synthesis via transfer of stereochemistry from the olefin to the heterocycle.

3.3.3.2 Diastereomers

Although the rationalization of the regiochemical outcome and relative stereochemistry was somewhat straightforward, investigating the mechanistic details of the diastereomeric outcome of the reaction between NBS and **2.41** to form oxazepanes and morpholines was more difficult as no obvious preference for one stereoisomer over the other can be predicted using simple models. For example, the role of each of the two stereogenic centers (i.e., C2 methyl and C3 methyl ester) of the threonine-based amino alcohol derivative **2.41a** in the observed stereoselectivity (dr > 20:1, Table 2.6, entry 1) was evaluated. First, the methyl ester of **2.41a** was found to be critical as its removal (**2.41m**) led to virtually no selectivity (dr 1.2:1, Table 2.6, entry 13). Removal of the methyl group (**2.41f**) retained the high level of selectivity (dr > 20:1, Table 2.6, entry 6), however, the methyl group was also important as its inversion (**2.41n**) led to loss of stereoselectivity (dr 2:1, Table 2.6, entry 14) and poor yield (42 %). Thus, we believed that the major factor impacting the stereoselectivity of **2.41a** was the methyl ester while the methyl group, if in the right configuration (matched case) was not essential. We initially postulated that the *cis* configuration of **2.41n** might cause distortion and disruption of the transition states (TS) conformation adopted by **2.41a** and **2.41f**. However, derivative **2.41p**, although also in the *cis* configuration, led to high yield and stereoselectivity (98 %, dr > 20:1, Table 2.6, entry 16). In addition, derivative **2.41k** in the *trans* configuration did not proceed with high selectivity (dr 2.0:1, Table 2.6, entry 11). The rigid nature of **2.41p** and **2.41k** may explain their behavior in our cyclization reactions. It rapidly appeared that the flexible nature of 7-membered rings made the rationalization difficult.

In light of this, we turned to computational chemistry to guide the investigation into the mechanistic details of this reaction. We first investigated the addition of bromine to a model system. It was our initial hypothesis that the reaction involved two different TS's, one upon addition of bromine to the double bond and one upon formation of the ring by nucleophilic attack of the alcohol onto the bromonium. With this in mind, considering the first step, we modeled the reaction of NBS (protonated by (\pm)-CSA) and *trans*-butene as a simple model of the olefin. To our surprise, no TS was observed and the resulting structure was a cage-like system around the bromine

and not a conventional bromonium ion (Figure 3.7). We further confirmed this observation, replacing butene with **2.41p**, indicating that this was not an artefact of the model.

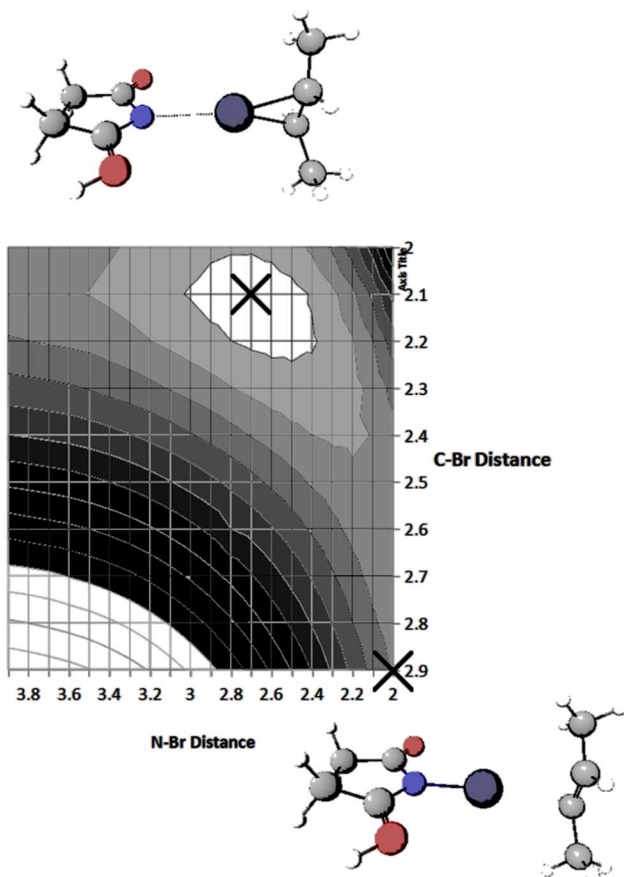


Figure 3.7. Potential energy surface of the reaction between NBS-H⁺ and *trans*-butene.

Since the addition of bromine at this early stage determines the stereochemistry and no isomerization through intermolecular alkene-to-alkene transfer is expected, we concluded that a conformational bias opening preferentially one face of the alkene to NBS should determine the predominance of one diastereomer. Thus, in practice this reduced our study to a simple conformational search rather than a TS analysis. Indeed, the computational prediction agreed, within error, with the experimentally observed products, predicting a 4:1 ratio of the *R* isomer of **2.42c** over the *S* isomer (Figure 3.8). Thus, the stereoselectivity can indeed be rationalized by simple conformational analysis of ground state reactants.

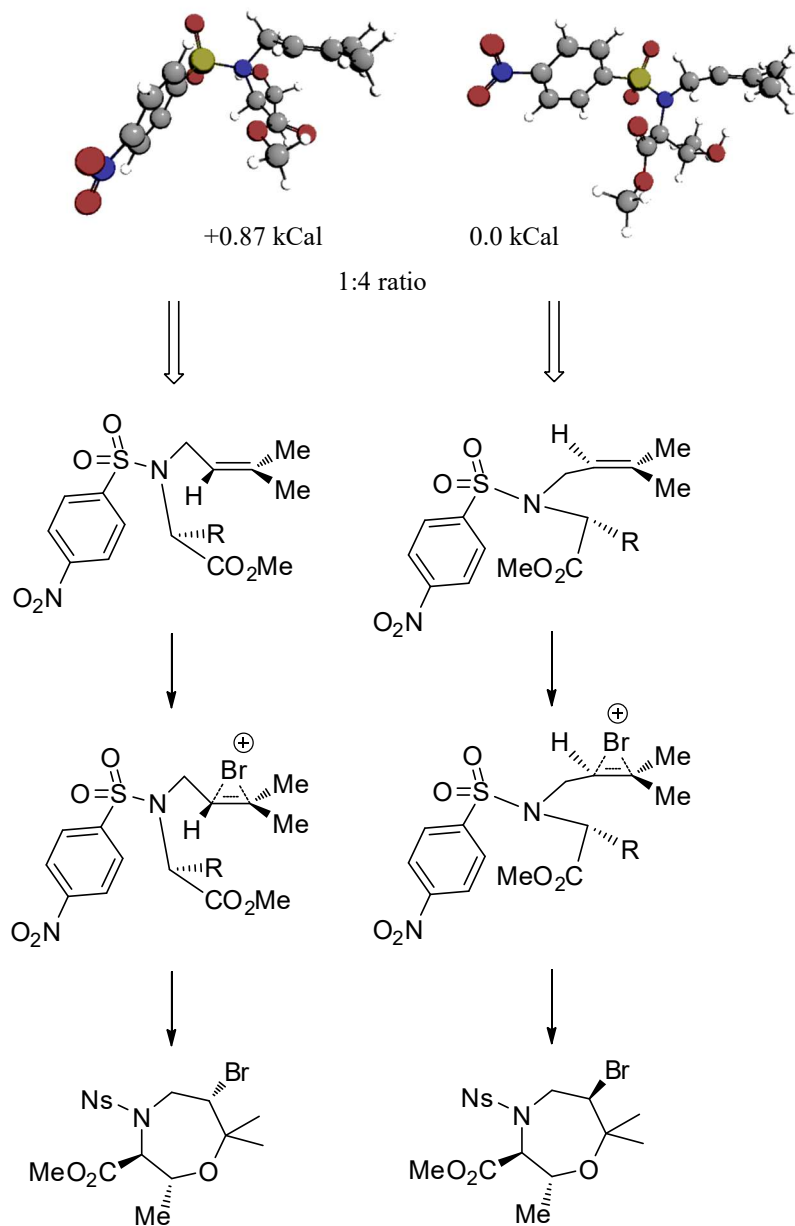


Figure 3.8. Stereochemical outcome from simple conformational analysis (2.41c).

3.4 Conclusions

The reaction mechanism of formation of oxazepanes and morpholines was probed extensively. The products were meticulously characterized using many different NMR techniques as well as X-ray crystallography to determine their structures and assess the regioselectivity and stereoselectivity of the reaction. Figure 3.9 summarizes the results.

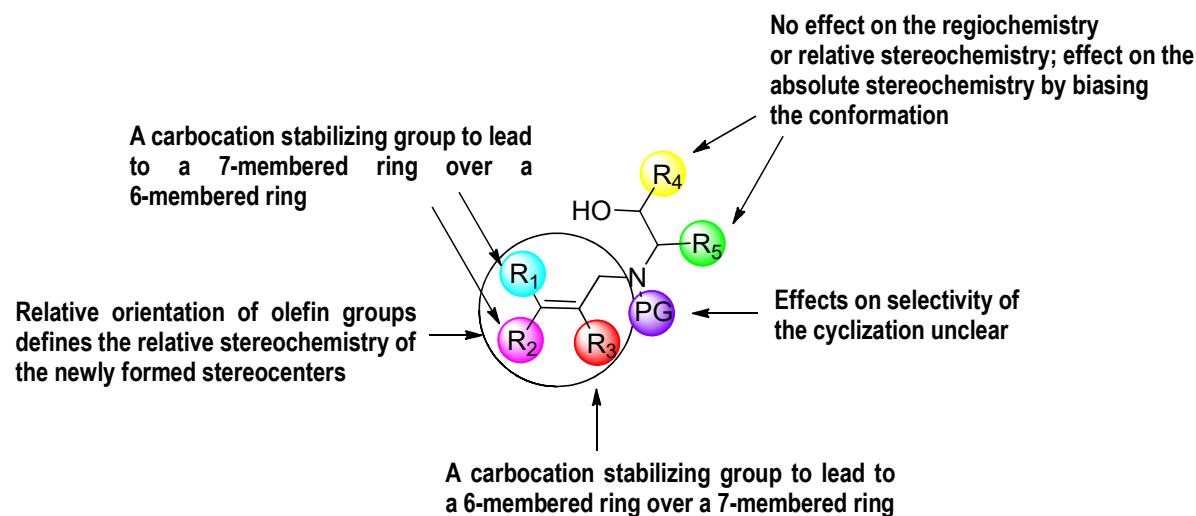


Figure 3.9. Summary of observed selectivity based on the structure of the starting material.

The regiochemistry of products was assigned as either the *7-endo* oxazepane product or the *6-exo* morpholine product after extensive 2-D NMR spectroscopy. This led to the observation of a trend in the shift of C7 in the ^{13}C NMR, with C7 of oxazepanes (**2.42**) showing up around 84 – 92 ppm while C7 of morpholines (**2.43**) showing up between 47 – 57 ppm. The regioselectivity was attributed to the desymmetrization of the bromonium ion, depending on the substitution at the olefin of the starting materials (**2.41**).

The relative stereochemistry of the products was determined to arise from nucleophilic attack at a haliranium being a stereospecific reaction and therefore the geometry of the olefin in **2.41** sets the relative stereochemistry observed in the cyclized products. The absolute stereochemistry was assigned using NOE signals or in cases where that was not possible, by analogy to other compounds. The origin of absolute stereoselectivity was less obvious and after computational investigation was found to come from reaction of the lowest energy ground state conformation.

3.5 Experimental

3.5.1 General considerations and procedure

Chemical shift (δ) are reported in parts per million (ppm) relative to CDCl_3 (7.26 ppm for ^1H and 77.160 ppm for ^{13}C). ^1H and ^{13}C NMR spectra were recorded at 400 or 500 and 100 or 125 MHz, respectively, and assignments were confirmed by 2D COSY, HSQC, HMQC and NOESY experiments or by X-ray crystallography.

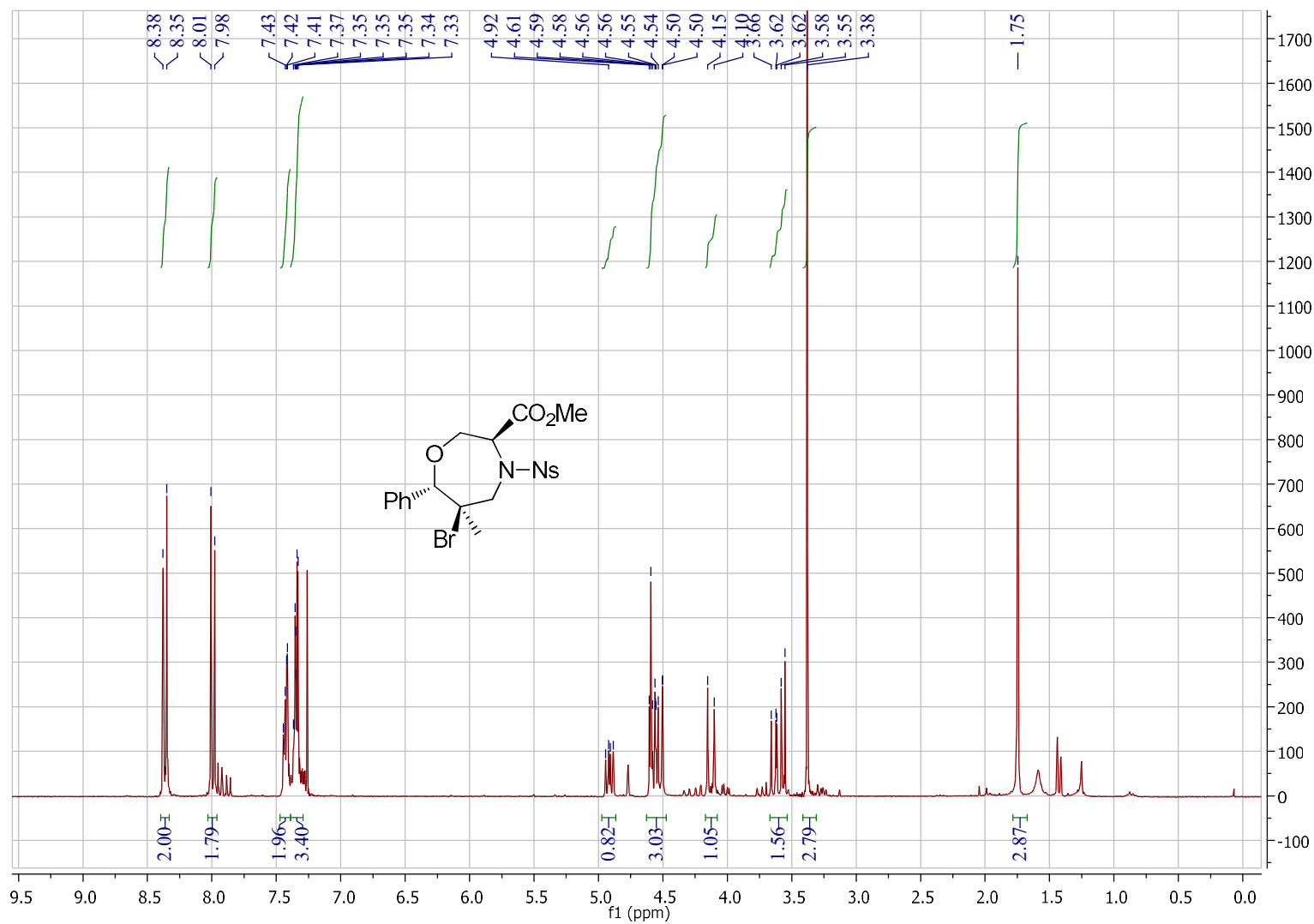
3.5.2 Computational methods

General Considerations. The quantum mechanical calculations were performed using density functional theory (DFT), more specifically the M06 functional (restricted Hartree-Fock) and the diffuse 6-31G(d,p) basis set. Certain convergence parameters were loosened slightly, due to the degrees of freedom in the molecules and difficulties acquiring a minimum state. No frequency analysis was required for this work. All calculations were carried out in a PCM (polarizable continuum model) solvent model of tetrahydrofuran. The M06 calculations were performed using GAMESS-US v.Aug2011-64bit.

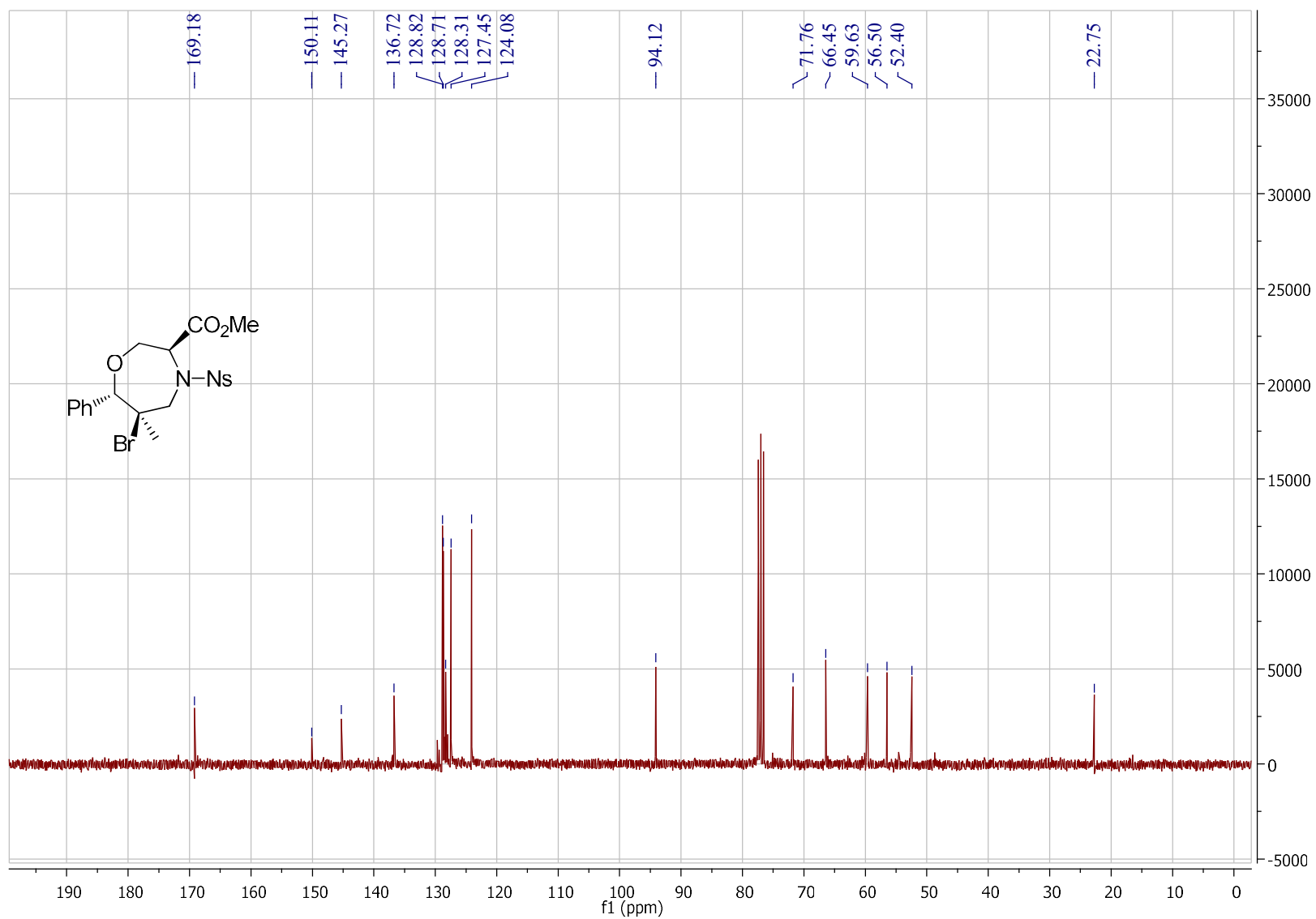
Butene NBS Study. The modeling of the reaction of NBS with *trans*-butene involved the exploration of two reaction coordinates. We systematically varied the length of the C-Br forming bonds along with the length of the N-Br breaking bonds. The energies of these systems were compared to the sum of the reactants and plotted in 3D.

Conformational analysis of 2.41c. The conformational search was done in a stepwise fashion. First, molecular mechanics (MM3* as a forcefield, MacroModel, Schrödinger) was used to generate a set of over 50 stable conformations. Then, the semiempirical function PM3 (MOPAC) was used to minimize the energy of all generated conformations. Upon sorting, these more accurate energies, we selected the top 5 structures for the formation of each of the *R* and the *S* conformers and finally optimized their structure by DFT (basis set/functional mentioned above).

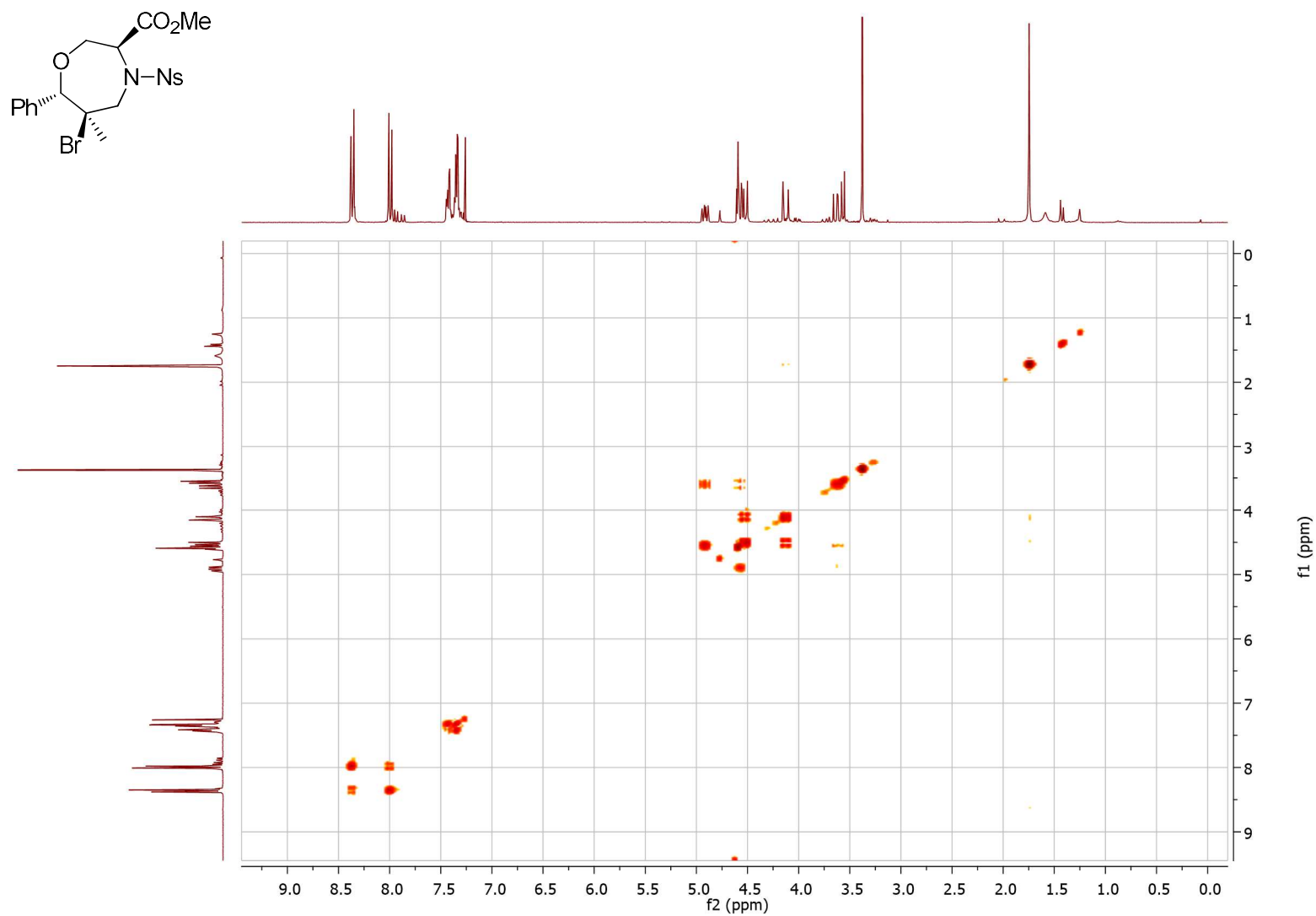
3.5.3 Experimental data



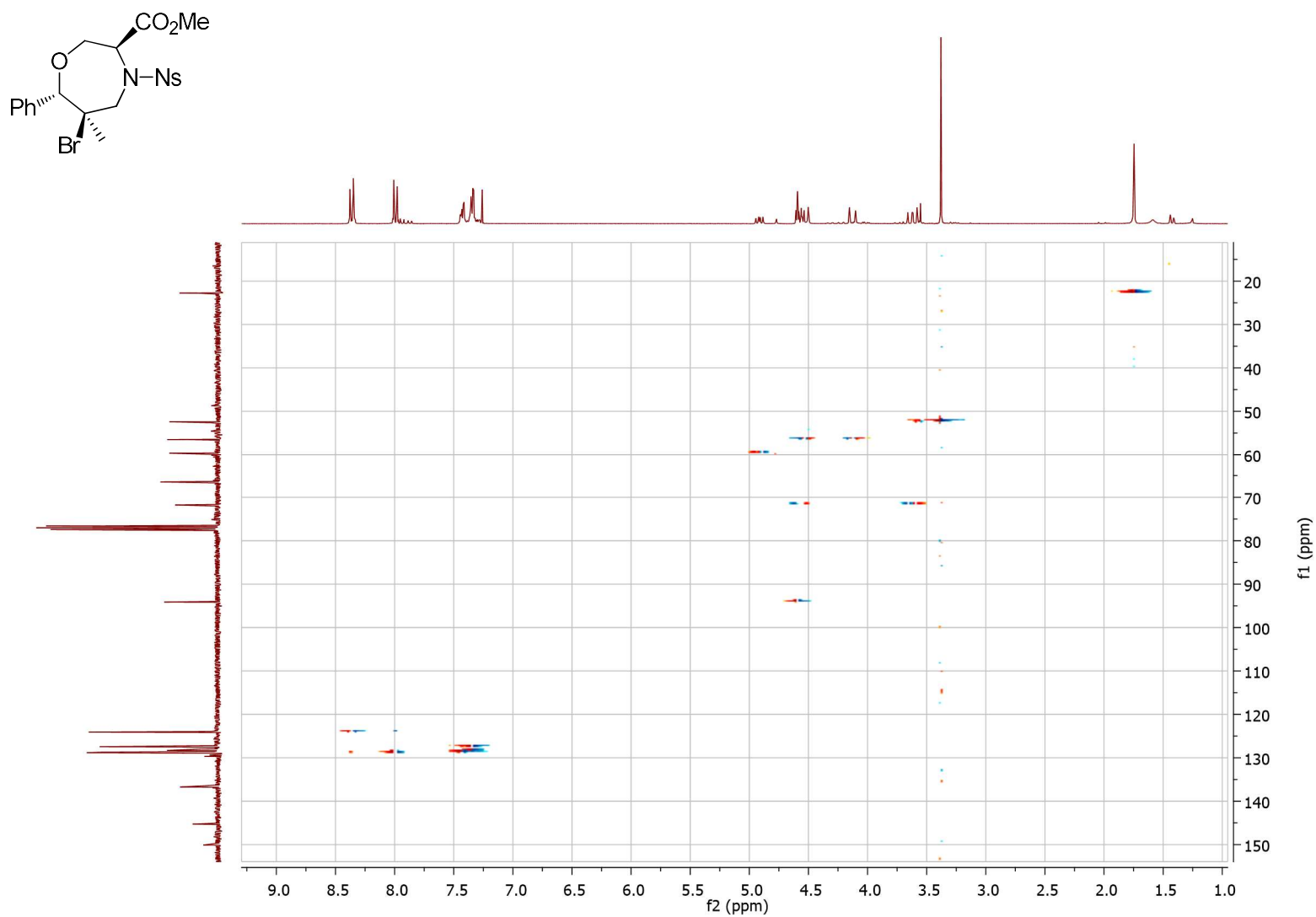
^1H NMR for methyl (3*S*,6*R*,7*S*)-6-bromo-6-methyl-4-((4-nitrophenyl)sulfonyl)-7-phenyl-1,4-oxazepane-3-carboxylate (**2.42j**).



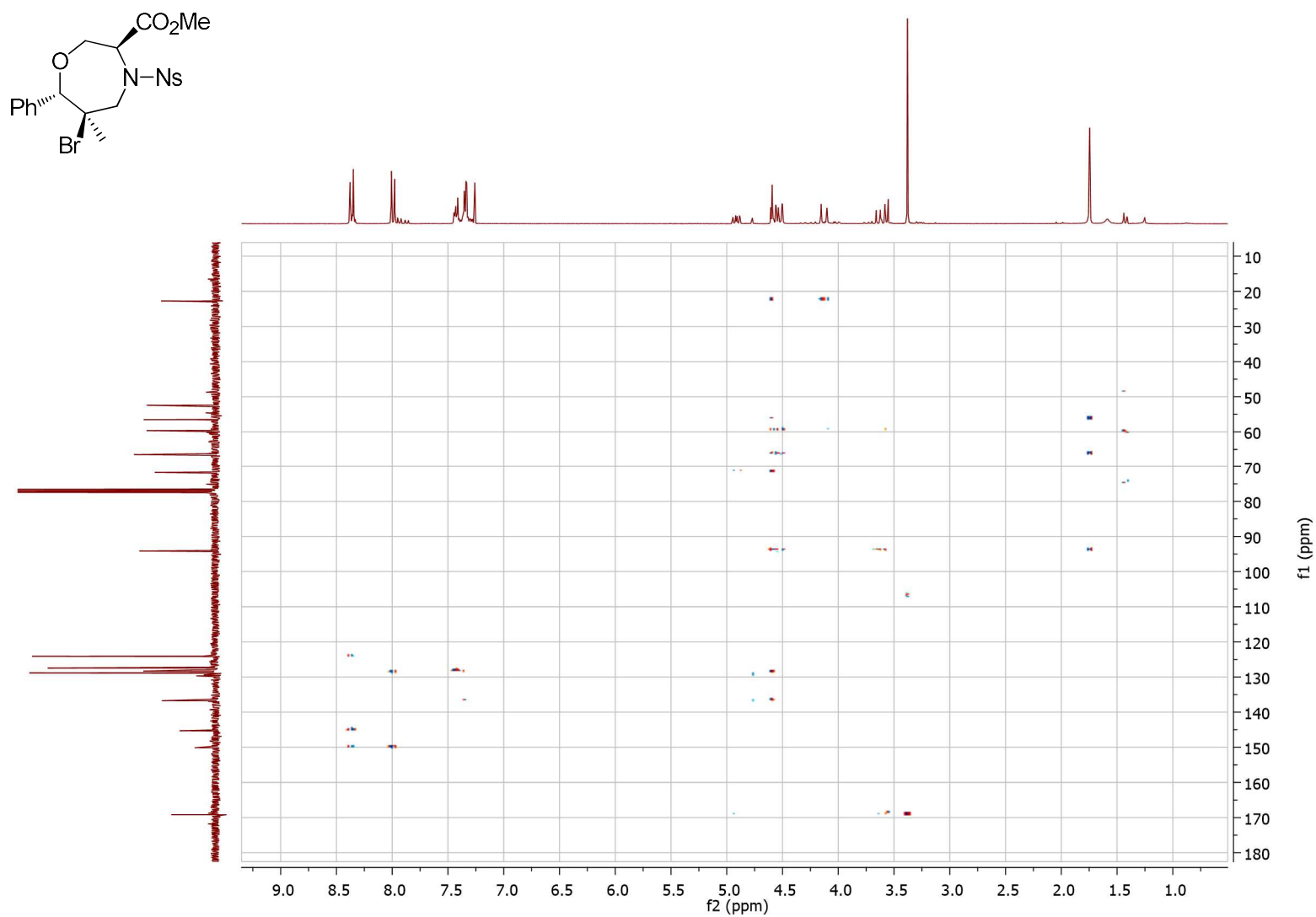
^{13}C NMR for methyl (3*S*,6*R*,7*S*)-6-bromo-6-methyl-4-((4-nitrophenyl)sulfonyl)-7-phenyl-1,4-oxazepane-3-carboxylate (**2.42j**).



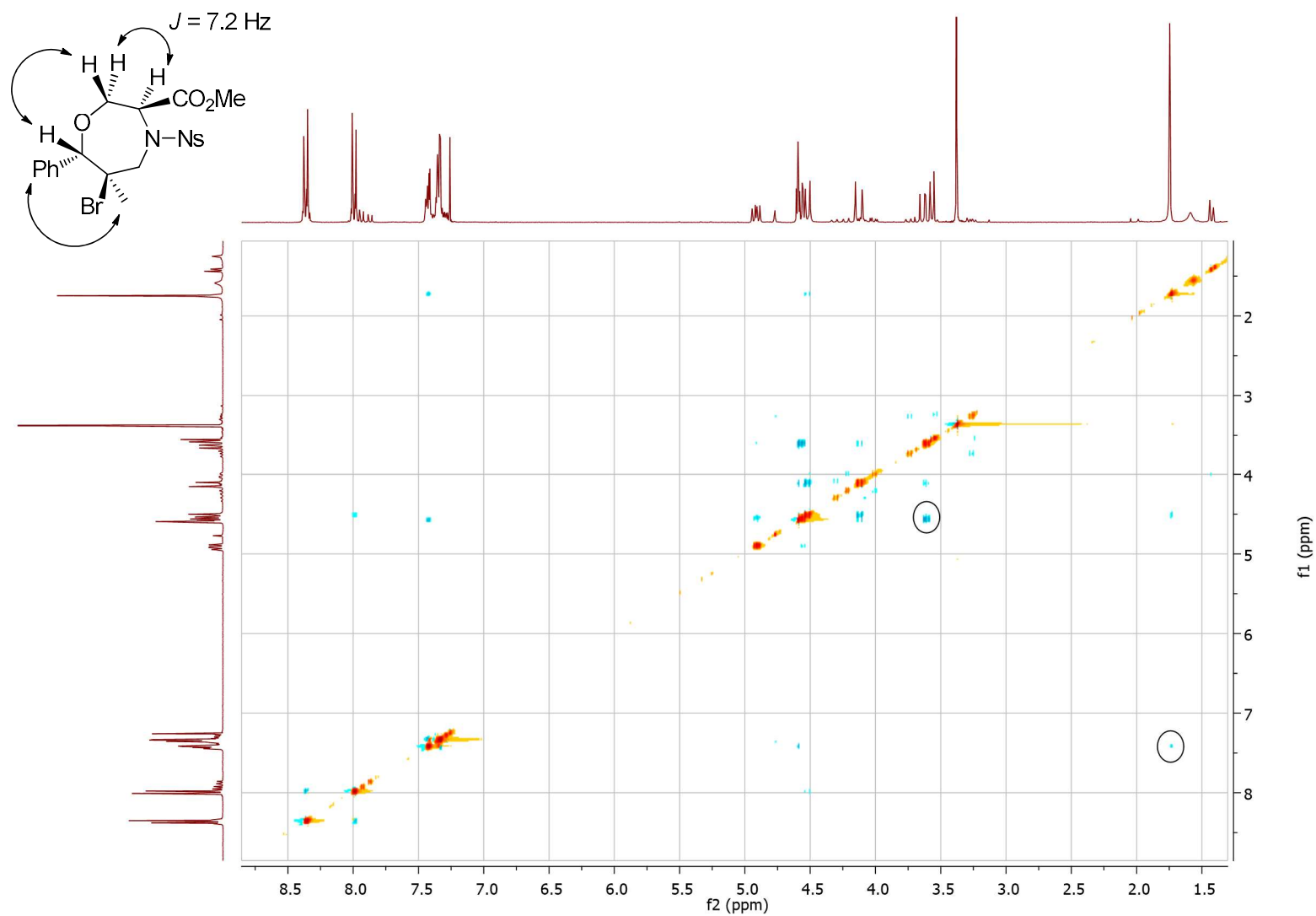
COSY NMR for methyl (3*S*,6*R*,7*S*)-6-bromo-6-methyl-4-((4-nitrophenyl)sulfonyl)-7-phenyl-1,4-oxazepane-3-carboxylate (**2.42j**).



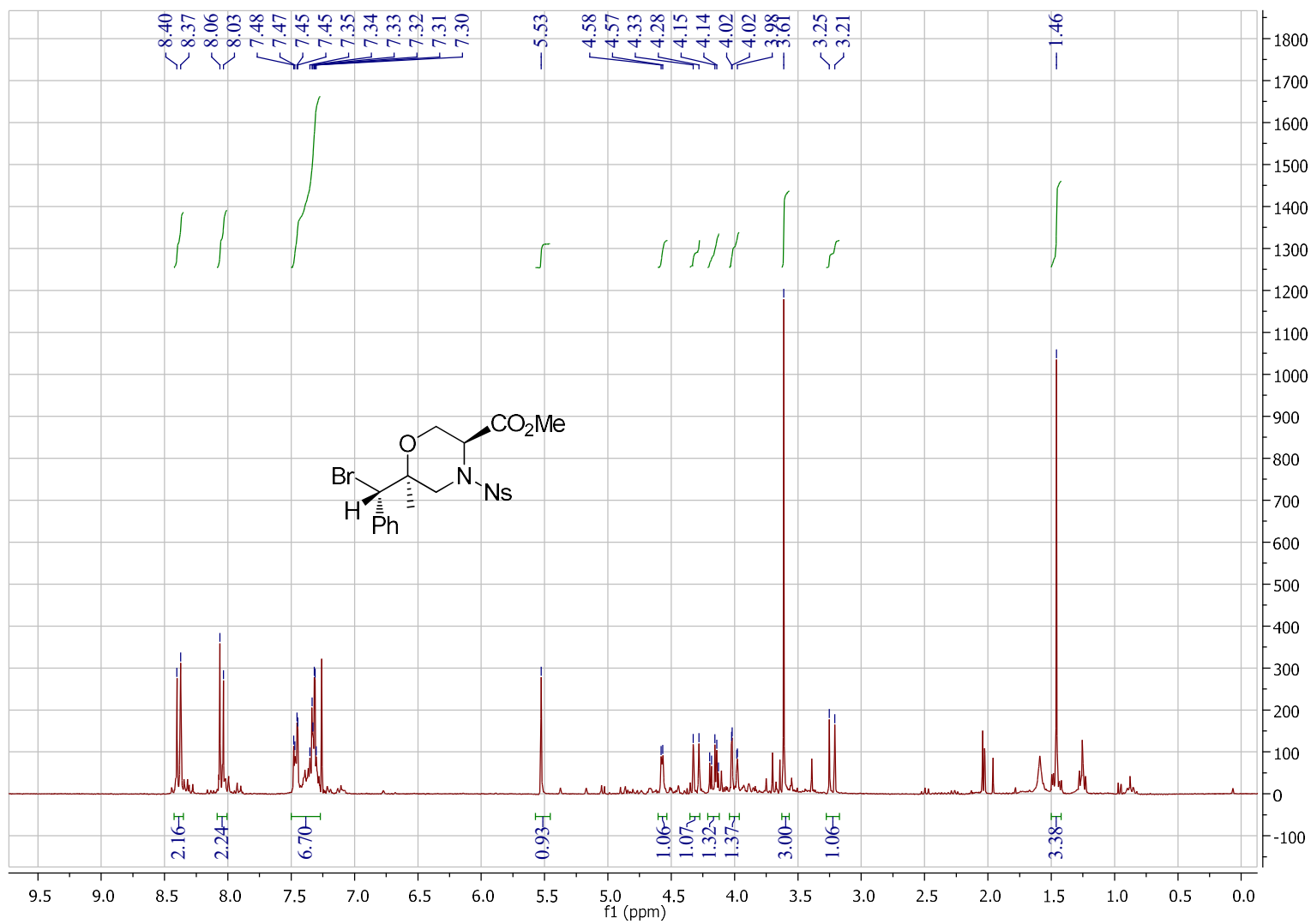
HSQC NMR for methyl (3*S*,6*R*,7*S*)-6-bromo-6-methyl-4-((4-nitrophenyl)sulfonyl)-7-phenyl-1,4-oxazepane-3-carboxylate (**2.42j**).



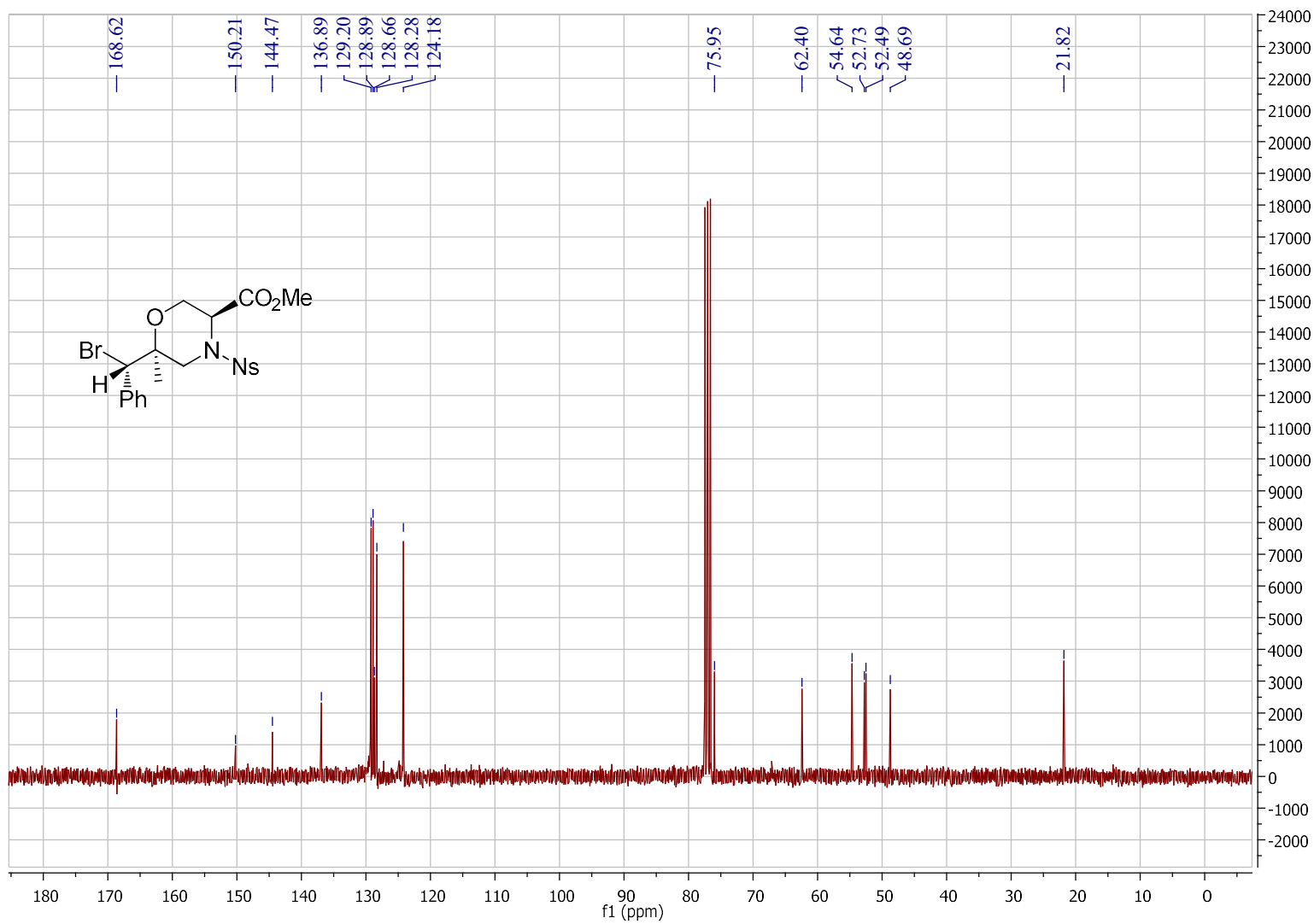
HMBC NMR for methyl (3*S*,6*R*,7*S*)-6-bromo-6-methyl-4-((4-nitrophenyl)sulfonyl)-7-phenyl-1,4-oxazepane-3-carboxylate (**2.42j**).



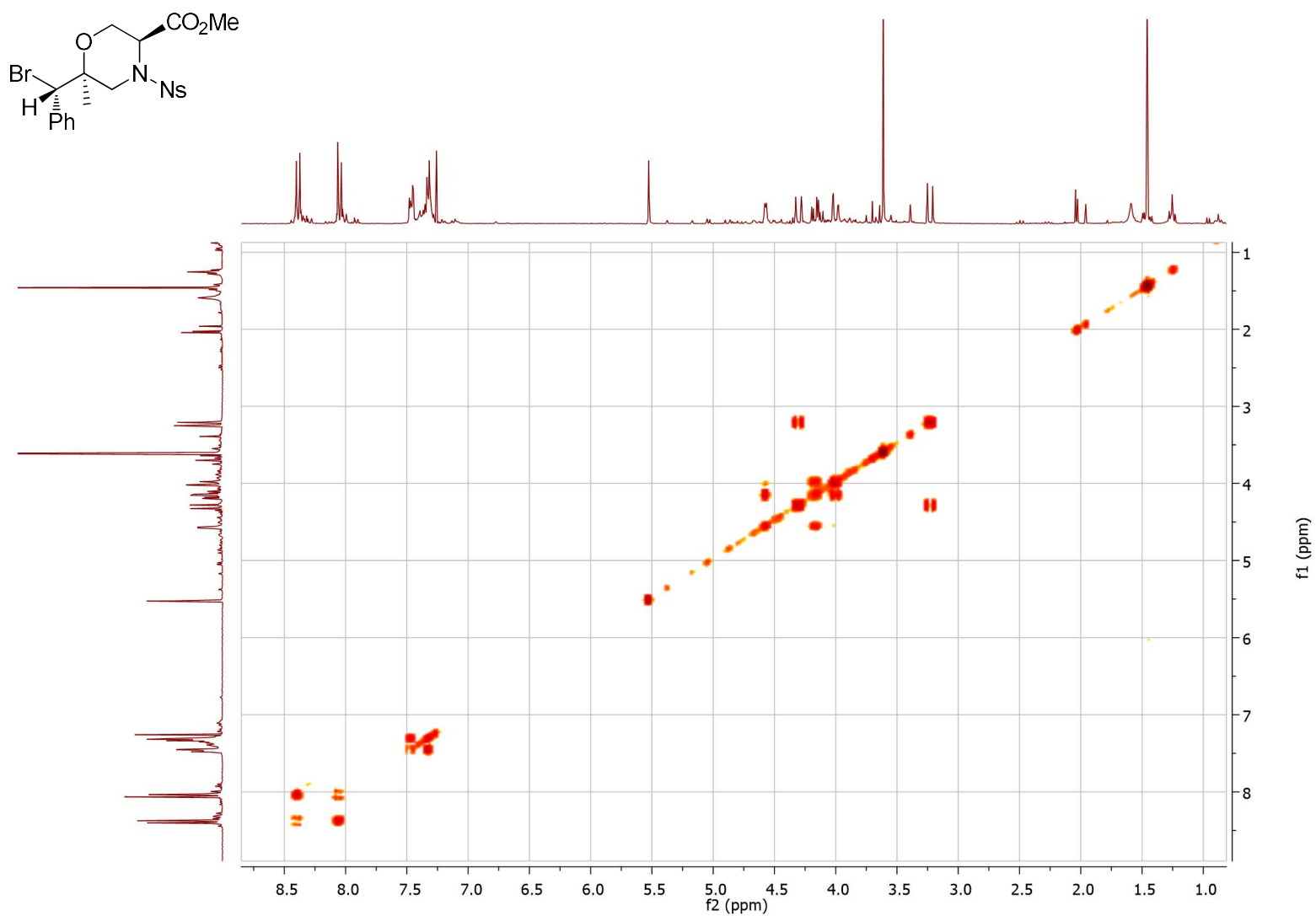
NOESY NMR for methyl (3*S*,6*R*,7*S*)-6-bromo-6-methyl-4-((4-nitrophenyl)sulfonyl)-7-phenyl-1,4-oxazepane-3-carboxylate (**2.42j**).



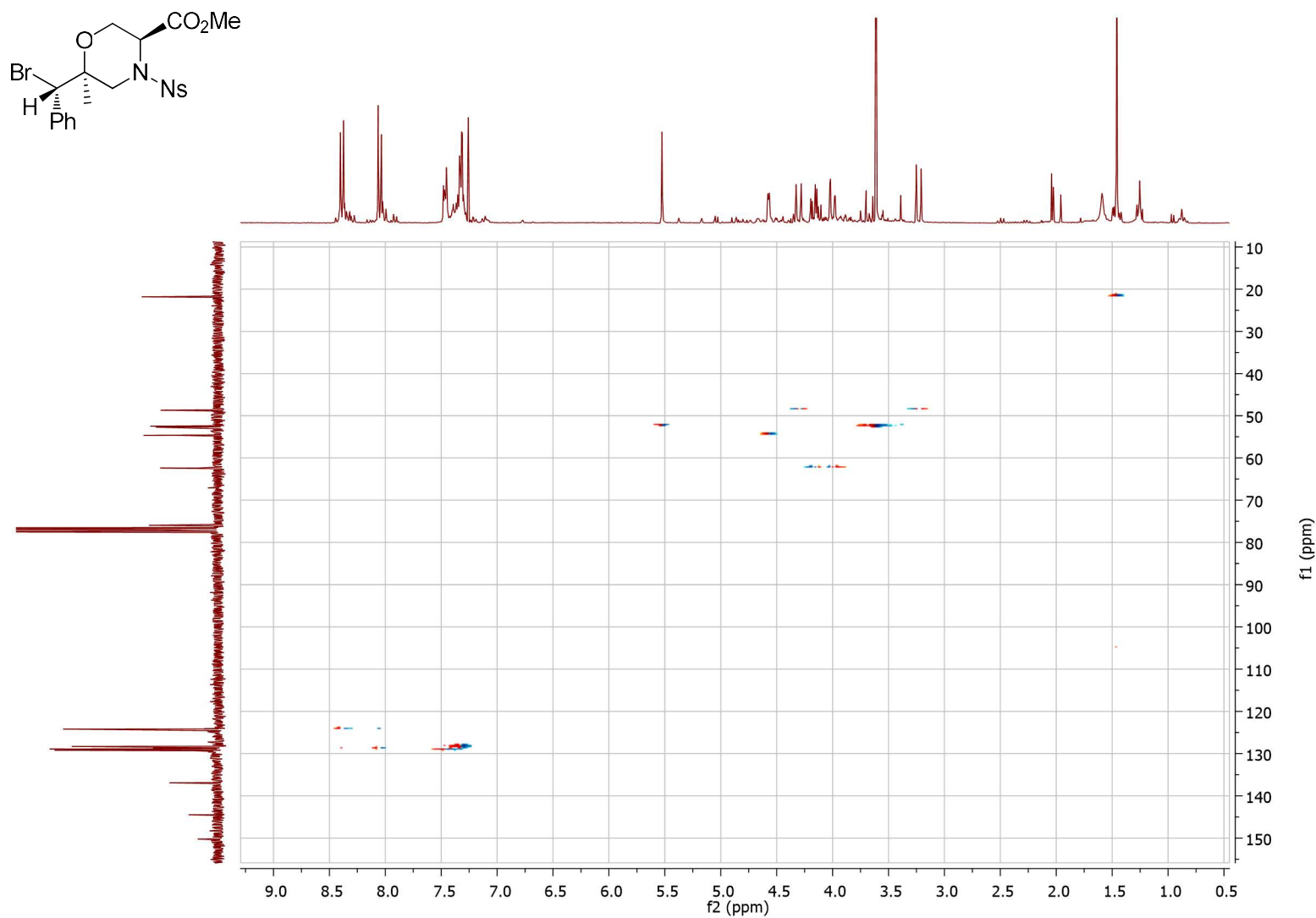
^1H NMR of methyl (3*S*,6*S*)-6-((*S*)-bromo(phenyl)methyl)-6-methyl-4-((4-nitrophenyl)sulfonyl)morpholine-3-carboxylate (**2.43j**).



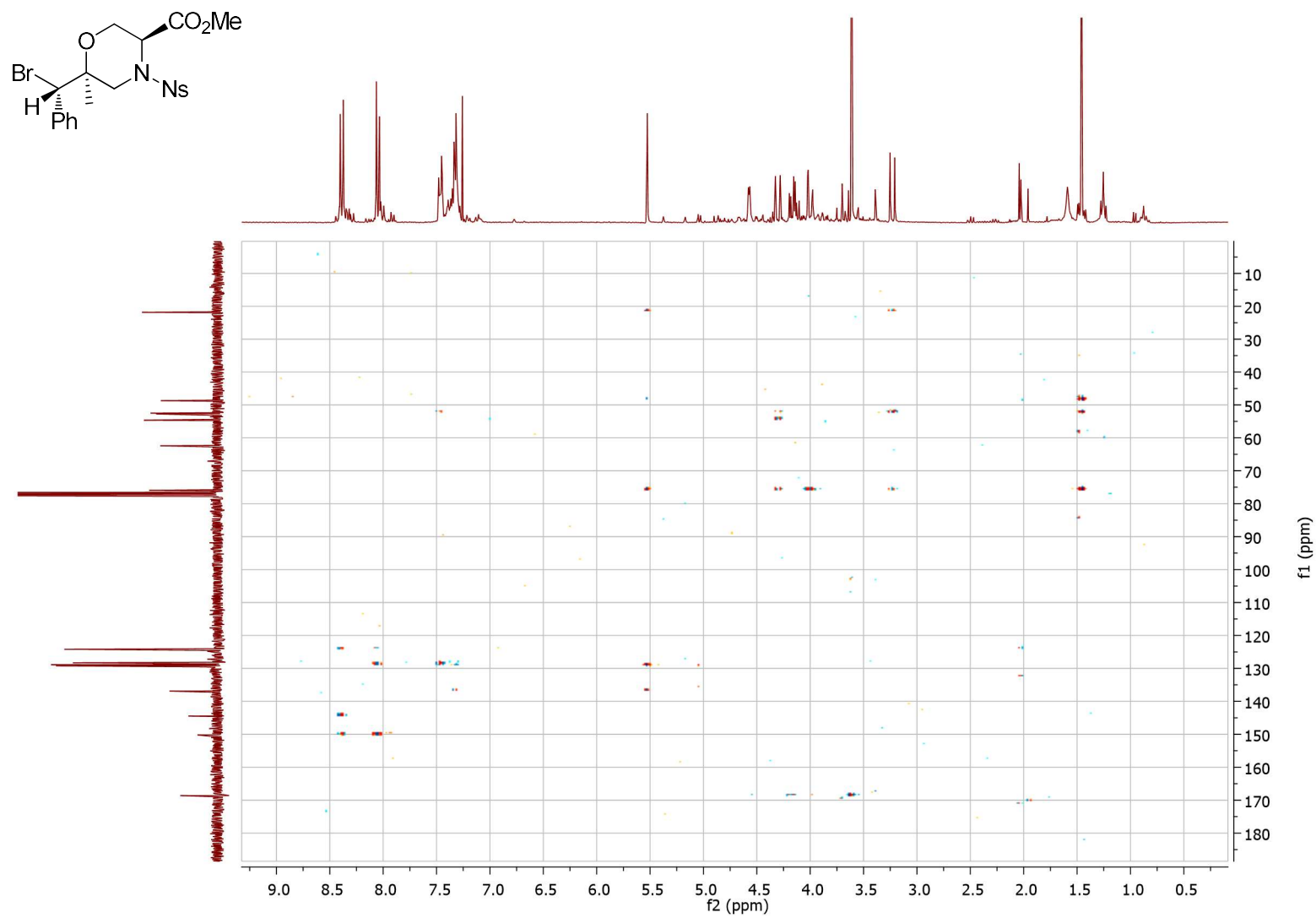
^{13}C NMR of methyl (3*S*,6*S*)-6-((*S*)-bromo(phenyl)methyl)-6-methyl-4-((4-nitrophenyl)sulfonyl)morpholine-3-carboxylate (**2.43j**).

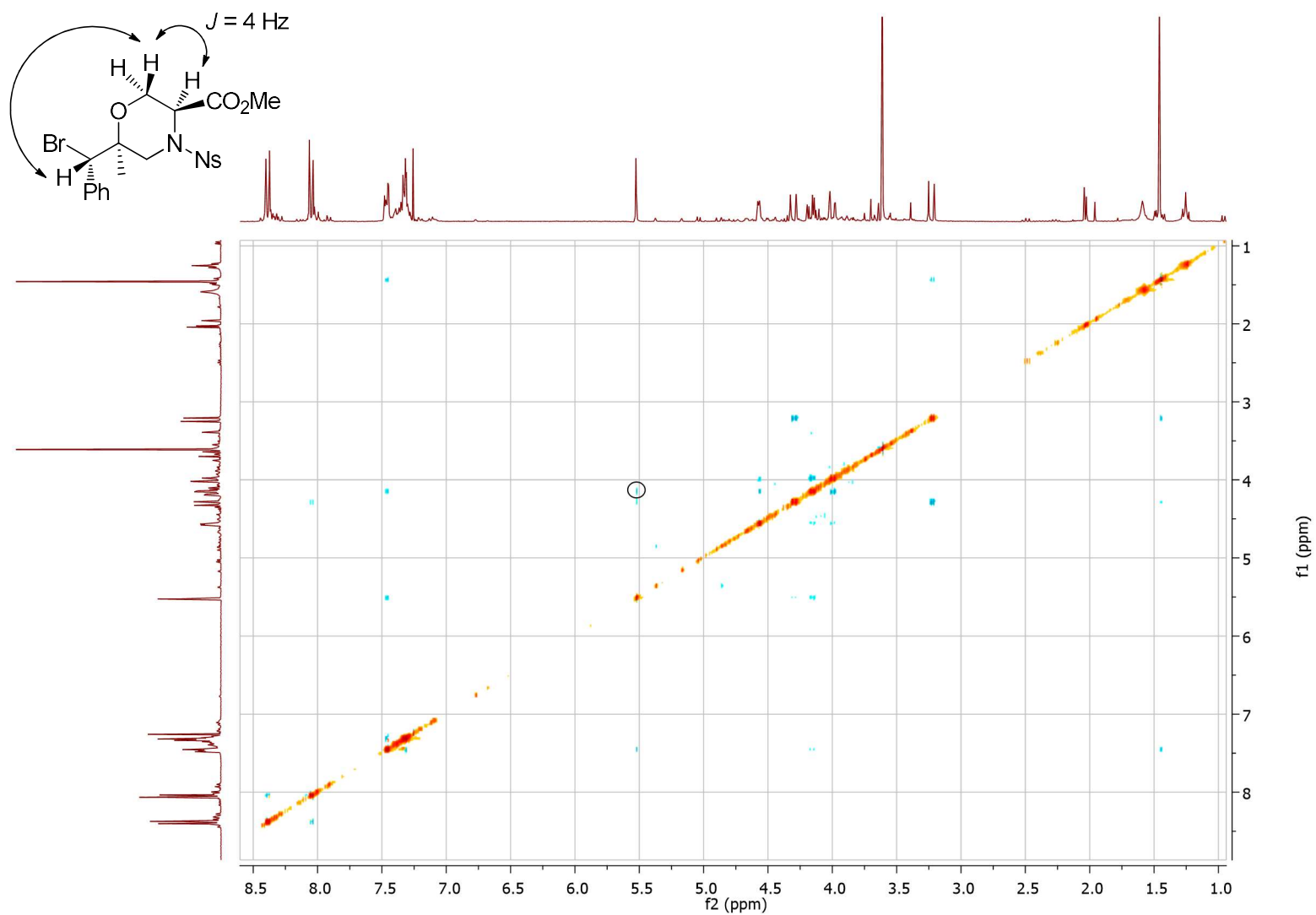


COSY NMR of methyl (3*S*,6*S*)-6-((*S*)-bromo(phenyl)methyl)-6-methyl-4-((4-nitrophenyl)sulfonyl)morpholine-3-carboxylate (**2.43j**).



HSQC NMR of methyl (3*S*,6*S*)-6-((*S*)-bromo(phenyl)methyl)-6-methyl-4-((4-nitrophenyl)sulfonyl)morpholine-3-carboxylate (**2.43j**).

HMBC NMR of methyl (3*S*,6*S*)-6-((*S*)-bromo(phenyl)methyl)-6-methyl-4-((4-nitrophenyl)sulfonyl)morpholine-3-carboxylate (**2.43j**).



NOESY NMR of methyl (3*S*,6*S*)-6-((*S*)-bromo(phenyl)methyl)-6-methyl-4-((4-nitrophenyl)sulfonyl)morpholine-3-carboxylate (**2.43j**).

3.6 References

- (1) Yamabe, S.; Minato, T. *Bull. Chem. Soc. Jpn.* **1993**, *66*, 3339.
- (2) Ko, C.; Hsung, R. P.; Al-Rashid, Z. F.; Feltenberger, J. B.; Lu, T.; Yang, J.-H.; Wei, Y.; Zifcsak, C. A. *Org. Lett.* **2007**, *9*, 4459.
- (3) Bezanson, M.; Pottel, J.; Bilbeisi, R.; Toumieux, S.; Cueto, M.; Moitessier, N. *J. Org. Chem.* **2013**, *78*, 872.
- (4) Zhou, J.; Zhou, L.; Yeung, Y.-Y. *Org. Lett.* **2012**, *14*, 5250.
- (5) Zhou, J.; Yeung, Y. Y. *J. Org. Chem.* **2014**, *79*, 4644.
- (6) Wong, E. H.; Ahmed, S.; Marshall, R. C.; McArthur, R.; Taylor, D. P.; Birgeron, L.; Cetera, P.; Organization, W. I. P., Ed. 2001.
- (7) Brenner, E.; Baldwin, R. M.; Tamagnan, G. *Org. Lett.* **2005**, *7*, 937.
- (8) Pedrosa, R.; Andrés, C.; Mendiguchía, P.; Nieto, J. *J. Org. Chem.* **2006**, *71*, 8854.
- (9) Nieto, J.; Andres, C.; Perez-Encabo, A. *Org. Biomol. Chem.* **2015**.
- (10) Kishore Vandavasi, J.; Hu, W.-P.; Chandru Senadi, G.; Chen, H.-T.; Chen, H.-Y.; Hsieh, K.-C.; Wang, J.-J. *Adv. Synth. Catal.* **2015**, *357*, 2788.
- (11) Denmark, S. E.; Burk, M. T.; Hoover, A. J. *J. Am. Chem. Soc.* **2010**, *132*, 1232.
- (12) Denmark, S. E.; Burk, M. T. *Proc. Natl. Acad. Sci. U. S. A.* **2010**, *107*, 20655.
- (13) Denmark, S. E.; Burk, M. T. *Org. Lett.* **2012**, *14*, 256.
- (14) Baldwin, J. E. *J. Chem. Soc., Chem. Commun.* **1976**, 734.

Chapter 4 Fluoride-mediated desulfonylative intramolecular cyclization to fused and bridged bicyclic compounds

4.1 Preface

Some of the most important and fundamental reactions in organic chemistry were discovered by serendipity. This chapter will discuss a rearrangement reaction of the oxazepane and morpholine products that were discussed in Chapter 2 and Chapter 3. While attempting to remove the sulfonamide protecting group, an unexpected product was obtained from a desulfonylative intramolecular cyclization to give a fused 4-oxa-1-azabicyclo[4.1.0]heptane ring system. A variety of conditions were investigated and it was found that the reaction was specific to TBAF initiated conditions. A mechanism is proposed along with evidence supporting the mechanism from testing a variety of different substrates under the reaction conditions. There are also extensive computational investigations presented supporting the proposed mechanism. Any computational work presented was done by Anna Tomberg.

4.2 Introduction

One powerful method of introducing molecular complexity is through intramolecular rearrangements of heterocyclic compounds with perhaps some of the best examples being in the context of diversity oriented synthesis.^{1,2} Many of these methods are metal catalyzed, decreasing the applicability of such reactions in green processes or significantly increasing the associated costs.³⁻⁶ Over the past century, several very different rearrangements were discovered such as the very well-known Claisen and Wittig rearrangements of allylic systems, the Brook rearrangement of α -silyl carbinols⁷ and the Wolff rearrangement to name a few.⁸ Other rearrangements on aromatic molecules are also well established such as the Snieckus-Fries rearrangement.^{9,10} Over the years, complex rearrangements were also discovered from judiciously designed experiments leading to unexpected results such as those reported by Ivachtchenko and co-workers and Kutateladze and co-workers.^{11,12}

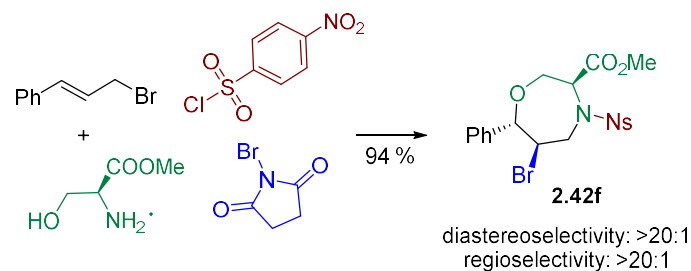


Figure 4.1. Complexity from simple building blocks

In recent years, we reported the design, development and use of a number of chiral molecular scaffolds. Among those are bicyclic dipeptide mimetics,¹³ carbohydrates,¹⁴ and polysubstituted oxazepanes and morpholines.¹⁵ The latter were prepared in three steps from commercially available starting materials in good to excellent stereoselectivity and regioselectivity (Figure 4.1). In order to use these scaffolds, the two protecting groups (methyl ester and nosyl) should be removed to release the two functionalizable anchors (carboxylic acid and secondary amine). In an

attempt to remove the sulfonamide protecting group on oxazepane **2.42f** using tetrabutylammonium fluoride (TBAF), we observed full conversion to a non-racemic mixture of enantiomeric products.

Herein we report a unique fluoride-mediated rearrangement of 1,4-oxazepanes and morpholines together with an extensive mechanistic study revealing a complex series of reactions.

4.3 Results and Discussion

4.3.1 Characterization

NMR characterization indicated that the *para*-substituted phenyl group of the nosyl protecting group was still present with a significant shift upfield of the aromatic protons. Additional investigations by mass spectrometry (MS) suggested loss of SO₂ and led us to consider an intramolecular rearrangement. Extensive NMR studies as well as X-ray crystallography confirmed the structure of the obtained product to be **4.1** (Figure 4.2). Although oxazepane **2.42f** was enantiopure, the crystal structure of **4.1** was of the racemic compound while chiral HPLC showed that the reaction proceeded with 36 %ee (see Supplementary Information).

Overall the process included desulfurization, migration of a *para*-nitrophenyl group, intramolecular cyclization to an aziridine and racemization. This uncommon process may represent a powerful method for introducing significant complexity in very few steps, including bridged and fused ring systems, and deserved to be further investigated and its mechanism should be elucidated.

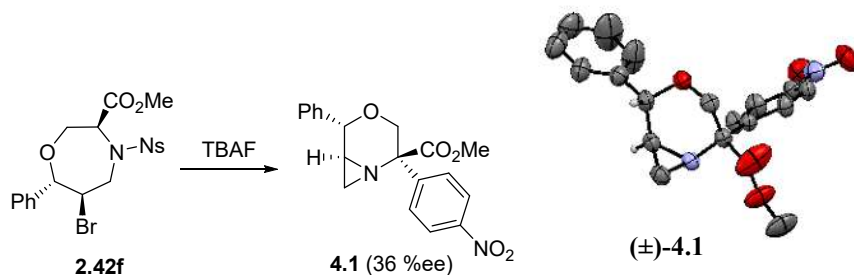
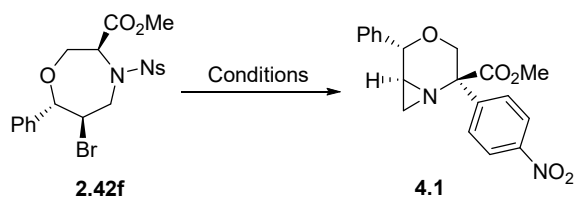


Figure 4.2. Fluoride-mediated intramolecular rearrangement of 2.42f. Ellipsoids shown at 50 % probability level; crystal structure is of (±)-4.1 (the enantiomer shown will be referred to as 4.1a, the enantiomer not shown will be referred to as 4.1b).

4.3.2 Probing the reaction conditions

In an effort to understand the mechanism, we examined a variety of conditions (Table 4.1). Surprisingly, TBAF was the only additive that initiated this unique rearrangement efficiently. It is known that TBAF can act as a strong base and is able to initiate amides and carbamates to undergo intramolecular cyclization.^{16,17} Additionally, there has been a few reports of aryl migration of nosyl protecting groups accompanied by extrusion of sulfur dioxide under basic conditions.^{18,19} In light of this known reactivity, we first reasoned that TBAF was acting as a base to initiate the reaction. The presence of the large nosyl group close to the enolizable proton may be preventing larger anions like chloride, bromide and iodide from initiating the reaction. Alternatively, these halides may not be basic enough to promote the reaction (Table 4.1, entries 2-4). The lack of reactivity observed when pyridinium fluoride was employed was thought to arise from the stronger ion pair formed compared to TBAF reducing the fluoride reactivity (Table 4.1, entry 5). However, when NaF was employed in conjunction with 15-crown-5 ether, no reaction was observed indicating that the availability of the fluoride ion may not be the issue, unless an ion pair is retained with the crown ether complex (Table 4.1, Entry 6).

Table 4.1. Reaction condition evaluation.



Entry	Reagent ^a	Conversion (%) ^b
1	TBAF ^c	100
2	TBACl	0
3	TBAB	0
4	TBAI	0
5	Pyridinium fluoride	0
6	NaF + 15-crown-5	0
7	K ₂ CO ₃	0
8	NEt ₃	< 5
9	KO ^t Bu + 18-crown-6	Complex mixture
10	NaOH	0 ^d
11	AgOTf	0
12	0.2 eq. TBAF	35
13	1 eq. TBAF	38
14 ^e	Reflux	Complex mixture
15	-78 °C	100
16	[2.42f] = 0.20 M	100
17	Solid TBAF ^f	100
18	Solid TBAF ^f , MeOH	0
19	Solid TBAF ^f , toluene	100

a) Reaction conditions: [**2.42f**] = 0.02 M, Reagent (5 eq.), THF, rt; b) Determined by HPLC; c) TBAF is a 1 M solution in THF; d) Starting material is completely consumed; e) An intermediate was observed in the HPLC trace of this crude mixture however it converted completely to the expected product within an hour; f) Solid TBAF is tetrabutylammonium fluoride hydrate.

Bases other than TBAF such as K_2CO_3 and NEt_3 did not initiate this reaction or did so with low conversion (Table 4.1, entries 7, 8). This observation ruled out the possibility that NBu_3 , a decomposition product of TBAF, played any substantial role. This prompted us to question if TBAF was indeed acting as a simple base and to look at stronger bases. When KO^tBu was employed, the starting material was completely consumed but only a complex mixture was obtained and no rearranged product was observed (Table 4.1, entry 9) indicating that the starting material and/or the products were not stable under strongly basic conditions. Similarly, when we employed NaOH, the starting material was again completely consumed but no rearranged product was obtained indicating that any basic hydroxides present in the commercial TBAF were not responsible for the observed reactivity (Table 4.1, entry 10). We also investigated using Lewis acids as activating agents to increase reactivity yet when $AgOTf$ was employed only starting material was recovered (Table 4.1, Entry 11).

An excess of TBAF was required to drive the reaction to completion; however, the similar conversions observed when employing substoichiometric or one equivalent of TBAF did not allow us to rule out a catalytic mechanism (Table 4.1, entries 12, 13).

We next examined the effect of temperature on the reaction (Table 4.1, entries 14, 15). Interestingly, at $-78\text{ }^\circ\text{C}$, a short half-lived intermediate was observed by monitoring the reaction by HPLC. This intermediate converted completely to **4.1** over time. At elevated temperatures, only decomposition was observed.

The effect of concentration of the starting material on the reaction seemed to be unimportant as increasing the concentration by up to an order of magnitude had little effect on the reaction (Table 4.1, entry 16). Lastly, we examined the effect of solvent on the reaction. The TBAF used under the standard conditions was a 1 M solution in THF. To vary the solvents, solid TBAF hydrate was also assessed. This was tested first in THF to ensure that the outcome was similar to that observed when TBAF solution was employed (Table 4.1, entry 17). At this stage, we could assume that solid TBAF hydrate was an acceptable substitute for TBAF solution. Performing the reaction in toluene gave similar results to using THF. However only starting material was isolated when methanol was employed (Table 4.1, entry 18, 19). This observation was consistent to TBAF acting as a weaker base in protic solvents such as methanol.

4.3.3 Substrate scope

We strategically chose a substrate scope not to show how widely applicable this chemistry was to various substrates, but rather to glean as much mechanistic details as we could. The selected set of substrates and the observed products are presented in .

As the bromine atom acts as a leaving group, substituting it with iodine should not affect the outcome. Unsurprisingly, the 6-iodo derivative (**10a**) gave the same product as **2.42f** (, entry 2).

When an analogous morpholine substrate (**10b**) was subjected to the reaction conditions, the major product isolated was fused bicycle **4.2b** (, entry 3). The structure of the product suggested that formation of an enolate occurred, followed by displacement of the bromide (Figure 4.3). This is an additional evidence of the fluoride acting as a base.

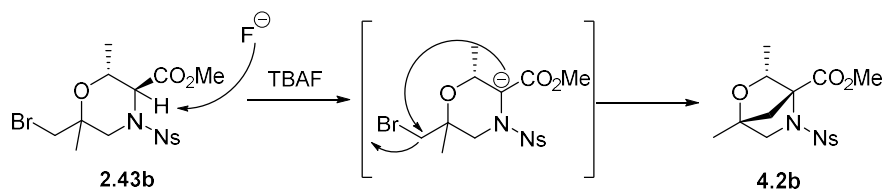


Figure 4.3. Mechanism for the formation of 4.2b.

We hypothesized that in the absence of an enolizable proton that no rearrangement would occur (, entry 4) and carried out the reaction with the 3-unsubstituted derivative **10c**. Only the elimination product **4.2c** was observed. Importantly, no rearranged bicycle product was observed, indicating an enolizable proton is required. Together with the previous observation with the morpholine substrate (, entry 3) and literature precedents,¹⁹ this piece of information strongly suggests that an enolate is involved in the mechanism.

In order to rationalize the isomerization of the benzylic position, we imagined that a possible mechanistic pathway might involve participation of the benzylic proton. To examine this potential mechanism, we replaced the phenyl group by an achiral gem dimethyl moiety in **10d** (, entry 5). The only product observed was **4.2d**, indicating that the benzylic proton was not necessary for the reaction to proceed and therefore unlikely to be involved in the mechanism. However, the presence of a single stereoisomer does not provide any information about the role of this hydrogen in the isomerization of the product as this could indicate a highly stereoselective isomerization or no isomerization.

We next wanted to examine the electronic effects of the sulfonamide group on the observed reactivity. We hypothesized that migration of the aryl group occurred from attack of an enolate at C3 onto the *ipso* carbon of the nosyl protecting group. We thought that the *ipso* carbon of a tosyl protecting group (**10e**) would be less electrophilic. In addition, the lower electron-withdrawing abilities of the tosyl relative to nosyl may also have an effect on the acidity of the C3 proton, making the enolate more difficult to form, possibly even shutting down the reaction. In light of these hypotheses, we were pleased to see that while a reaction indeed occurred with the tosylated derivative, the reaction resulted in a very complex mixture that did not seem to follow the same

trends as the reactivity of the nosylated derivative (, entry 6). This observation is also consistent with previous observations on proline esters where moving from nosyl to tosyl shut down the migration reaction (Figure 4.4).¹⁹

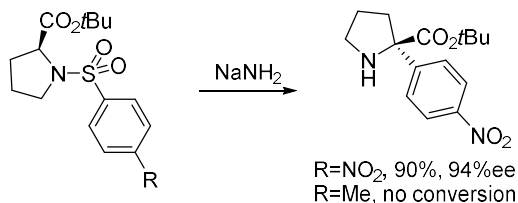


Figure 4.4. Migration of *para*-nitrophenyl in nosyl-protected proline ester reported previously.¹⁹

While the migration of aryl sulfonamide proline esters is documented to occur under strongly basic conditions (Figure 4.4), the partial racemization we observed was puzzling. Mechanistically, the partial racemization that we observed for the formation of **4.1** indicated that all three of the stereocenters on the molecule must participate in the mechanism. We thought that the addition of another stereocenter would give information about if that center was also involved in the mechanism and additionally wanted to examine the effect that this additional stereocenter had on the selectivity of the reaction. For this purpose, we looked at threonine analogue **10f** and isolated not a single compound as we did with **2.42f** but in fact a mixture of several compounds (, entry 7). After tedious purification and characterization, we were able to assign structures as **4.2fa**, **4.2fb**, **4.2fc** and **4.2fd**. Interestingly, **4.2fa** was very difficult to isolate reproducibly. Despite this poor stability, we were able to get a crystal structure of **4.2fa** to confirm the structure we had initially assigned by NMR (Figure 4.5). We previously mentioned a short half-life intermediate observed at low temperature when reacting **2.42f**. At this point, we assigned the structure of the intermediate isolated at low temperatures mentioned above (Table 4.1, entry 14) to be **4.1c** based on analogy of the ¹H NMR spectrum with that of **4.2fa**. It is important to note that the stereochemistry at the C7

phenyl group had inverted relative to the stereochemistry of the starting material. As this was the only substrate isolated from the reaction that had the nosyl protecting group intact, this was strong evidence that the stereochemistry at C7 was effected prior to migration of the *para*-nitrophenyl group.

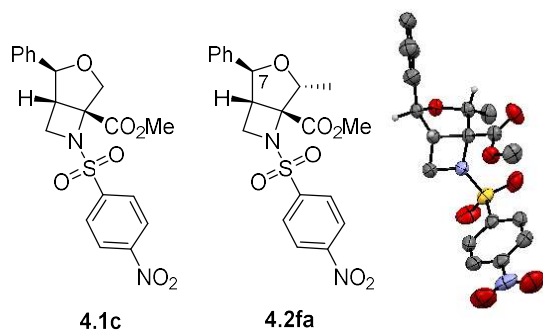


Figure 4.5. Assigned structure of 4.1c based on analogy of its NMR spectrum with that of 4.2fa. Ellipsoids shown at 50 % probability level.

Extensive NMR studies suggested that the structures of **4.2fb** and **4.2fc** were diastereomeric. When we strategically designed this experiment, we proposed to introduce an additional stereocenter relative to **4.1** (i.e., additional methyl from **2.42f** to **10f**) to determine if that carbon atom was also involved in the mechanism. The formation of diastereomers differing in all but this center indicated that the C2 center was not involved in the isomerization mechanism. There was an obvious matched/mismatched effect happening however, as **4.2fb** was significantly favored over **4.2fc**.

The epoxide **4.2fd** represented an interesting scaffold and exemplified how fascinating this reaction was mechanistically. Two possible mechanisms for the formation of **4.2fd** are presented in Figure 4.6. With threonine, the additional methyl enables the formation of an epoxide after migration of the *para*-nitrophenyl, with elimination/ring opening taking place on the threonine side chain methyl group to produce **4.2fd** after loss of SO₂ (Figure 4.6, pathway 1). Alternatively,

fluoride abstraction of the enolizable proton may lead to a retro-Michael addition and the generated alkoxide then concertedly displaced the bromide to form epoxide **4.2fd** (Figure 4.6, pathway 2).

Assistance of the sulfonamide oxygen is possible and has not been investigated further.

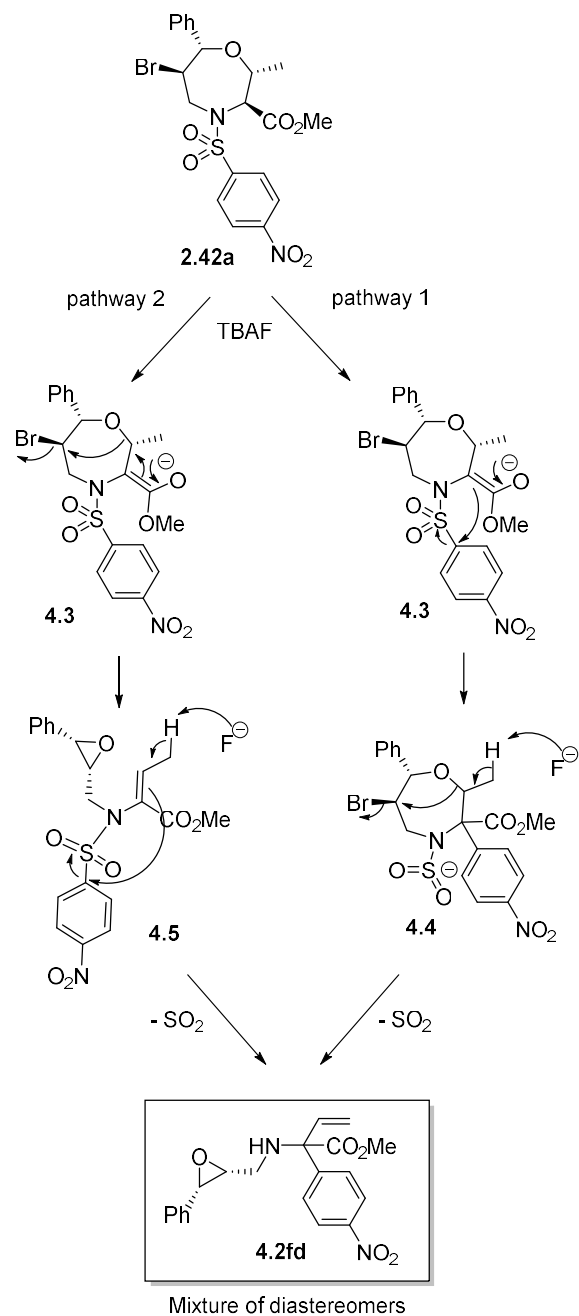
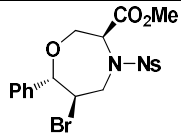
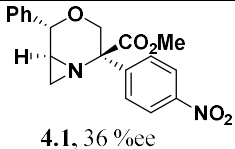
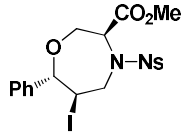
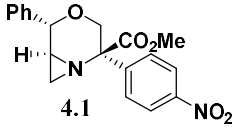


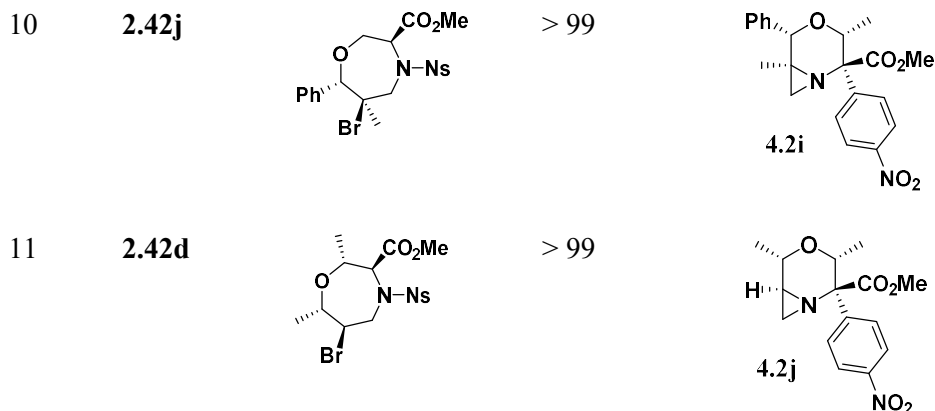
Figure 4.6. Tentative mechanisms for the formation of 4.2fd.

When comparing the stereochemical outcome of the reactions with serine derivative **2.42f** and with threonine derivative **10f**, it was clear that the additional stereogenic center was modulating the stereoselectivity. We reasoned that inverting the C2 stereochemistry, which was responsible for the matched/mismatched behavior, may invert the stereo-preference. To probe this hypothesis, we varied the stereochemistry at C6 and C7 using *allo*-threonine derived starting oxazepane. As predicted, when reacting **10g**, the C2 epimer of **10f**, only one product was isolated, **4.2g** (, entry 8). Once more the relative stereochemistry between the three isomerizable centers was identical to **4.1** and was unique as no diastereomers were observed. When reacting **10h**, which was diastereomeric of **10f** at C2, C6 and C7, the HPLC trace was identical to the crude of **10f**. This indicated that since the C2 stereocenter is not involved in the reaction, then the transition states of reaction of **10h** were enantiomeric of those from **10f** (, entry 9). Indeed, isolation of the major compound from this reaction, **4.2hb**, showed an identical proton NMR as that of **4.2fb** together with an optical rotation measurement of the opposite sign, lending even further evidence towards this hypothesis.

Table 4.2. Substrate screen.

Entry	Compound	Starting Material	% Conversion ^a (Isolated Yield)	Product(s) Isolated
1	2.42f		> 99 (46)	 4.1 , 36 %ee
2	2.42r		> 99 ^b	 4.1

3	2.43b		> 99 (27)		4.2b		
4	2.42o		- ^c		4.2c		
5	2.42c		> 99 (69)		4.2d		
6	2.39a		-	Complex mixture			
7	2.42a		> 99		4.2fa		4.2fb
					4.2fc		4.2fd
8	2.42n		> 99 (69)		4.2g		
9 ^d	2.42n'		> 99		4.2ha		4.2hb
					4.2g		4.2hd



a) Determined by HPLC, > 99 % indicates no remaining starting material could be detected; b) **10a'**, with the opposite stereochemistry at C6 and C7, also gave **4.1** exclusively with full conversion, no %ee was measured for either reaction; c) HPLC signals for starting material overlapped with those of the products so conversion could not be reported, no starting material was recovered; d) Products shown were assumed based on the proposed mechanism and isolation of **4.2hb** proving to be the enantiomer of **4.2fb**.

4.3.4 Proposed mechanism

At this point, we would like to point out that while we believe we present herein a reasonable suggestion that is supported by extensive computational investigations, the proposal is still a tentative mechanism. The calculations were performed using DFT in THF implicit solvent (see SI for details).

To account for the clean conversion of medium-sized ring derivative **2.42f** into bicyclic molecule **4.1** we undertook computational modeling of the reaction mechanism. With the substrate scope in hand, we had a wealth of information to consider when developing a proposed mechanism. One particularly significant observation was the isolation of **10fa**, which suggested that the inversion of stereochemistry at C7 occurs before migration of the *para*-nitrophenyl group.

This inversion likely goes through an sp^2 intermediate, via either a carbocationic intermediate or an olefin intermediate.

To probe inversion of stereochemistry going through a carbocation, we analyzed computationally the formation of a carbon-oxygen bond (marked red in Figure 4.7). By computing the energies along the varying bond length between these two atoms, we estimated the energy barrier required for this step to be over 30 kcal/mol, which indicated that this pathway is unlikely.

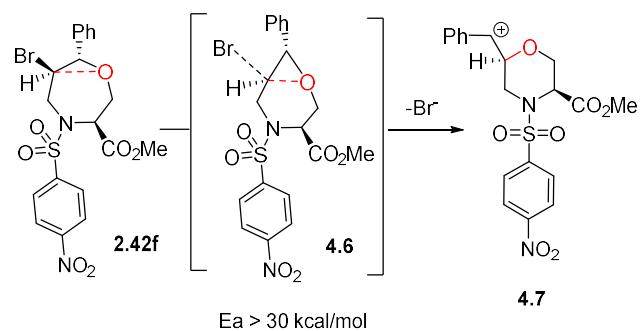


Figure 4.7. Formation of carbocation intermediate 4.7 from 2.42f.

The alternative way of inverting the stereochemistry at C7 is through an olefin formed through opening the 7-membered ring by an elimination reaction. This step required a specific conformation of the ring where the C6 proton oriented almost perfectly anti-periplanar to the ether oxygen, making elimination a favorable option (Figure 4.8).

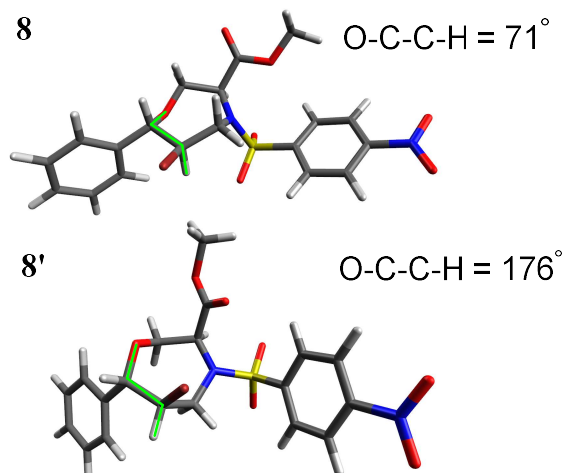


Figure 4.8. Compound 2.42f: conformation leading towards 4.1a (top), conformation with C6 proton anti-periplanar to the ether oxygen leading to elimination of bromine (bottom).

This conformation (**2.42f'**), stabilized by a fluoride anion and an HF molecule, was 3.1 kcal/mol lower than compound **2.42f** in the presence of the same molecules. An energy barrier of 14.9 kcal/mol was required to produce the open structure **4.8** (Figure 4.9) though an E2 mechanism from **2.42f'**. The free rotation around the carbon-carbon bond to yield **4.8'** is energetically favorable by 4.3 kcal/mol, thereby allowing the substituents at C6 and C7 to invert relative to **2.42f** once the ring closes to **4.9**. The two structures, **2.42f** and **4.9**, have similar energies with **4.9** being 0.9 kcal/mol lower.

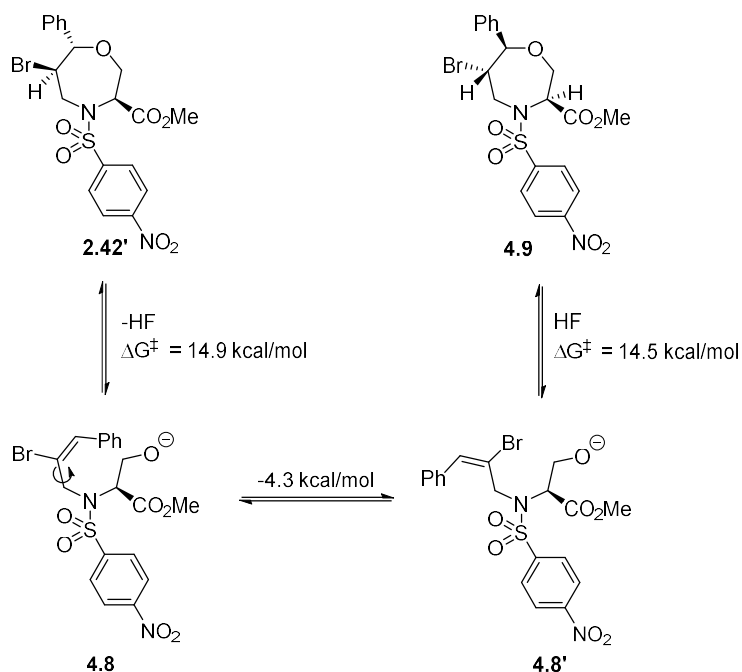


Figure 4.9. Ring opening of **2.42f** leading to the production of its diastereomer **4.9**.

It is worth noting that only one conformation of compound **2.42f** possess this anti-periplanar geometry and will undergo the elimination mechanism. Similarly, we suggest that this elimination becomes more or less favorable for other substrates such as threonine (**10f**) or *allo*-threonine (**10g,h**) based substrates, depending on the energy associated with their conformations. This would account for the matched/mismatched effect that is observed, particularly between **10g** and **10h**.

The formation of this double bond conjugated with the phenyl ring explaining the isomerization is in agreement with the single isomer (no isomerization) observed with substrates which can either not form this double bond (**10i**, Table 2, entry 10) or would lead to a non-conjugated double bond (**10j**, Table 2, entry 11).

With a reasonable mechanism to give both stereoisomers at C7, we proposed the next step to be the formation of enantiomeric enolates **4.10a** and **4.10b** from **2.42f** and **4.9**, respectively. An energy of activation of 1.3 kcal/mol and 4.9 kcal/mol was predicted, respectively (Figure 4.10).

Thus, computation confirmed that enolization is possible and that fluoride ion is basic enough in THF for this step to take place.

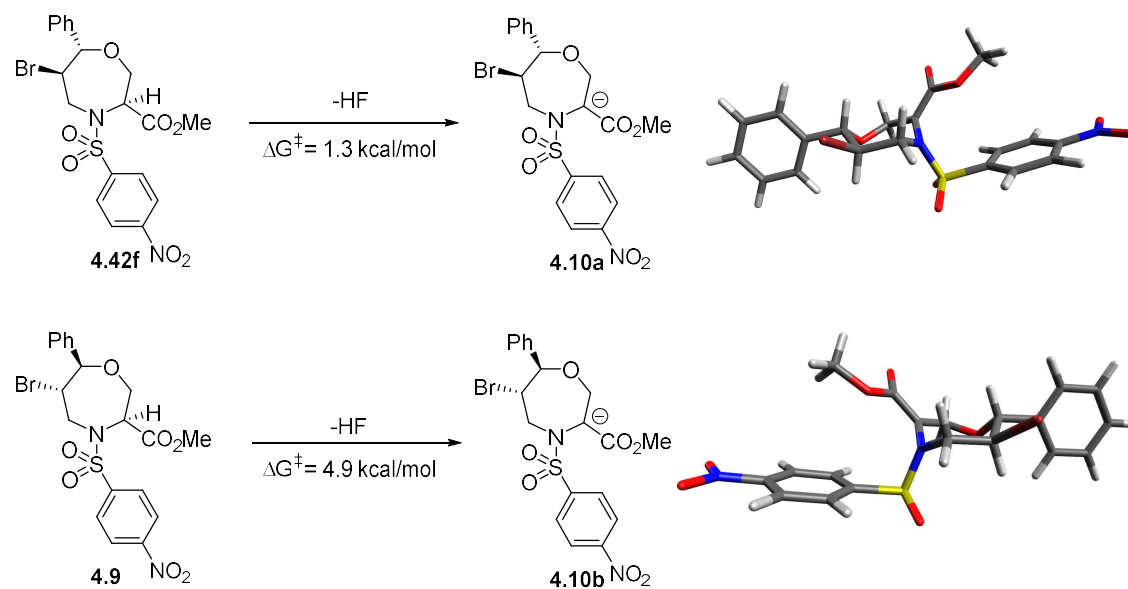


Figure 4.10. Loss of HF to produce the intermediate enolates **4.10a** and **4.10b** from **4.42f** and **4.9**, respectively.

We investigated migration of the *para*-nitrophenyl as the next step in the mechanism. Since the enolates **4.10a** and **4.10b** are enantiomeric, for simplicity, only **4.10a** will be discussed below. The process for **4.10b** is the mirror image and will have identical energies. The formation of **4.11a** from **4.10a** (Figure 4.11) needed to overcome an energy barrier of 10.3 kcal/mol, going through a highly exothermic process. The last step connecting this pathway to the observed products **4.1a** was the loss of SO₂, ring contraction to form the aziridine and displacement of bromide anion. This process has an energy of activation of 12.8 kcal/mol.

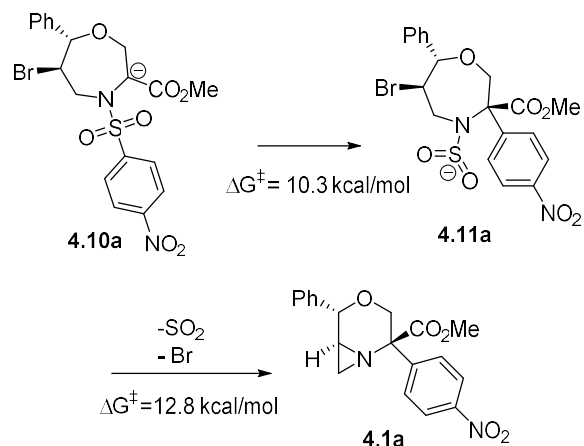


Figure 4.11. Formation of product **4.1a** from enolate **4.10a** (same for **4.1b** from **4.10b**).

Keeping in mind there could be other pathways explaining the formation of **4.1b**, we investigated other possibilities producing this enantiomer. For example, **4.10a** could change conformations, prompting the nosyl on top of the neighboring $-\text{CO}_2\text{Me}$ (**4.10a'**), which would allow the formation of **4.12** after the migration of *para*-nitrophenyl (Figure 4.12). Then, similarly to the process described in Figure 4.7, a cation **4.13''** would form through the epoxidation of **4.12** could lead to the inverted stereochemistry of the phenyl group. However, these structures were not stable: the optimizations led to ring opening or loss of SO_2 and high energies relative to **4.12** (see SI for details). From the data obtained, it was clear that **4.10a**, when formed, can only produce one diastereoisomer with no possible racemization during the course of the reaction. All other attempts to obtain **4.1b** suffered from high energies and unstable structures as well. Therefore, we believe that the ring opening process shown in Figure 4.9 is responsible for formation of product **4.1b**.

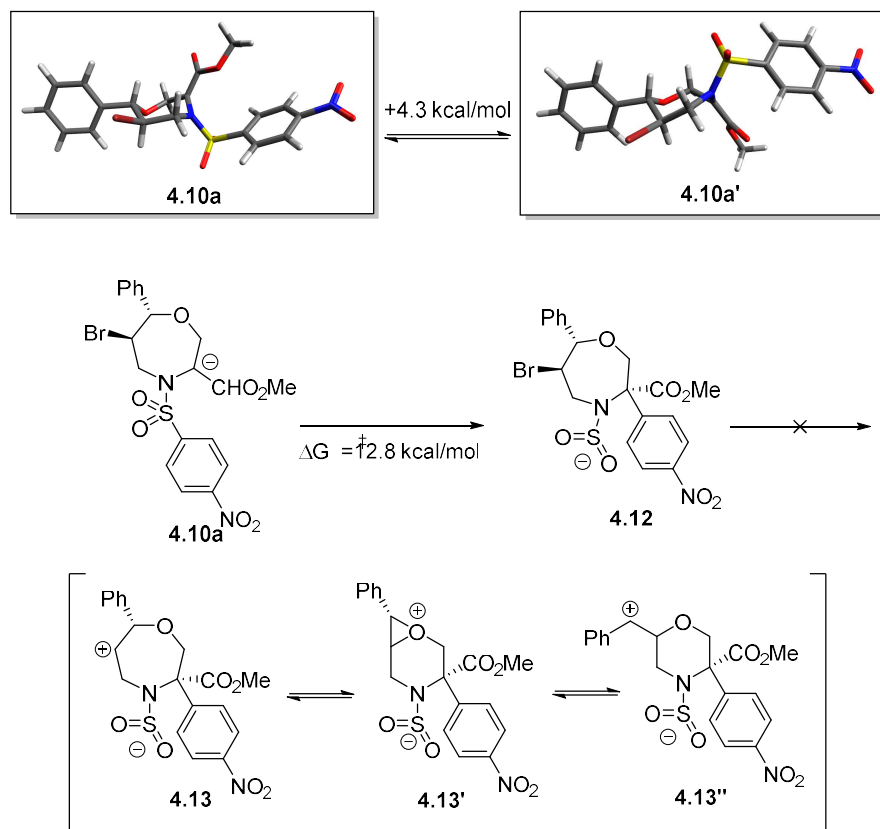


Figure 4.12. Investigation of alternative pathways leading to 4.1b.

Overall, based on the results obtained from the computational study, we propose that the mechanism to form **4.1a** starts with an enolate alkylation followed by a highly stereospecific mechanism leading to **4.1a**. The mechanism of formation of **4.1b**, on the other hand, begins with a conformational change induced by a catalytic amount of HF, followed by an elimination/ring opening step and subsequent ring closure allows inversion of the C6 and C7 substituents, forming **4.9**, a diastereomer of **2.42f**. Compound **4.9** then follows the same mechanism as described above to produce **4.1b**. The entire energy profile relative to **2.42f** for the pathways we describe is shown in Figure 4.13.

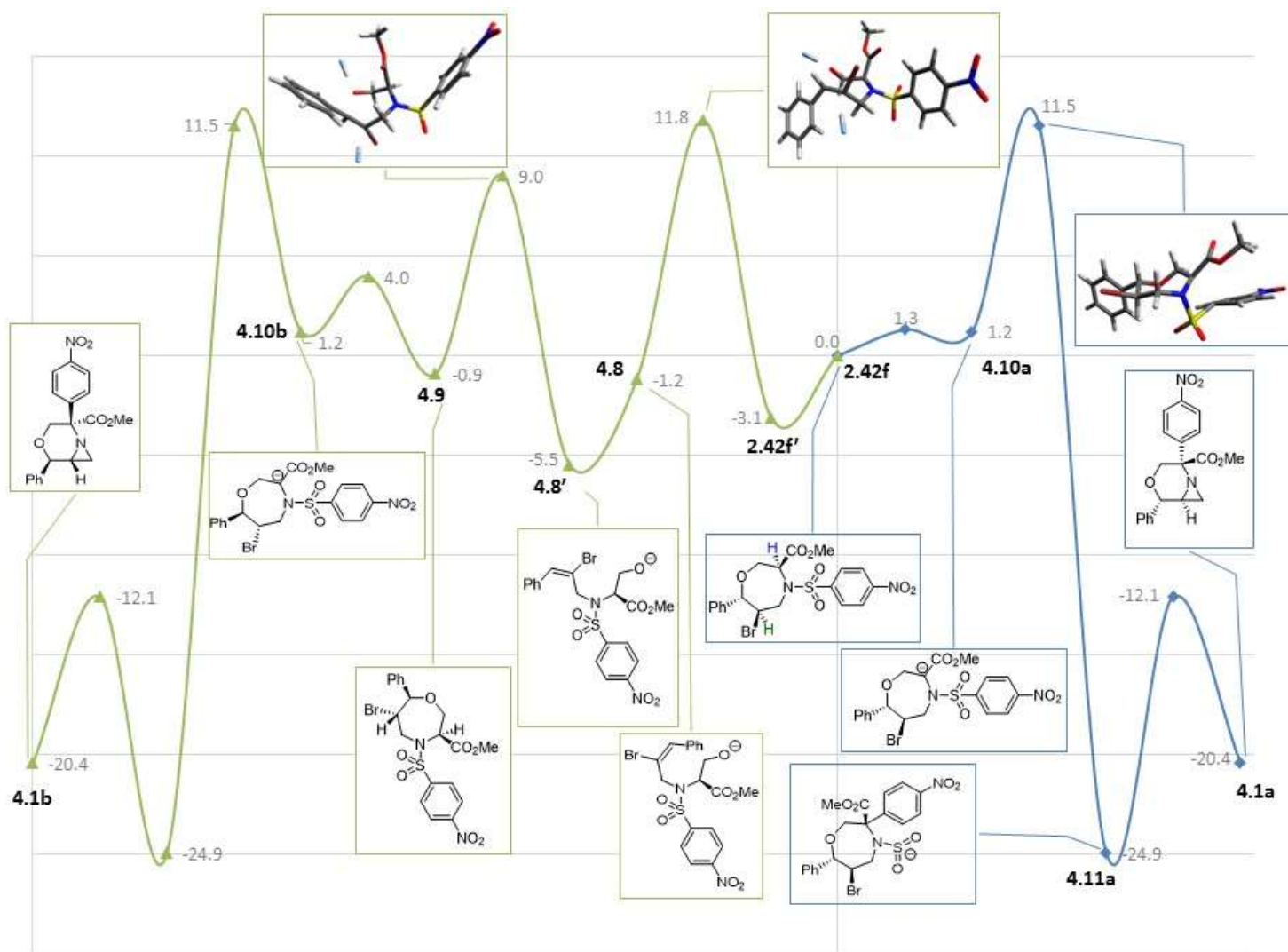


Figure 4.13. Overall energy profile (kcal/mol) for reaction mechanism leading from 2.42f to 4.1a (blue) and to 4.1b (green).

4.4 Conclusion

In summary, we have discovered a mild, environmentally-friendly fluoride-mediated intramolecular rearrangement of 1,4-oxazepanes and morpholines featuring an enolizable proton in C3. This reaction created significant complexity in one step including generating fused (**4.1**, **4.2d,g**) and bridged (**4.2b**) ring systems in good conversions. We have presented a tentative mechanism supported by extensive computational data. We propose that the formation of **4.9**, a diastereomer of **2.42f**, occurs through an olefin intermediate, **4.8**. Subsequent formation of enantiomeric enolates from **2.42f** and **4.9** is followed by migration of *para*-nitrophenyl, loss of SO₂ and ring contraction to give **4.1a** and **4.1b**, respectively. This mechanism is consistent with the experimental observations we have made. At this stage, methods for increasing stereoselectivity are currently under progress in our lab and will be reported in due course.

4.5 Experimental Section

4.5.1 General considerations

All commercially available reagents were used without further purification. All melting points are uncorrected. Chemical shifts (δ) are reported in parts per million (ppm) relative to CDCl₃ (7.26 ppm for ¹H and 77.160 ppm for ¹³C). ¹H and ¹³C NMR spectra were recorded at 400 or 500 and 100 or 125 MHz, respectively, and assignments were confirmed by 2D COSY, HSQC, HMQC and NOESY experiments or by X-ray crystallography. Chromatography was performed on silica gel 60 (230-40 mesh). Visualization was performed by UV or by development using ceric ammonium molybdate, KMnO₄ or ninhydrin stains. Infrared spectra were recorded on an FT-IR spectrometer. HRMS were obtained by ESI-QTOF unless otherwise stated. Optical rotations were measured at the wavelength 589 nm (sodium D line). Compounds **2.42f**, **10b-h** were made according to literature procedure.¹⁵

4.5.2 Experimental Data

General procedure for TBAF-mediated intramolecular rearrangement of oxazepanes and morpholines. **2.42f** (49 mg, 0.10 mmol) was dissolved in THF (4.5 mL). TBAF (1 M in THF, 500 μ L, 0.50 mmol) was added and the mixture immediately turned very dark. The mixture was stirred at rt for 1 - 16 h. The mixture was filtered through a Celite plug and then concentrated under reduced pressure. The crude was purified by column chromatography (7:3 Hexanes:EtOAc) or by semi-preparative HPLC (95:5 H₂O:MeOH to 5:95 H₂O:MeOH, retention time 19.5 min, Zorbax Bonus-RP column) and **4.1** was isolated as a white solid.

Methyl 2-(4-nitrophenyl)-5-phenyl-4-oxa-1-azabicyclo[4.1.0]heptane-2-carboxylate (4.1): White solid; 38 mg isolated (46 % yield, 36 %ee); $[\alpha]^{22}_{\text{D}} = +55.7^{\circ}$ (*c* 1.90, CHCl₃); R_f: 0.16 (7:3 Hexanes:EtOAc); MP 165 - 168 $^{\circ}$ C; IR (film, cm⁻¹) 2998, 2954, 2866, 1730, 1606, 1597, 1519, 1349, 1260, 1062, 856, 751, 740, 699; ¹H NMR (500 MHz, CDCl₃) δ 8.27 (d, *J* = 9.0 Hz, 2H), 7.89 (d, *J* = 9.0 Hz, 2H), 7.37 – 7.25 (m, 6H), 4.83 (d, *J* = 3.2 Hz, 1H), 4.01 (d, *J* = 12.9 Hz, 1H), 3.89 (d, *J* = 12.8 Hz, 1H), 3.80 (s, 3H), 2.68 (dt, *J* = 5.2, 3.5 Hz, 1H), 2.37 (d, *J* = 5.2 Hz, 1H), 2.09 (d, *J* = 3.6 Hz, 1H); ¹³C NMR (125 MHz, CDCl₃) δ 171.3, 148.3, 147.5, 140.6, 128.8, 128.4, 127.5, 126.6, 123.7, 75.1, 64.8, 62.5, 53.2, 35.6, 30.9; HRMS: (M + Na) for C₁₉H₁₈O₅N₂Na calcd 377.1113, found 377.1111.

(1*S*,2*S*,5*R*)-methyl 6-((4-nitrophenyl)sulfonyl)-2-phenyl-3-oxa-6-azabicyclo[3.2.0]heptane-5-carboxylate (4.1c). ¹H NMR (400 MHz, CDCl₃) δ 8.38 (d, *J* = 8.9 Hz, 2H), 8.12 (d, *J* = 8.9 Hz, 2H), 7.40 – 7.28 (m, 5H), 5.21 (s, 1H), 4.62 (d, *J* = 11.1 Hz, 1H), 4.18 – 4.10 (m, 2H), 4.07 (dd, *J* = 7.1, 4.4 Hz, 1H), 3.69 (s, 3H), 3.51 (dd, *J* = 7.2, 4.1 Hz, 1H), 3.36 (m, 6.6 Hz, 1H).

(3*S*,6*R*,7*S*)-methyl 6-iodo-4-((4-nitrophenyl)sulfonyl)-7-phenyl-1,4-oxazepane-3-carboxylate (10a): Colourless oil; 60 mg isolated (46 % yield); $[\alpha]^{22}_{\text{D}} = +8.2^{\circ}$ (*c* 1.20, CHCl₃);

R_f: 0.65 (CH₂Cl₂); IR (film, cm⁻¹) 3105, 3066, 3035, 2955, 2882, 1745, 1530, 1349, 1160, 1094, 1019, 1011, 890, 855, 777, 759, 745, 735, 700; ¹H NMR (400 MHz, CDCl₃) δ 8.40 (d, *J* = 8.9 Hz, 2H), 8.08 (d, *J* = 8.9 Hz, 2H), 7.35 (dd, *J* = 5.2, 1.9 Hz, 3H), 7.28 (d, *J* = 3.1 Hz, 2H), 5.07 (dd, *J* = 10.1, 7.1 Hz, 1H), 4.56 – 4.48 (m, 2H), 4.34 (ddd, *J* = 10.6, 9.9, 3.2 Hz, 2H), 3.75 (ddd, *J* = 17.2, 14.9, 11.4 Hz, 2H), 3.64 (s, 3H); ¹³C NMR (100 MHz, CDCl₃) δ 169.3, 150.2, 145.5, 138.8, 129.0, 128.7, 128.5, 127.4, 124.4, 92.1, 69.4, 59.5, 52.7, 52.1, 32.0; HRMS: (M + Na) for C₁₉H₁₉IN₂O₇SNa calcd: 568.9855, found: 568.9851.

(3*S*,6*S*,7*R*)-methyl 6-iodo-4-((4-nitrophenyl)sulfonyl)-7-phenyl-1,4-oxazepane-3-carboxylate (10a'): White solid; 14 mg isolated (11 % yield); MP 211 - 215 °C; [α]²²_D = - 87.6 ° (*c* 0.43, CH₂Cl₂); R_f: 0.54 (CH₂Cl₂); IR (film, cm⁻¹) 3105, 3066, 3035, 2953, 2871, 1747, 1530, 1349, 1164, 1091, 855, 759, 744, 735, 700, 686; ¹H NMR (500 MHz, CDCl₃) δ 8.39 (d, *J* = 9.0 Hz, 2H), 8.09 (d, *J* = 9.0 Hz, 2H), 7.37 – 7.29 (m, 3H), 7.26 – 7.21 (m, 2H), 4.80 – 4.75 (m, 2H), 4.58 (dd, *J* = 13.5, 2.7 Hz, 1H), 4.46 – 4.40 (m, 1H), 4.32 (dd, *J* = 15.5, 2.6 Hz, 1H), 4.17 (dd, *J* = 13.5, 2.6 Hz, 1H), 3.99 (dd, *J* = 15.3, 7.6 Hz, 1H), 3.73 (s, 3H); ¹³C NMR (125 MHz, CDCl₃) δ 169.6, 150.3, 145.0, 140.3, 129.0, 128.8, 128.6, 126.6, 124.3, 90.1, 69.8, 61.7, 52.9, 52.3, 32.5; HRMS: (M + Na) for C₁₉H₁₉IN₂O₇SNa calcd: 568.9855, found: 568.9848.

(1*R*,3*R*,4*R*)-methyl 1,3-dimethyl-5-((4-nitrophenyl)sulfonyl)-2-oxa-5-azabicyclo[2.2.1]heptane-4-carboxylate (4.2b): Colourless oil; 10 mg isolated (27 % yield); [α]²²_D = -0.96 ° (*c* 0.50, CHCl₃); R_f 0.31 (7:3 Hexanes:EtOAc); IR (film, cm⁻¹) 3107, 2957, 1745, 1529, 1349, 1166, 1144, 1098, 1077, 855, 687; ¹H NMR (400 MHz, CDCl₃) δ 8.35 (d, *J* = 9.0 Hz, 2H), 8.11 (d, *J* = 9.0 Hz, 2H), 4.54 (q, *J* = 6.2 Hz, 1H), 3.84 (s, 3H), 3.59 (dd, *J* = 8.3, 1.5 Hz, 1H), 3.17 (d, *J* = 8.3 Hz, 1H), 2.28 (dd, *J* = 9.9, 1.5 Hz, 1H), 2.14 (d, *J* = 9.9 Hz, 1H), 1.53 (d, *J* = 6.2 Hz, 3H), 1.40 (s, 3H); ¹³C NMR (125 MHz, CDCl₃) δ 199.0, 163.9, 147.6, 130.3, 128.8, 123.1,

122.8, 96.8, 52.3, 28.5, 12.8; HRMS: (M + Na) for C₁₅H₁₈N₂O₇SNa calcd 393.0732 found 393.0730.

4-((4-nitrophenyl)sulfonyl)-7-phenyl-2,3,4,7-tetrahydro-1,4-oxazepine (4.2c): Yellow oil; 6 mg isolated (25 % yield); R_f: 0.65 (7:3 Hexanes:EtOAc); IR (film, cm⁻¹) 3293, 3106, 2928, 2872, 1720, 1529, 1349, 1310, 1166, 1107, 1091, 855, 737; ¹H NMR (500 MHz, CDCl₃) δ 8.41 (d, *J* = 9.0 Hz, 2H), 8.05 (d, *J* = 9.0 Hz, 2H), 7.37 – 7.27 (m, 3H), 7.25 – 7.21 (m, 2H), 6.67 (dd, *J* = 9.8, 2.0 Hz, 1H), 5.18 – 5.15 (m, 1H), 5.12 (dd, *J* = 9.8, 3.2 Hz, 1H), 4.03 – 3.93 (m, 2H), 3.69 (ddd, *J* = 9.6, 7.9, 3.0 Hz, 1H), 3.60 – 3.51 (m, 1H); ¹³C NMR (125 MHz, CDCl₃) δ 150.4, 144.2, 140.4, 128.6, 128.3, 128.2, 126.9, 126.6, 124.6, 116.8, 79.9, 67.0, 51.7; HRMS (APCI): (M + H) for C₁₇H₁₇N₂O₅S calcd: 361.0853, found 361.0848.

(2*S*,3*R*,6*S*)-methyl 3,5,5-trimethyl-2-(4-nitrophenyl)-4-oxa-1-azabicyclo[4.1.0]heptane-2-carboxylate (4.2d): Colourless oil; 42 mg isolated (61 % yield); [α]²²_D = +96.1 ° (*c* 0.84, CHCl₃); R_f: 0.14 (7:3 Hexanes:EtOAc); IR (film, cm⁻¹) 2979, 1732, 1520, 1345, 1256, 1074, 1050, 852, 709; ¹H NMR (400 MHz, CDCl₃) δ 8.22 (d, *J* = 8.9 Hz, 2H), 7.51 (d, *J* = 8.9 Hz, 2H), 3.94 (q, *J* = 6.2 Hz, 1H), 3.81 (s, 3H), 2.54 (dd, *J* = 5.6, 4.4 Hz, 1H), 1.93 (m, 2H), 1.53 (s, 3H), 1.30 (s, 3H), 0.96 (d, *J* = 6.2 Hz, 3H); ¹³C NMR (125 MHz, CDCl₃) δ 171.9, 147.1, 145.6, 129.2, 122.5, 68.4, 66.5, 62.2, 52.9, 41.2, 31.8, 26.8, 25.0, 18.3; HRMS: (M + Na) for C₁₆H₂₀N₂O₅Na calcd: 343.1270, found 343.1264.

(1*S*,2*S*,4*R*,5*R*)-methyl 4-methyl-6-((4-nitrophenyl)sulfonyl)-2-phenyl-3-oxa-6-azabicyclo[3.2.0]heptane-5-carboxylate (4.2fa): Colourless crystalline solid; 1 mg isolated (<1 % yield); [α]²²_D = 18.8 ° (*c* 1.05, CHCl₃); R_f: 0.36 (7:3 Hexanes:EtOAc); MP 175-181 °C; IR (film, cm⁻¹) 2962, 2877, 1740, 1530, 1350, 1275, 1164, 1108, 855, 738; ¹H NMR (400 MHz, CDCl₃) δ 8.39 (d, *J* = 8.9 Hz, 2H), 8.04 (d, *J* = 8.9 Hz, 2H), 7.35 (dd, *J* = 8.0, 6.5 Hz, 2H), 7.29 (d, *J* = 7.2

Hz, 1H), 7.23 (d, $J = 7.6$ Hz, 2H), 5.16 (s, 1H), 4.54 (dd, $J = 8.6, 7.1$ Hz, 1H), 4.36 (q, $J = 6.1$ Hz, 1H), 3.85 (dd, $J = 7.1, 3.7$ Hz, 1H), 3.83 (s, 3H), 3.53 (dd, $J = 8.6, 3.7$ Hz, 1H), 1.37 (d, $J = 6.1$ Hz, 3H); ^{13}C NMR (125 MHz, CDCl_3) δ 168.3, 150.1, 145.7, 139.4, 128.8, 128.3, 128.0, 125.7, 124.3, 84.4, 82.6, 76.2, 54.1, 53.1, 45.1, 14.5; HRMS: (M + Na) for $\text{C}_{20}\text{H}_{20}\text{N}_2\text{O}_7\text{SNa}$ calcd 455.0889, found 455.0886.

Methyl (2*S*,3*R*,5*R*,6*R*)-3-methyl-2-(4-nitrophenyl)-5-phenyl-4-oxa-1-azabicyclo[4.1.0]heptane-2-carboxylate (4.2fb): Colourless oil; 56 mg isolated (14 % yield); R_f 0.19 (7:3 Hexanes:EtOAc); IR (film, cm^{-1}) 2951, 1741, 1521, 1349, 1220; ^1H NMR (400 MHz, CDCl_3) δ 8.18 (d, $J = 9.0$ Hz, 2H), 7.62 (d, $J = 9.0$ Hz, 2H), 7.55 (m, 2H), 7.41 (m, 2H), 7.33 (m, 1H), 5.45 (s, 1H), 3.84 (s, 3H), 3.33 (q, $J = 6.7$ Hz, 1H), 3.00 (dd, $J = 5.2, 4.0$ Hz, 1H), 2.32 (d, $J = 5.2$ Hz, 1H), 2.21 (d, $J = 4.0$ Hz, 1H), 1.27 (d, $J = 6.7$ Hz, 3H); ^{13}C NMR (100 MHz, CDCl_3) δ 170.0, 149.6, 147.1, 139.2, 128.8, 128.2, 128.2, 127.4, 123.2, 72.1, 70.7, 67.8, 52.4, 32.5, 30.0 15.7; HRMS: (M + Na) for $\text{C}_{20}\text{H}_{20}\text{N}_2\text{O}_5\text{Na}$ calcd 391.1270, found 391.1269.

(2*S*,3*R*,5*S*,6*S*)-methyl 3-methyl-2-(4-nitrophenyl)-5-phenyl-4-oxa-1-azabicyclo[4.1.0]heptane-2-carboxylate (4.2fc): Colourless oil; 4 mg isolated (1 % yield); $[\alpha]_D^{22} = +298.8^\circ$ (c 0.85, CHCl_3); R_f 0.15 (7:3 Hexanes:EtOAc); IR (film, cm^{-1}) 2952, 1732, 1606, 1519, 1345, 1254, 1220, 1112, 1065, 1038, 853, 740; ^1H NMR (400 MHz, CDCl_3) δ 8.25 (d, $J = 8.9$ Hz, 2H), 7.58 (d, $J = 8.9$ Hz, 2H), 7.47 – 7.32 (m, 5H), 4.84 (d, $J = 4.7$ Hz, 1H), 3.95 (q, $J = 6.2$ Hz, 1H), 3.87 (s, 3H), 2.76 (td, $J = 4.7, 3.5$ Hz, 1H), 2.25 (d, $J = 5.2$ Hz, 1H), 2.07 (d, $J = 3.5$ Hz, 1H), 1.05 (d, $J = 6.2$ Hz, 3H); ^{13}C NMR (125 MHz, CDCl_3) δ 171.7, 147.2, 145.8, 141.3, 129.1, 128.9, 128.2, 125.8, 122.6, 77.1, 69.2, 65.7, 53.0, 38.0, 30.9, 18.2; HRMS: (M + H) for $\text{C}_{20}\text{H}_{21}\text{N}_2\text{O}_5$ calcd 369.1445, found 369.1454.

Methyl 4-hydroxy-1-((4-nitrophenyl)sulfonyl)-3-phenyl-2-vinylpyrrolidine-2-carboxylate (4.2fd). Characterized as a 1:1 mixture of diastereomers: Yellow oil; 44 mg isolated (11 % yield); R_f 0.56 (7:3 Hexanes/EtOAc); IR (film, cm^{-1}) 2953, 1733, 1605, 1519, 1236, 854, 751, 698; ^1H NMR (500 MHz, CDCl_3) δ 8.20 (d, $J = 8.7$ Hz, 2H), 7.64 (m, 2H), 7.39 – 7.29 (m, 3H), 7.25 – 7.22 (m, 2H), 6.30 (m, 1H), 5.50 – 5.41 (m, 2H), 3.82 (m, 1H), 3.77 (s, 3H), 3.19 – 3.14 (m, 1H), 2.87 (m, 1H), 2.65 (m, 1H); ^{13}C NMR (125 MHz, CDCl_3) δ 172.6, 147.8, 147.3, 136.9, 136.5, 136.5, 128.5, 128.3, 128.2, 128.1, 125.6, 125.6, 123.6, 118.1, 118.0, 69.8, 69.7, 62.1, 62.0, 56.9, 56.7, 52.9, 45.1, 44.8; HRMS: (M + Na) for $\text{C}_{20}\text{H}_{20}\text{N}_2\text{O}_5\text{Na}$ calcd 391.1270, found 391.1274.

(2R,3S,5R,6R)-methyl 3-methyl-2-(4-nitrophenyl)-5-phenyl-4-oxa-1-azabicyclo[4.1.0]heptane-2-carboxylate (4.2g): Colourless oil; 87 mg isolated (69 % yield); $[\alpha]_D^{22} = 53.4^\circ$ (c 4.35, CHCl_3); R_f : 0.16 (7:3 Hexanes:EtOAc); IR (film, cm^{-1}) 2950, 2898, 1739, 1519, 1347, 1239, 1037, 999, 853, 753; ^1H NMR (500 MHz, CDCl_3) δ 8.18 (d, $J = 9.0$ Hz, 2H), 7.62 (d, $J = 9.0$ Hz, 2H), 7.54 (d, $J = 7.4$ Hz, 2H), 7.41 (t, $J = 7.6$ Hz, 2H), 7.33 (t, $J = 7.4$ Hz, 1H), 5.44 (s, 1H), 3.83 (s, 3H), 3.33 (q, $J = 6.7$ Hz, 1H), 2.99 (dd, $J = 5.0, 4.1$ Hz, 1H), 2.31 (d, $J = 5.3$ Hz, 1H), 2.21 (d, $J = 3.9$ Hz, 1H), 1.26 (d, $J = 6.7$ Hz, 3H); ^{13}C NMR (125 MHz, CDCl_3) δ 170.0, 149.6, 147.1, 139.2, 128.8, 128.2, 128.2, 127.4, 123.2, 72.1, 70.7, 67.8, 52.4, 32.5, 30.0, 15.7; HRMS: (M + H) for $\text{C}_{20}\text{H}_{21}\text{N}_2\text{O}_5$ calcd 369.1445, found 369.1451.

(2R,3S,5S,6S)-methyl 3-methyl-2-(4-nitrophenyl)-5-phenyl-4-oxa-1-azabicyclo[4.1.0]heptane-2-carboxylate (4.2hb): $[\alpha]_D^{22} = -12.7^\circ$ (c 0.30, CHCl_3); ^1H NMR (400 MHz, CDCl_3) δ 8.18 (d, $J = 9.0$ Hz, 2H), 7.62 (d, $J = 9.0$ Hz, 2H), 7.55 (m, 2H), 7.41 (m, 2H), 7.33 (m, 1H), 5.45 (s, 1H), 3.84 (s, 3H), 3.33 (q, $J = 6.7$ Hz, 1H), 3.00 (dd, $J = 5.2, 4.0$ Hz, 1H), 2.32 (d, $J = 5.2$ Hz, 1H), 2.21 (d, $J = 4.0$ Hz, 1H), 1.27 (d, $J = 6.7$ Hz, 3H).

Molecular Modeling. All calculations were performed using ORCA 3.0.1²⁰ *ab initio* software. The structures were obtained by B3LYP/def2-SVP and recomputed to get single point energies at the def2-TZVP level. An implicit solvent model COSMO was used to take THF influence into account. The molecular orbitals, frequencies, and structures were visualized using Avogadro²¹ and Iboview.²²

X-Ray Crystallography. Crystal and molecular structures of **4.1** and **4.2fa** were determined by single crystal X-ray diffraction. Diffraction measurements were made on a Bruker D8 APEX2 X-ray diffractometer instrument using graphite-monochromated MoK α ($\lambda = 0.71073 \text{ \AA}$) radiation. The X-ray diffraction data sets were collected using the ω scan mode over the 2θ range up to 54° . The structures were solved by direct methods implemented in SHELXS and refined using SHELXL.²³ Structure refinement was performed on F^2 using all data, and hydrogen atoms were located from the electron difference map whenever data quality was sufficient. Otherwise, hydrogen atoms on carbon centres were modelled with appropriate riding-hydrogen models. Calculations were performed and the drawings were prepared using the WINGX²⁴ suite of crystallographic programs. The compound **4.1** crystalizes in a centrosymmetric space group $P2_1/n$ and is not enantiopure. The compound **4.2fa** crystalizes in an enantiomorphic space group $P2_12_12_1$. The absolute configuration of **4.2fa** was determined from anomalous scattering, with the Flack parameter of 0.04(3). Structures have been deposited with the Cambridge Structural Database, deposition codes 1429192 and 1429193.

Supporting Information Available: Spectroscopic data of all new compounds, chiral HPLC chromatograms, X-ray crystallographic files (CIF), theoretical calculations. The Supporting Information is available free of charge via the Internet at <http://pubs.acs.org>.

4.6 References

- (1) Schreiber, S. L. *Science* **2000**, *287*, 1964.
- (2) Burke, M. D.; Schreiber, S. L. *Angew. Chem. Int. Ed.* **2004**, *43*, 46.
- (3) Padwa, A. *Chem. Soc. Rev.* **2009**, *38*, 3072.
- (4) Shi, M.; Wu, L.; Lu, J. M. *J. Org. Chem.* **2008**, *73*, 8344.
- (5) Yao, L. F.; Wei, Y.; Shi, M. *J. Org. Chem.* **2009**, *74*, 9466.
- (6) Sun, Y. W.; Tang, X. Y.; Shi, M. *Chem. Commun.* **2015**, *51*, 13937.
- (7) Brook, A. G. *Acc. Chem. Res.* **1974**, *7*, 77.
- (8) Meier, H.; Zeller, K.-P. *Angew. Chem. Int. Ed.* **1975**, *14*, 32.
- (9) Sibi, M. P.; Snieckus, V. *J. Org. Chem.* **1983**, *48*, 1935.
- (10) Riggs, J. C.; Singh, K. J.; Yun, M.; Collum, D. B. *J. Am. Chem. Soc.* **2008**, *130*, 13709.
- (11) Ilyin, A.; Kysil, V.; Krasavin, M.; Kurashvili, I.; Ivachtchenko, A. V. *J. Org. Chem.* **2006**, *71*, 9544.
- (12) Kumar, N. N. B.; Kuznetsov, D. M.; Kutateladze, A. G. *Org. Lett.* **2015**, *17*, 438.
- (13) Huot, M.; Moitessier, N. *Tetrahedron Lett.* **2010**, *51*, 2820.
- (14) Moitessier, N.; Henry, C.; Aubert, N.; Chapleur, Y. *Tetrahedron Lett.* **2005**, *46*, 6191.
- (15) Bezanson, M.; Pottel, J.; Bilbeisi, R.; Toumieux, S.; Cueto, M.; Moitessier, N. *J. Org. Chem.* **2013**, *78*, 872.
- (16) Charrier, J.-D.; Hadfield, D. S.; Hitchcock, P. B.; Young, D. W. *Org. Biomol. Chem.* **2004**, *2*, 474.
- (17) Duttagupta, I.; Goswami, K.; Sinha, S. *Tetrahedron* **2012**, *68*, 8347.
- (18) Patonay, T.; Hegedus, L.; Patonay-Peli, E. *J. Heterocyclic Chem.* **1993**, *30*.
- (19) Foschi, F.; Landini, D.; Lupi, V.; Mihali, V.; Penso, M.; Pilati, T.; Tagliabue, A. *Chem. Eur. J.* **2010**, *16*, 10667.
- (20) Neese, F. *WIREs Comput. Mol. Sci.* **2012**, *2*, 73.
- (21) Avogadro: an open-source molecular builder and visualization tool. Version 1.1.1 ed.
- (22) Knizia, G.; Klein, J. E. M. N. *Angew. Chem. Int. Ed.* **2015**, *54*, 5518.
- (23) Sheldrick, G. M. *Acta Crystallogr., Sect. A: Found. Crystallogr.* **2008**, *64*, 112.
- (24) Farrugia, L. *J. Appl. Crystallogr.* **1999**, *32*, 837.

<p style="text-align: center;">Chapter 5 Efforts in the synthesis of cyclic chiral amines for applications in asymmetric organocatalysis</p>

5.1 Preface

Chapter 2 introduced the synthesis of a variety of chiral polysubstituted oxazepanes while Chapter 4 described the rearrangement of these oxazepanes into predominantly 4-oxa-1-azabicyclo[4.1.0]heptanes as the major product, depending on the substrate used. Many of these products were either synthesized in a diastereoselective fashion or the mixture of diastereomers was separated and each diastereomer isolated.

This chapter outlines the examination of some 4-oxa-1-azabicyclo[4.1.0]heptane products directly as catalysts for asymmetric dihydroxylation. The manipulation of sulfonamide protected oxazepanes to make chiral secondary amines as organocatalysts of asymmetric Diels-Alder cycloaddition and aldol reactions as well as manipulations of some 4-oxa-1-azabicyclo[4.1.0]heptanes to make amino alcohols as organocatalysts for asymmetric diethylzinc addition to aldehydes is also presented. Additionally, work on synthesizing carbohydrate-based amino alcohols as organocatalysts for asymmetric diethylzinc addition is presented.

5.2 Introduction

Catalysis has become ubiquitous in chemistry. Of particular importance is asymmetric catalysis, whereby a chiral catalyst directs the formation of a chiral compound such that the formation of one particular stereoisomer is preferred. This preference is a result of a lowered activation energy for one of the diastereomeric transition states to form one enantiomer over another, rendering the energy profile for the formation of enantiomers asymmetric (Figure 5.1).

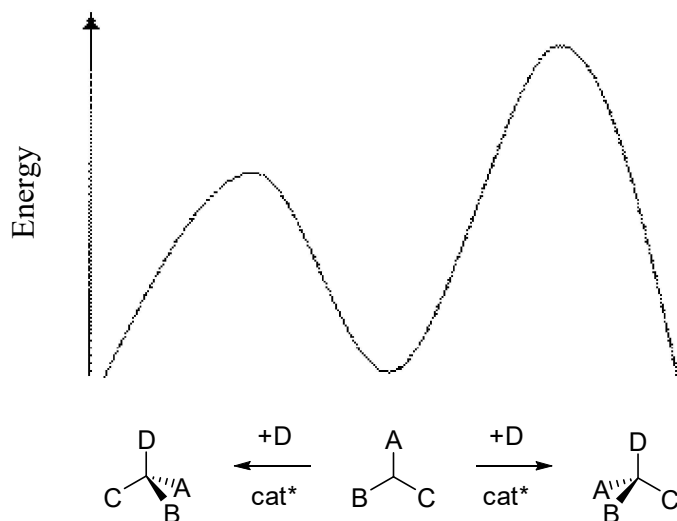


Figure 5.1. Gibbs free energy profile of an asymmetrically catalyzed addition reaction.

Asymmetric catalysis can be divided into three major categories: metal-mediated catalysis, biocatalysis and organocatalysis. The category that this chapter examines is organocatalysis. Asymmetric catalysis is advantageous over historically more common methods of obtaining enantioenriched materials either 1) directly or indirectly from the chiral pool or 2) by resolving a racemic mixture because, unlike the former method, it utilizes sub-stoichiometric amounts of chiral materials, and, unlike the latter method, can furnish yields higher than 50%.¹ Additionally, organic catalysts, relative to transition metal catalysts and biocatalysts, are insensitive to air and moisture, inexpensive, operationally easy to handle, non-toxic and often readily available.

Organocatalysis, a term first coined in 2000 by MacMillan, is the use of small organic molecules to catalyze organic transformations.² While there had previously been several reports of organocatalytic reactions, those manuscripts involved the use of a single catalyst for a single reaction type; none of them identified a general mode of activation. For example, it can be seen in Figure 5.2 a secondary amine operates via iminium catalysis through the same LUMO-activating

mechanism that Lewis acids are known to go through. This iminium catalysis generic mode of activation has been used to catalyze dozens of reactions including Diels-Alder², cyclopropanation³, epoxidation⁴, nitronc cycloaddition⁵ and hydrogenation of enals⁶ and enones⁷ to name a few.

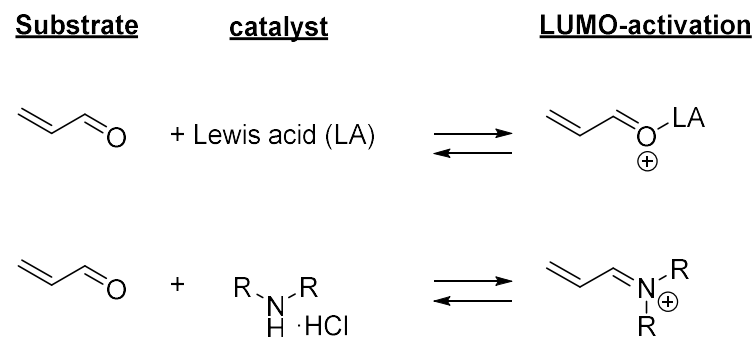
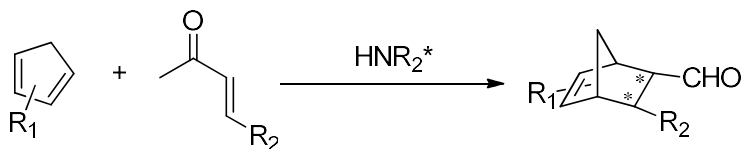


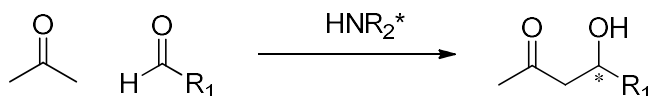
Figure 5.2. LUMO-activation mechanism of α,β -unsaturated carbonyls via Lewis acids or amines.

Organocatalysis has been used to catalyze various different reactions. In the context of this chapter, the specific reactions of interest are highlighted in Figure 5.3. As well as being the reaction of interest in the seminal paper on organocatalysis², Diels-Alder reactions are one of the most common methods for assembling cyclohexyl rings in a stereoselective manner.^{2,8} Aldol reactions, used to make β -hydroxy carbonyls, are one of the most fundamental reactions in the organic chemist toolbox and are often used as a standard reaction for assessing the selectivity of organocatalysts and chiral auxiliaries.⁹ Diels-Alder and aldol reactions are known to be catalyzed by secondary amines operating by an iminium mechanism. Asymmetric dihydroxylation is an important oxidation reaction that earned a Nobel Prize in 2001. Sharpless developed a method using cinchona alkaloids featuring chiral tertiary amines as ligands and employed either *N*-methylmorpholine *N*-oxide (NMO) or potassium ferricyanide to regenerate osmium tetroxide (OsO_4), rendering the reaction catalytic in the toxic and expensive metal.^{10,11} The last reaction of interest is diethylzinc addition to carbonyl compounds, a valuable method for synthesizing optically active secondary alcohols. This reaction is well documented to be catalyzed by chiral amino alcohols.^{12,13}

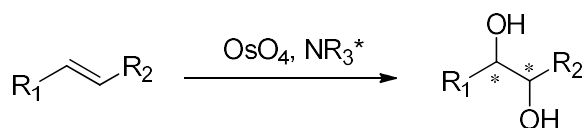
Diels-Alder cycloaddition



Aldol reaction



Asymmetric dihydroxylation



Diethylzinc addition

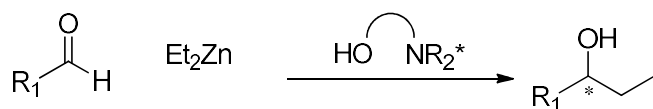


Figure 5.3. Asymmetric reactions catalyzed by chiral amines.

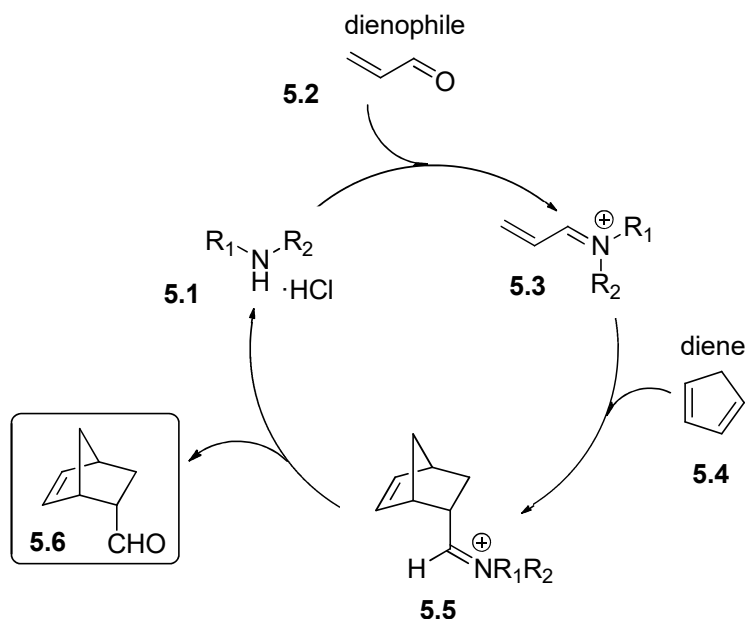
The following chapter highlights our efforts towards developing various chiral amines, specifically secondary amines, tertiary amine and amino alcohols, as asymmetric organocatalysts for the reactions mentioned above. The reactivity and selectivity of those compounds is discussed below.

5.3 Results and Discussion

5.3.1 Development of chiral polysubstituted oxazepane and morpholine secondary amines as organocatalysts for Diels-Alder and aldol reactions

As mentioned in the introduction of this chapter, both Diels-Alder cycloadditions and aldol reactions are known to be catalyzed by chiral secondary amines operating through an iminium catalysis generic mode of action. The mechanism of the organocatalyzed Diels-Alder reaction can be seen in Scheme 5.1. Secondary amine **5.1** condenses onto the dienophile **5.2** to generate

LUMO-lowering iminium ion **5.3** which subsequently reacts with the diene **5.4**, to yield **5.5**. Upon hydrolysis, the Diels-Alder cycloaddition product **5.6** is obtained and the catalyst is regenerated.



Scheme 5.1. Catalytic cycle for Diels-Alder cycloadditions catalyzed by secondary amines operating via an iminium catalysis generic mode of activation.

It is typical that higher selectivities are generally obtained using small ring systems owing to their rigidity offering a well-defined chiral space in which the reaction occurs. In Chapter 2, we discussed the synthesis of several oxazepanes, **2.42**. We reasoned that due to the polysubstitution of these oxazepanes with reasonably large substituents in a stereoselective fashion the natural flexibility of a 7-membered ring would be significantly reduced. In light of this hypothesis, we undertook efforts to remove the sulfonamide protecting group to obtain the secondary free amine (Figure 5.4, **5.8**) and subsequently test it as an organocatalyst in Diels-Alder cycloaddition and aldol reactions.

Additionally, it is known that some of the most efficient organocatalysts for aldol reactions are bifunctional catalysts featuring both a secondary amine and a pendent carboxylic acid to activate and position the substrates together (Figure 5.4, **5.7**). In light of this, it was desirable to install a carboxylic acid at C3 (Figure 5.4, **5.9**) or, analogous to Jørgensen's catalysts, a

diphenyl(trimethylsilyl)oxy moiety onto the carbonyl (Figure 5.4, **5.10**). Efforts into the synthesis of these structures will also be presented herein.

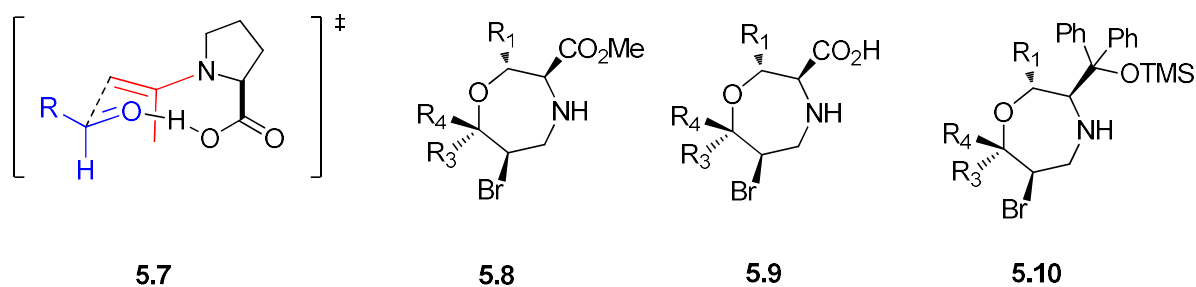
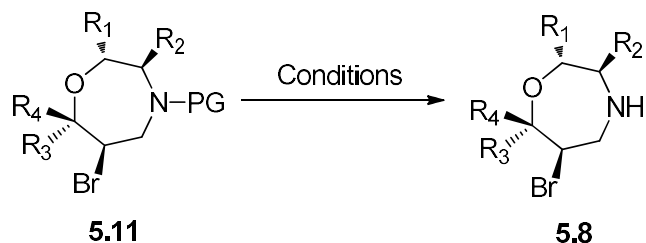


Figure 5.4. Suggested TS for the proline-catalyzed aldol reaction (5.7) and oxazepane-based potential organocatalysts featuring a secondary amine (5.8), an amino acid (5.9) and diphenyl(trimethylsilyl)oxy amine (5.10).

5.3.2 Efforts into removal of sulfonamide protecting groups

The original deprotection strategy was to directly remove the sulfonamide group. However, these efforts were only marginally successful, affording free amines in yields only as high as 65 %. Table 5.1 summarizes the substrates and conditions used for the direct removal.

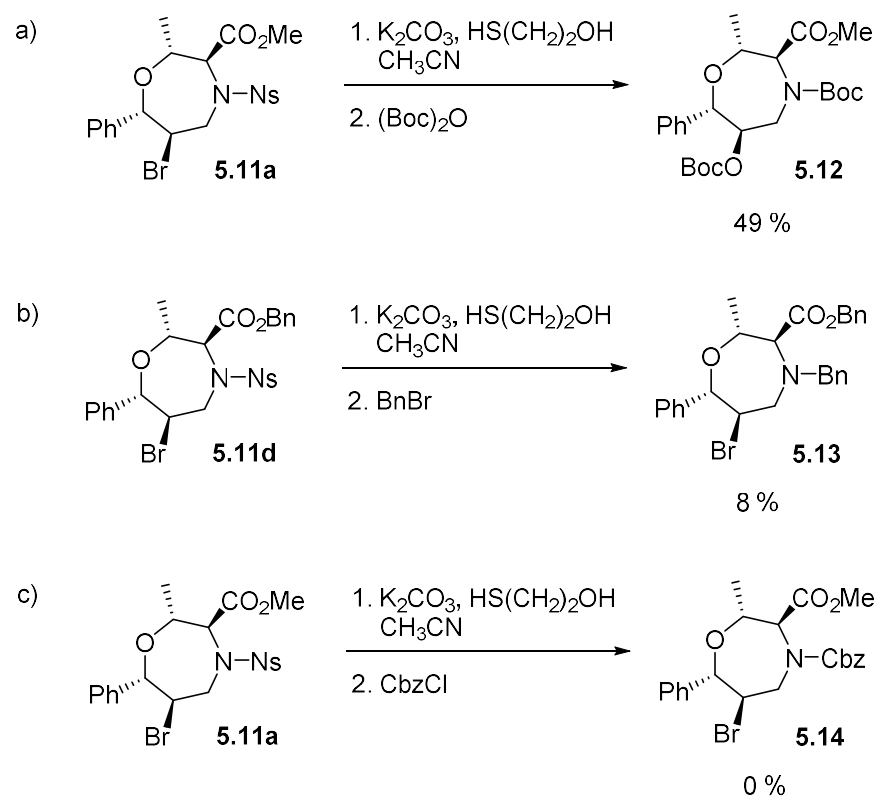
Table 5.1. Efforts to remove sulfonamide protecting group directly.^a

Entry	Starting Material	Base	Thiol	Solvent	Product	Yield
1	 5.11a	K ₂ CO ₃	PhSH	CH ₃ CN	 5.8a	50 %
2		K ₂ CO ₃	HSCH ₂ CO ₂ H	CH ₃ CN		25 %
3		K ₂ CO ₃	HS(CH ₂) ₂ OH	CH ₃ CN		63 %
4		K ₂ CO ₃	HS(CH ₂) ₂ OH	DMF		0 % ^b
5		LiOH	HS(CH ₂) ₂ OH	CH ₃ CN		41 %
6	 5.11b	K ₂ CO ₃	HS(CH ₂) ₂ OH	CH ₃ CN	 5.8b	65 %
7		LiOH	HS(CH ₂) ₂ OH	CH ₃ CN		42 %
8	 5.11c	LiOH	HS(CH ₂) ₂ OH	CH ₃ CN		0 % ^b
9		Sodium naphthalide	HS(CH ₂) ₂ OH	CH ₃ CN		0 % ^c

^a Reaction conditions: substrate (0.04 mmol), base (2 mmol), thiol (2 mmol), 0.1 M in solvent, rt, 6-12 h; ^b Starting material recovered; ^c No starting material or product recovered.

The nosyl protecting group was successfully removed by employing thiols. Thiophenol, thioglycolic acid and β -mercaptoethanol all worked but the latter afforded the product in the highest yields (Table 5.1, entry 1-3). The deprotection did seem to be sensitive to solvent effects as only starting material was recovered when the reaction was run in DMF (Table 5.1, entry 4). The source of base seemed to be unimportant though as LiOH and K_2CO_3 both afforded the product (Table 5.1, entry 3,5). These conditions were only applicable to removing nosyl protecting groups however as efforts to remove tosyl protecting groups were unsuccessful, perhaps because the *ipso* carbon that is less electrophilic and therefore less susceptible to nucleophilic attack by thiol (Table 5.1, entry 8). Alternative conditions to remove the tosyl protecting group using sodium naphthalide were also unfruitful (Table 5.1, entry 9).

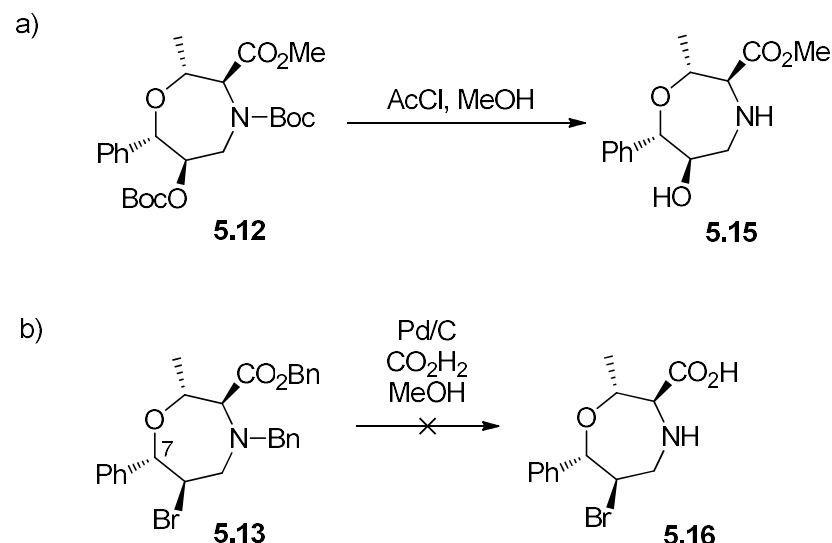
Initial difficulties with conditions optimization and isolation of the amines led us to simultaneously look for alternative conditions to obtain the free amine in hand. As such, we also examined a strategy that included an *in situ* protection with a protecting group that was facile to remove. The results of this strategy are presented in Scheme 5.2.



Scheme 5.2. Efforts to remove sulfonamide protecting groups via a deprotection-protection strategy.

Sulfonamide deprotection followed by *in situ* Boc protection afforded **5.12** in 49 % yield over two steps. Other protecting groups like Bn and Cbz were less successful, with **5.13** being isolated in only 8 % yield and **5.14** not isolated at all. Interestingly, by mass spectrometry and NMR, **5.12** was determined to have had the bromide displaced by an OBoc group with retention of stereochemistry. This phenomenon was not observed under any other deprotection conditions and the mechanism of this displacement is still unclear.

The subsequent deprotection of **5.12** and **5.13** was performed as shown in Scheme 5.3. The Boc-deprotection using methanolic HCl worked well, affording secondary amine **5.15** in quantitative yield (Scheme 5.3a). The Bn-deprotection, in attempt to afford amino acid **5.16**, was less successful, yielding only degraded product by NMR, probably from cleavage of the benzylic C7-O bond (Scheme 5.3b).

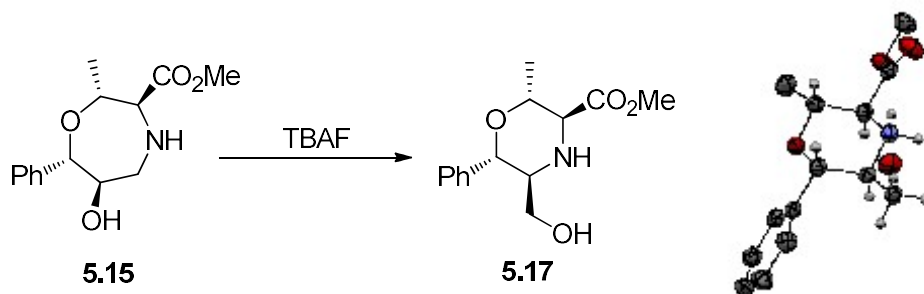


Scheme 5.3. a) Boc-deprotection and b) Bn deprotection attempt.

The strategy to isolate the amine from a precursor that is easier to deprotect proved to be less successful than the direct isolation and when considering that such a strategy inherently contradicts the principles of green chemistry, this methodology was not pursued or optimized.

The rearrangement of oxazepanes and morpholines was discussed extensively in Chapter 4. An interesting and unexpected reaction that was observed during that investigation is shown in Scheme 5.4. **5.15** features no sulfonamide to undergo migration and was expected to be inert under the rearrangement conditions. However, when **5.15** was subjected to TBAF, it underwent ring

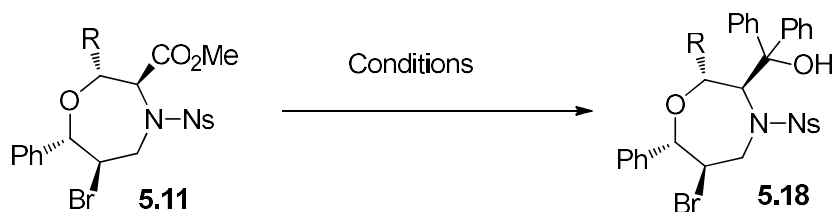
contraction to give **5.17** in 23 % isolated yield. This structure was confirmed by X-ray crystallography. This secondary amine was also tested for catalytic activity and selectivity in Diels-Alder cycloaddition.



Scheme 5.4. Fluoride-mediated rearrangement of **5.15** to morpholine **5.17**.

To synthesize **5.10**, a simple Grignard addition was envisioned to be the easiest method. Attempts to install the diphenyl onto the methyl ester of **5.11a** and **5.11b** are summarized in Table 5.2. Unfortunately, all attempts led to only recovery of the starting material. The use of commercially available Grignard reagent or freshly made Grignard reagent had no impact. This may be because the ester is sterically inaccessible because of the nearby large Ns group.

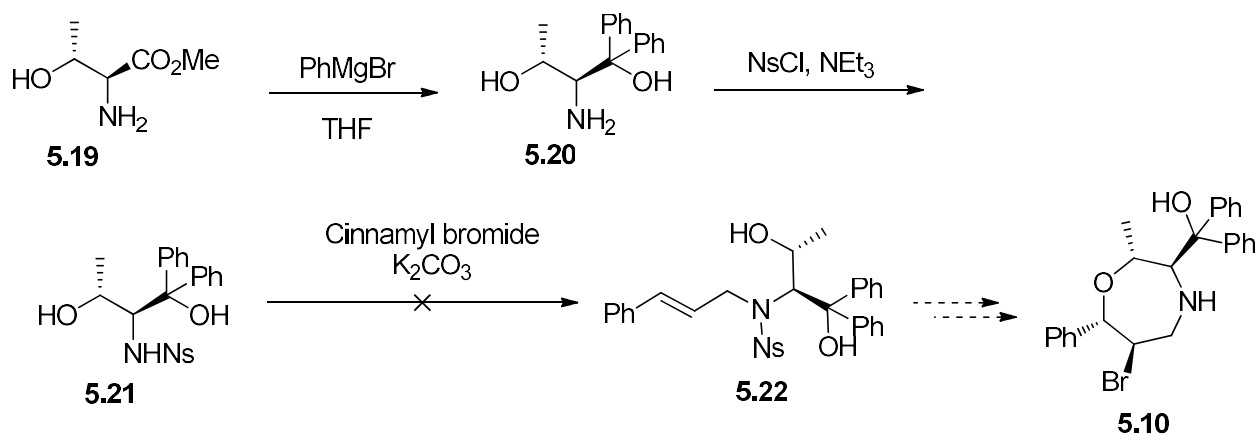
Table 5.2. Attempts to install diphenyl onto methyl ester via Grignard reaction.



Entry	R	Starting Material	Conditions	Yield
1 ^a	Me	5.11a	PhBr, Mg	0 % ^c
2 ^b	Me	5.11a	PhMgBr	0 % ^c
3 ^a	H	5.11b	PhBr, Mg	0 % ^c
4 ^b	H	5.11b	PhMgBr	0 % ^c

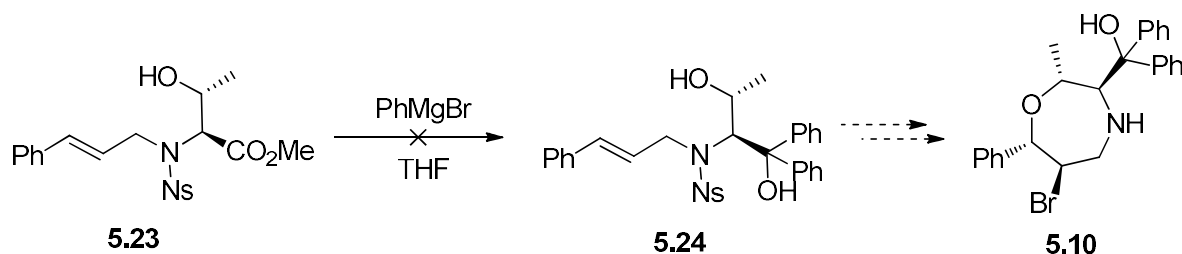
^a Reaction conditions: Substrate (0.4 mmol), PhBr (0.8 mmol), Mg turnings (excess), 0.2 M in ether; ^b Reaction conditions: Substrate (0.2 mmol), PhMgBr (0.8 mmol), 0.2 M in THF; ^c Starting material isolated.

As the late installation of the diphenyl group was unsuccessful, the synthetic route was reworked to introduce the group earlier in the synthesis (Scheme 5.5). The Grignard addition to threonine methyl ester was successful, affording **5.20** in 43 % yield. This was subsequently nosylated to obtain **5.21** in 30 % yield. Unfortunately, all attempts to alkylate **5.21** with cinnamyl bromide were unsuccessful, making this route synthetically unfeasible. This lack of reactivity towards alkylation may potentially be from an intramolecular hydrogen bond between the free tertiary amine and the sulfonamide nitrogen.



Scheme 5.5. Attempt to synthesize **5.10** by introducing diphenyl addition to the synthesis at an early stage.

The last attempt that was made to make **5.10** was to introduce the diphenyl moiety at a point in the middle of the synthesis (Scheme 5.6). **5.23** was subjected to a Grignard reaction however no product was isolated, only starting material was recovered. Similar to when trying to install the diphenyl moiety at a late stage in the synthesis, this reaction may be problematic for steric reasons due to the large Ns nearby.

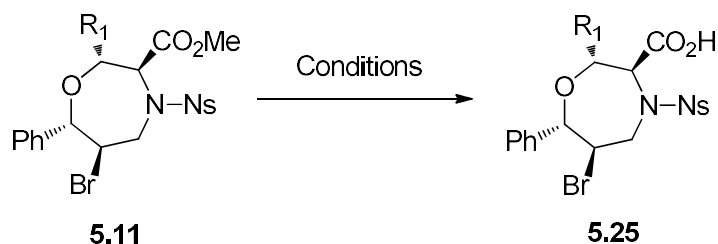


Scheme 5.6. Attempt to synthesize **5.10** by introducing diphenyl addition to the synthesis at a middle stage.

Unfortunately, as all attempts to install the diphenyl moiety had not worked, efforts to synthesize **5.10** were not pursued any further.

Efforts to convert the methyl ester to a carboxylic acid towards the synthesis of **5.9** were more successful. Regular saponification conditions with aqueous base had no effect, yielding only recovered starting material. Thankfully, treatment with lithium iodide in ethyl acetate (Table 5.3, entry 4) successfully afforded carboxylic acid **5.25a** in 76 % yield.

Table 5.3. Ester hydrolysis.

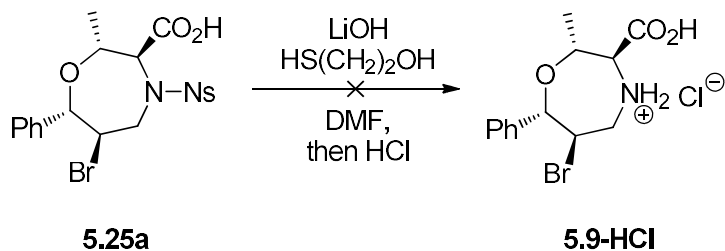


Entry	R ₁	Starting Material	Conditions	Product	Yield
1 ^a	Me	5.11a	NaOH, THF/H ₂ O	5.25a	0 %
2 ^a	Me	5.11a	NaOH, MeOH	5.25a	0 %
3 ^a	H	5.11b	NaOH, THF/H ₂ O	5.25b	0 %
4 ^b	Me	5.11a	LiI, Pyr, EtOAc	5.25a	76 %

^a Reaction conditions: Substrate (0.2 mmol), NaOH (2 mmol), 0.1 M, reflux; ^b Reaction conditions: Substrate (0.2 mmol), LiI (1 mmol), 0.2 M, reflux.

With **5.25a** in hand, removal of the sulfonamide protecting group was attempted. Upon treatment with base and thiol to remove the sulfonamide and then subsequent treatment with

hydrochloric acid to try to crash **5.9-HCl** out of the organic solvent, no solid was collected (Scheme 5.7). NMR of the crude mixture was very messy and appeared as though the reaction had perhaps not gone. However, purification by column chromatography yielded a thiol-nosyl adduct, indicating that the deprotection reaction had proceeded. Unfortunately, no amino acid was isolated as it was very likely lost on the column.



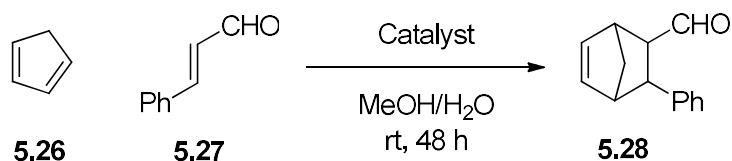
Scheme 5.7. Attempt to remove sulfonamide protecting group and isolate 5.9-HCl.

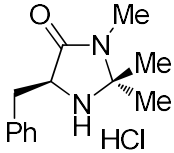
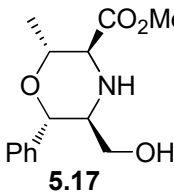
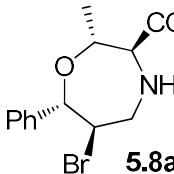
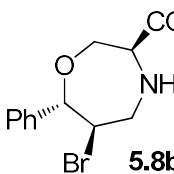
Unfortunately, efforts to synthesize **5.9** and **5.10** were unsuccessful. However, our efforts to deprotect the sulfonamide group to the secondary amine were happily more fruitful. With **5.8a**, **5.8b** and **5.17** in hand, the catalytic activity and selectivity of those compounds was tested. The conditions optimization and preliminary results of these compounds as organocatalysts in Diels-Alder cycloaddition and aldol reactions are described below.

5.3.3 Diels-Alder catalysis

We tested oxazepane and morpholine compounds **5.8a**, **5.8b** and **5.17** for their catalytic ability in Diels-Alder cycloaddition. The results of this as well as literature results of (*L*)-proline (Table 5.4, entry 1) and MacMillan's catalyst (Table 5.4, entry 2) are presented in Table 5.4. Morpholine-based **5.17** afforded the cycloaddition product in low yield (Table 5.4, entry 4). This entry is very promising and as it is currently unoptimized, after some condition optimization such as perhaps an increased catalyst loading, this yield may be increased markedly. The selectivity of this reaction was not determined at the time due to the poor yield but the rigidity of the polysubstituted morpholine indicates that it has potential to be a selective catalyst and this will be examined more closely in the future. Unfortunately, both oxazepane-based secondary amines **5.8a** and **5.8b**, yielded only starting material (Table 5.4, entry 5,6). This may be caused by the amine and the aldehyde failing to form the iminium ion required for the organocatalysis to occur, perhaps due to the presence of water influencing the equilibrium towards hydrolysis of the iminium.

Table 5.4. Organocatalyzed Diels-Alder reaction condition screen.



Entry	Catalyst (mol %)	(mol %)	Solvent	Yield ^a	<i>exo</i> : <i>endo</i> ^b	<i>exo</i> %ee
1 ²	(<i>L</i>)-Pro-OMe-HCl	(10)	MeOH/H ₂ O	81 %	2.7 : 1	48 (<i>2R</i>)
2 ²		(5)	MeOH/H ₂ O	99 %	1.3 : 2	93 (<i>2S</i>)
3	None		MeOH/H ₂ O	0 % ^d	-	-
4		(10)	MeOH/H ₂ O	15 %	1 : 1.2	nd ^c
5		(10)	MeOH/H ₂ O	0 % ^d	-	-
6		(10)	MeOH/H ₂ O	0 % ^d	-	-

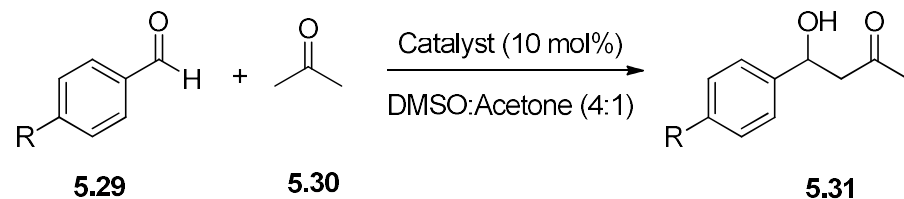
^a Isolated yields; ^b Determined by NMR; ^c nd = not determined; ^d Starting material recovered.

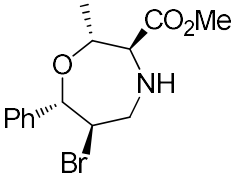
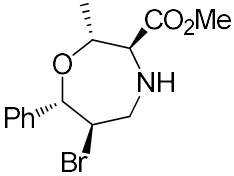
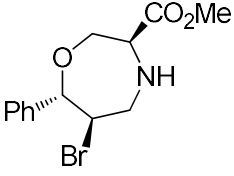
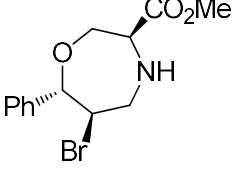
5.3.4 Aldol catalysis

Despite previous reports of various secondary amines, proline among them, catalyzing aldol reactions effectively¹⁴, attempts to use oxazepane-based secondary amines to catalyze aldol reactions were ineffective (Table 5.5). This likely indicates that, similar to attempts to catalyze Diels-Alder cycloaddition with the same compounds, conditions were unfavourable to form the

iminium. The conditions for this reaction are unoptimized and need to be examined more thoroughly.

Table 5.5. Preliminary attempts of using 5.8a,b as organocatalysts for aldol reactions.^a



Entry	R	Catalyst (mol %)	Yield	% ee
1 ¹⁴	H	(<i>L</i>)-Pro	62 %	60
2 ¹⁴	NO ₂	(<i>L</i>)-Pro	68 %	76
3	H	None	0 % ^b	-
4	NO ₂	None	0 % ^b	-
5	H		0 % ^b	-
6	NO ₂		0 % ^b	-
7	H		0 % ^b	-
8	NO ₂		0 % ^b	-

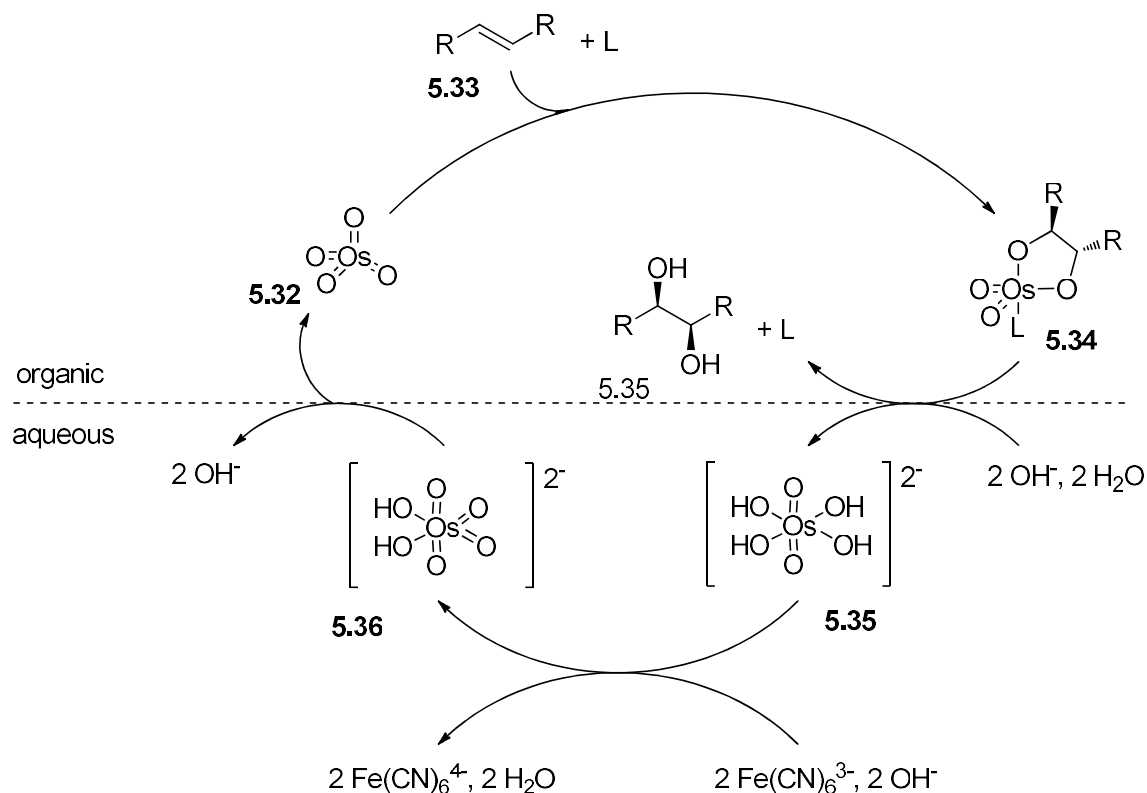
^a Reaction conditions: aryl aldehyde (1 eq), acetone (5 eq), catalyst (0.1 eq), DMSO (20 eq), rt, 12-72 h; ^b Starting material recovered.

5.3.5 Chiral tertiary amines as ligands for catalytic asymmetric dihydroxylation

Asymmetric dihydroxylation is a powerful reaction that oxidizes olefins into chiral diols. The reaction has proved to be extremely useful in the synthesis of pharmaceuticals, agrochemicals and other fine chemicals. As such, Sharpless was recognized for the importance of his work by being awarded the Nobel Prize in Chemistry in 2001 “for his work on chirally catalyzed oxidation reactions” which included his contributions to asymmetric dihydroxylations, epoxidations and oxyaminations.¹⁵

Asymmetric dihydroxylation was first reported by Hentges and Sharpless in 1980 when they discovered that using chiral pyridines as ligands for OsO_4 in the dihydroxylation of olefins afforded enantiomerically enriched *vicinal*-diols.¹⁶ Since then, it has been realized that tertiary amines form considerably stronger complexes with OsO_4 ^{17,18} and tertiary amine containing cinchona alkaloids have been discovered to be a particularly good class of ligands, often yielding stereoselectivities greater than 90 %ee.¹⁰

The mechanism of asymmetric dihydroxylation when employing $\text{K}_3\text{Fe}(\text{CN})_6$ as the co-oxidant is shown in Scheme 5.8. In this heterogeneous reaction, OsO_4 complexed to the chiral ligand is the only oxidant in the organic phase as the inorganic co-oxidant is insoluble in the organic layer. The complexation of OsO_4 with tertiary amines significantly increases its reactivity making this reaction suitable to catalysis. Oxidation of the osmium glycolate cannot occur because the co-oxidant is insoluble in the organic layer and rather, hydrolysis of the glycolate must occur to yield the chiral diol product in the organic phase and water-soluble $\text{Os}(\text{VI})$. The $\text{Os}(\text{VI})$ is then re-oxidized in the aqueous phase by the co-oxidant to $\text{Os}(\text{VIII})$ to complete the catalytic cycle.



Scheme 5.8. Catalytic cycle of asymmetric dihydroxylation with K₃Fe(CN)₆ as the co-oxidant.

The compounds of interest for use as catalysts in asymmetric dihydroxylation were some of the 4-oxa-1-azabicyclo[4.1.0]heptanes presented in Chapter 4 as they featured tertiary amines (Figure 5.5). It was hypothesized that they may strongly coordinate to the osmium metal center due to the strained ring system resulting in a distorted amine. This distortion would possibly render the lone pairs of the amine more sterically available than those of the tertiary amines of cinchona alkaloids, perhaps leading to an increased rate of catalysis or higher selectivity.

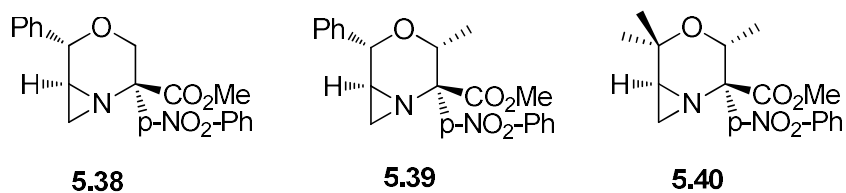
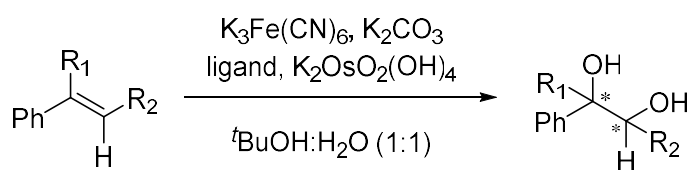


Figure 5.5. 4-oxa-1-azabicyclo[4.1.0]heptane scaffolds of interest as tertiary amine organocatalysts in the asymmetric dihydroxylation reaction.

Unfortunately, as can be seen in Table 5.6, none of the compounds tested showed any catalytic selectivity, yielding racemates for all the substrates tested. This may be because the

tertiary aziridine did not coordinate to the osmium center, as aziridines are less basic than other alkyl amines due to the increased *s*-character of the orbital the lone pair occupies. This poor coordination would there was no chiral pocket available to induce asymmetry. Alternatively, perhaps the chiral pocket of the ligated osmium complex was not well defined and so no stereinduction occurred. It is difficult to definitely say that no catalysis took place as there was an increased yield relative to the control reactions that had no ligand present, markedly so when **5.41c** was used as a substrate.

Table 5.6. Asymmetric dihydroxylation.



5.41

5.42a-c

5.41a: R₁ = H, R₂ = Ph

5.41b: R₁ = H, R₂ = H

5.41c: R₁ = Me, R₂ = H

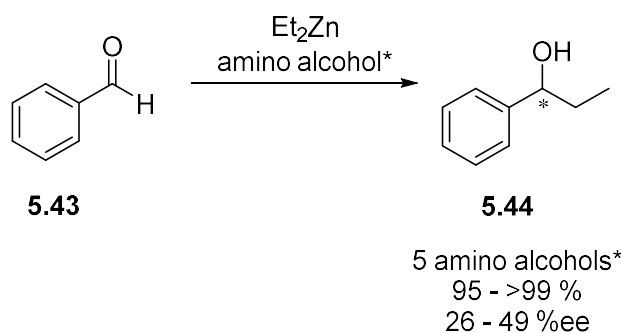
Entry	Substrate	Ligand	Yield (%)	% ee	Entry	Substrate	Ligand	Yield (%)	% ee
1 ^{b,c}	5.41a	AD-mix- α	99	>99.5 (<i>R,R</i>)	10 ^b	5.41a	4.38	27	0
2 ^{b,c}	5.41a	AD-mix- β	95	>99.5 (<i>S,S</i>)	11	5.41a	4.38	75	0
3 ^c	5.41b	AD-mix- α	78	97 (<i>S</i>)	13 ^b	5.41a	4.40	12	0
4 ^c	5.41b	AD-mix- β	70	97 (<i>R</i>)	14	5.41b	4.39	>99	0
5 ^c	5.41c	AD-mix- α	> 99	93 (<i>S</i>)	15 ^b	5.41b	4.39	34	0
6 ^c	5.41c	AD-mix- β	> 99	94 (<i>R</i>)	16	5.41b	4.40	67	0
7 ^b	5.41a	None	7	0	17	5.41c	4.38	60	0

8	5.41b	None	35	0	18	5.41c	4.39	>99	0
9	5.41c	None	11	0	19	5.41c	4.40	>99	0

^a Reaction conditions: Olefin (1 mmol), Ligand (0.01 mmol), K₂OsO₂(OH)₄ (0.002 mmol), K₂CO₃ (3 mmol), K₃Fe(CN)₆ (3 mmol), 0.1 M (1:1 v/v ^tBuOH:H₂O), 0 °C, 24 h; ^b MeSO₂NH₂ (1 mmol) was also added; ^c Literature values¹⁹

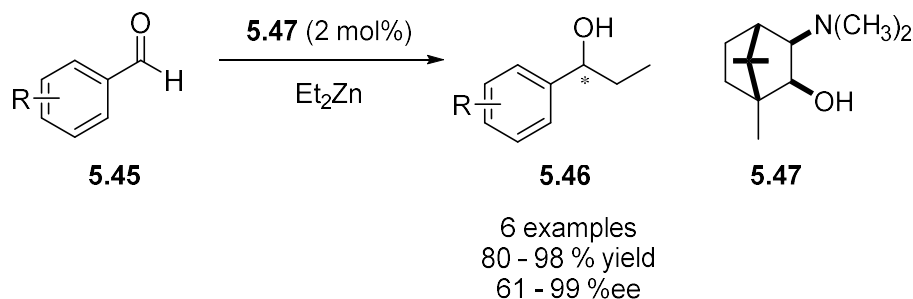
5.3.6 Chiral bicyclic aziridinols as organocatalysts for diethylzinc addition to benzaldehyde

Diethylzinc addition to benzaldehyde was first reported in 1984 in a report from Oguni and Omi.²⁰ They showed that chiral amino alcohols catalyzed the asymmetric addition of diethylzinc to benzaldehyde in up to 49 %ee (Scheme 5.9). Most of the amines tested were primary amines and one secondary amine, (*S*)-prolinol, and of those tested, (*S*)-leucinol gave the best results.



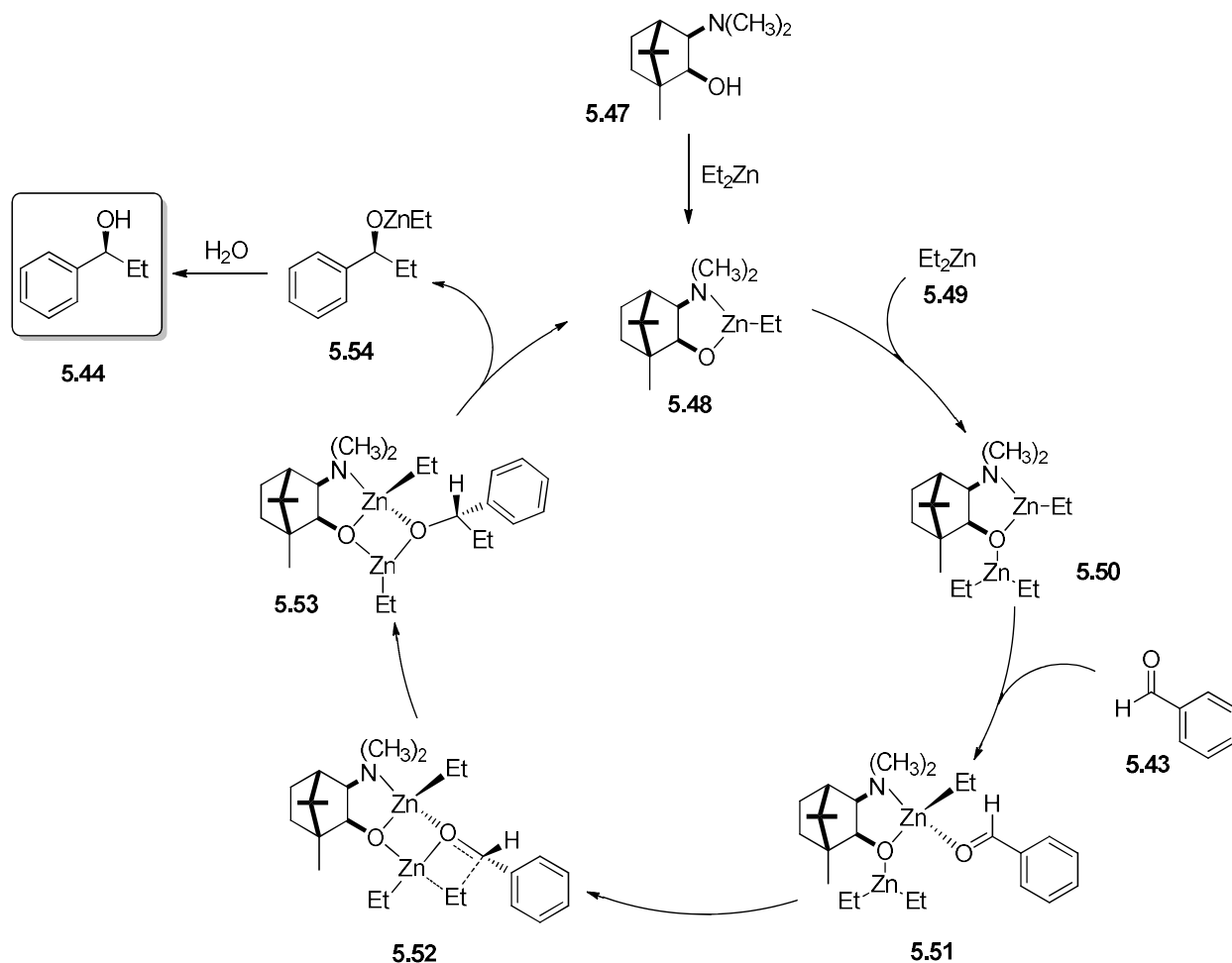
Scheme 5.9. Amino alcohol organocatalyzed diethylzinc addition to benzaldehyde.

It was discovered in 1986 by Noyori and coworkers that tertiary amines were more efficient at catalyzing diethylzinc addition to aryl aldehydes.²¹ They employed (-)-3-*exo*-(dimethylamino)isoborneol (DAIB, **5.47**) as a chiral catalyst and obtained >90 %ee for alkyl addition to a variety of aryl aldehydes (Scheme 5.10). This report also noted that the ratio of dialkylzinc reagent to amino alcohol had to be at least 2:1, indicating that two zinc species per aldehyde were required for the alkylation.



Scheme 5.10. DAIB-catalyzed diethylzinc addition to aryl aldehydes.

Studies have shown that coordination of a ligand to dialkylzinc changes the geometry at the metal center from linear to tetrahedral, thereby reducing the bond order of the Zn-C bond and increasing the nucleophilicity of the zinc alkyl groups.²² The generally accepted mechanism of dialkylzinc addition to aldehydes is shown in Scheme 5.11. First, amino alcohol **5.47** reacts with one equivalent of dialkyl zinc (**5.49**) to generate **5.48**, a species that is not itself reactive towards benzaldehyde. This *in situ* generated zinc complex goes on to coordinate both another equivalent of dialkylzinc and aldehyde, acting as Lewis base to activate the dialkylzinc reagent, a Lewis acid to activate the carbonyl, and additionally positions the reagents close together in space, thereby accelerating the reaction. *Anti*-addition of the aldehyde relative to the ligand leads to a 5,4,4-tricyclic transition state structure (**5.52**).^{23,24} Subsequent migration of the alkyl group to the *si* face of the aldehyde affords **5.53** which give chiral alcohol **5.44** upon aqueous workup.



Scheme 5.11. Catalytic cycle diethylzinc addition to benzaldehyde as catalyzed by DAIB (applies generally to amino alcohols).

Diethylzinc addition to aldehydes also exhibits the interesting property of asymmetric amplification, a phenomenon whereby the enantiomeric excess of the product is higher than that of the catalyst used in the synthesis. This non-linear effect (NLE) was first observed by Oguni and coworkers²⁵ and also later by Noyori, who showed that using DAIB in as low as 15 %ee yielded ethylated product in 95 %ee.²⁶ This is suggested to arise from the formation of dimers of zinc-complex (Figure 5.6). Both the heterodimer (5.55) and the homodimer (5.56) can form, however the heterodimer is more stable than the homodimer (ca. 3.4 kJ/mol). This means that the homodimer will dissociate much more easily while the minor enantiomer of the mixture will be unavailable as it participates in the stable heterodimer, thereby leading to asymmetric amplification.

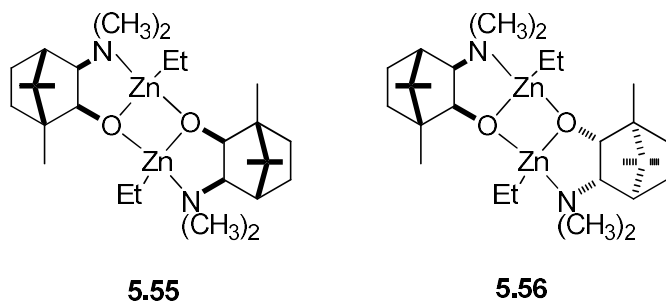
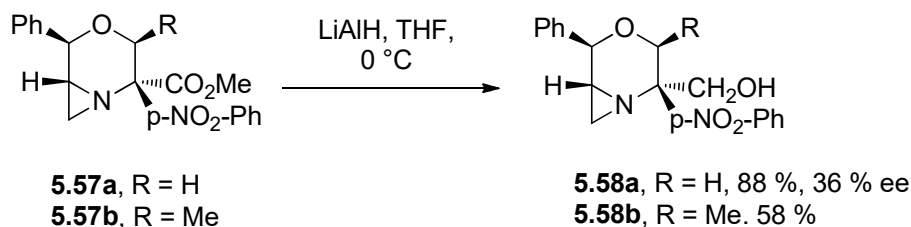


Figure 5.6. Heterodimer (5.55) and homodimer (5.56).

5.3.7 Synthesis of amine alcohols

As discussed in Chapter 4, a series of 4-oxa-1-azabicyclo[4.1.0]heptane scaffolds were obtained from the rearrangement of 1,4-oxazepanes. These 4-oxa-1-azabicyclo[4.1.0]heptanes featured a tertiary amine and a methyl ester beta to the amine. Reduction of the ester to an alcohol would afford beta amino alcohols, a motif that is well known to catalyze diethylzinc addition to carbonyl compounds. It can be seen in Scheme 5.12 that reduction of the methyl ester using LiAlH₄ proceeded smoothly to afford **5.58a** and **5.58b** in 88 % and 58 % yield respectively.



Scheme 5.12. Ester reduction.

5.3.8 Diethylzinc addition catalysis

With **5.58a,b** in hand we tested their catalytic ability in the addition of diethylzinc to benzaldehyde. The results are presented in Table 5.7. While the amino alcohols do catalyze the reaction in low to moderate yields, there seems to be either a conservation of enantioselectivity observed or even a slight negative NLE.

Table 5.7. Organocatalyzed diethylzinc addition to benzaldehyde using 5.58a,b.^a

Entry	Amino alcohol	Yield ^b	% ee ^c
1	None	0 %	-
2 ²⁰	Leucinol	96 %	49
3	<p style="text-align: center;">5.58a</p>	25 %	33
4	<p style="text-align: center;">5.58b</p>	78 %	5

^a Reaction conditions: **5.62** (1 mmol), toluene (dry and degassed, 2 mL), **5.58** (0.20 mmol), diethylzinc (1 M solution in hexanes, 2 mL), 0 °C, 24 h; ^b Isolated yields; ^c Measured by optical rotation.

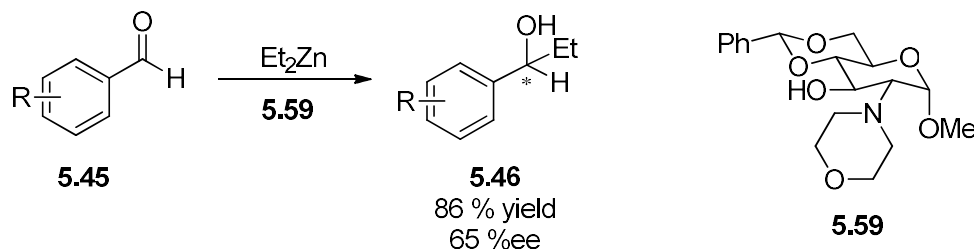
5.3.9 Carbohydrate-based amino alcohols as organocatalysts for diethylzinc addition to benzaldehyde

For reasons described above, diethylzinc addition to benzaldehyde is obviously an interesting reaction. This chapter discusses efforts to synthesize carbohydrate based amino alcohols for the purpose of catalyzing this reaction.

5.3.10 Asymmetric Catalyst Evaluation (ACE)

Utilization of computational chemistry has started to become more mainstream in the synthetic organic chemistry world. It has proved particularly useful in the field of pharmaceutical chemistry where it is often used to dock small molecule libraries into macromolecular structures such as proteins.²⁷ However in synthetic chemistry, it is still mostly used to explain results *post facto* rather than in a predictive manner as with computer-aided drug design.

Reports of carbohydrate-based compounds being used to catalyze the addition of dialkylzinc to aldehydes in the literature is very rare. In fact, to the best of our knowledge, the only report was in 2003 from Davis and coworkers.²⁸ Unfortunately, despite testing 25 different carbohydrate-based catalysts, the best enantioselectivity they obtained was 65 %ee using glucosamine derivative **5.59** (Scheme 5.13).



Scheme 5.13. Organocatalyzed diethylzinc addition to benzaldehyde using carbohydrate-based amino alcohol 5.59.

Using carbohydrates as catalysts has several benefits including that they are inexpensive, readily available, enantiopure and available as both pseudo-enantiomers. (Figure 5.7). However, they also have the drawback in that there are many different carbohydrates available and identifying which stereochemistry and subsequently which substituents on a specific carbohydrate would be a selective catalyst based on chemical intuition alone is impossible. Synthesizing many different carbohydrate compounds to then test as catalysts would be incredibly time consuming and expensive. In light of this, we were interested in a computational tool that could be used in a predictive fashion to evaluate the stereoselectivity of a catalyst *in silico*.

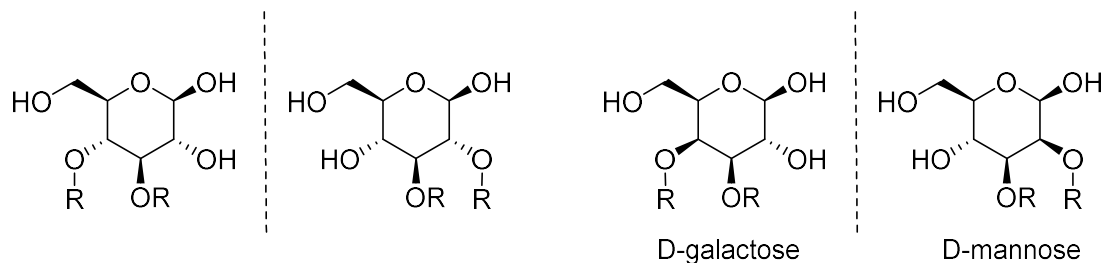


Figure 5.7. Pseudo-enantiomeric structures of carbohydrates.

In 2008, our group published a report on ACE (Aymmetric Catalyst Evaluation), a molecular-mechanics-based (MM) program that constructs transition states (TSs) from a linear combination of reactants and products and includes a factor, λ , which uses chemical principles described by the

Hammond-Leffler postulate (“the TS looks most like the species it is closest to in energy”) to describe the position of the TS on the potential-energy surface (PES).^{29,30} Our group validated the program by examining several organocatalysts and chiral auxiliaries in Diels-Alder cycloadditions, proline-catalyzed aldol reactions and asymmetric epoxidation reactions and found that in the majority of cases, they predicted the correct stereoisomer as obtained experimentally and with acceptable accuracy compared to DFT-derived results when comparing the CPU-time required.

We envisioned using this program to screen a library of carbohydrate-based amino alcohols, choosing a compound that is predicted to be a selective catalyst to synthesize in the lab, testing the catalytic ability of that compound and using the results to update the program to improve its predictive ability. To ensure the program is indeed predictive, we would also choose a compound that is predicted to not be selective to synthesize and test. A preliminary screen yielded the compounds shown in Figure 5.8. Mannose-derived **5.60** was predicted to catalyze diethylzinc addition to benzaldehyde with good selectivity while glucose-derived **5.61** was predicted to catalyze the same reaction with relatively poor selectivity. Efforts to synthesize these compounds are highlighted below. Unfortunately, all attempts were ultimately unsuccessful and the use of these compounds as catalysts in diethylzinc addition to benzaldehyde was never tested.

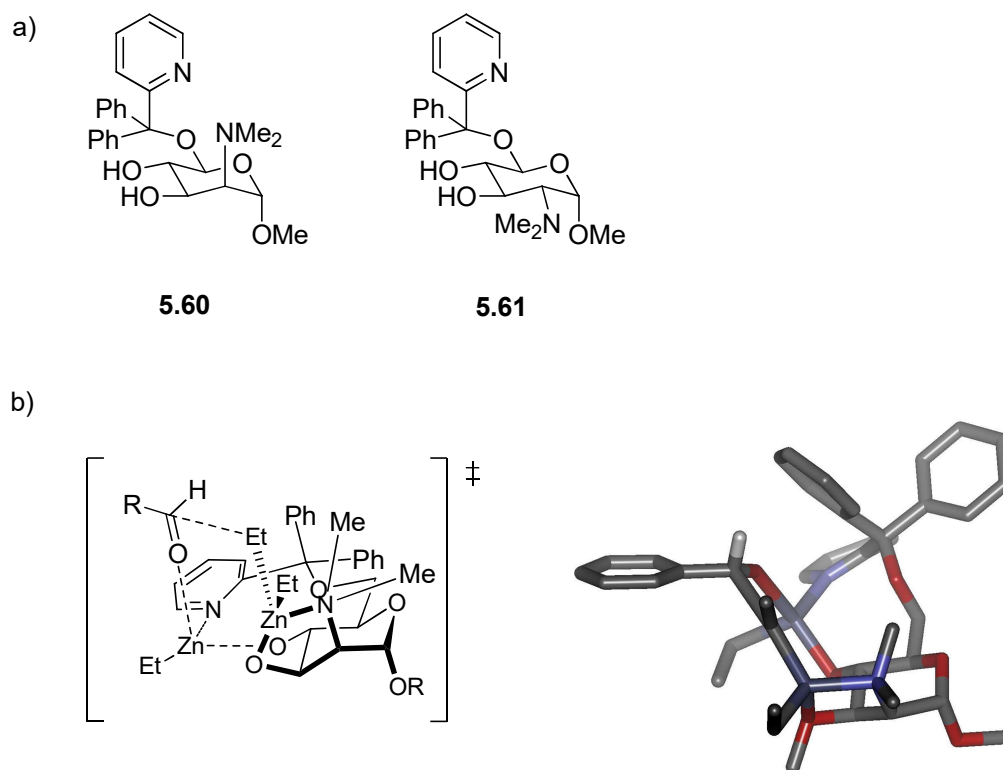
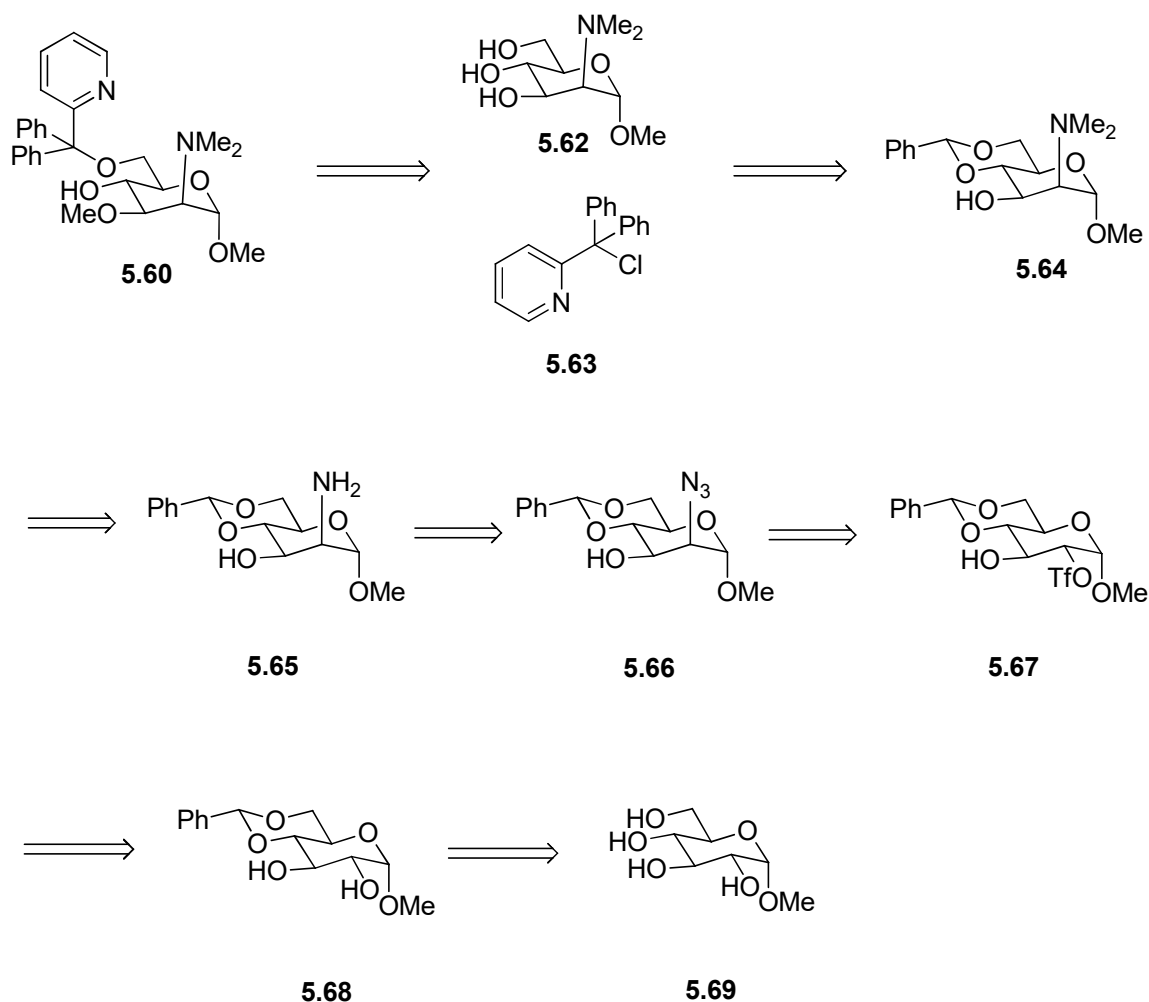


Figure 5.8. a) Predicted selective mannose-based amino alcohol **5.60** and predicted less selective glucose-based amino alcohol **5.61**; b) ACE output of highly structured transition state of diethylzinc addition to benzaldehyde using **5.60** as an organocatalyst.

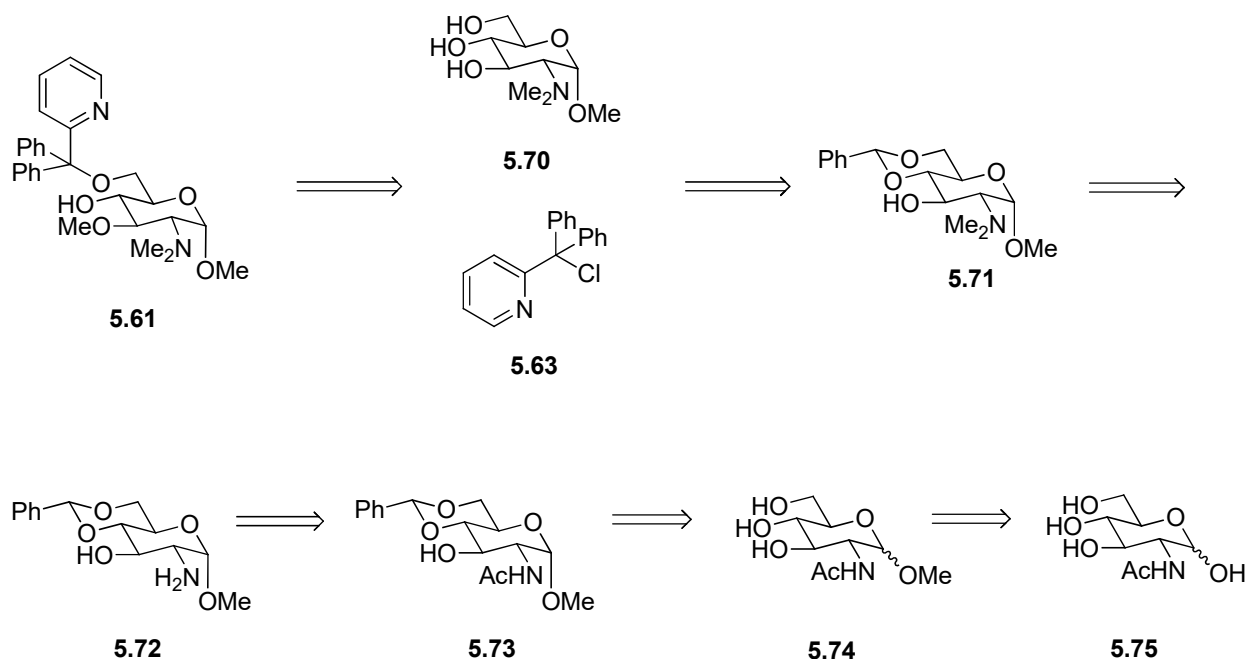
5.3.11 Efforts into the synthesis of carbohydrate-based amino alcohols

A retrosynthetic analysis of **5.60** is presented in Scheme 5.14. Functionalization of the C6 hydroxyl of **5.62** could be achieved by reaction with **5.63**. **5.62** would be easily obtained from reductive amination of **5.65** with formaldehyde and subsequent removal of the benzylidene protecting group from **5.64**. Making **5.66** was the key step in this synthesis. We envisioned that we could obtain **5.66** from S_N2 displacement of the C2-triflate of **5.67** with sodium azide to give an inversion of stereochemistry at C2, making mannose derivative **5.65** after reduction of the azide. **5.67** would be readily available in two steps starting from α -methyl glucose.



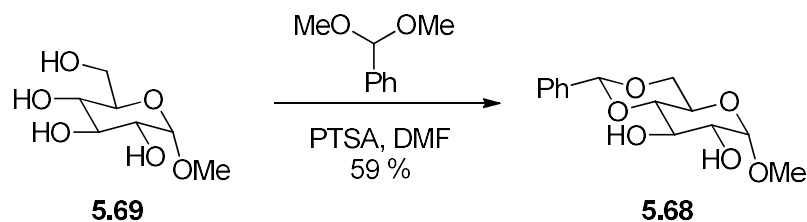
Scheme 5.14. Retrosynthetic analysis of **5.60**.

The retrosynthetic analysis for **5.61** is slightly simpler since there was no need to undergo an inversion of stereochemistry (Scheme 5.15). **5.70** should be easily obtained from removal of the benzylidene protecting group of **5.71** and subsequent functionalization of C6 hydroxyl with **5.63**. **5.71** is simply the reductive amination product of **5.72** with formaldehyde, which can be obtained from the deacetylation of **5.73**. **5.73** is readily available in two steps from commercially available and very inexpensive N-acetyl-2-deoxy-2-glucosamine (**5.75**).



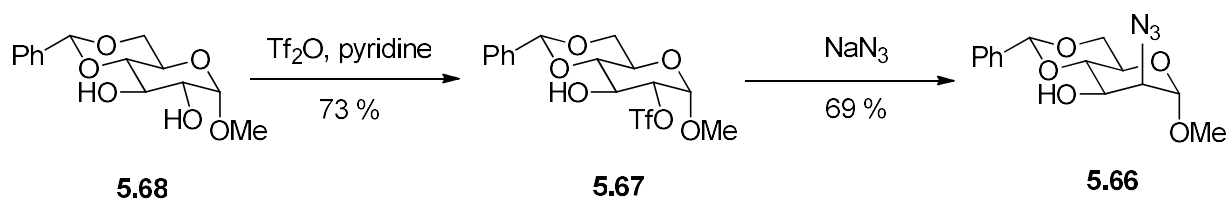
Scheme 5.15. Retrosynthetic analysis of **5.61**.

Efforts into the synthesis of **5.60** began by installing a benzylidene protecting group at the C4 and C6 hydroxyls of α -methylglucose (**5.69**), affording **5.68** in 59 % yield (Scheme 5.16).



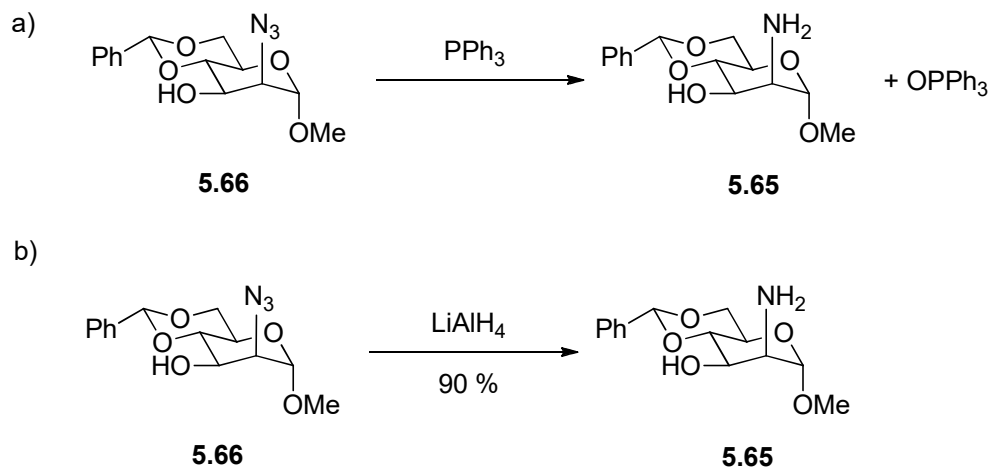
Scheme 5.16. Benzylidene protection of **5.69**.

Installation of the triflate group at the C2 hydroxyl was achieved in 73 % yield (**5.67**) and subsequent inversion of the C2 stereocenter by S_N2 displacement of the installed triflate leaving group with sodium azide (**5.66**).



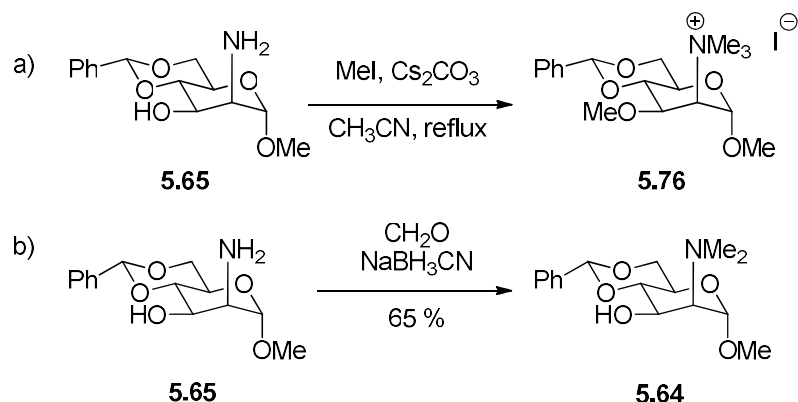
Scheme 5.17. Triflation of C2 hydroxyl to give 5.67 followed by $\text{S}_{\text{N}}2$ displacement of triflate by NaN_3 to give 5.66.

With 5.66 in hand, we tried different conditions to reduce the azide to the amine 5.65. Hydrogenation with palladium and hydrogen would have cleaved the benzylidene, which, since we also were interested in testing 5.64 as a catalyst, was undesirable. As such, we did a Staudinger reduction using PPh_3 . This reaction did afford the desired amine however, all attempts to remove the triphenylphosphine oxide byproduct proved unsuccessful. In light of this purification difficulty, we opted to use LiAlH_4 reduction conditions instead. This successfully afforded 5.65 in 90% yield after purification (Scheme 5.18).



Scheme 5.18. Reduction of azide 5.66 to amine 5.65 using a) PPh_3 and b) LiAlH_4 .

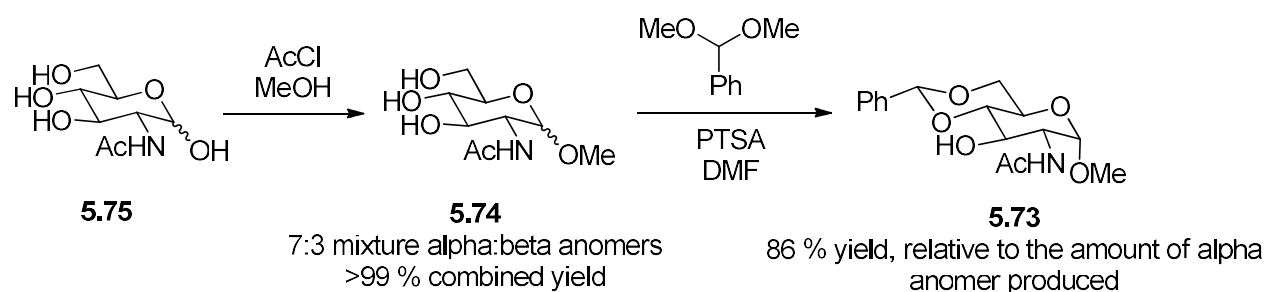
Attempts to alkylate the nitrogen of 5.65 using only two equivalents of methyl iodide and CsCO_3 to prevent over-alkylation was unsuccessful as the over-alkylated product was the major product isolated. As such, alternative Escheweiler-Clarke conditions were employed to necessarily prevent this over-alkylation and afforded 5.64 in 65% yield.



Scheme 5.19. a) Over-alkylation of **5.72** using MeI and b) Escweiler-Clarke reaction to yield **5.64**.

Preliminary attempts to hydrogenate the benzylidene protecting group on **5.64** were unsuccessful and unfortunately, at this point **5.60** was not obtained and tested as a catalyst for diethyl zinc addition to benzaldehyde.

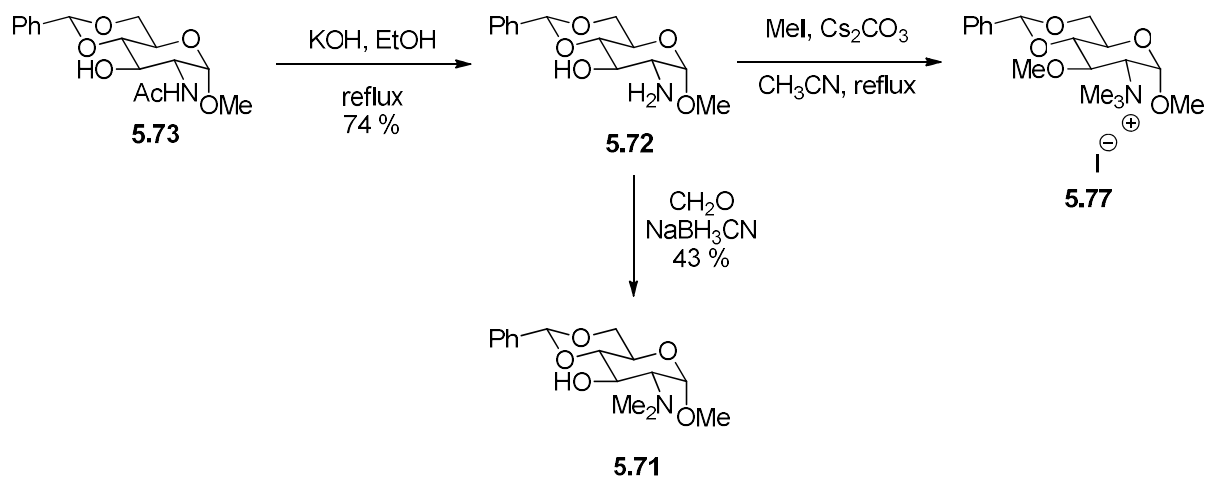
Simultaneously to efforts to synthesize **5.60**, efforts were also ongoing to synthesize glucose analogue, **5.61**. Fischer glycosylation of **5.75** led to **5.74** in quantitative yields and gave a mixture of roughly 7:3 of α : β anomers. This was followed by installation of a benzylidene protecting group onto the C4 and C6 hydroxyls to give **5.73** in 19 % yield as only the α -anomer after recrystallization. Yields could be increased up to 86 % (relative to the amount of alpha anomer produced) by separating the anomers by column chromatography. (Scheme 5.20)



Scheme 5.20. Fischer glycosylation to yield **5.74** followed by subsequent benzylidene protection to afford **5.73**.

The *N*-acetyl group was successfully removed by refluxing **5.73** in KOH in ethanol to afford amine **5.72** in 74 % yield. Similar to the mannose analogue, attempts to alkylate amine **5.72** using

MeI yielded only the over-alkylated product. This over-alkylation was avoided by employing Eschweiler-Clarke conditions, affording **5.71** in 43 % yield (Scheme 5.21).



Scheme 5.21. Deacetylation of 5.73 followed by over-alkylation of 5.72 using MeI or alternative Eschweiler-Clarke conditions to successfully yield 5.71.

Again, similar to the mannose analogue, preliminary attempts to hydrogenate the benzylidene protecting group were unsuccessful and unfortunately **5.61** was not obtained and tested as a catalyst for diethyl zinc addition to benzaldehyde.

More investigations into the removal of the benzylidene protecting groups of **5.64** and **5.71** would likely to yield the deprotected products **5.62** and **5.70**, at which point, reaction of both with **5.63** would lead to **5.60** and **5.61**, respectively. This work is currently being completed in our laboratories and will be reported in due course.

5.4 Conclusion

Herein we have described many of our efforts to synthesize and utilize chiral cyclic amine compounds as organocatalysts in several different organic transformations. The successful synthesis of **5.8a**, **5.8b** and **5.17** was demonstrated and were subsequently tested for their catalytic selectivity in Diels-Alder cycloadditions and aldol reactions. Unfortunately, oxazepane-based secondary amines **5.8a** and **5.8b** were not active catalysts in either reaction. Morpholine-based **5.17** did afford the cycloaddition product in low yields, showing its promise as an organocatalyst. This reaction is currently being investigated further to identify conditions to increase the yield to a point of usefulness and the stereoselectivity needs to be analyzed further.

The synthesis of **5.38**, **5.39** and **5.40** was described in Chapter 4. These compounds featured a tertiary amine that was of interest as a ligand in the asymmetric dihydroxylation reaction. Unfortunately, none of these compounds showed any selectivity, yielding only racemic mixtures. In some cases, however, the yields of the oxidations were greatly improved over control reactions containing no ligand.

Lastly, diethylzinc addition to benzaldehyde was studied. Our computationally guided efforts to synthesize carbohydrate-based amino alcohols **5.60** and **5.61** were unsuccessfully completed due to many synthetic issues that carbohydrates are typically associated with. However, efforts to synthesize amino alcohols **5.58a** and **5.58b** from the 4-oxa-1-azabicyclo[4.1.0]heptane scaffolds disclosed in Chapter 4 were more successful. Simple reduction of methyl ester containing compounds led to amino alcohols **5.58a** and **5.58b**. These amino alcohols were shown to successfully catalyze diethylzinc addition to benzaldehyde, affording 1-phenylpropan-1-ol in yields ranging from 25 – 78 % and up to 33 %ee,.

5.5 Experimental

General Considerations. All commercially available reagents were used without further purification, unless otherwise stated. Chemical shift (δ) are reported in parts per million (ppm) relative to CDCl_3 (7.26 ppm for ^1H and 77.160 ppm for ^{13}C). ^1H and ^{13}C NMR assignments were confirmed by 2D COSY, HSQC HMBC and NOESY experiments recorded using 400 MHz and 500 MHz spectrometers. Chromatography was performed on silica gel 60 (230-240 mesh). Visualization was performed by UV unless otherwise stated. Mass spectra were obtained from the McGill University mass spectral facilities. A Perkin Elmer Spectrum One FT-IR spectrometer was used to collect spectra of the samples at resolution of 4 cm^{-1} and 32 scans.

General procedure for sulfonamide deprotection. Base (0.2 mmol) was added to a flask containing sulfonamide-protected oxazepane (0.04 mmol) in solvent (4 mL). Subsequently, thiol (0.2 mmol) was added and the reaction mixture was stirred at rt for 12-20 h. The mixture was diluted with 1 M HCl and extracted with EtOAc. The remaining aqueous mixture was made basic by addition of NaHCO_3 and then extracted with EtOAc. This basic extraction organic layer was dried over Na_2SO_4 , filtered and concentrated under reduced pressure. The crude mixture was purified by column chromatography on silica gel.

General procedure for Diels-Alder cycloaddition. To a solution of catalyst in MeOH/H₂O (95:5 v/v, 1.0 M), was added cinnamaldehyde. The solution was stirred for 5 minutes before the addition of freshly cracked cyclopentadiene. Upon consumption of the limiting reagent, the reaction mixture was diluted with Et₂O and washed successively with H₂O and brine. The organic layer was dried over Na₂SO₄, filtered and concentrated under reduced pressure. Hydrolysis of the product dimethyl acetal was performed by stirring the crude product in TFA:H₂O:CHCl₃ (1:1:2) for 2 h at rt, followed by neutralization with saturated aqueous NaHCO₃ and extraction with Et₂O. The crude mixture was purified by column chromatography on silica gel.

General procedure for aldol reactions. The amine (0.03-0.04 mmol) was stirred in 1 mL of DMSO/acetone (4:1) for 15 minutes. Aldehyde (0.1 mmol) was added and the reaction mixture was stirred until consumption of aldehyde was observed by TLC. The mixture was treated with 1 mL of saturated aqueous NH₄Cl solution and extracted with EtOAc. The organic layer was dried over Na₂SO₄, filtered and concentrated under reduced pressure. The crude mixture was purified by column chromatography on silica gel.

General procedure for dihydroxylation. A solution of olefin (1.0 mmol) was added to a vigorously stirred solution of K₂CO₃ (3.0 mmol), K₃Fe(CN)₆ (3.0 mmol), K₂OsO₂(OH)₄ (0.001 mmol) and ligand (0.01 mmol) in *t*-BuOH:H₂O (10 mL, 1:1 v/v) at rt. MeSO₂NH₂ (1.00 mmol) was also added in cases where the olefin was either 1,2-disubstituted, trisubstituted or tetrasubstituted. Upon consumption of the olefin, sodium sulfite (1.5 g) was added and the mixture was stirred for an additional 30 minutes. The products were extracted with CH₂Cl₂ and the organic layer was dried over Na₂SO₄, filtered and concentrated under reduced pressure. The crude mixture was purified by column chromatography on silica gel.

General procedure for methyl ester reduction. **5.60** (0.50 mmol) was added to a dry flask, flushed with argon and dissolved in dry THF (5 mL). The mixture was cooled to 0 °C. LiAlH₄ (5.0 mmol) was added to the mixture in small portions and the mixture was stirred for 1 hour at 0 °C (follow reaction by TLC). The mixture was diluted with ether. Water was slowly added dropwise (90 uL) followed by 15 % NaOH_{aq} (90 uL) followed by an additional aliquot of water (270 uL) and the solution was warmed to rt and stirred for 15 min. Anhydrous Na₂SO₄ was added and stirred for another 15 min and the solution was then filtered through Celite to remove any salts. The filtrate

was concentrated under reduced pressure. The crude was purified by column chromatography on silica gel to yield **5.61**.

General procedure for diethylzinc addition to benzaldehyde. To a flame dried round bottom flask was added amino alcohol (0.20 mmol) and dry toluene (2 mL). The solution was degassed with argon for 20 min and the flask was then completely flushed with argon. To this, a solution of 1.0 M Et₂Zn (2.0 mmol) was added slowly and the mixture was stirred at 15 °C for 15 min. The solution was then cooled to -78 °C and benzaldehyde (1.0 mmol) was added and the solution was warmed up to 0 °C and stirred for 24 h. The reaction was quenched by addition of saturated NH₄Cl solution (5 mL) at 0 °C and the crude product was extracted into EtOAc. The organic layers were dried over Na₂SO₄, filtered and concentrated under reduced pressure. . The crude mixture was purified by column chromatography on silica gel.

(2R,3S,6R,7S)-methyl 6-bromo-2-methyl-7-phenyl-1,4-oxazepane-3-carboxylate (5.8a). Colourless oil; 18 % isolated yield; R_f 0.41 (1:9 MeOH:CH₂Cl₂, Ninhydrin Stain); IR (film, cm⁻¹) 3309, 9253, 2873, 1736, 1436, 1294, 1202, 1067, 1043, 932, 758 700; ¹H NMR (400 MHz, CDCl₃) δ 7.43 – 7.30 (m, 5H), 4.42 (d, *J* = 9.2 Hz, 1H), 3.80 (s, 3H), 3.71 (dq, *J* = 9.3, 6.1 Hz, 1H), 3.52 (d, *J* = 9.3 Hz, 1H), 3.43 (dd, *J* = 11.3, 2.8 Hz, 1H), 3.33 (dd, *J* = 11.3, 5.7 Hz, 1H), 3.01 (ddd, *J* = 8.8, 5.7, 2.8 Hz, 1H), 2.38 (s, 1H), 1.28 (d, *J* = 6.1 Hz, 3H); ¹³C NMR (75 MHz, CD₃OD) δ 171.1, 138.1, 128.7, 128.7, 127.1, 81.4, 74.8, 64.1, 59.3, 52.3, 45.8; HRMS: (M + Na) for C₁₄H₁₉BrNO₄ calcd 328.0548, found 328.0543.

(3S)-methyl 6-bromo-7-phenyl-1,4-oxazepane-3-carboxylate (5.8b). Colourless oil; 65 % isolated yield; IR (film, cm⁻¹) 2954, 5863, 1741, 1436, 1299, 1219, 1081, 760, 701; ¹H NMR (400 MHz, CDCl₃) δ 7.43 – 7.28 (m, 5H), 4.28 (dd, *J* = 11.1, 3.6 Hz, 1H), 4.20 (d, *J* = 9.1 Hz, 1H), 3.93 (dd, *J* = 10.6, 3.6 Hz, 1H), 3.79 (s, 3H), 3.61 (t, *J* = 10.9 Hz, 1H), 3.35 (dd, *J* = 5.0, 2.5 Hz, 2H), 3.09 – 3.01 (m, 1H); ¹³C NMR (125 MHz, CDCl₃) δ 170.3, 137.7, 128.9, 128.8, 127.2, 81.6, 68.9, 60.2, 57.3, 52.4, 45.8; HRMS: (M + H) for C₁₃H₁₇BrNO₃ calcd 314.0392, found 314.0386.

(2R,3S,6R,7S)-4-tert-butyl 3-methyl 6-((tert-butoxycarbonyl)oxy)-2-methyl-7-phenyl-1,4-oxazepane-3,4-dicarboxylate (5.12). K₂CO₃ (0.2 mmol) was added to a flask containing **2.XX** (0.04 mmol) in CH₃CN (4 mL). Subsequently, β-mercaptoethanol (0.2 mmol) was added and the reaction mixture was stirred at rt for 12 h. (Boc)₂O (0.08 mmol) was added to the mixture and the reaction was stirred at rt for 5 h. The mixture was concentrated under reduced pressure and

the residue was extracted with EtOAc and washed with water. The organic layer was dried over Na_2SO_4 , filtered and concentrated under reduced pressure. The crude mixture was purified by column chromatography on silica gel. Colourless oil; 49 % yield; $[\alpha]_D^{22} = -11.39$ (c 2.18, CHCl_3); R_f 0.60 (7:3 Hexanes:EtOAc, Ninhydrin Stain); IR (film, cm^{-1}) 2979, 1745, 1700, 1456, 1394, 1369, 1331, 1276, 1255, 1161, 860, 766, 700; ^1H NMR (400 MHz, CDCl_3) δ 7.39 – 7.24 (m, 5H), 4.65 (d, $J = 4.8$ Hz, 1H), 4.46 (ddd, $J = 10.0, 5.2, 4.8$ Hz, 1H), 4.37 – 4.29 (m, 2H), 4.25 (dd, $J = 11.0, 5.2$ Hz, 1H), 3.95 (dq, $J = 8.7, 6.1$ Hz, 1H), 3.76 (s, 3H), 1.45 (s, 9H), 1.43 (d, $J = 6.1$ Hz, 3H), 1.42 (s, 9H); ^{13}C NMR (125 MHz, CDCl_3) δ 171.8, 153.2, 141.5, 128.6, 128.2, 126.4, 82.1, 81.3, 77.9, 70.1, 67.6, 60.5, 53.4, 52.3, 28.2, 27.7; HRMS: (M + Na) for $\text{C}_{24}\text{H}_{35}\text{NO}_8\text{Na}$ calcd 488.2255, found 488.2260.

(S)-methyl 3-hydroxy-2-(naphthalene-2-sulfonamido)propanoate. Colourless oil; 13 % isolated yield; $R_f = 0.54$ (9:1 CH_2Cl_2 :MeOH +1 % NH_3OH , UV); IR (film, cm^{-1}) 3292, 2925, 1742, 1530, 1349, 1167, 1091, 855, 767; ^1H NMR (500 MHz, CD_3OD) δ 8.41 (d, $J = 1.2$ Hz, 1H), 8.03 (d, $J = 8.9$ Hz, 2H), 7.98 (d, $J = 8.0$ Hz, 1H), 7.85 (dd, $J = 8.7, 1.8$ Hz, 1H), 7.70 – 7.62 (m, 2H), 4.06 (t, $J = 5.2$ Hz, 1H), 3.75 (dd, $J = 11.4, 5.2$ Hz, 1H), 3.68 (dd, $J = 11.1, 5.5$ Hz, 1H), 3.30 (s, 3H); ^{13}C (125 MHz, CDCl_3) δ 169.6, 145.6, 134.5, 128.9, 128.8, 128.7, 128.5, 128.4, 128.2, 124.1, 68.3, 67.8, 61.0, 20.1; HRMS: (M + Na) for $\text{C}_{17}\text{H}_{18}\text{N}_2\text{O}_7\text{SNa}$ calcd 417.0732, found 417.0727.

(2S,3R)-benzyl 2-(N-cinnamyl-4-nitrophenylsulfonamido)-3-hydroxybutanoate. Made according to the general procedure for N-alkylation of N-protected amino alcohols as presented in Chapter 2. Colourless oil; 57 % isolated yield; $R_f = 0.29$ (3:1 Hexanes:EtOAc); IR (film, cm^{-1}) 3547, 3033, 2980, 1735, 1529, 1348, 1160, 1088, 1023, 854, 741; ^1H NMR (300 MHz, CDCl_3): δ 7.93 (d, $J = 9.0$ Hz, 2H), 7.84 (d, $J = 9.1$ Hz, 2H), 7.40 – 7.21 (m, 6H), 7.21 – 7.10 (m, 4H), 6.47 (d, $J = 16.0$ Hz, 1H), 5.98 (ddd, $J = 15.9, 7.8, 6.1$ Hz, 1H), 4.97 (d, $J = 1.8$ Hz, 2H), 4.62 (d, $J = 5.2$ Hz, 1H), 4.55 – 4.44 (m, 1H), 4.32 – 4.14 (m, 2H), 2.60 (s, 1H), 1.35 (d, $J = 6.3$ Hz, 3H); ^{13}C (125 MHz, CDCl_3) δ 169.4, 149.7, 145.9, 135.8, 134.4, 134.3, 129.0, 128.8, 128.7, 128.6, 126.4, 123.8, 67.9, 67.3, 65.0, 49.7, 20.0; HRMS: (M + Na) for $\text{C}_{26}\text{H}_{26}\text{N}_2\text{O}_7\text{SNa}$ calcd 533.1358, found 533.1353.

(2R,3S,6R,7S)-benzyl 6-bromo-2-methyl-4-((4-nitrophenyl)sulfonyl)-7-phenyl-1,4-oxazepane-3-carboxylate (5.11d). Made according to the general procedure for cyclization of N-sulfonamide protected amino alcohols as presented in Chapter 2. Colourless oil; >99 % isolated

yield; $R_f = 0.60$ (7:3 Hexanes:EtOAc); IR (film, cm^{-1}) 3035, 2980, 1736, 1530, 1348, 1159, 1089, 1008, 771, 738, 398; ^1H NMR (300 MHz, CDCl_3): δ 8.13 (d, $J = 8.7$ Hz, 2H), 7.88 (d, $J = 8.7$ Hz, 2H), 7.40 – 7.27 (m, 8H), 7.21 (dd, $J = 6.5, 2.7$ Hz, 2H), 4.99 (d, $J = 2.9$ Hz, 2H), 4.57 (d, $J = 9.5$ Hz, 1H), 4.40 (d, $J = 10.0$ Hz, 1H), 4.20 (dd, $J = 11.4, 6.2$ Hz, 2H), 4.03 – 3.93 (m, 1H), 3.87 (dd, $J = 16.3, 12.4$ Hz, 1H), 1.35 (d, $J = 6.1$ Hz, 3H); ^{13}C (125 MHz, CDCl_3) δ 169.7, 150.0, 145.3, 139.1, 134.4, 129.0, 128.8, 128.7, 128.5, 128.3, 128.2, 127.4, 124.3, 90.2, 67.6, 64.8, 51.6, 50.6, 20.6; HRMS: (M + Na) for $\text{C}_{26}\text{H}_{25}\text{BrN}_2\text{O}_7\text{SNa}$ calcd 611.0464, found 611.0458.

(2R,3S,6R,7S)-benzyl 4-benzyl-6-bromo-2-methyl-7-phenyl-1,4-oxazepane-3-carboxylate (5.13d). K_2CO_3 (0.2 mmol) was added to a flask containing **5.11d** (0.04 mmol) in CH_3CN (4 mL). Subsequently, β -mercaptoethanol (0.2 mmol) was added and the reaction mixture was stirred at rt for 12 h. Hünig's base (0.06 mmol) was added followed by benzyl bromide (0.044 mmol) and the reaction was stirred at rt for 5 h. The mixture was concentrated under reduced pressure and the residue was extracted with EtOAc and washed with water. The organic layer was dried over Na_2SO_4 , filtered and concentrated under reduced pressure. The crude mixture was purified by column chromatography on silica gel. Colourless oil; 8 % yield over two steps; $R_f = 0.81$ (7:3 Hexanes:EtOAc, CAM stain); IR (film, cm^{-1}) 2917, 2849, 1736, 1455, 1263, 1115, 1072, 751, 698; ^1H NMR (500 MHz, CDCl_3): δ 7.36 – 7.04 (m, 16H), 4.84 (dd, $J = 28.5, 12.2$ Hz, 2H), 4.66 (d, $J = 9.0$ Hz, 1H), 3.85 (dq, $J = 9.1, 6.2$ Hz, 1H), 3.72 (s, 2H), 3.50 (dd, $J = 11.9, 3.1$ Hz, 1H), 3.25 (d, $J = 9.2$ Hz, 1H), 2.88 (d, $J = 11.0$ Hz, 1H), 2.52 (d, $J = 8.1$ Hz, 1H), 1.01 (d, $J = 6.2$ Hz, 3H); HRMS: (M + Na) for $\text{C}_{27}\text{H}_{28}\text{BrNO}_3\text{Na}$ calcd 516.1150, found 516.1145.

(2R,3S,6R,7S)-methyl 6-hydroxy-2-methyl-7-phenyl-1,4-oxazepane-3-carboxylate (5.15). **5.12** (0.10 mmol) was dissolved in dry MeOH (10 mL) and AcCl (5 mmol) was added and the mixture was stirred at rt for 16 h. The mixture was concentrated under reduced pressure and the product was crystallized from CHCl_3 . White solid; 53 % isolated yield; $[\alpha]_D^{22} = +20.0$ (c 0.80, MeOH); R_f 0.59 (5:95 MeOH: CH_2Cl_2 , Ninhydrin Stain); MP: 124 – 129 °C; IR (film, cm^{-1}) 3325, 2954, 1578, 1151 1455, 1338, 1315, 1229, 1068, 761, 702; ^1H NMR (400 MHz, CD_3OD) δ 7.45 (s, 5H), 4.68 (d, $J = 9.7$ Hz, 1H), 4.15 (d, $J = 9.7$ Hz, 1H), 4.12 – 4.05 (m, 1H), 3.95 (s, 3H), 3.54 (dt, $J = 13.2, 5.6$ Hz, 2H), 3.43 (t, $J = 5.1$ Hz, 1H), 1.46 (d, $J = 5.9$ Hz, 3H); ^{13}C NMR (75 MHz, CD_3OD) δ 166.7, 136.0, 129.2, 128.5, 127.1, 77.8, 72.0, 61.5, 60.7, 57.5, 52.5, 17.3; HRMS: (M + Na) for $\text{C}_{14}\text{H}_{19}\text{NO}_4\text{Na}$ calcd 288.12118, found 288.1206.

(2R,3S,5S,6S)-methyl 5-(hydroxymethyl)-2-methyl-6-phenylmorpholine-3-carboxylate (5.17). Made according to the general procedure of TBAF-mediated intramolecular rearrangement of oxazepanes and morpholines as described in Chapter 4. White crystalline solid; 23 % isolated yield; $[\alpha]_D^{22} = +107.67$ ($c = 0.06$, MeOH); R_f 0.12 (7:3 Hexanes:EtOAc, Ninhydrin Stain); MP: 99 - 101 °C; IR (film, cm^{-1}) 3309, 2934, 1737, 1454, 1437, 1342, 1280, 1264, 1201, 1141, 1087, 785, 701; ^1H NMR (400 MHz, CD_3OD) δ 7.41 – 7.22 (m, 5H), 4.37 (d, $J = 9.6$ Hz, 1H), 3.78 (s, 3H), 3.65 (ddd, $J = 12.3, 9.3, 6.2$ Hz, 1H), 3.44 (d, $J = 9.3$ Hz, 1H), 3.35 – 3.23 (m, 3H), 2.79 (ddd, $J = 9.5, 5.2, 3.2$ Hz, 1H), 1.23 (d, $J = 6.2$ Hz, 3H); ^{13}C NMR (100 MHz, CD_3OD) δ 171.3, 139.0, 128.0, 127.9, 127.2, 80.6, 74.4, 63.8, 60.6, 60.1, 51.2, 26.5, 17.3; HRMS: (M + Na) for $\text{C}_{14}\text{H}_{19}\text{NO}_4\text{Na}$ calcd 288.12118, found 288.1216.

(S)-2-amino-1,1-diphenylpropane-1,3-diol (5.19).³¹ Yellow oil; 43 % isolated yield; $R_f = 0.71$ (9:1 CH_2Cl_2 :MeOH); IR (film, cm^{-1}): 3359, 3060, 2942, 1597, 1492, 1449, 1385, 1175, 1032, 908, 731; ^1H NMR (300 MHz, CDCl_3) δ 7.58 – 7.46 (m, 4H), 7.38 – 7.26 (m, 4H), 7.20 (ddd, $J = 9.4, 7.3, 3.1$ Hz, 2H), 3.88 (dd, $J = 5.1, 3.6$ Hz, 1H), 3.61 (t, $J = 4.0$ Hz, 2H), 3.24 (br s, 3H); ^{13}C NMR (125 MHz, CDCl_3) δ 128.32, 126.93, 125.50, 125.17, 77.29, 77.04, 76.79, 53.43; HRMS: (M + Na) for $\text{C}_{15}\text{H}_{17}\text{NO}_2\text{Na}$ calcd 266.1157, found 266.1151.

(S)-N-(1,3-dihydroxy-1,1-diphenylpropan-2-yl)-4-nitrobenzenesulfonamide (5.20). Colourless oil; 30 % isolated yield; $R_f = 0.30$ (7:3 Hexanes:EtOAc); IR (film, cm^{-1}) 3366, 1607, 1450, 1348, 1162, 1093, 1061, 910, 854, 734, 704; ^1H NMR (300 MHz, CDCl_3) δ 8.04 (d, $J = 8.9$ Hz, 2H), 7.58 (d, $J = 8.9$ Hz, 2H), 7.47 (d, $J = 7.4$ Hz, 2H), 7.27 (ddd, $J = 16.3, 9.5, 4.6$ Hz, 7H), 7.05 – 6.87 (m, 3H), 6.13 (d, $J = 7.2$ Hz, 1H), 4.82 (s, 1H), 4.30 (d, $J = 5.5$ Hz, 1H), 4.04 (qd, $J = 11.7, 1.9$ Hz, 2H); ^{13}C NMR (75 MHz, CDCl_3) δ 149.50, 145.73, 144.23, 143.47, 128.66, 128.10, 127.72, 127.44, 126.83, 125.10, 124.73, 124.07, 80.81, 64.58, 59.63; HRMS: (M + Na) for $\text{C}_{21}\text{H}_{20}\text{N}_2\text{O}_6\text{SNa}$ calcd 451.0940, found 451.0934.

((2R,3R,6R,7S)-6-bromo-2-methyl-4-((4-nitrophenyl)sulfonyl)-7-phenyl-1,4-oxazepan-3-yl)methanol (5.25a). **5.11a** (0.2 mmol) was dissolved in EtOAc (10 mL) and solid LiI (1.0 mmol) was added. The mixture was protected from light and heated at reflux for 16 h. The mixture was diluted with 1 M HCl and extracted with EtOAc. The organic phase was washed successively with water and brine, dried over Na_2SO_4 , filtered and concentrated under reduced pressure to yield **5.XX**. Yellow oil; >99 % isolated yield; $R_f = 0.58$ (5:95 MeOH: CH_2Cl_2); IR (film, cm^{-1}): 3462.

1717. 1531. 1350. 1161 1088. 1008. 738; ^1H NMR (400 MHz, CD_3OD) δ 8.46 (d, $J = 8.9$ Hz, 2H), 8.16 (d, $J = 8.9$ Hz, 2H), 7.32 (m, 3H), 7.26 (m, 2H), 4.54 (d, $J = 10.2$ Hz, 1H), 4.42 (d, $J = 9.6$ Hz, 1H), 4.31 (dd, $J = 14.9, 2.9$ Hz, 1H), 4.17 – 4.07 (m, 2H), 4.00 (dd, $J = 15.3, 11.7$ Hz, 1H), 1.39 (d, $J = 6.1$ Hz, 3H); ^{13}C NMR (100 MHz, CD_3OD): δ 150.4. 145.6. 139.8. 128.4. 128.1. 127.8. 127.2. 124.2. 89.4. 77.1. 65.3. 51.4. 50.3. 19.5; HRMS: (M - H) for $\text{C}_{19}\text{H}_{18}\text{BrN}_2\text{O}_7$ calcd: 497.00236, found: 497.0031.

((2S,5R,6R)-2-(4-aminophenyl)-5-phenyl-4-oxa-1-azabicyclo[4.1.0]heptan-2-yl)methanol (5.58a). Yellow oil; 88 % isolated yield; IR (film, cm^{-1}) 3994, 2871, 1675, 1598, 1517, 1348, 1072, 856, 700; ^1H NMR (400 MHz, CDCl_3) δ 8.28 (d, $J = 9.0$ Hz, 2H), 7.93 (d, $J = 9.0$ Hz, 2H), 7.34 – 7.25 (m, 4H), 7.22 – 7.15 (m, 2H), 4.82 (d, $J = 3.2$ Hz, 1H), 3.92 (m, 3H), 3.48 (d, $J = 12.6$ Hz, 1H), 2.53 (dt, $J = 5.1, 3.2$ Hz, 1H), 2.21 (d, $J = 3.8$ Hz, 2H); ^{13}C NMR (125 MHz, CDCl_3) δ 151.1, 147.0, 141.2, 129.0, 128.7, 128.3, 126.6, 123.4, 75.7, 67.9, 64.1, 58.0, 34.0, 29.0; HRMS: (M + Na) for $\text{C}_{18}\text{H}_{18}\text{N}_2\text{O}_4\text{Na}$ calcd 349.1164, found 349.1159.

((2S,3S,5R,6R)-3-methyl-2-(4-nitrophenyl)-5-phenyl-4-oxa-1-azabicyclo[4.1.0]heptan-2-yl)methanol (5.58b). Yellow oil; 58 % isolated yield; $R_f = 0.68$ (9:1 CH_2Cl_2 :MeOH + 1 % NH_4OH , *p*-anisaldehyde stain); IR (film, cm^{-1}) 3417, 2881, 1603, 1454, 1100, 1027, 909, 759, 732, 701; ^1H (500 MHz, CDCl_3) δ 8.05 (d, $J = 8.6$ Hz, 2H), 7.89 (d, $J = 8.6$ Hz, 2H), 7.24 (dd, $J = 4.9, 1.7$ Hz, 3H), 7.09 (dd, $J = 6.7, 2.9$ Hz, 2H), 4.97 (q, $J = 6.5$ Hz, 1H), 4.68 (d, $J = 9.7$ Hz, 1H), 3.66 (s, 2H), 3.42 (dd, $J = 11.0, 2.7$ Hz, 1H), 3.34 (dd, $J = 11.1, 5.7$ Hz, 1H), 2.92 (ddd, $J = 8.7, 5.6, 2.7$ Hz, 1H), 1.67 (d, $J = 6.6$ Hz, 3H); ^{13}C (125 MHz, CDCl_3) δ 151.8, 145.3, 138.9, 128.6, 128.5, 127.2, 123.1, 72.9, 69.8, 69.5, 61.6, 55.5, 46.7, 14.1.

5.5 References

- (1) Halpern, J.; Trost, B. M. *Proc. Natl. Acad. Sci. U.S.A.* **2004**, *101*, 5347.
- (2) Ahrendt, K. A.; Borths, C. J.; MacMillan, D. W. C. *J. Am. Chem. Soc.* **2000**, *122*, 4243.
- (3) Kunz, R. K.; MacMillan, D. W. C. *J. Am. Chem. Soc.* **2005**, *127*, 3240.
- (4) Lee, S.; MacMillan, D. W. C. *Tetrahedron* **2006**, *62*, 11413.
- (5) Jen, W. S.; Wiener, J. J. M.; MacMillan, D. W. C. *J. Am. Chem. Soc.* **2000**, *122*, 9874.
- (6) Ouellet, S. G.; Tuttle, J. B.; MacMillan, D. W. *J. Am. Chem. Soc.* **2005**, *127*, 32.
- (7) Tuttle, J. B.; Ouellet, S. G.; MacMillan, D. W. *J. Am. Chem. Soc.* **2006**, *128*, 12662.
- (8) Herrera, R.; Merino, P.; Marqués-López, E.; Tejero, T. *Synthesis* **2009**, *2010*, 1.

- (9) Notz, W.; Tanaka, F.; Barbas, C. F. *Acc. Chem. Res.* **2004**, *37*, 580.
- (10) Kolb, H. C.; VanNieuwenhze, M. S.; Sharpless, K. B. *Chem. Rev.* **1994**, *94*, 2483.
- (11) Zaitsev, A. B.; Adolfsson, H. *Synthesis* **2006**, *2006*, 1725.
- (12) Noyori, R.; Kitamura, M. *Angew. Chem. Int. Ed.* **1991**, *30*, 49.
- (13) Pu, L.; Yu, H.-B. *Chem. Rev.* **2001**, *101*, 757.
- (14) List, B.; Lerner, R. A.; Barbas, C. F. *J. Am. Chem. Soc.* **2000**, *122*, 2395.
- (15) MSc. Thesis, Rana Bilbeisi, 2001.
- (16) Hentges, S. G.; Sharpless, K. B. *J. Am. Chem. Soc.* **1980**, *102*, 4263.
- (17) Cleare, M. J.; Hydes, P. C.; Griffith, W. P.; Wright, M. J. *J. Chem. Soc., Dalton Trans.* **1977**, 941.
- (18) Griffith, W. P.; Skapski, A. C.; Woode, K. A.; Wright, M. J. *Inorg. Chim. Acta* **1978**, *31*, L413.
- (19) Sharpless, K. B.; Amberg, W.; Bennani, Y. L.; Crispino, G. A.; Hartung, J.; Jeong, K. S.; Kwong, H. L.; Morikawa, K.; Wang, Z. M. *J. Org. Chem.* **1992**, *57*, 2768.
- (20) Oguni, N.; Omi, T. *Tetrahedron Lett.* **1984**, *25*, 2823.
- (21) Kitamura, M.; Suga, S.; Kawai, K.; Noyori, R. *J. Am. Chem. Soc.* **1986**, *108*, 6071.
- (22) Hursthouse, M. B.; Motevalli, M.; O'Brien, P.; Walsh, J. R.; Jones, A. C. *J. Mater. Chem.* **1991**, *1*, 139.
- (23) Goldfuss, B.; Houk, K. N. *J. Org. Chem.* **1998**, *63*, 8998.
- (24) Goldfuss, B.; Steigelmann, M.; Khan, S. I.; Houk, K. N. *J. Org. Chem.* **2000**, *65*, 77.
- (25) Oguni, N.; Matsuda, Y.; Kaneko, T. *J. Am. Chem. Soc.* **1988**, *110*, 7877.
- (26) Kitamura, M.; Yamakawa, M.; Oka, H.; Suga, S.; Noyori, R. *Chem. Eur. J.* **1996**, *2*, 1173.
- (27) Young, D. C. *Computational Drug Design: A Guide for Computational and Medicinal Chemists*; John Wiley and Sons: New York, USA, 2009.
- (28) Emmerson, D. P. G.; Villard, R.; Mugnaini, C.; Batsanov, A.; Howard, J. A. K.; Hems, W. P.; Tooze, R. P.; Davis, B. G. *Org. Biomol. Chem.* **2003**, *1*, 3826.
- (29) Corbeil, C. R.; Thielges, S.; Schwartzentruber, J. A.; Moitessier, N. *Angew. Chem. Int. Ed.* **2008**, *47*, 2635.
- (30) Weill, N.; Corbeil, C. R.; De Schutter, J. W.; Moitessier, N. *J. Comput. Chem.* **2011**, *32*, 2878.

(31) Sibi, M. P.; Despande, P. K.; LaLoggia, A. J.; Patent, U. S., Ed.; NDSU-Research Foundation: United States, 1997, p 13.

Chapter 6 Conclusions and Perspectives

6.1 Conclusions

In this thesis, we first reviewed the synthesis of small and medium sized heterocycles by haliranium-mediated cyclization, specifically through halocycloetherification reactions. The inherent ambiguity of the naming system accompanying Baldwin's rules was also discussed. The limited methods of making small 3-membered oxiranes and 4-membered oxetanes, was presented, predominantly in a diastereoselective or non-stereoselective fashion. Overwhelmingly, the literature focused on the synthesis of 5-membered tetrahydrofurans as this method of cyclization allowed for good stereocontrol, importantly in a catalytic asymmetric fashion. The synthesis of the 6-membered tetrahydropyrans is touched upon in the context of synthesis of natural products or biologically important molecules. Fundamental research into methods of halocycloetherification to make 6-membered and larger rings was chiefly lacking in the literature. The importance of these reactions is obviated by the number of organohalogen containing natural products that exist, the interesting motifs that halocycloetherification facilitate, and the synthetic handles that halogens provide.

In Chapter 2, we presented a novel methodology that was developed to synthesize polysubstituted 7-membered oxazepanes and 6-membered morpholines and the optimization of this methodology was discussed. Starting from enantiopure amino alcohols and alkyl bromides, the products were obtained in only 3 steps: N-protection, N-alkylation and a key bromocycloetherification. The final products were obtained in good to excellent yields and moderate to excellent diastereoselectivities.

In Chapter 3, we thoroughly probed the reaction mechanism of the methodology developed in Chapter 2. Through a combination of NMR characterization and X-ray crystallography, the structure of the oxazepanes and morpholines were confirmed. Using both strategically chosen substrates to obtain experimental evidence and complimented by employing computational techniques, the reaction mechanism was explained. The regiochemistry was determined to arise from desymmetrization of the bromiranium ion, dependent on the substitution of the olefin of the starting material. The relative stereochemistry was attributed to nucleophilic addition to a haliranium ion being a stereospecific reaction and therefore the stereochemistry of the starting

olefin was transferred to the product. Less straightforwardly, the absolute stereochemistry originated from reaction of the lowest energy ground state conformation. The explanation of absolute stereochemistry was aided extensively by computational work.

In Chapter 4, we presented the unexpected and virtually unprecedented fluoride-mediated intramolecular rearrangement of the 1,4-oxazepanes that was presented in Chapter 2 and Chapter 3. This rearrangement afforded several fused and bridged bicyclic compounds featuring a quaternary stereocenter. We present a strategic substrate scope as well as a tentative mechanism for the reaction. Transition state calculations are currently in progress to support our proposed mechanism.

Chapter 5 goes on to examine utilizing the structures described in Chapter 2, 3 and 4 as organocatalysts. Efforts into making chiral secondary amines via sulfonamide deprotection of oxazepanes were discussed for the purpose of catalyzing Diels-Alder cycloaddition and aldol reactions, both of which are well known to be catalyzed by secondary amines operating through a LUMO-lowering iminium generic mode of activation. Preliminary results showed 1,4-morpholine derivatives promisingly catalyzed the unoptimized Diels-Alder cycloaddition in low yields. Unfortunately, 1,4-oxazepanes did not catalyze either Diels-Alder cycloaddition or aldol reactions. The 4-oxa-1-azabicyclo[4.1.0]heptanes containing tertiary amines discussed in the Chapter 4 were tested as ligands for OsO₄ in the dihydroxylation of olefins. Unfortunately, no stereoselectivity was observed for this reaction and only racemates were obtained. Lastly, efforts into synthesizing chiral amino alcohols were presented for the purpose of catalyzing diethylzinc addition to benzaldehyde. Scaffolds that were examined included 4-oxa-1-azabicyclo[4.1.0]heptanes as well as two carbohydrate-based compounds. Preliminary results for the addition reaction were presented with non-optimized reactions affording up to 33 %ee using a catalyst with only 36 %ee, a result that may be a side effect of negative non-linear effects.

In conclusion, this thesis presents the synthesis of medium-sized heterocycles, namely oxazepanes and morpholines, using halide-mediated cycloetherification (Chapter 2) followed by extensive studies into the reaction mechanism (Chapter 3). The reactivity of oxazepanes and morpholines under alternate halide-mediated conditions, specifically fluoride-mediated conditions, was examined and a mechanism proposed for an unexpected rearrangement (Chapter

4). Lastly, the application of oxazepanes, morpholines and 4-oxa-1-azabicyclo[4.1.0]heptanes as organocatalysts in various organic reactions was examined (Chapter 5).

6.2 Perspectives

The oxazepane products presented in Chapter 2 and 3 represent an interesting class of cyclic compounds. Due to the difficulty in making 7-membered rings, they are currently underexplored in pharmaceutical chemistry, generally only included in substrate screenings as an analogue of morpholine. There are several examples of oxazepanes having biological activity, particularly as glycosidase inhibitors¹, anti-fungals², anti-convulsants³ and recently as peripheral-selective noradrenaline reuptake inhibitors.⁴⁻⁶ This new methodology could lend itself to making similar molecules that have potentially interesting biological activity.

The various synthetic handles that these structures possess such as an amine and functionalizable ester and bromide groups, in addition to their propensity to undergo rearrangement chemistry makes these structures very versatile (Figure 6.1).

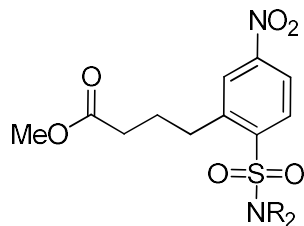


Figure 6.2. Potential sulfonamide protecting group.

Organocatalysis has become the third major faction of catalysis, alongside metal-mediated catalysis and biocatalysis. They are particularly appealing alternatives as they are inexpensive, air and water stable, readily available and have low toxicity, all industrially desirable qualities. Being a field only since 2000, this area of research is still quite young. While there have been huge strides in finding highly active and selective organocatalysts, there is still areas left to be explored including, for example, finding catalysts that exhibit selectivities rivaling metal catalysts and biocatalysts, particularly at similar catalyst loadings as opposed to the typical >5 mol % that organocatalysts typically require. Expanding the toolbox of reactions that can be organocatalyzed would also be attractive. Organocatalysis is likely the future of catalysis when considering its availability and applicability and as such, strong efforts into this field are still needed.

6.3 References

- (1) Burland, P. A.; Osborn, H. M.; Turkson, A. *Bioorg. Med. Chem.* **2011**, *19*, 5679.
- (2) Kaneko, S.; Arai, M.; Uchida, T.; Harasaki, T.; Fukuoka, T.; Konosu, T. *Bioorg. Med. Chem. Lett.* **2002**, *12*, 1705.
- (3) Sharma, G.; Park, J. Y.; Park, M. S. *Bioorg. Med. Chem. Lett.* **2008**, *18*, 3188.
- (4) Fujimori, I.; Yukawa, T.; Kamei, T.; Nakada, Y.; Sakauchi, N.; Yamada, M.; Ohba, Y.; Takiguchi, M.; Kuno, M.; Kamo, I.; Nakagawa, H.; Hamada, T.; Igari, T.; Okuda, T.; Yamamoto, S.; Tsukamoto, T.; Ishichi, Y.; Ueno, H. *Bioorg. Med. Chem.* **2015**.
- (5) Yukawa, T.; Fujimori, I.; Kamei, T.; Nakada, Y.; Sakauchi, N.; Yamada, M.; Ohba, Y.; Ueno, H.; Takiguchi, M.; Kuno, M.; Kamo, I.; Nakagawa, H.; Fujioka, Y.; Igari, T.; Ishichi, Y.; Tsukamoto, T. *Bioorg. Med. Chem.* **2016**, *24*, 3207.
- (6) Yukawa, T.; Nakada, Y.; Sakauchi, N.; Kamei, T.; Yamada, M.; Ohba, Y.; Fujimori, I.; Ueno, H.; Takiguchi, M.; Kuno, M.; Kamo, I.; Nakagawa, H.; Fujioka, Y.; Igari, T.; Ishichi, Y.; Tsukamoto, T. *Bioorg. Med. Chem.* **2016**, *24*, 3716.